Dependence of learning and memory consolidation on spatiotemporal expression of Arc/Arg3.1 in hippocampal-cortical networks

Dissertation

Zur Erlangung des akademischen Grades

des Doktors der Naturwissenschaften (Dr.rer.nat.)

des Fachbereichs Biologie,

der Fakultät für Mathematik, Informatik und Naturwissenschaften,

der Universität Hamburg

vorgelegt von

Xiaoyan Gao

aus Shandong, China

Hamburg, 2016

1st Gutachter: Prof. Dr. Dietmar Kuhl

2nd Gutachter: Prof. Dr. Christian Lohr

Die Arbeit wurde im Zeitraum von November 2011 bis Juli 2016 im Institut für Molekulare und Zelluläre Kognition, des Zentrum für Molekulare Neurobiologie Hamburg (ZMNH) unter der Anleitung von Herrn Prof. Dietmar Kuhl und Frau Dr. Ora Ohana angefertigt.

Tag der Disputation: 04.11.2016

Eidesstattliche Versicherung

Hiermit erkläre ich an Eides statt, dass ich die vorliegende Dissertationsschrift selbst verfasst und keine anderen als die angegebenen Quellen und Hilfsmittel benutzt habe.

Hamburg, den 09.11.2016 Xiang Gao

Unterschrift

Table of contents

Acknowledgement / Danksagung

First of all, I would like to thank Prof. Dietmar Kuhl for providing me the opportunity to work in his lab as a doctoral student. With his supervision, I learned how to do serious science. I thank Prof. Christian Lohr from the Department of Biology of Hamburg University for his efforts as the second supervisor and reviewer of the thesis. I am also indebted to the China Scholarship Council (CSC) who awarded me the stipend that enabled my study in Germany.

Especially, I would like to thank Dr. Ora Ohana for her excellent supervision of my doctoral projects, critical corrections of this thesis as well as her warm-hearted help in life. Her support and help were indispensable for my work and life in the past several years in Hamburg.

I am indebted to my close friends and colleagues Mario Sergio Castro Gómez and Jasper Grendel, two very talented PhD students and to Ms. Sabine Graf, an outstanding technician, whose collaboration and contribution to my work were invaluable to this thesis. I really enjoyed the time spent together with them and cherish their sincere friendship.

I would also like to thank Dr. Lars Binkle, Dr. Daniel Mensching, Miss Helia Saber, Dr. Ingke Braren (Vector facility of UKE), PD. Dr. Sabine Hoffmeister-Ullerich, PD. Dr. Irm Hermanns-Borgmeyer, Ms. Ute Süsens and Ms. Eva Kronberg for their kind help during experiments and for their contributions to this project. Thanks Dr. Mary Muhia and Dr. Fabio Morrelini for kindly sharing their experience and knowledge of rodent behaviors. I also would like to thank all of the other colleagues from ‘Cool-lab’ who shared their experience, knowledge and many happy and wonderful moments with me. They are Francesca, Xiaosong, Jerome, Jakob, Daks, Uwe, Ralf, Joachim, Sandra, Abuzar, Christina, Barbara, Andrea, Guido.

Particularly, I am very grateful for the support of my family. Especially, my highest respect and gratitude belong to Dr. Shu-Ting Yin, my wife and the mother of my daughter for her love, support and selfless dedication.

Abbreviations

ACC	anterior cingulate cortex
AMPA	α-amino-3-hydroxy-5-methyl-4-isoxazolepropionat
Arg3.1	activity-regulated gene 3.1
BDNF	brain-derived neurotrophic factor
BLA	basolateral amygdala
BNST	bed nuclei of the stria terminalis
CA	cornus ammonis
CaMKII	calcium calmodulin-dependent kinase 2
CFC	contextual fear conditioning
ChR2	channelrhodopsin 2
cKO	conditional knock out
CREB	cAMP response element binding protein
CS	conditioned stimulus
CTA	conditioned taste aversion
DCM	dynamic consolidation model
DG	dentate gyrus
DHPG	dihydroxyphenylglycine
DMN	default mode network
EJCs	exon junction complexes
fEPSP	field excitatory postsynaptic potential
fMRI	functional magnetic resonance imaging
HFS	high frequency stimulation
IEGs	immediate early genes
IHC	immunohistochemistry
IO	input/output
KD	knock down
KO	knock out
LA	lateral amygdala
LFP	local field potential
LFS	low frequency stimulation
LTD	long-term depression
LTM	long-term memory
LTP	long-term potentiation
MAPK	mitogen-activated protein kinase
MEC	medial entorhinal cortex
MEF2	myocyte enhancer factor 2
mEPSC	miniature excitatory postsynaptic current

MS	medial septum
DBB	diagonal band of Broca
MTL	medial temporal lobe
MTT	multiple trace theory
MWM	morris water maze
NAcc	nucleus accumbens
NMD	nonsense mediated decay
NMDA	N-methyl-D-aspartate
NOR	novel object recognition
ODNs	oligodeoxynucleotides
ORF	open reading frame
PBN	parabrachial nucleus
PEC	perirhinal cortex
PFA	paraformaldehyde
PKA	protein kinase A
PKC	protein kinase C
PP	perforant path
PRPs	plasticity related proteins
PS	population spike
rAAV	recombinant adeno-associated virus
REM	rapid eye movement
rISH	radiaoacitve *in situ* hybridization
RSC	retrosplenial cortex
SAM	schema assimilation model
SARE	synaptic activity response element
SCT	standard consolidation theory
SPWs	sharp waves
SRE	serum response element
STDP	spike timing-dependent plasticity
STM	short-term memory
SWRs	sharp wave ripples
SWS	slow-wave sleep
TBS	theta-burst stimulation
TTT	trace transformation theory
US	unconditioned stimulus
UTR	untranslated region
WT	wild type

Abstract

Despite decades of intense research, the process of memory formation and storage in the brain remains enigmatic. While information processing occurs in large and distributed neural networks, the actual sites of storage are unknown as well as the content of the information stored. The temporal aspects of generating and storing memories are likewise unknown; in particular, whether the capacity for learning and memory is differentially modulated during development and in adulthood. These questions have proven so far difficult to answer because learning and memory consolidation could not be well isolated from information processing in the brain. In this thesis I address these questions by targeting the memory-specific gene Arc/Arg3.1.

Arc/Arg3.1 is an activity regulated gene whose expression is rapidly upregulated following memory acquisition and retrieval, and is essential for synaptic and memory consolidation. However, how postnatal Arc/Arg3.1 expression contributes to learning and memory consolidation, and whether memory consolidation necessitates continuous Arc/Arg3.1 expression during adulthood remain unclear. Moreover, how Arc/Arg3.1-mediated synaptic plasticity in specific brain regions underlies learning and memory consolidation is also not fully elucidated. To address these questions, Arc/Arg3.1 was conditionally ablated either pre- or postnatally or was removed locally in specific brain regions of adult Arc/Arg3.1 floxed mice together with Cre-carrying mice or viral vectors. The contribution of spatiotemporal Arc/Arg3.1 expression to learning and memory consolidation was assessed in different behavioral tests. Underlying mechanisms were explored using *in vivo* electrophysiological recordings and brain IEG mapping.

First, I observed that prenatal Arc/Arg3.1 ablation (KO mice) led to retarded spatial learning, significantly reduced brain rhythmic activity, attenuated synaptic consolidation in the hippocampus and strongly impaired long-term explicit memory consolidation in novel object recognition, contextual fear conditioning and Morris water maze. Strikingly, late postnatal Arc/Arg3.1 ablation (Late-cKO mice) left spatial learning, brain rhythmic activity and hippocampal synaptic plasticity largely intact, but also caused explicit memory loss. These data suggest that long-term explicit memory consolidation requires lifelong Arc/Arg3.1 expression, while intact spatial learning and hippocampal oscillatory activity highly rely on Arc/Arg3.1 expression during early brain development, indicating two essential yet different roles of Arc/Arg3.1 in establishing memory and learning capacity.

Further, I discovered that local removal of Arc/Arg3.1 mediated by rAAV-Cre in selected one or two mnemonic regions, such as hippocampus, medial prefrontal cortex, anterior

cingulate cortex, retrosplenial cortex and basolateral amygdala did not significantly block contextual fear memory retrieval. Loss of memory was only observed when Arc/Arg3.1 was ablated in the entire forebrain of Late-cKO mice, indicating that contextual fear memory is stored broadly in hippocampal-cortical networks and its consolidation requires Arc/Arg3.1 mediated plasticity in adulthood. Notably, local ablation of Arc/Arg3.1 in the adult hippocampus led to impaired hippocampal synaptic plasticity, inefficient reactivation of ensembles in the medial prefrontal cortex and basolateral amygdala and thereby caused declined specificity of remote memory, implying an essential role of Arc/Arg3.1 mediated plasticity in the hippocampus in controlling precise remote memory processing. This study allows us to better understand the contribution of spatial Arc/Arg3.1 expression in different brain regions to system memory consolidation.

Finally, I reported that complete Arc/Arg3.1 KO mice showed strong deficits in consolidation of implicit memory assessed by auditory fear conditioning and conditioned taste aversion. Surprisingly, I did not observe such deficits in the Late-cKO mice. However, when Arc/Arg3.1 was acutely ablated in the amygdala of adult mice via local rAAV-Cre injection, tone fear memory was strongly impaired. Put together, these findings suggest that early expression of Arc/Arg3.1 during development is indispensable for acquisition of implicit memory, whereas its prolonged absence in adulthood could be compensated through recruitment of different brain regions or cellular mechanisms. Acute rAAV-Cre mediated Arc/Arg3.1 ablation in the hippocampus did not impact auditory fear memory formation, consolidation or retrieval, suggesting that the hippocampus is not essential for this implicit memory.

In summary, findings reported in this thesis support a new model of memory consolidation in which different aspects of information are stored as complementary memory traces in a broad network of brain regions. Interactions between these regions contribute to memory stability in the face of ongoing time and local damage. In addition, I provide first evidence that the capacity for learning and memory is established during early development by Arc/Arg3.1 dependent plasticity mechanisms.

Zusammenfassung

Auch nach Jahrzehnten intensiver Forschung sind die Prozesse der Gedächtnisbildung und des Gedächtnisses rätselhaft. Während die Informationsverarbeitung in großen und verteilten Netzwerken erfolgt, sind der tatsächliche Speicherort und der Gehalt der gespeicherten Information unbekannt. Die zeitlichen Aspekte der Generierung und Speicherung von Erinnerungen sind im gleichen Maße unbekannt; insbesondere die Frage, ob die Kapazität zum Lernen und Speichern während der Entwicklung und im Erwachsenenalter unterschiedlich moduliert wird, bleibt ungeklärt. Die Beantwortung dieser Fragen hat sich bis heute als äußerst schwierig herausgestellt, da das Lernen und die Konsolidierung des Gedächtnisses nur schlecht von der Informationsverarbeitung des Gehirns zu trennen sind. In dieser Arbeit adressiere ich diese Fragen mit Hilfe des gedächtnisspezifischen Gens Arc/Arg3.1.

Arc/Arg3.1 ist ein aktivitätsreguliertes Gen, dessen Expression während der Bildung des Gedächtnisses und dem Abrufen von Erinnerungen rasch hochreguliert wird und das essenziell für die Konsolidierung des Gedächtnisses und der synaptischen Plastizität ist. Es ist jedoch unklar, inwiefern die postnatale Arc/Arg3.1 Expression zu Lernprozessen und Gedächtniskonsolidierung beiträgt und ob diese im Erwachsenenalter weiterhin notwendig ist. Darüber hinaus ist es kaum verstanden, in welcher Weise Arc/Arg3.1-vermittelte synaptische Plastizität in spezifischen Hirnarealen dem Lernen und der Gedächtniskonsolidierung zugrunde liegt. Zur Beantwortung dieser Fragen wurde Arc/Arg3.1 entweder prä- oder postnatal durch die konditionale Expression der Cre-Rekombinase entfernt. Zusätzlich wurde Arc/Arg3.1 lokal durch virale Injektionen entfernt. Die Beteiligung der räumlich-zeitlichen Expression von Arc/Arg3.1 am Lernen und der Gedächtniskonsolidierung wurde mit Hilfe von verschiedenen Verhaltensversuchen überprüft. Die zugrunde liegenden Mechanismen wurden durch die Verwendung von *in vivo* Elektrophysiologie und IEG-Kartierung des Gehirns untersucht.

Zunächst konnte ich feststellen, dass die pränatale Entfernung von Arc/Arg3.1 (KO Mäuse) zu folgenden Beeinträchtigungen führt: verzögertes räumliches Lernen, signifikante Reduktion der rhythmischen Hirnaktivität, abgeschwächte synaptische Konsolidierung im Hippocampus und stark gestörte Langzeitkonsolidierung des expliziten Gedächtnisses in Verhaltensexperimenten wie neue Objekterkennung, kontextuelle Angstkonditionierung und Morris water maze. Auffälligerweise bleibt das räumliche Lernen, die rhythmische Hirnaktivität und synaptische Plastizität im Hippocampus in postnatal ablatierten Mäusen (Late-cKO) weitestgehend intakt. Das explizite Gedächtnis ist jedochin diesen Tieren weiterhin gestört. Diese Ergebnisse weisen darauf hin, dass für ein intaktes, explizites Langzeitgedächtnis eine lebenslange Expression von Arc/Arg3.1 notwendig ist, wohingegen räumliches Lernen und hippocampale, oszillatorische Aktivität im hohen Maße von einer Arc/Arg3.1-Expression während der Entwicklung abhängig sind. Dies deutet auf zwei

essenzielle, jedoch unterschiedliche Rollen von Arc/Arg3.1 in der Etablierung von Lern- und Gedächtnisfähigkeiten hin.

Im Weiteren konnte ich zeigen, dass die lokale Entfernung von Arc/Arg3.1 in einer oder zwei mnemonischen Hirnregionen wie dem Hippocampus, des medialen präfrontalen Cortex, anterioren cingulären Cortex, und der basolateralen Amygdala, keine signifikante Störung des kontextualen Angstgedächtnisses zur Folge haben. Der Verlust des Gedächtnisses konnte ausschließlich beobachtet werden, wenn Arc/Arg3.1 im gesamten Vorderhirn (Late-cKO) entfernt wurde, was darauf hinweist, dass das kontextuale Angstgedächtnis verteilt im hippocampalen-corticalen Netzwerk gespeichert ist und dass die Arc/Arg3.1-vermittelte Plastizität für dessen Konsolidierung im adulten Tier notwendig ist. Bemerkenswerterweise führt die lokale Entfernung von Arc/Arg3.1 im adulten Hippocampus zu einer Beeinträchtigung der synaptischen Plastizität, ineffektiver Reaktivierung von Engrammzellen im medialen präfrontalen Cortex und der basolateralen Amygdala und dadurch zu einer Schwächung der Spezifität des Altgedächtnisses. Dies deutet auf eine essenzielle Rolle der hippocampalen, Arc/Arg3.1-vermittelten Plastizität in der präzisen Kontrolle der Langzeitgedächtnisverarbeitung hin. Meine Arbeit leistet einen grundlegenden Beitrag zum besseren Verständnis der systemweiten Gedächtniskonsolidierung, die durch die räumliche Arc/Arg3.1-Expression in verschiedenen Hirnarealen bestimmt wird.

Zuletzt zeige ich in auditorischen Angstkonditionierungsversuchen und der konditionierten Geschmacksabneigung, dass konstitutive Arc/Arg3.1 KO Mäuse auch starke Defizite in der Konsolidierung des impliziten Gedächtnisses aufweisen. Überraschender Weise konnte ich solche Defizite nicht in Late-cKO Mäusen finden. Wird Arc/Arg3.1 jedoch akut in der Amygdala adulter Mäuse entfernt, zeigt sich eine starke Beeinträchtigung des auditorischen Angstgedächtnisses. Zusammengenommen legen diese Ergebnisse nahe, dass die Expression von Arc/Arg3.1 während der frühen Entwicklung unerlässlich für die Ausbildung des impliziten Gedächtnisses ist, wohingegen der permanente Verlust von Arc/Arg3.1 im adulten Tier durch die Einbeziehung von anderen Hirnregionen oder zellulären Mechanismen kompensiert werden kann. Die akute Entfernung von Arc/Arg3.1 im Hippocampus hat keinen Einfluss auf die Generierung, Konsolidierung oder das Abrufen des auditorischen Angstgedächtnisses und legt damit nahe, dass der Hippocampus nicht essentiell für implizites Gedächtnis ist.

Zusammengefasst unterstützen die Ergebnisse meiner Arbeit ein neues Modell der Gedächtniskonsolidierung, in welchem verschiedene Aspekte von Gedächtnisinformationen in komplementären Gedächtnisspuren in einem breiten Netzwerk verschiedener Hirnregionen gespeichert werden. Die Interaktion dieser Regionen trägt angesichts voranschreitender Zeit und lokalen Schäden zur Gedächtnisstabilität bei. Zusätzlich zeige ich, dass die Fähigkeit für Lernen und Gedächtnis früh während der Entwicklung durch Arc/Arg3.1-abhängige Mechanismen der Plastizität etabliert wird.

1 Introduction

Every day, we as humans try to perceive, understand and interact with our surrounding, based on information from our senses, our internal representation of the world and our emotions. This never ending flow of thoughts and emotions is captured in our brains for an indefinite amount of time. Probably, you never want to forget some joyful experience, but following the time they are gradually degraded, whereas, some unhappy experience cannot be erased easily and sometimes come to your mind again and again. However, where and how experience is selected for storage by the brain remain paramount questions of modern research.

For generations, neuroscientists have taken various theoretical and experimental approaches to reveal the workings of the brain. Molecular and cellular neuroscientists mainly focus on identifying molecules and signaling cascades that are crucial for brain function and how these cooperate to define neuronal specificity and build neural circuits. On the basis of their work, system and behavioral neuroscientists further investigate how neural circuits perform specific functions and how these circuits are controlled, modulated and coordinated to produce integrated behavior. Highly challenging work is done by cognitive neuroscientists who try to understand how complex activities in the human brain enable us to think, to feel and to act.

1.1 Learning and memory

Learning is the process of acquiring new information, or updating and strengthening existing information or knowledge. Memory is the process of stabilizing, consolidating and retaining learned information or knowledge. Psychologists and neuroscientists distinguish different forms of learning and memories rely on different brain structures and networks.

1.1.1 Learning

The two major forms of learning are procedural learning and episodic learning. Procedural learning describes the acquisition of a motor response in reaction to a visual, tactile or olfactory sensory input. It can be classified as either non-associative or associative learning. Non-associative learning is a simple form of learning induced by certain repetitive stimuli that could cause long-lasting behavioral responses. It is categorized into habituation and sensitization. These two subtypes of learning exist in all species of animals from invertebrate to vertebrate, and are especially well studied by using *Aplysia* (Castellucci et al., 1970; Pinsker et al., 1970; Kandel, 2001).

Studies in this thesis mainly focus on associative learning. Associative learning refers to the process of acquiring an association between two stimuli, or between a behavior and a stimulus. Classical conditioning and operant conditioning are the two major forms. Classical conditioning, first introduced by the Russian physiologist Ivan Pavlov, involves associating

two previously unrelated stimuli. One is called conditioned stimulus (CS, e.g. a light or a tone), and the other one is called unconditioned stimulus (US, e.g. food or foot shocks). Pairing of the reward or aversive US with the neutral CS repeatedly, results in the CS becoming a predication signal for the US such that the CS alone can induce the behavioral response. For example, in the auditory fear conditioning experiment, a CS tone presented alone can evoke freezing responses in mice that had been exposed to several pairs of tone/foot shocks presentation. So, during classical conditioning, animals can learn to predict shock events with the help of a neutral stimulus (LeDoux, 1995; LeDoux, 2003; Johansen et al., 2011). Amygdala has been always considered as the main player involved in fear learning. It is composed of heterogeneous nuclei, including lateral nucleus, basal lateral nucleus, basal medial nucleus and central nucleus. These nuclei work together for controlling of fear acquisition and expression. Briefly, lateral nucleus converge the auditory CS information relayed from thalamic regions and auditory cortex, and the aversive US collected and transmitted by somatosensory and nociceptive systems. These converging synaptic inputs potentiate synapses in the lateral amygdala to encode fear and then trigger fear expression by recruiting neurons in the central amygdala and its targeted hypothalamic and brainstem areas that control fear responses, such as freezing (LeDoux, 2000; Duvarci and Pare, 2014; Herry and Johansen, 2014). In the fear conditioning, there is also episodic component which is linked with fear. Conditioned mice could also generate fear in the conditioning environment without tone CS presentation because they learn that this is where they have previously experienced electrical foot shocks (Curzon et al., 2009; Izquierdo et al., 2016). In addition to amygdala, hippocampi as well as neocortical regions are reported to involve in contextual fear learning (Fanselow, 2010; Izquierdo et al., 2016). A second form of associative learning is called operant or instrumental learning which refers to the process of acquiring an association between a specific behavior and a meaningful stimulus. A widely used animal model for this form of learning is the lever pressing paradigm in which a hungry or thirsty animal can receive food or water by pressing a lever. Learning starts through an accidental lever pressing experience and proceeds by reinforcing the positive outcome, namely, that pressing the lever leads to a food or water reward (Wilkenfield et al., 1992; Nabavi et al., 2014). Thus, an action-outcome association is formed and strengthened during operant conditioning.

Spatial learning based on spatial cue guided allocentric navigation is another important ability for almost all organisms for survival. It is a process that animals are motivated by some stimuli (e.g. searching water or food; escaped from danger and return home safely) to learn to locate and memorize a specific place and find their own routes to get there by using some available distal or proximal cues in the space. The most commonly used paradigm for assessing spatial learning in rodents is Morris water maze (MWM). In this task animals learn

to reach a hidden escape platform guided by spatial visual cues in the nearby environment (Morris, 1984; D'Hooge and De Deyn, 2001; Vorhees and Williams, 2006). Successful spatial learning primarily needs the involvement of functional hippocampus and entorhinal cortex for generating precise cognitive maps (Vorhees and Williams, 2014). Lesions of hippocampus impaired spatial navigation (Morris et al., 1982). Specific populations of cells named place cells has been identified in the hippocampus. These cells are firing sequentially in a high rate when animals are approaching a hidden escape platform in the MWM. During this process, a neural map for locating the platform is established (Hollup et al., 2001). Later on, scientists also identified special types of neurons named grid cells (Hafting et al., 2005) for generating tiling patterns of spatial map, head direction cells for directional orientation (Buzsaki and Moser, 2013a) and border cells for reacting to edges (Solstad et al., 2008) in the entorhinal cortex. Together, all of these specific types of cells in the hippocampus and entorhinal cortex communicate with each other during spatial navigation to encode spatial information for generating functional mapping networks that finally facilitate navigation to a specific place avoiding getting lost.

1.1.2 Explicit and implicit memory

Long-term memory (LTM) had been classically divided into two categories: explicit and implicit memory, based on how memory related information is collected, consolidated, stored and retrieved. Different learning processes generate difference forms of memories supported by different brain regions. Procedural learning generates implicit memory, while episodic learning produces explicit memory.

Explicit memory is the memory people use every day in life. It can be subdivided into episodic and semantic memory concerning specific events in one’s life and learned facts, respectively. For example, you remember that you attended a concert. The place was in People’s Art Theater of Shanghai, and the time is last Saturday night. After that you still can vividly recall the actors' performances and give a verbal description to your friends. Besides, you also may know the facts that Beijing is the capital of China and the seawater is salty. The psychologist Endel Tulving first developed the idea that explicit memory can be further classified as episodic memory, a memory for events or personal experience, and semantic memory, a memory for facts (Tulving, 1972). All of these events and facts related memories are also called declarative memories. Retrieval of declarative memory is conscious recollection of previous experiences, information and knowledge. Unlike explicit declarative memory, implicit memory is unconscious and cannot be verbally declared. Therefore, it is also frequently called nondeclarative memory. Implicit memory includes the retrieval of specific step-by-step procedures, or specific conditioned responses. For example, you can unconsciously drive a car or ride a bike after procedural learning. Moreover, you can

generate conditioned aversion towards food that caused you strong allergies and diarrhea. Similarly, as shown in the conditioned taste aversion (CTA) experiment, mice are scary to drink sugar water because they still remember they had gastrointestinal discomfort after drinking sugar water, although this effect is induced by US stimulus (here refer to LiCl) not by sugar water (Rosenblum et al., 1993; Welzl et al., 2001a; Sano et al., 2014). Therefore, implicit memory retrieval is a process of unconsciously retrieving previously learned skills, simple forms of conditioning as well as habit and priming. Together, “explicit declarative memory provides a way to represent the external world, while implicit nondeclarative memory provides for myriad unconscious ways of responding to the world” (Squire and Dede, 2015).

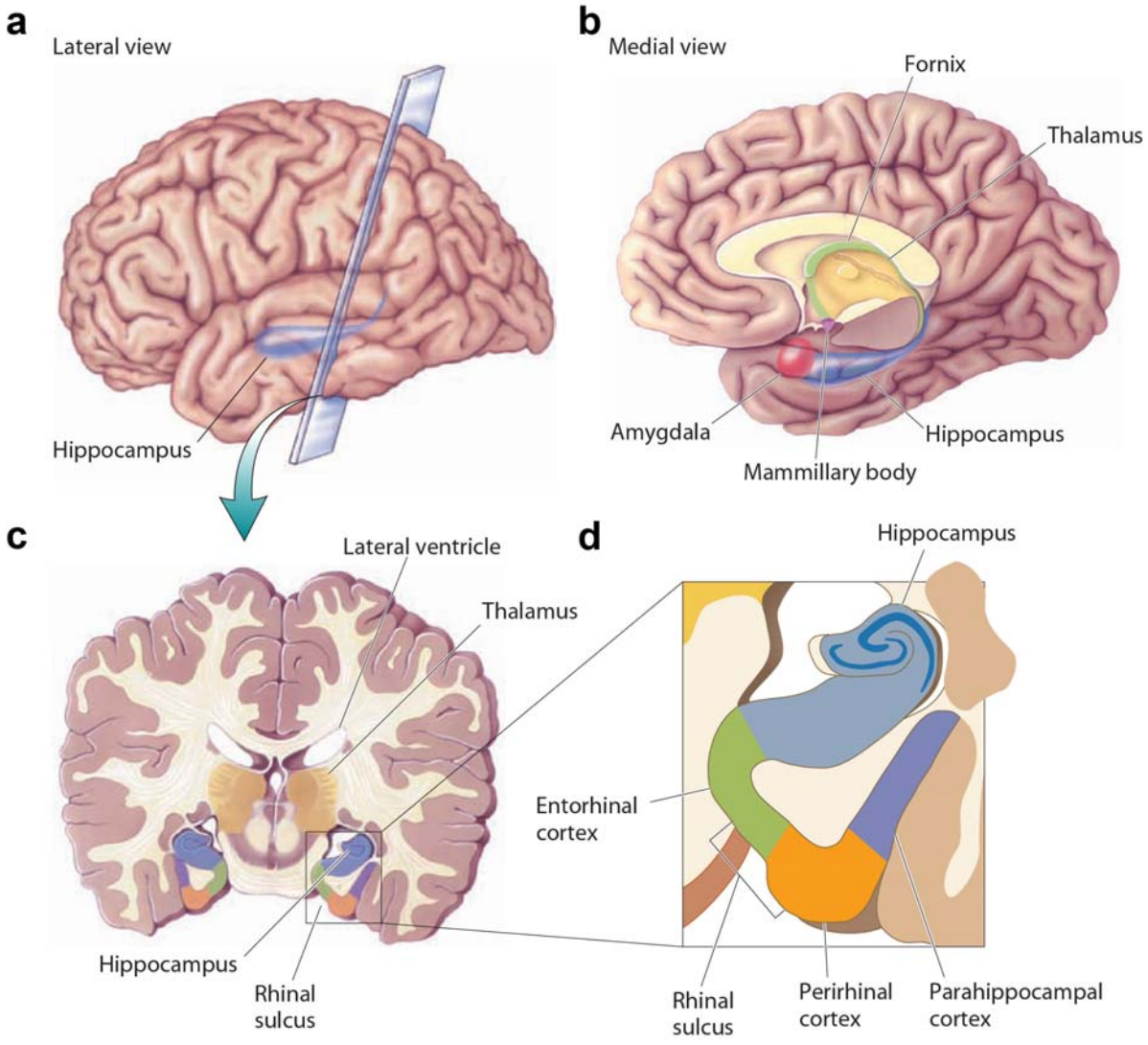

Fig. 1.1 Structures in the medial temporal lobe and diencephalon involved in memory processing. a, Lateral views show the location of the hippocampus in the temporal lobe. **b,** Medial views show the location of the hippocampus in the temporal lobe and structures in the diencephalon. The thalamus and mammillary bodies receive afferents from structures in the medial temporal lobe. **c-d,** Coronal section show the hippocampus and cortex of the medial temporal lobe. (Adapted and modified from Neuroscience-exploring the brain, third edition)

1.1.3 Brain systems for explicit and implicit memory

The dissociation of explicit and implicit memory started with the investigations of the famous patient H.M. (full name Henry Molaison) whose medial temporal lobe (MTL) was removed bilaterally by a neurosurgeon named William B. Scoville, in order to relieve his severe epilepsy. The operation was very successful and his epilepsy was largely cured. However, later on studies by the Canadian neuropsychologist Brenda Milner and her colleagues reported that H.M. had strong memory deficits (Scoville and Milner, 1957; Penfield and Milner, 1958; Squire and Wixted, 2011) mainly for memorizing and retaining new information about place, objects and people which nowadays is considered as declarative information, but he still had normal short-term memory. Moreover, H.M. could also recall most of the memory events that happened before operation, but with mild temporally graded retrograde amnesia indicated by loss of some memories acquired several years before the surgery. In the beginning, Milner thought that H.M. lost the ability to form all types of LTM, but later she surprisingly found that H.M. could still learn to draw a star based on an image displayed in a mirror after 3 days practice, although he could not remember he did the same thing yesterday. This mirror-drawing task needs hand-eyes coordination, a form of motor based procedural skill learning. Since then scientists began to realize that the MTL including the regions that were removed in H.M. (Fig. 1.1a, c, d; hippocampus and the adjacent cortical structures) (Squire and Zola-Morgan, 1991; Squire and Wixted, 2011) were mainly important for acquiring, consolidating and storing long-term explicit declarative memories, but not for skill learning or implicit memory. Since these findings, knowledge about brain regions important for memory expanded. Now we also know that perirhinal cortex (Ho et al., 2015; Olarte-Sanchez et al., 2015) is important for novel object recognition memory encoding and hippocampus (Bannerman et al., 1999) and entorhinal (Hardman et al., 1997) are essential for spatial memory. Meanwhile, scientists discovered that the frontal lobes, in addition to MTL structures, are also involved in explicit episodic memory acquisition (Shimamura AP, 1991). Besides, it was also reported that nuclei located in the diencephalic midline (Fig. 1.1b), such as mammillary nuclei and anatomically connected with the MTL, are also important for declarative memories (Squire et al., 2004; Staresina et al., 2011). In 1960s, scientists knew from the studies of H.M. that there a specific form of memory now defined as implicit memory, is preserved in absence of other explicit forms. Later on, different forms of implicit memories, such as habituation, sensitization, classical conditioning, and operant conditioning were clarified. All of them do not depend on MTL. Now accumulated data and knowledge reveal that different forms of implicit memory are acquired through different forms of learning and involve different brain regions. For example, the amygdala is mainly responsible for memory containing an emotional component, such as auditory fear memory (LeDoux, 2003) and CTA memory (Reilly and Bornovalova, 2005). Memory acquired through

procedural learning requires the striatum, while memory acquired through operant conditioning also needs the participation of the cerebellum. Some neocortical regions are also necessary for memory acquired through priming or perceptual learning, such as the insular cortex for CTA memory (Yamamoto, 2007). The two simple forms of learning, habituation and sensitization also need the involvement of sensory and motor cortex. Together, different types of memory processing, both explicit and implicit memory, require the participation of different one or more combined brain regions (Squire, 1992). In general, explicit and implicit memories depend on different brain systems.

1.2 Memory consolidation

Memory consolidation is a process that acquired memory traces are gradually transformed from a fragile state to a stabilized state for permanent storage. The main theory about memory consolidation posits that memory is first consolidated at the synaptic level (rapid process within minutes or hours) involving experience-induced activation of intracellular signaling cascades, leading to memory related gene expression and modifications. In turn, these cause subsequent synaptic remodeling and synaptic strength and efficacy alteration. Finally, acquired information is stored in modified local synapses and neural circuits which involve memory encoding (Kandel et al., 2014). The second phase, system consolidation (slow process, from days to months, even years) involves recurrent waves of synaptic consolidation in the brain regions that receive fresh or reinforced information. Then the brain systems participated in this process integrate all the information and reorganize the representations of LTM in a time-dependent manner in distributed hippocampal-cortical networks (Dudai et al., 2015).

1.2.1 Synaptic memory consolidation

In 1949, Donald Hebb proposed in his seminal book that the basic mechanism for memory storage is due to the enhancement of synaptic strength and morphological changes of the synaptic contacts (Hebb, 1949). Based on that, modern memory consolidation theory postulates that memories are stored in the connections between synapses which are plastic. The strength of the synapses can be changed or modulated by plasticity related stimulus, such as behavior. The process of stimulus-induced alteration of synaptic efficacy and retention of these synaptic strength changes for a longer time is called synaptic or cellular memory consolidation (Fig. 1.2). For the underlying mechanisms, activity-dependent synaptic plasticity and its based synaptic tagging and capture dominate the current theory (Redondo and Morris, 2011; Clopath, 2012). Activity-dependent synaptic plasticity such as long-term potentiation (LTP) (Bliss and Lomo, 1973), long-term depression (LTD) (Lynch et al., 1977) or spike timing-dependent plasticity (STDP) (Markram et al., 1997; Bi and Poo, 1998) have

been identified as the causal link that occur at individual synapses mediating long-lasting changes of synaptic efficacy.

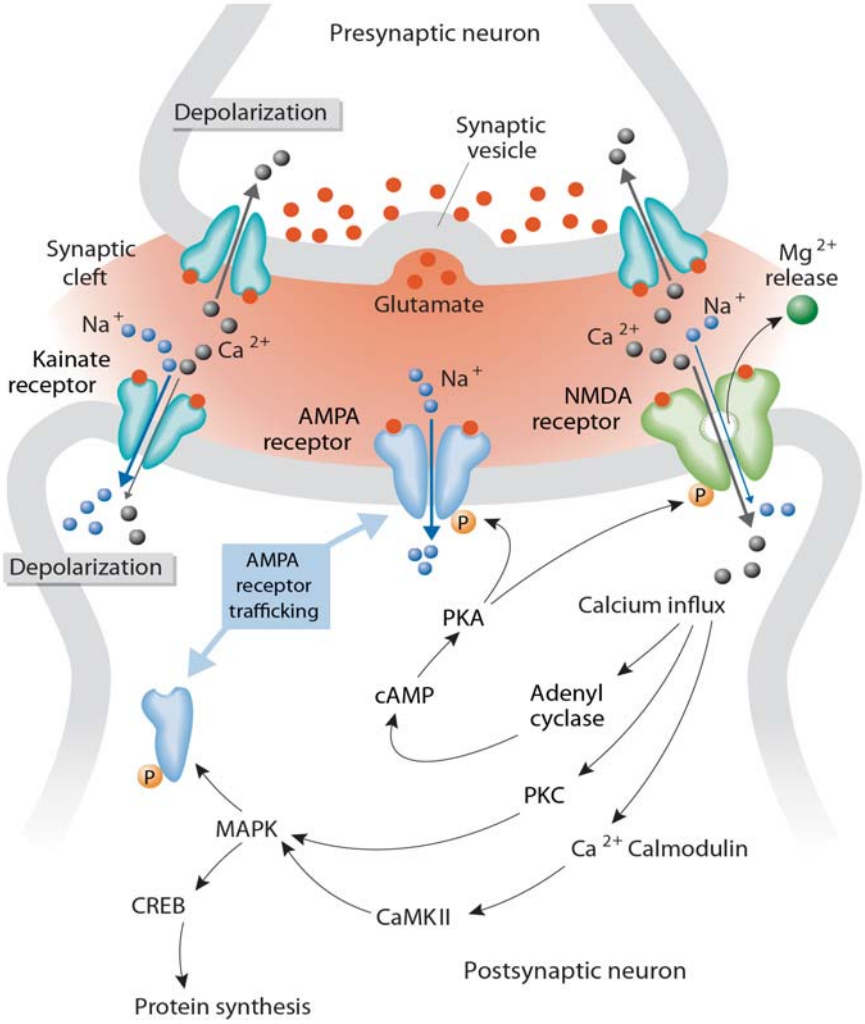

Fig. 1.2 Process of synaptic consolidation. Upon stimulation, presynaptic terminal release glutamate and binds to glutamate receptors at the postsynaptic membrane. Activation of AMPA and Kainate receptors initiates postsynaptic depolarization and further remove magnesium that block NMDA receptors. Calcium influx through NMDA receptors triggers various cascade signaling pathways to regulate AMPA receptors trafficking and plasticity related proteins synthesis that are responsible for synaptic consolidation. AMPA, α-amino-3-hydroxy-5-methyl-4-isoxazolepropionate; CaMKII, calcium/calmodulin-dependent kinase II; CREB, cAMP response element binding protein; MAPK, mitogen-activated protein kinase; NMDA, N-methyl-D-aspartate; PKA, protein kinase A; PKC, protein kinase C. ［Adapted from (Voglis and Tavernarakis, 2006)］

Memory encoding stimuli can selectively recruit cells that are at a high state of excitability. These selected cells are often termed “engram cells” (Josselyn et al., 2015). During the encoding phase, stimuli induce early-LTP by triggering presynaptic neuronal transmitter release such as glutamate which bind to postsynaptic receptors such as AMPA receptors, depolarizing postsynaptic membrane and then activate NMDA receptors, eliciting Ca^{2+} influx and activating CaMKII and further increase the synaptic weight by promoting the conductance of AMPA receptors mediated by phosphorylation and the AMPA receptor

insertion promoted by cytoskeletal changes (Fig. 1.2) (Shi et al., 1999; Lynch, 2004). Meanwhile, in the postsynaptic site the number of dendritic spines for supporting postsynaptic machinery is rapidly increased (Engert and Bonhoeffer, 1999). It was reported that local translation of dendritically localized mRNA could alter the structure of activated synapses and therefore support plasticity (Miyashiro et al., 1994; Steward et al., 1998; Wang et al., 2009; Kim and Martin, 2015). In parallel with the early-LTP induction, several activity regulated immediate early genes (IEGs), such as c-fos, arc/arg3.1 and zif268 are induced in the activated neurons (Alberini, 2009) and synaptic plasticity related kinases (e.g. CaMKII) are phosphorylated such that recruited cells are tagged as engram cells (Redondo and Morris, 2011). After initial memory encoding, if the stimulus is strong enough to create sufficient amount of tags that exceed the threshold, protein synthesis dependent late-LTP process is triggered (Fig. 1.2). Plasticity related proteins (PRPs) are synthesized by activating series of intracellular signaling cascades, including activation of MAPK/ERK and subsequent activation of transcription factor such as CREB to modulate gene expression. During the process of *de novo* protein synthesis, the steady state synthesis of AMPA receptors is shifted to a higher level and newly synthesized PRPs (reviewed by (Katche et al., 2013a)) undergo posttranslational modification, captured by tagged synapses for synaptic remodeling and help to stabilize the existing synaptic connections which are already potentiated during leaning process. Besides, new synaptic connections can also emerge though the activation of silent connections (Liao et al., 1995; Le Be and Markram, 2006) to facilitate memory information processing. Finally, all of these changes shape synaptic connectivity among the engram cells and then memory traces are consolidated into stable and precise mode in the synaptic level.

1.2.2 System memory consolidation

Compared with synaptic consolidation, system consolidation is much slower. It requires the participation and interaction of hippocampal and multiple cortical structures where recently acquired memory representations are reorganized for long-term storage. It is widely considered that the hippocampus plays a critical role in system memory consolidation, but its involvement is time limited. Originally, this idea emerged from the observations that amnesic patients (e.g. H.M.) whose MTL, especially hippocampus was damaged also show temporally graded retrograde amnesia apart from showing severe anterograde amnesia, implying less dependence of older memories on intact MTL (Scoville and Milner, 1957; Corkin, 2002). To explain this phenomenon, scientists proposed a standard consolidation theory (SCT) (Alvarez and Squire, 1994; McClelland et al., 1995; Squire, 2004; Frankland and Bontempi, 2005). The SCT posits that declarative information is encoded in parallel in the hippocampus and relevant neocortical areas. The retention and retrieval of those encoded information initially rely on hippocampus. Subsequently, reactivation of

hippocampus can replay encoded information to the neocortical regions. Continuous reactivation and coordinated replay from the hippocampus to the cortical regions leads to persistent adjustments of cortical-cortical connections, and establishment of reorganized long-lasting cortical representations. During this process, new memories are gradually getting independent of the hippocampus. In this model, the hippocampus is considered only as a temporary storage region for memory and the neocortex is the final place for long-term memory storage (Fig. 1.3).

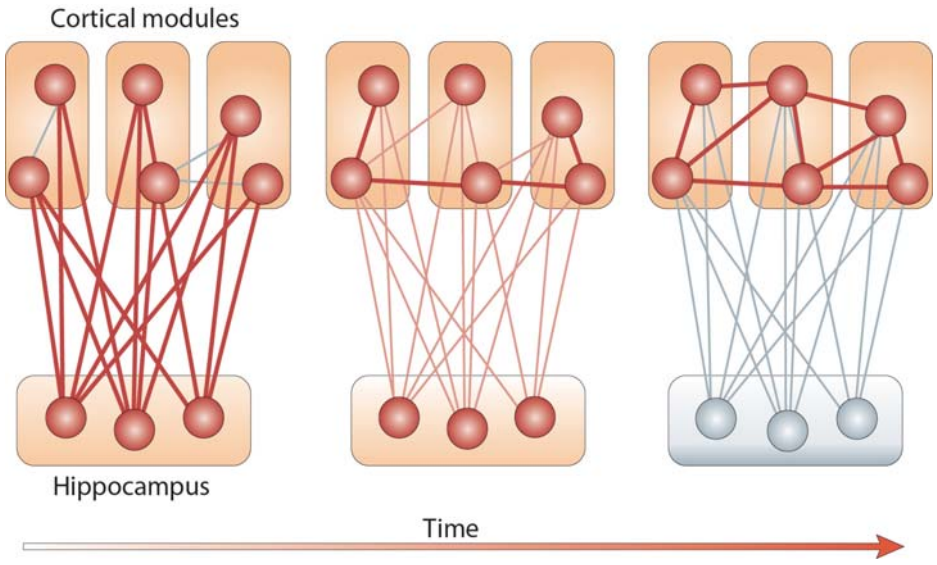

Fig. 1.3 Standard system memory consolidation model. Memory is encoded in parallel in the hippocampus and relevant neocortical areas. Hippocampus undergoes rapid process of memory consolidation and replay encoded information to the neocortical regions to help establish reorganized long-lasting cortical representations. This allows new memories to become independent of hippocampus. ［Adapted from (Frankland and Bontempi, 2005) ］

However, there are more and more literatures reporting that hippocampal disruption can affect both recent and remote LTM, indicating that the hippocampus also participates in remote memory processing (Viskontas et al., 2000; Lehmann et al., 2007; Goshen et al., 2011; Winocur et al., 2013). Moreover, retrieval of detailed remote declarative memories engages the hippocampus (Ryan et al., 2001; Addis et al., 2004; Wiltgen et al., 2010). With the accumulation of scientific data, the system memory consolidation theory has been continuously updated. The current dominant view is called multiple trace theory (MTT) which was first proposed by Lynn Nadel and Morris Moscovitcht (Nadel and Moscovitch, 1997) and later reviewed by other neuroscientists (Frankland and Bontempi, 2005; Dudai, 2012; Kandel et al., 2014). MTT holds that episodic information is rapidly and sparsely encoded in distributed hippocampal ensembles which act as an index to neocortical ensembles that represent attended information. These connections bind together to generate coherent memory trace stored in the hippocampal–cortical networks. Reactivation of this memory trace creates newly encoded hippocampal traces binding new traces in the cortex leading to

generation of multiple traces. These memory traces share some or all of the details about the initial representation. Another main feature of this theory is that unlike SCT, it dissociates the two subtypes of declarative memories (episodic and semantic memory) and proposes that retrieval of contextually rich episodic memories always depends on the hippocampus together with the cortex, because hippocampal traces provide spatial and temporal contextual information. However, semantic memories can be stored in the cortex and can be retrieved independent of functional hippocampus. Compared with SCT, MTT predicts that reactivation initiated memory reorganization also happens in the hippocampus like cortex. Due to the proliferation of memory traces, remote episodic memories are likely to have more traces in the hippocampus which could facilitate memory retrieval and make memories more resistant to hippocampus damage. Thus, partial hippocampus lesion would cause temporally graded retrograde amnesia whose extent would be determined by the size of hippocampal lesion. Complete hippocampal lesions should abolish all episodic memories, regardless of their age. In general, MTT suggests that hippocampus is still actively recruited and required for remote LTM retrieval. Yet, some recent evidence seems incompatible with MTT. For example, patients with well characterized MTL lesions show intact remote memory, unless the damage exceeds the MTL (Squire and Bayley, 2007). Goshen et al. also reported that optogenetic inhibition of hippocampus disrupted remote memory retrieval, suggesting ongoing involvement of hippocampus in remote LTM which fits MTT. However, when the silencing was extended for 30 min prior to memory retrieval to mimic lesion based studies, remote memory was successfully retrieved, indicating that with prolonged loss of hippocampal networks some underlying compensatory mechanisms render remote memory retrieval independent of the hippocampus (Goshen et al., 2011).

Afterwards, Winocur and his colleagues updated MTT and proposed a trace transformation theory (TTT) (Winocur et al., 2010; Winocur and Moscovitch, 2011). The main features are that acquired episodic memory keeps dependence on the hippocampus where episodic features are stored. During the transformation process, episodic memory is transformed from being hippocampus-represented and context-dependent to neocortex represented and context-independent. During this process, some detailed contextual features are lost and memory becomes schematized or semanticized. Most importantly, the transformed memory is posited to co-exist and interact with the initial more detailed memory that remains hippocampus dependent.

According to MTT, different circuits encode different memories handled by different brain regions. The allocation of specific memory to a particular circuit is due to hardwired organization of the brain. By using fear conditioning paradigm, Michael S. Fanselow challenged this view and proposed a dynamic consolidation model (DCM) (Fanselow, 2010).

He hypothesized that there are different circuits which can mediate fear related learning and memory. These circuits compete with each other and the winner will encode memories. The most efficient circuit wins the competition and then work as a primary circuit dominating learning. Once the primary circuit learns (e.g. contextual information in the hippocampus), the alternative ones do not. Moreover, if the dominant primary circuit is compromised (e.g. by inhibition or lesion), the alternate circuits can compensate it. However, the compensatory circuits are less efficient. Similarly, Brian J. Wiltgen and Kazumasa Z. Tanaka recently also proposed that during memory retrieval a competition exists between the hippocampus and neocortex. If the hippocampus wins the competition, detailed context memories are retrieved. In contrast, when the neocortex wins, imprecise context memories are retrieved but the retrieved memories are with loss of details (Wiltgen and Tanaka, 2013). This model provides new insights in how the brain selects efficient circuits through competition to produce specific behaviors.

Earlier system memory consolidation theories considered that memory encoding occurs rapidly, but memory consolidation, especially in the cortex undergoes a slow gradual process. In disagreement with this assumption, Tse et al. propose schema assimilation model (SAM) for system consolidation which posits that systems consolidation could also be accomplished extremely quickly if a previously created associative “schema” is available for incorporation of new information (Tse et al., 2007; Tse et al., 2011). This proposal was raised based on the observations from a hippocampus-dependent learning task. In these experiments, they trained rats to learn a set of different flavor-place associations which become persistent over time and form a cortical schema. Once the cortical schema is developed, new representations from one-trial learning could be assimilated and rapidly consolidated. This schema-dependent fast system consolidation is associated with a striking up-regulation of IEGs (e.g. zif268 and Arc/Arg3.1) in the prelimbic area of the medial prefrontal cortex (mPFC). Their findings challenge the concept that hippocampus represent fast learning system while cortical areas undergo slow learning and memory process.

At present, multiple theories for system memory consolidation exist. This is a fruitful ground for investigations in this field. As Yadin Dudai said “That different systems consolidation models coexist is a stimulating situation, as they provide opportunities for new hypothesis-driven experiments, which are likely to generate not only new data but also new models” (Dudai, 2012).

1.3 Role of Arc/Arg3.1 in synaptic plasticity and memory consolidation

1.3.1 Arc/Arg3.1

Activity-regulated gene (Arg3.1, also known as Arc) was identified in 1995 during a screening for genes upregulated by seizures in the hippocampus (Link et al., 1995; Lyford et al., 1995). The Arc/Arg3.1 gene is located on chromosome 15, 7 and 8 in the mouse, rat and human, respectively. It is a pretty conserved gene and only has low homology to α-spectrin sequence (Lyford et al., 1995). It composes 3 exons and 2 introns and transcribes a 3.1kb mRNA with a large 3 prime untranslated region (3' UTR) (Fig. 1.4) which contains a sequence for dendritic targeting (Kobayashi et al., 2005) and sites for two exon junction complexes (EJCs) that make Arc/Arg3.1 a natural target for nonsense mediated decay (NMD) (Giorgi et al., 2007). The entire open reading frame (ORF) is located in exon 1 and encodes a protein of 396 amino acids with a predicted molecular weight 55 kDa (Link et al., 1995; Lyford et al., 1995).

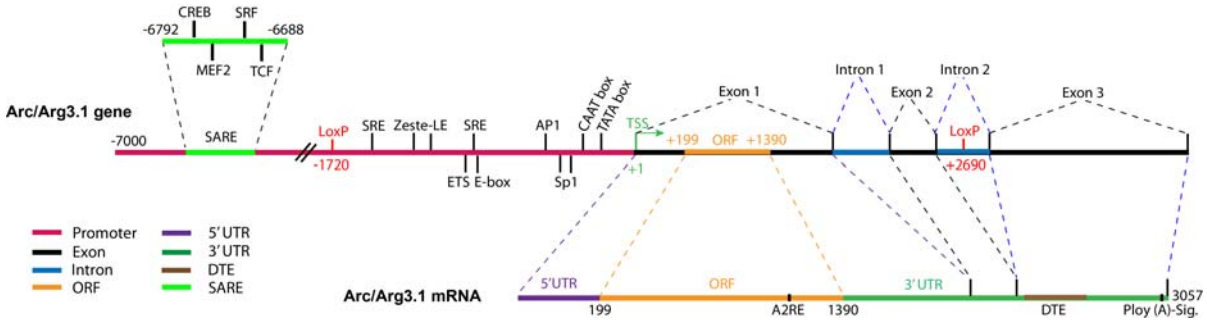

Fig. 1.4 Schematic of Arc/Arg3.1 DNA and mRNA elements. CREB, cAMP response element-binding protein; MEF2, myocyte enhancer factor-2; SRF, serum response factor; TCF, T-cell factor; SARE, synaptic activity response element; 5'UTR, 5 prime untranslated region; 3'UTR, 3 prime untranslated region; ORF, open reading frame; DTE, dendritic targeting element; AP1, activator protein 1; ETS, E26 transformation-specific family; E-BOX, enhancer-box; TSS, transcription start site; A2RE; A2 response element; Sp1, specificity protein 1. (Adapted and modified from Dr. Lars Binkle)

As an IEG, Arc/Arg3.1 expression can be regulated by plasticity related stimuli (Steward et al., 1998; Ying et al., 2002; Rodriguez et al., 2005; Chotiner et al., 2010) or behaviors (Gusev and Gubin, 2010a; Lonergan et al., 2010; Lv et al., 2011; Santini et al., 2011; Chau et al., 2013). For the regulation of activity-dependent transcription, several regions have been identified in the promoter region of Arc/Arg3.1 gene (Fig. 1.4). It includes a synaptic activity response element (SARE) that contains binding sites for 3 major transcription factors: cyclic AMP response element-binding protein (CREB), myocyte enhancer factor 2 (MEF2), and serum response factor (SRF) (Kawashima et al., 2009). Two serum response element (SRE) and one "Zeste-like" element that can be recruited by synaptic activity and enhance Arc/Arg3.1 induction were also identified in the promoter region (Waltereit et al., 2001; Pintchovski et al., 2009). Arc/Arg3.1 mRNA can be induced within several minutes upon

stimulation and then transported to the dendrites, especially to the activated synapses (Steward et al., 1998; Moga et al., 2004) as synaptic tags. However, Okuno et al. reported that Arc/Arg3.1 was selectively transported to the inactive synapses. This process needs the binding an inactive form of CaMKIIβ to promote AMPARs removal (Chowdhury et al., 2006; Rial Verde et al., 2006). With this it avoids the undesired potentiation of weak synapses in activated neurons (Okuno et al., 2012). In addition, Arc/Arg3.1 can be locally translated in the activated synapses (Steward et al., 1998; Yin et al., 2002; Moga et al., 2004). All of these unique characteristics of Arc/Arg3.1 imply that Arc.Arg3.1 could possibly couple synaptic activity to protein synthesis dependent synaptic plasticity and indicate a potential role in memory consolidation.

1.3.2 Arc/Arg3.1 and synaptic plasticity

Synaptic plasticity, in neuroscience is the ability of synapses to regulate their strength in response to activity. LTP, LTD and homeostatic plasticity are the common forms of synaptic plasticity. It was reported that Arc/Arg3.1 is essential for all of these forms of plasticity (Fig. 1.5).

LTP is the persistent increase of synaptic strength in response to high frequency stimulation (HFS) or chemical induction, such as brain-derived neurotrophic factor (BDNF). The first discovery about of the role of Arc/Arg3.1 in LTP was demonstrated by John F. Guzowski et al. in 2000. They found that intrahippocampal infusions of Arc/Arg3.1 antisense oligodeoxynucleotides (ODNs) to inhibit Arc/Arg3.1 expression impaired HFS induced LTP maintenance without affecting its induction in rats (Guzowski et al., 2000). Six years later, our colleagues further confirmed that early-LTP was enhanced while late-LTP was significantly impaired in the Arc/Arg3.1 knock out (KO) mice, indicating an essential role of Arc/Arg3.1 in synaptic consolidation (Plath et al., 2006). Afterwards, Elhoucine Messaoudi (2007) probed the dynamic function of Arc/Arg3.1 during LTP *in vivo* and reported that application of Arc/Arg3.1 antisense ODNs 2 hours but not 4 hours after LTP induction resulted in a reversal of LTP, while ODNs infusion 5 min before or 15 min after HFS only caused transient suppression of LTP and ODNs infusion 15 min or 90 min before HFS did not affect LTP expression and maintenance, suggesting temporal requirements for Arc/Arg3.1 expression in LTP (Messaoudi et al., 2007a). However, Sjoukje D. Kuipers et al. recently reported that local infusion of Arc/Arg3.1 ODNs prior to BDNF infusion also blocked BDNF-LTP induction in the adult dentate gyrus (Kuipers et al., 2016).

LTD is the persistent reduction of synaptic strength in response to low frequency stimulation (LFS) or chemical induction, such as dihydroxyphenylglycine (DHPG). The role of Arc/Arg3.1 in LTD expression was first reported by our colleagues in 2006. Low LFS-induced LTD was significantly impaired in Arc/Arg3.1 KO mice *in vitro* (Plath et al., 2006). Later

studies also demonstrated that mGluR-LTD induced either by paired-pulse LFS (PP-LFS) or mGluR agonist DHPG highly depends on local translation of Arc/Arg3.1 from pre-existing mRNA in the dendrites, but it does not rely on new transcription (Park et al., 2008; Waung et al., 2008; Jakkamsetti et al., 2013). Acute inhibition of new Arc/Arg3.1 expression with antisense ODNs blocks mGluR-LTD (Waung et al., 2008). Besides, Arc/Arg3.1 is also required for the late phase of cerebellar LTD in cultured Purkinje cells. This form of LTD is transcription dependent. It needs the binding of transcription factor SRF to SRE 6.9 in the Arc/Arg3.1 promoter (Smith-Hicks et al., 2010).

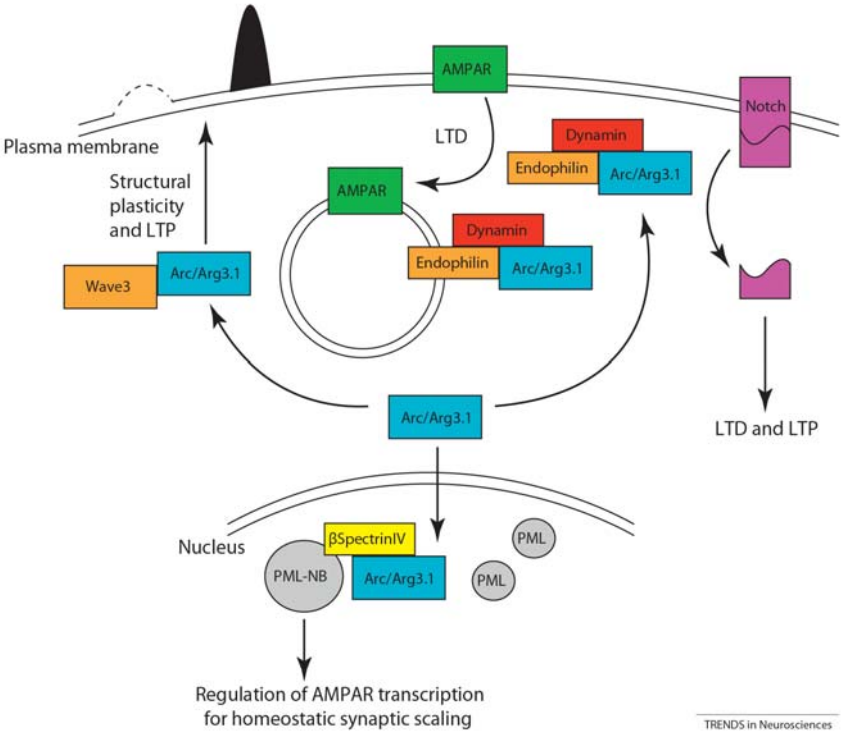

Fig. 1.5 Arc/Arg3.1 and synaptic plasticity. By interacting with other proteins, Arc/Arg3.1 might regulate structural plasticity, hebbian plasticity (LTP and LTD) and homeostatic plasticity. ［Adapted and modified from (Korb and Finkbeiner, 2011)］

What are the underlying molecular mechanisms of Arc/Arg3.1 in synaptic consolidation? Synaptic plasticity can be modulated by modifying synapse structure. For example, LTP induction can increase spinogenesis via promoting actin polymerization and stabilization (Yuste and Bonhoeffer, 2001; Dillon and Goda, 2005). Essentially, Carol L. Peebles et al. reported that over-expression of Arc/Arg3.1 increases spine density in cultured neurons. Specifically, the proportion of more plastic thin spines was significantly increased (Peebles et al., 2010), suggesting that Arc/Arg3.1 involves structural plasticity modulation (Fig. 1.5). Moreover, the increased thin spines could contribute to LTP expression (Popov et al., 2004). As mentioned above, actin cytoskeleton dynamics modulate spine morphology. Originally, it was reported that Arc/Arg3.1 protein co-localizes with actin cytoskeletal matrix (Lyford et al.,

1995). More directly, knock down (KD) of Arc/Arg3.1 with local infusion of ODNs 2 hours after induction impaired LTP consolidation. In parallel, cofilin was dephosphorylated and F-actin was lost at activated synapses. This LTP impairment can be reversed when the F-actin was stabilized by infusing jasplakinolide during LTP consolidation. This experiment directly linked Arc/Arg3.1 expression with actin cytoskeleton for long-lasting LTP (Messaoudi et al., 2007a). Another interesting study showed that Arc/Arg3.1 positively regulates Notch signaling by promoting the cleavage and activation of Notch in response to activity in the activated synapses therefore contribute to synaptic consolidation (Fig. 1.5, both LTP and LTD). Clear evidence was shown that the proteolytic activation of Notch1 is disrupted in the Arc/Arg3.1 KO neurons both *in vivo* and *in vitro* (Alberi et al., 2011). It might explain the observed deficits of synaptic consolidation in the KO mice. Meanwhile, current evidences mainly demonstrate that Arc/Arg3.1 mediated AMPARs trafficking is essential for LTD. It has been reported that Arc/Arg3.1 expression enhances AMPARs endocytosis by interacting with endophlin 3 and dynamin 2 (Fig. 1.5). Without Arc/Arg3.1 expression, endocytosis was remarkably reduced and the level of steady state surface AMPARs was significantly increased in the Arc/Arg3.1 KO neurons (Chowdhury et al., 2006). Over-expression of Arc/Arg3.1 reduced AMPARs mediated synaptic transmission indicated by decreased amplitude of AMPAR-EPSC which further confirmed former observations (Verde et al., 2006). Later studies showed that nuclear Arc/Arg3.1 can promote expression of promyelocytic leukemia nuclear bodies (PML bodies) upon activity, which decreases GluA1 transcription (Fig. 1.5) (Korb et al., 2013). A recent study reported that the RING E3 Ligase Triad3A can ubiquitinates Arc/Arg3.1 and promote its degradation leading to increased surface AMPARs. Knock down of Triad3A results in Arc/Arg3.1 accumulation which reduces surface AMPARs (Mabb et al., 2014). Byers et al. presented further evidence for explaining Arc/Arg3.1 mediated AMPARs endocytosis. They found that Arc/Arg3.1 expression can facilitate dynamin polymerization and assembly and stabilize pre-formed dynamin 2 polymers which are important for constructing the endocytic machinery that promotes AMPARs internalization (Byers et al., 2015). Yet, so far that how Arc/Arg3.1 supports LTP and LTD is still far from being fully understood. Additional studies are needed to better understand the underlying mechanism of Arc/Arg3.1 mediated synaptic consolidation.

Homeostatic plasticity in neuroscience refers to the process that maintains stability of neuronal functions through scaling neuronal response to activity up or down. It is a compensatory mechanism for hebbian plasticity (e.g. LTP and LTD). One of the proposed mechanisms of homeostatic is synaptic scaling (Turrigiano, 2012). Arc/Arg3.1 mediates synaptic scaling of AMPARs (Shepherd et al., 2006). Specifically, chronic blockade of network activity by 2 days Tetrodotoxin (TTX, a selective sodium blocker) treatment down regulated Arc/Arg3.1 protein expression which then upregulated surface AMPARs and

increased synaptic strength in cultured wild type neurons. Conversely, over activation by 2 days Bicuculline treatment (a competitive antagonist of $GABA_A$ receptors) upregulated Arc/Arg3.1 expression leading to reduced surface AMPARs and synaptic strength. However, this up or down synaptic scaling of AMPARs upon neuronal activation or inactivation was completely abolished in cultured Arc/Arg3.1 KO neurons (Shepherd et al., 2006). Similar results were obtained when activity manipulation was performed on single synapse of KO neurons (Beique et al., 2011). These data suggest that Arc/Arg3.1 controls the level of surface AMPARs in a homeostatic manner. To directly verify the importance of Arc/Arg3.1 in homeostatic plasticity, an *in vivo* study showed Arc/Arg3.1 expression was significantly elevated in the visual cortical neurons of animals which were reared in the dark environment for 2 days compared with normal reared ones. In parallel, miniature excitatory postsynaptic current (mEPSC) amplitude was also clearly increased in the dark reared animals, indicating up scaling of synaptic strength. A down scaling effect was observed when these animals were taken into the lighted environment. Similarly with *in vitro* observation, the bidirectional scaling of synaptic strength in the visual cortex induced by light deprivation or re-exposure was also abolished in the Arc/Arg3.1 KO mice (Gao et al., 2010). For the underlying mechanism of Arc/Arg3.1 mediated synaptic scaling, Tim J. Craig et al. proposed a model based on their discovery revealing that inhibition of neuronal activity by TTX reduces the level of deSUMOylating enzyme SENP1 that in turn prevents deSUMOylation of Arc/Arg3.1 protein. SUMOlated Arc/Arg3.1 cannot bind to its interaction partners (e.g. endophilin and dynamin) to promote AMPARs endocytosis therefore upregulates surface AMPARs leading to increased synaptic strength (Craig and Henley, 2012; Craig et al., 2012).

In summary, *in vitro* and *in vivo* studies demonstrate that activity-dependent Arc/Arg3.1 expression can dynamically regulate synaptic strength and is essential for both hebbian and homeostatic plasticity which are the potential mechanisms for memory formation and consolidation.

1.3.3 Arc/Arg3.1 and memory consolidation

The role of Arc/Arg3.1 in memory consolidation has been investigated by many neuroscientists. It was first reported by John F. Guzowski et al by specifically blocking new Arc/Arg3.1 protein synthesis with local intrahippocampal infusion of antisense ODNs. They found that pretraining infusion of ODNs impaired long-term spatial memory retention 2 days after water maze training without affecting spatial learning and short-term memory (STM). Similarly, infusion of ODNs immediately after training also impaired long-term spatial memory retention. However, infusion of ODNs 8 hours after training left memory intact (Guzowski et al., 2000). These data suggest a temporal requirement for Arc/Arg3.1 expression during memory consolidation. The importance of Arc/Arg3.1 in memory consolidation was further

convinced when Arc/Arg3.1 KO mice were available. KO mice showed strong impairments in long-term novel object recognition memory, spatial memory, fear memory and conditioned taste aversion memory but no deficit was observed in short-term novel object recognition memory (10 min) and fear memory (4 hours) (Plath et al., 2006; Yamada, 2011). Not consistent with the observation from ODNs experiment, KO mice showed retarded spatial learning (Plath et al., 2006) as well as inefficient motor learning (Ren et al., 2014). To study the role of Arc/Arg3.1 in different brain areas for different forms of memory, antisense Arc/Arg3.1 ODNs were locally infused into specific regions. Inhibition of Arc/Arg3.1 synthesis in the lateral amygdala (LA) before fear conditioning did not affect fear memory acquisition and STM, but significantly impaired long-term tone memory retrieval (Ploski et al., 2008) as well as reconsolidation of fear memory (Maddox and Schafe, 2011). Intra-BLA infusion of ODNs before extinction training impaired extinction of long-term fear memory (Onoue et al., 2014). A recent report demonstrated that inhibiting late Arc/Arg3.1 expression by intra-BLA infusion of ODNs 7 hours either after conditioning or after 1 day memory retrieval test impaired memory retention 7 d, but not 2 d, after fear conditioning and memory retrieval, suggesting that late Arc/Arg3.1 expression in the BLA is essential for persistence of newly acquired and reactivated contextual fear memories (Nakayama et al., 2016). They acquired similar results when ODNs were infused into hippocampus *in vivo* (Nakayama et al., 2015). Previously published data from other labs also showed that specific knockdown of Arc/Arg3.1 pretraining in the either dorsal or ventral hippocampus dramatically impaired trace and contextual fear conditioning, but not delayed fear conditioning, a hippocampus independent paradigm (Czerniawski et al., 2011), whereas pretesting infusion of antisense Arc/Arg3.1 ODNs into ventral hippocampus had little effect on memory retrieval, but it significantly impaired the subsequent memory retrieval tests which underwent a reconsolidation process (Chia and Otto, 2013). In addition, posttraining disruption of Arc/Arg3.1 expression in the anterior cingulate cortex (ACC) either immediately or 6 hours after training impaired long-term fear memory, while inhibition of Arc/Arg3.1 expression 3 hour before test did not affect memory retrieval (Holloway and McIntyre, 2011). All of the data summarized above converge to a consensus that Arc/Arg3.1 is essential for different forms of memory consolidation and reconsolidation. Arc/Arg3.1 expression in specific region may support specific memory.

1.4 Brain rhythmic activity in learning and memory

Our brain is always constantly running during day and night to process all of our acquired experiences. Especially during sleep, newly acquired information can be consolidated for long-term storage (Inostroza and Born, 2013). Information processing is closely correlated with vary rhythmic activities in the brain. Brain rhythms are periodically fluctuating waves of neuronal activity. They are not reflections of activity from individual neurons, but are reflections of synchronized activity of a population of neurons (Colgin, 2016).

Depending on the frequencies, three major types of rhythms are defined: theta rhythm, gamma rhythm, sharp waves-ripples complexes. These rhythmic activities can be detected and visualized by using local field potential (LFP) recordings during particular behaviors (Fig. 1.6). Different rhythms play distinct roles in memory related information processing.

1.4.1 Theta rhythms

Theta rhythms (Fig. 1.6) are neuronal activity in low frequency (~4-12 Hz). It usually occurs during active exploration and rapid eye movement (REM) sleep (Jouvet, 1969; Vanderwolf, 1969; Colgin, 2013) but are normally absent during immobility. Theta waves can be regularly observed in the *stratum lacunosum-moleculare layer* of hippocampal *cornus ammonis* (CA1) region. It can also be detected in the CA3 and dentate gyrus and other cortical regions, such as entorhinal cortex, prefrontal cortex, and amygdala (Buzsaki, 2002). However, these structures cannot generate theta waves by themselves. Several Subcortical nuclei have been identified to be essential for theta oscillation generation. The main generator and pacemaker is the medial septum-diagonal band of Broca (MS-DBB). Its involvement in theta generation was confirmed by the experiments that lesions or inactivation of MS-DBB neurons completely blocked theta activity (Stumpf et al., 1962; Stewart and Fox, 1990), while optogenetic activation of septal neurons drive or modulate hippocampal theta rhythms (Vandecasteele et al., 2014; Robinson et al., 2016). Functionally, theta oscillation is thought to represent the “on-line” state of the hippocampus and is believed to be critical for modulating synaptic strength and thereby for spatiotemporal coding of memory engrams (Buzsaki, 2002). Actually, theta-burst stimulation (TBS) has been used as an optimal protocol to induce LTP in hippocampal synapses and is believed to mimic the physiological situation (Larson and Lynch, 1986; Greenstein et al., 1988).

Eventually, theta oscillations are important for the performance during learning and memory process. Experiments have shown that theta oscillation inhibition by septum lesion reduced rats learning ability and let to spatial memory deficits (Winson, 1978) as well as reduced fear acquisition rate in classical conditionings (Berry and Seager, 2001). Especially, theta activity in the hippocampus is important for spatial navigation (Buzsaki, 2005) and is positively correlated with rats performance in Morris water maze task (Olvera-Cortes et al., 2002).

Furthermore, scientists propose that spatial representation is defined by theta sequence which is an ordered series of spikes generated by hippocampal place cells within individual theta cycles. Sufficient theta sequence could facilitate learning and memory formation (Colgin, 2016). All of the evidence mentioned above for the physiological functions of theta rhythms was obtained in behaving animals.

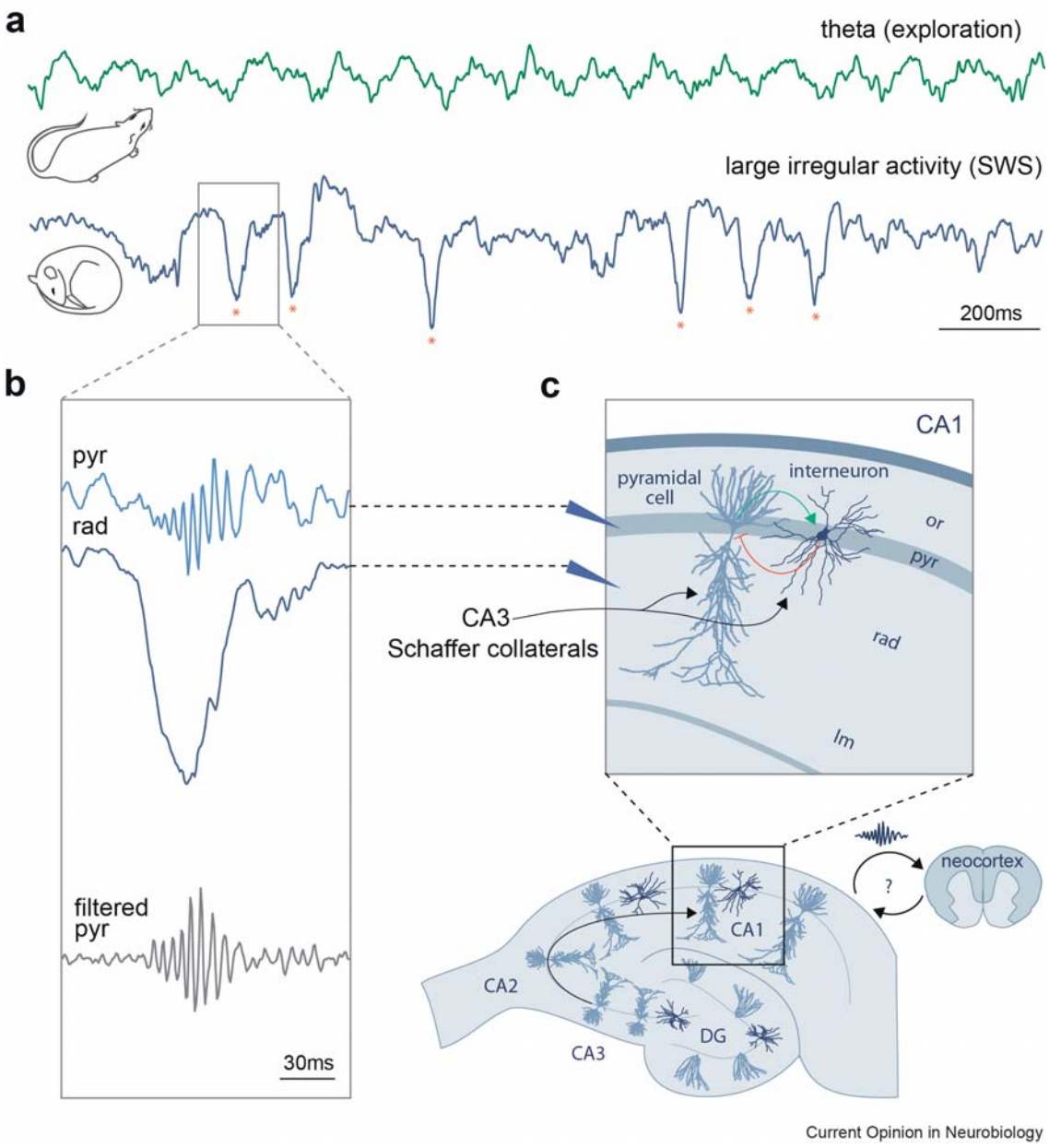

Fig. 1.6 Hippocampal rhythmic activities during exploration and rest/sleep. a, Theta rhythm appears during exploration, and is replaced by large irregular activity characterized by the occurrence of sharp wave events (red stars) during sleep and quiet wakefulness. **b,** Sharp wave recorded in *stratum radiatum* (rad) co-occurs with high frequency ripple oscillation in *stratum pyramidale* (pyr). **c,** Sharp waves reflect massive excitation of CA1 neurons triggered by CA3 pyramidal cells via the Schaffer collaterals. The interneuron network is synchronized at ~200 Hz that generates a ripple in the *pyramidal layer* (or: stratum oriens, lm: stratum lacunosum moleculare, CA1–3: cornu ammonis 1 and 3, DG: dentate gyrus).［Adapted from (Girardeau and Zugaro, 2011)］

However, theta rhythms are also observed in the hippocampus and cortical structures of mice and rats during REM sleep with a prominent frequency around 7 Hz. Unfortunately scientists have not yet reached a consensus about whether theta oscillations generated during REM sleep are also necessary for learning and memory. A recently published study presented a direct causality between theta activity and memory consolidation by optogeneticly silencing GABAergic neurons in the medial septum (MS). They found that

during a critical window of REM sleep after learning, silencing MS GABAergic neurons erased novel object recognition and impaired contextual fear memory, while no effect was observed on memory when silencing was performed outside REM sleep episodes, indicating that theta activity during REM sleep also plays a critical role in memory consolidation (Boyce et al., 2016).

1.4.2 Gamma rhythms

Gamma rhythms are neuronal oscillations with a broad range of frequency (~25-100 Hz). Gamma activity also can be detected in hippocampus and prefrontal cortex and some other brain regions of animals during a variety of behaviors (Csicsvari et al., 2003; Kay, 2003; van der Meer and Redish, 2009). They show lower amplitude than that of the co-occurring theta waves. Two distinct subtypes of gamma rhythms, termed “slow gamma” with frequency from 25 Hz to 55 Hz and “fast gamma” with frequency from 60 Hz to 100 Hz are categorized in the hippocampus. In hippocampal CA1, slow gamma activity is coupled by the activity inputs from CA3, while fast gamma is entrained by activity inputs from medial entorhinal cortex (MEC) (Colgin et al., 2009; Schomburg et al., 2014). Moreover, different gamma frequencies appear in different layers of CA1. Slow gamma activity mainly is detected in *stratum radiatum,* whereas fast gamma occurs mainly in *stratum lacunosum-moleculare layer* (Schomburg et al., 2014). It was hypothesized that slow and fast gamma play different role in information processing, but there is no consensus so far as a result of lacking sufficient experimental data accumulation. Some studies tend to support the hypothesis that slow gamma promotes memory retrieval and fast gamma encodes sensory information transmitted from the MEC to hippocampus. Meanwhile, some observations from other studies are against this hypothesis (Colgin, 2016). This hypothesis is yet to be tested with more direct evidence in the future. Even though there is no solid answer about the relation between gamma activity and memory, there is a theoretical support for the role of gamma rhythms played in synaptic plasticity, here referred to STDP. STDP relies on the occurrence of presynaptic firing in a restricted time course with postsynaptic depolarization (Bi and Poo, 1998). Presynaptic firing release glutamate and then glutamates bind to NMDARs within about 20 ms, while the postsynaptic depolarization occurs very fast within 1 ms. Gamma frequency is from 25 to 100 Hz, and the interval between two cycles is between 10 ms and 40 ms. Put together, it suggests that the input pattern of gamma rhythms shares the exact timing parameter which is necessary for STDP and thereby implies a potential role for gamma oscillation in learning and memory (Axmacher et al., 2006; Nyhus and Curran, 2010).

1.4.3 Sharp wave ripples

Sharp waves (SPWs, Fig. 1.6) are negative polarity deflections with large amplitudes and irregular occurrence patterns observed during LFP recordings (O'Keefe, 1976; Buzsaki,

2015). SPWs are generated mainly in the *stratum radiatum layer* of hippocampal CA1. They reflect massive excitation of CA1 cells evoked by activities received via the Schafer collaterals from CA3 cells. SPWs are very often associated with high frequency oscillations, termed “ripples” (with filtered band between 150 Hz and 250 Hz) that are detected in the CA1 *pyramidal layer*. Ripples are generated by concomitant synchronization of inhibition from activated interneurons in CA1 and strong excitation from CA3. SPWs and coupled ripples form the sharp wave-ripples complex (SPW-Rs). SPW-Rs can occur during slow-wave sleep (SWS) and nonexploratory wake states or immobility, such as drinking, eating, grooming and quiet wakefulness (Buzsaki et al., 1992; Girardeau and Zugaro, 2011; Buzsaki, 2015).

About the function of SPW-Rs, it is mainly hypothesized that SPW-Rs involve off-line memory consolidation process. The dominant scenario is that reactivation of neuronal ensembles encoding experiences acquired during wake state (a process called “neuronal replay”) by ripples trigger synaptic modifications in downstream neurons which then help to stabilize, enhance and reorganize acquired memory information. Some indirect and direct evidences have been discovered to support this scenario. First, the ripple frequency is around 200 Hz which is an ideal frequency to induce synaptic plasticity, such as LTP and STDP in the connected cortical regions with CA1 (e.g. PFC and RSC). These forms of plasticity have been consistently shown to closely correlate with certain types of learning and memory (Pastalkova et al., 2006; Whitlock et al., 2006). Second, studies showed that the exploration evoked spike sequences of place cells are frequently replayed mainly during SPW-Rs occurrence. The same order of spike sequence was maintained but was temporally compressed (Skaggs and McNaughton, 1996; Nadasdy et al., 1999; Lee and Wilson, 2002). A very recent study combing functional magnetic resonance (fMRI) imaging with *in vivo* ripple recordings in the hippocampus of monkeys demonstrated that ripple-associated activities in the hippocampus help to establish functional connections for acquired information processing within the default mode network (DMN), including parietal, prefrontal and medial temporal lobe. Neuronal reply in the hippocampus can thus promote neuronal reactivation in the other areas of DMN with plastic synaptic modification for memory consolidation (Kaplan et al., 2016; Walker and Robertson, 2016). Finally, Gabrielle Girardeau et al. (2009) presented the first direct evidence for the causal link between hippocampal ripples and memory consolidation. Specifically, selective suppression of online-detected SPW-Rs by applying electrical stimulation to ventral hippocampal commissural during posttraining rest and sleep apparently reduced rats’ performance in a food-rewarded eight arms radial maze, a hippocampus dependent spatial memory task, indicating impaired memory consolidation (Girardeau et al., 2009). After that, Ego-Stengel and Wilson (2010) also reported that disruption of neural activity during ripple events after control spatial training decreased leaning ability in the following training trials, suggesting impairments in spatial learning (Ego-

Stengel and Wilson, 2010). In general, SPW-Rs are important for spatial learning and memory consolidation. Additionally, there are some evidences implying that SPW-Rs might also involve memory transferring process from hippocampus to the neocortical regions by coordinately interacting with neocortical sleep rhythms, such as slow oscillation and neocortical spindles (Siapas and Wilson, 1998; Sirota et al., 2003) which are also thought to involve learning and memory (Marshall et al., 2006). However, there is still no direct evidence so far to proof the essential role of SPW-Rs in memory transferring.

1.5 Cre-loxP system

Cre-loxP recombination system was initially developed by Dr. Brian Sauer for activating gene expression in mammalian cell lines (Sauer, 1987; Sauer and Henderson, 1988). It is a site-specific recombination system which includes an enzyme, Cre recombinase and paired LoxP sequences. The Cre recombinase protein can recognize the inserted LoxP sites in the target genome and recombines them and thereby delete the foxed gene or activate specific gene expression by removal of floxed stop sequence. During the last decade, it has been widely used as gene targeting approach for studying gene function in mice. By expressing Cre recombinase driven under specific promoter, genomic DNA modification can be achieved in specific cell types, such as CaMKII promoter driving Cre expression to modify gene expression in principal neurons or parvalbumin (PV) promoter driving Cre expression to manipulate gene expression in PV positive interneurons (Tsien et al., 1996; Ito-Ishida et al., 2015; Rudenko et al., 2015; Tang et al., 2015) or can be triggered by chemicals (such as tamoxifen or doxcycline) at specific time points dependent on when the chemicals are applied (Erdmann et al., 2007). Therefore, this system allows researchers to manipulate gene expression in a spatiotemporally controlled way. It is especially useful for helping neuroscientists to explore the roles of specific genes in different cell types for brain cognitive functions and behaviors (McHugh et al., 1996; Rondi-Reig et al., 2001; Nakazawa et al., 2002; Nakazawa et al., 2003; Monteggia et al., 2004; Chen et al., 2010; Kim et al., 2014; Bacon et al., 2015).

1.6 Aims of the study

Previously published data collected from Arc/Arg3.1 KO mice demonstrate that Arc/Arg3.1 is essential for synaptic and memory consolidation. However, how postnatal Arc/Arg3.1expression contributes to learning and memory, and whether memory consolidation needs lifelong Arc/Arg3.1 expression during adulthood remains unclear. Moreover, it is also not well known that what is the specific role of Arc/Arg3.1 mediated synaptic plasticity in different brain regions for memory consolidation. Therefore, the main aim of this study is to investigate the contributions of spatiotemporal Arc/Arg3.1 expression to learning and memory consolidation.

Specific aims are:

1. To study the dependence of learning and explicit memory consolidation on Arc/Arg3.1 expression during early and late postnatal development.
2. To explore the role of Arc/Arg3.1 played in synaptic plasticity and oscillatory activity during early and late postnatal development.
3. To investigate whether and how Arc/Arg3.1 expression in specific brain regions of adult mice affect memory consolidation, and to further reveal the process of system memory consolidation by employing Arc/Arg3.1 as a molecular tool.
4. To uncover whether explicit and implicit memory consolidation similarly rely on spatiotemporal Arc/Arg3.1 expression.

2 Results

Part I Generation and verification of Arc/Arg3.1 mutants

2.1 Temporal expression of Arc/Arg3.1 mRNA in young wild type mice

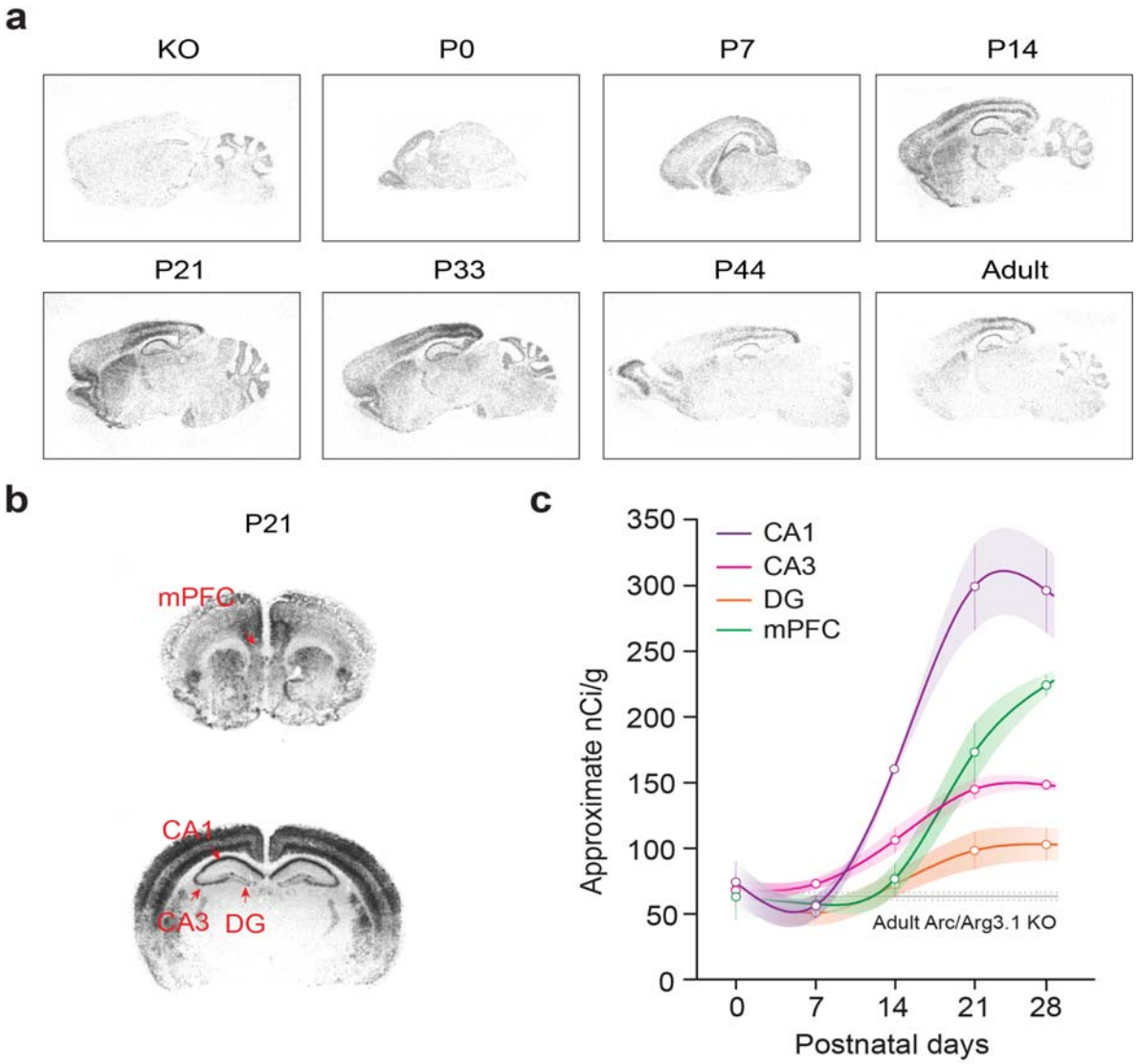

Fig. 2.1 Arc/Arg3.1 mRNA expression during postnatal development. a, Baseline level of Arc/Arg3.1 mRNA in the brain is low at birth and in adulthood but is strongly upregulated between the second and fourth postnatal week. **b,** Strong up-regulation is observed in mnemonic structures such as the dorsal hippocampus and the mPFC. (a-b) rISH on sagittal/coronal sections of WT brains, KO as negative control. **c,** Spatiotemporal profiles of Arc/Arg3.1 expression during development. Sections from WT brains (n = 3) were subjected to rISH, converted to a radioactive scale and averaged (circles represent means ± SEM). Shaded lines represent polynomial interpolation of the 5 time points and their SEM values.

I first investigated the spatiotemporal pattern of Arc/Arg3.1 expression in the brains of young wild type (WT) mice. Across the cerebrum, Arc/Arg3.1 mRNA was detectable starting at P7, increased dramatically between P14 and P33 and subsequently decreased to a lower baseline level in adulthood (Fig. 2.1a). The spatial pattern of Arc/Arg3.1 mRNA expression was highly heterogeneous with some regions strongly upregulated while others only weakly or not at all. The hippocampus and mPFC, two major mnemonic regions, exhibited strong up-regulation (Fig. 2.1b), but differed in their temporal expression pattern. Up-regulation started

earlier in the hippocampus, especially in the CA1 and CA3, and was later in the mPFC (Fig. 2.1c). The strong spatiotemporal expression pattern of Arc/Arg3.1 in the mPFC and in areas CA1 and CA3 of the hippocampus suggests a role for Arc/Arg3.1 in the development of these two mnemonic regions.

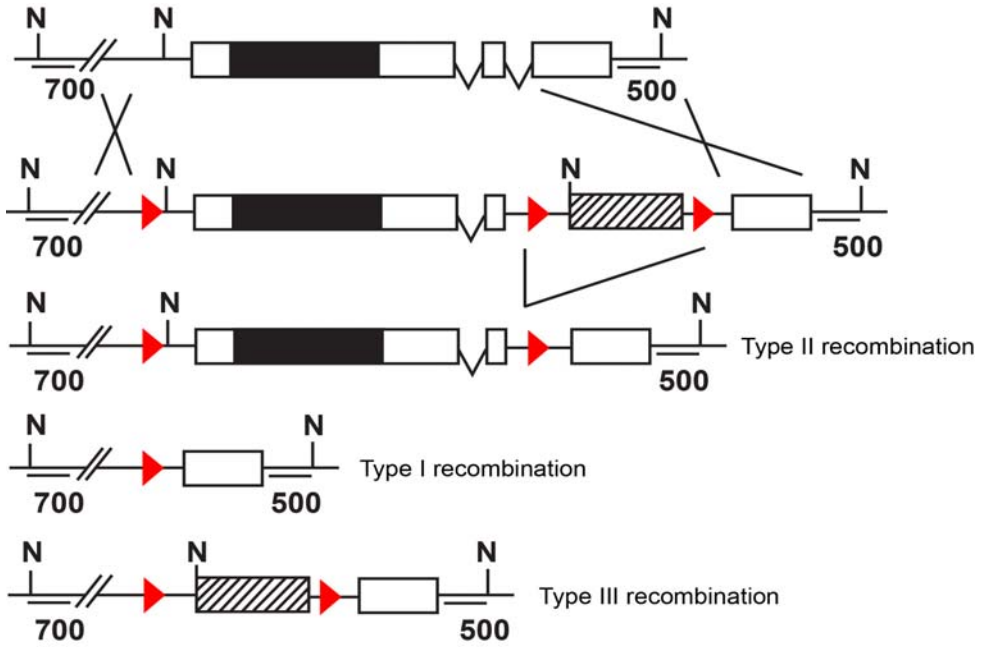

Fig. 2.2 Scheme of Arc/Arg3.1$^{f/f}$ mice generation. Arc/Arg3.1 ORF was flanked by inserting a loxP site at position -1720. A neomycin resistance cassette, flanked by two loxP sites, was inserted at position +2690 into the second intron. Positive clones were identified by Southern blot analysis and one targeted ES cell clone was transiently transfected with Cre recombinase. A type II recombination clone was injected into C57Bl/6J blastocytes. Male chimeras were backcrossed into C57Bl/6J. Top: Arc/Arg3.1 gene locus (N, NheI restriction sites; open boxes, exons; black box, ORF; horizontal lines, homology regions used in targeting construct; 500, 700, Southern blot probes). Middle: Floxed genes locus (triangles, loxP sites; hatched box, neomycin-resistance cassette). Bottom: Floxed Arc/Arg3.1 conditional mutants following Cre-mediated type II recombination; Arc/Arg3.1 KO mutants following Cre-mediated type I recombination, Arc/Arg3.1 KO mutants with neomycin cassette following Cre recombinase mediated type III recombination. (Lab resource of Dietmar Kuhl)

2.2 Generation and verification of Arc/Arg3.1$^{f/f}$ mice

Conventional Arc/Arg3.1 KO mice were previously generated in our laboratory and previous findings revealed that Arc/Arg3.1 is essential for memory consolidation and for maintenance of long-term synaptic plasticity in the hippocampus (Plath et al., 2006). However, the constitutive absence of Arg3.1 in these mice prevented examination of possible roles of Arc/Arg3.1 during early brain development and its distinction from lifelong support of memory consolidation. Moreover, the complete removal of Arc/Arg3.1 precluded revealing the precise identity of brain regions involved in memory consolidation and Arc/Arg3.1 mediated synaptic plasticity. In this project I proposed to dissect the spatiotemporal contribution of Arc/Arg3.1 to learning and memory by genetically ablating Arc/Arg3.1 in a

time or location specific manner. To do so, former colleagues from the lab of Dietmar Kuhl generated a line of conditional LoxP floxed Arc/Arg3.1 mice. By crossing Arc/Arg3.1 floxed mice with Cre transgenic mice in which Cre expression is driven by either CMV or CaMKIIα promoter, I could remove Arc/Arg3.1 either pre- or postnatally. Similarly, I could locally excise Arc/Arg3.1 in selected brain regions, by stereotactic injections of Cre-carrying viral vectors.

2.2.1 Generation of Arc/Arg3.1$^{f/f}$ mice

A floxed Arc/Arg3.1 mouse line (Arc/Arg3.1$^{f/f}$, Fig. 2.2) was generated in which the Arc/Arg3.1 ORF was flanked by two loxP sites. A type II recombination clone was selected after a transient transfection with a vector harboring Cre recombinase. Selected clones were injected into C57bl/6J blastocytes and male chimeras were backcrossed into C57bl/6J for at least ten generations (Dammermann, 1999; Bick-Sander, 2002; Plath et al., 2006). Arc/Arg3.1$^{f/f}$ mice are vital, breed normally according to the Mendelian law, and reach the same age and body weight as their wild type littermates.

2.2.2 Spatiotemporal expression of Arc/Arg3.1 in Arc/Arg3.1$^{f/f}$ mice

To examine whether the genetic modification of the Arc/Arg3.1 locus might have affected the gross brain morphology and layering, Nissl staining was conducted on coronal brain sections. Sections obtained from Arc/Arg3.1$^{f/f}$ mice and their WT littermates (Fig. 2.3a) were similar in layering and cellular density. Since a loxP site was inserted within the Arc/Arg3.1 promoter region upstream of the transcription starting site, it could, in theory, affect the spatiotemporal expression of Arc/Arg3.1.

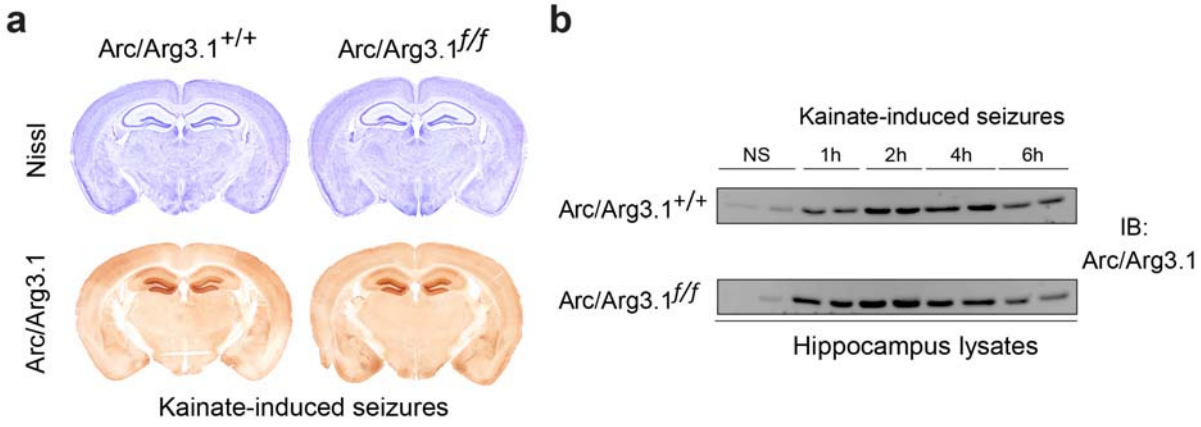

2.3 Spatiotemporal expression of Arc/Arg3.1$^{f/f}$ mice. a, Nissl staining indicated normal brain morphology and layering of Arc/Arg3.1$^{f/f}$ mice. Immunostaining analysis of Arc/Arg3.1 protein displayed similar spatial expression pattern and dendritic localization in the hippocampus of Arc/Arg3.1$^{+/+}$ and Arc/Arg3.1$^{f/f}$ mice after Kainate-induced seizures. **b,** Western blots analysis of Arc/Arg3.1 protein from hippocampal lysates showed similar temporal expression pattern under control conditions and 1, 2, 4, and 6 hours after Kainate-induced seizures in the Arc/Arg3.1$^{+/+}$ and Arc/Arg3.1$^{f/f}$ mice.

To test this possibility, immunohistochemistry (IHC) and western blots were performed after Kainate-induced seizures. Arc/Arg3.1 expression levels and dendritic localization pattern in the hippocampus were similar in WT and Arc/Arg3.1$^{f/f}$ mice (Fig. 2.3a). Spatial expression pattern in the brain was likewise similar. As in WT mice, Arc/Arg3.1 was induced within 1 hour after seizure onset, peaked around 2 hours and decayed within 6 hours in the Arc/Arg3.1$^{f/f}$ mice (Fig. 2.3b). There were no detectable alterations in the spatiotemporal expression pattern and levels of Arc/Arg3.1 in the Arc/Arg3.1$^{f/f}$ mice, confirming that the integrated loxP sites did not interfere with Arc/Arg3.1 gene expression.

2.2.3 Exploratory, anxiety-like behaviors and risk assessment ability in Arc/Arg3.1$^{f/f}$ mice

Exploration can drive Arc/Arg3.1 expression and conversely, genetic modification of Arc/Arg3.1 gene locus might also affect exploratory behaviors. I therefore examined Arc/Arg3.1$^{f/f}$ mice in an open field arena (Fig. 2.4a), where they were allowed to explore for 10 min. Both WT and Arc/Arg3.1$^{f/f}$ mice displayed similar degree of anxiety, indicated by the percent time spent in the center of the arena (Fig. 2.4b). Comparable path length and movement velocity between WT and Arc/Arg3.1$^{f/f}$ mice indicated intact locomotion and exploratory drive in the latter (Fig. 2.4c-d).

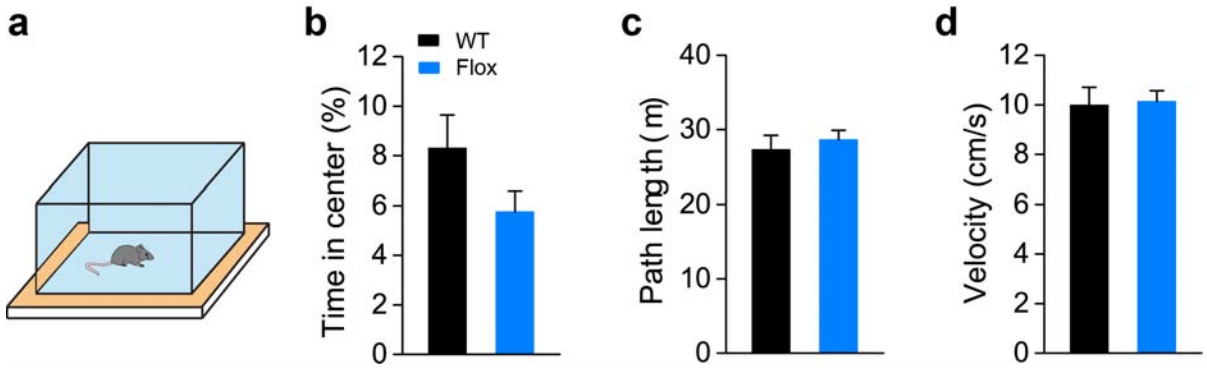

Fig. 2.4 Locomotion activity and exploratory behavior in Arc/Arg3.1$^{f/f}$ mice. a-d, Locomotion and exploratory activity in the open field test (**a**) was similar for WT and Arc/Arg3.1$^{f/f}$ mice. **b,** percent time spent in the center: WT, 8.30 ± 1.34%; Arc/Arg3.1$^{f/f}$, 5.75 ± 0.84%; t_{22} = 1.62, p = 0.12, NS; **c,** path length; WT, 27.31 ± 1.92 m; Arc/Arg3.1$^{f/f}$, 28.63 ± 1.28 m; t_{22} = -0.57, p = 0.57, NS; **d,** velocity; WT, 9.98 ± 0.73 cm/s; Arc/Arg3.1$^{f/f}$, 10.13 ± 0.44 cm/s; t_{22} = - 0.18, p = 0.86, NS; n = 12 per group. All error bars show mean ± S.E.M. Two sample t-tests were performed between genotypes.

Mice were additionally tested in the elevated zero maze (Fig. 2.5a), a more precise behavioral paradigm for assessing innate anxiety-like behavior and risk assessment ability. Arc/Arg3.1$^{f/f}$ mice spent similar amount of time in the open arms of the maze (Fig. 2.5b) and entered the open arms as frequently as WT littermates (Fig. 2.5c).

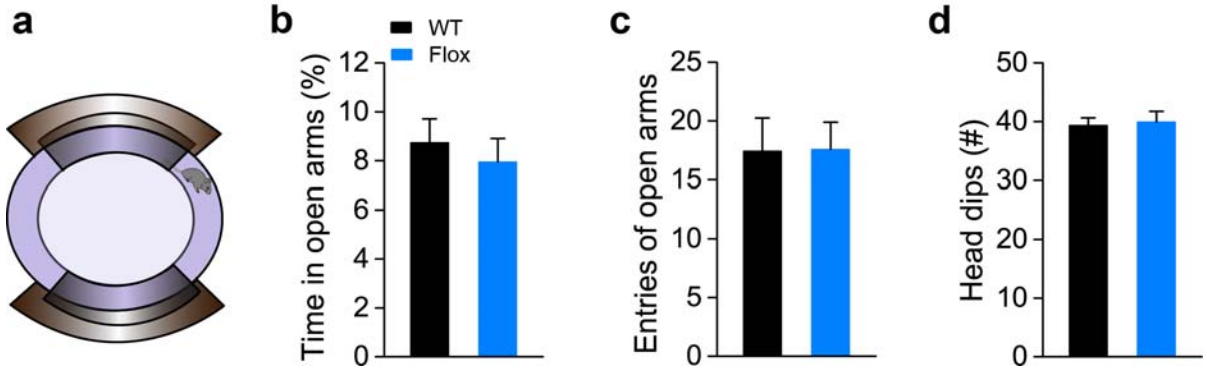

Fig. 2.5 Anxiety-like behavior and risk assessment ability in Arc/Arg3.1$^{f/f}$ mice. a-c, Anxiety-like behavior and risk assessment in the elevated zero maze (**a**) were similar for WT and Arc/Arg3.1$^{f/f}$ mice. **b,** percent time spent in the open arms: WT, 8.74 ± 0.97%, Arc/Arg3.1$^{f/f}$, 7.95 ± 0.96%; t_{22} = 0.57, p = 0.57, NS; **c,** entries of open arms: WT, 17.42 ± 2.83; Arc/Arg3.1$^{f/f}$, 17.58 ± 2.32; t_{22} =-0.05, p = 0.96, NS; **d,** number of head dips beyond the open arms edges: WT, 39.33 ± 1.30; Arc/Arg3.1$^{f/f}$ 39.92 ± 1.82, t_{22} = -0.26, p = 0.80, NS; n = 12 per group). All error bars show ± S.E.M. Two sample t-tests were performed between genotypes.

In summary, Arc/Arg3.1$^{f/f}$ mice displayed exploratory activity and anxiety-like behavior that were indistinguishable from WT mice. Similarly, risk assessment of Arc/Arg3.1$^{f/f}$ mice was identical to their WT littermates, judged by the similar number of head dips beyond the open arms edges (Fig. 2.5d).

2.2.4 Pain sensitivity and fear memory capacity of Arc/Arg3.1$^{f/f}$ mice

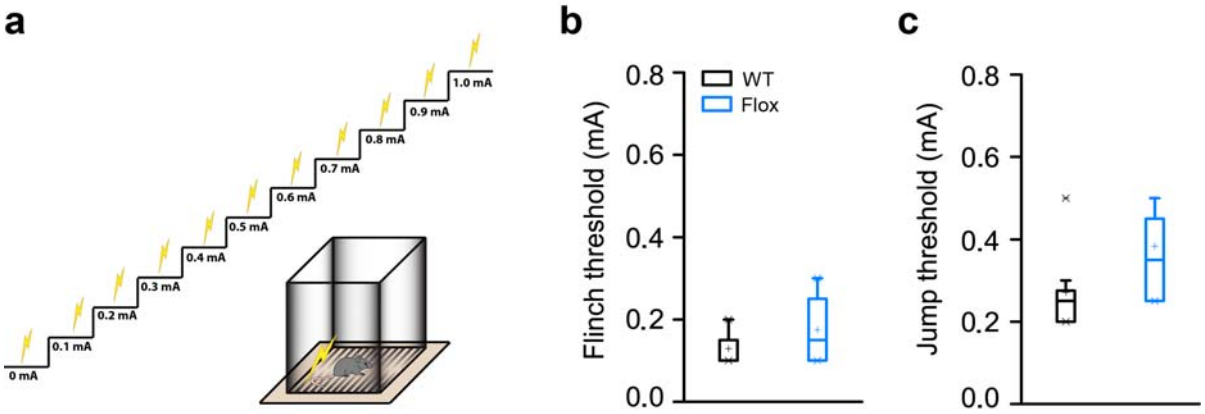

Fig. 2.6 Pain sensitivity in Arc/Arg3.1$^{f/f}$ mice. a, Sensitivity to the electrical shock thresholds (mA) to elicit stereotypic responses were measured for WT and Arc/Arg3.1$^{f/f}$ mice with a flinch-jump test. No difference was found in the first flinch (**b,** median in mA: WT, 0.10; Arc/Arg3.1$^{f/f}$, 0.15; U = 45.50, p = 0.11, NS) or first jump (**c,** Median in mA: WT, 0.25; Arc/Arg3.1$^{f/f}$, 0.35; U = 41.00, p = 0.07, NS; WT, n = 12; Arc/Arg3.1$^{f/f}$, n = 12). Box plots show median (-), 25th and 75th percentiles, mean (+) and outliers (×). Mann-Whitney test was performed between genotypes.

A central memory test in this study is fear conditioning in which mice learn to associate an environment or tone with pain sensation induced by mild electrical shocks. To make sure

that Arc/Arg3.1$^{f/f}$ mice had intact pain sensitivity, a flinch-jump test (Fig. 2.6a) was performed in the Multi-Conditioning System (TSE Systems). During this test, a train of consecutive 0.5 s long foot shocks was administered stepwise from 0.1 mA to 1.0 mA in steps of 0.1 mA. Shocks were separated by 30 s intervals. The lowest shock intensity eliciting flinch and/or jump was considered as threshold value. The threshold to first flinch was around 0.1 mA and 0.15 mA for WT and Arc/Arg3.1$^{f/f}$ mice, respectively. Slightly higher currents evoked jump response in all mice. The median value of jump threshold was 0.25 mA for WT and 0.35 mA for Arc/Arg3.1$^{f/f}$ mice. No significant difference was observed between WT and Arc/Arg3.1$^{f/f}$ mice neither for the flinch threshold (Fig. 2.6b) nor for the jump threshold (Fig. 2.6c).

Next, I tested Arc/Arg3.1$^{f/f}$ mice in contextual fear conditioning (Fig. 2.7a). Following conditioning, fear memory was assessed at different time points to evaluate memory persistence. Arc/Arg3.1$^{f/f}$ mice acquired fear memory as well as WT mice and maintained it for 4 weeks, a time at which it is considered as remote memory (Fig. 2.7b-d).

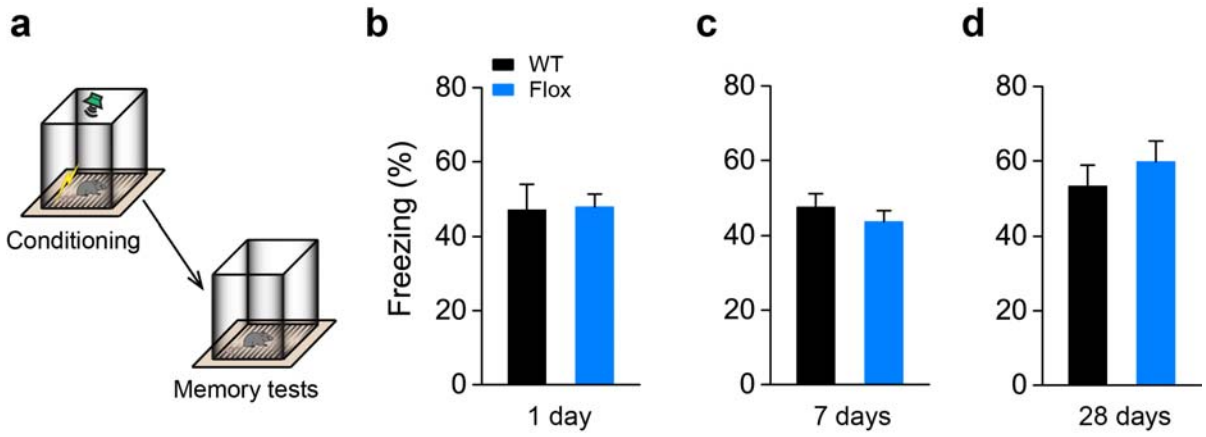

Fig. 2.7 Contextual fear memory in Arc/Arg3.1$^{f/f}$ mice. a-d, Long-term and remote memory of contextual fear was comparable in WT and Arc/Arg3.1$^{f/f}$ mice in the contextual fear conditioning test (**a**) (**b,** 1 day; WT, 47.01 ± 6.92%; Arc/Arg3.1$^{f/f}$, 47.81 ± 3.45%; t_{10} = -0.10, p = 0.92, NS; WT, n = 6; Arc/Arg3.1$^{f/f}$, n = 6; **c,** 7 days; WT, 47.45 ± 3.63%; Arc/Arg3.1$^{f/f}$, 43.49 ± 3.05%; t_{10} = 0.83, p = 0.42, NS; WT, n = 6; Arc/Arg3.1$^{f/f}$, n = 6; **d,** 28 days; WT, 53.26 ± 5.63%; Arc/Arg3.1$^{f/f}$, 59.84 ± 5.51%; t_{10} = -0.84, p = 0.42, NS; WT, n = 6; Arc/Arg3.1$^{f/f}$, n = 6). All error bars show ± S.E.M. Two sample t-tests were performed between genotypes.

Taken together, I conclude that insertion of loxP sites in the Arc/Arg3.1 locus did not change pain sensitivity, exploration, general anxiety and memory capacity in the Arc/Arg3.1$^{f/f}$ mice.

2.3 Generation and verification of Arc/Arg3.1 KO and Late-cKO mice

To dissect the contribution of temporal Arc/Arg3.1 expression to learning and memory, and especially to study the role of Arc/Arg3.1 during postnatal development, Arc/Arg3.1 was

ablated either pre- or postnatally by crossing Arc/Arg3.1 floxed mice with Cre transgenic mice in which Cre expression was driven by time restricted promoters.

2.3.1 Generation of Arc/Arg3.1 KO and Late-cKO mice

To generate postnatal Arc/Arg3.1 conditional KO mice, I bred Arc/Arg3.1$^{f/f}$ mice with CaMKIIα-Cre mice (Tsien et al., 1996) starting to express Cre recombinase postnatally. I termed the resulting offspring (progeny) "Late-cKO" (Fig. 2.8a-b). For comparison, I also generated complete KO mice in which Arc/Arg3.1 was removed in the germ line using a CMV-Cre transgenic strategy (Schwenk et al., 1995). To test Cre activity and successful Cre mediated Arc/Arg3.1 ablation, I crossed Late-cKO mice with ROSA26-LacZ reporter mice (Soriano, 1999) and detected β-Gal activity and Arc/Arg3.1 mRNA expression, in parallel.

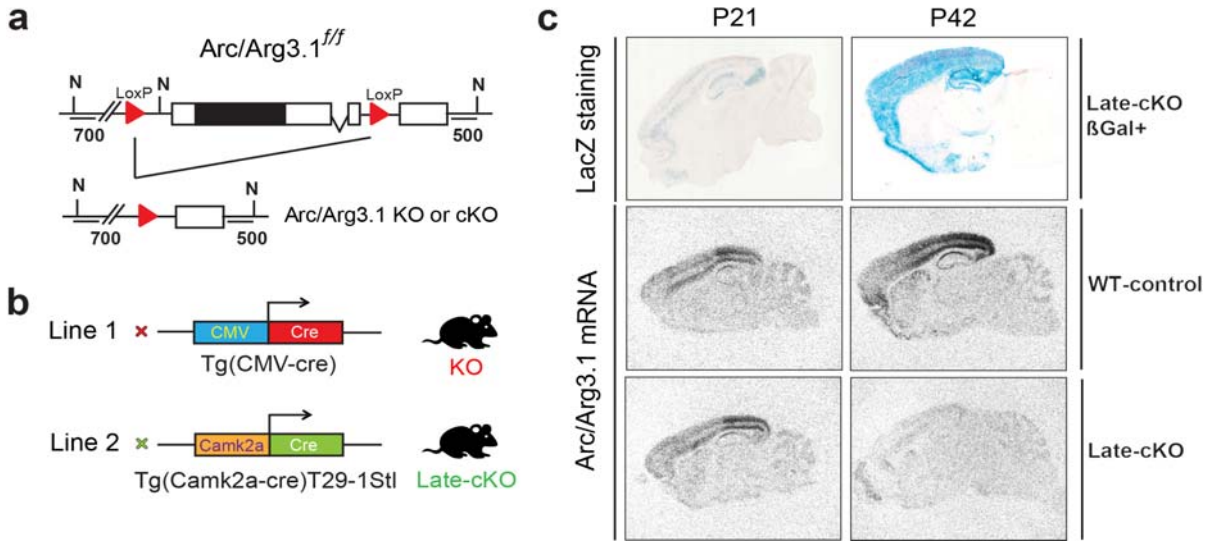

Fig. 2.8 Generation of Arc/Arg3.1 KO and Late-cKO mice. a-b, Arc/Arg3.1$^{f/f}$ mice were bred with Cre transgenic lines to generate constitutive (red) KO and Late-postnatal Arc/Arg3.1 conditional KO (Late-cKO, green) progeny. **c,** Cre transgenic mouse was crossed with a R26R reporter line. LacZ staining of brain sections indicated that Cre activity was detectable starting from P21 and peaked around P42. rISH showed that ablation of Arc/Arg3.1 takes place between P21 and P42 in the Late-cKO mice.

Brains from neonatal Late-cKO mice were extracted at different time points during development. LacZ staining revealed that Cre expression driven by CaMKIIα promoter (8.5kb) started around P21 in the forebrain (Tsien et al., 1996). At this time Arc/Arg3.1 was already broadly expressed in the brain, at levels comparable to Cre- mice, suggesting that Cre activity was still too low to remove Arc/Arg3.1. However, 42 days after birth, Cre activity was increased, and Arc/Arg3.1 mRNA was clearly reduced in the cortex and hippocampus (Fig. 2.8c). Between P21 and P42 Cre activity increased and consequently Arc/Arg3.1 ablation intensified.

2.3.2 Arc/Arg3.1 expression in adult KO and Late-cKO mice

Next, I checked the spatial expression pattern of Arc/Arg3.1 in adult KO and Late-cKO mice after Kainate-induced seizures. Radioactive *in situ* hybridization (rISH) and immunohistochemistry (IHC) were performed on coronal slices (Fig. 2.9).

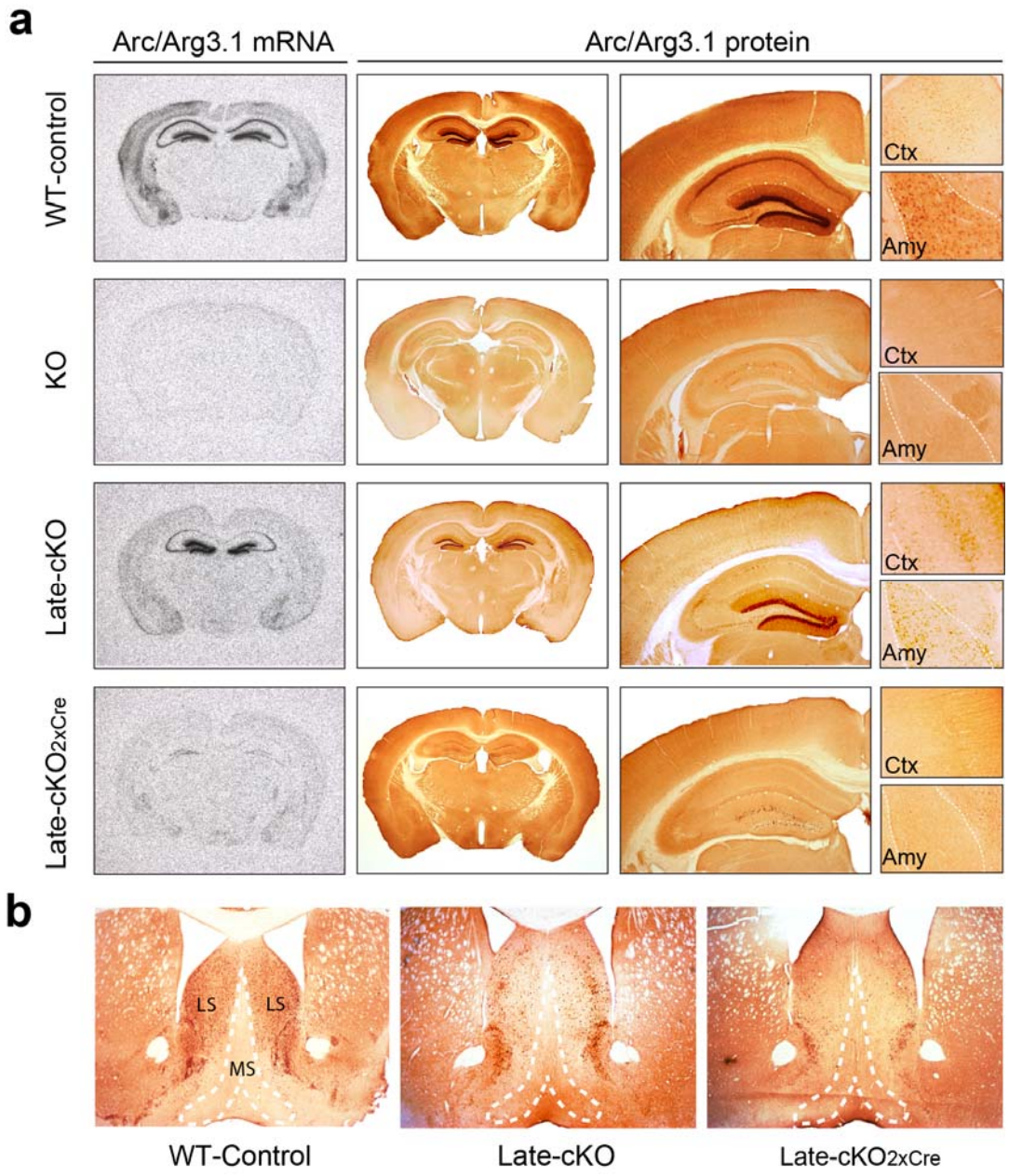

Fig. 2.9 Arc/Arg3.1 expression in the adult constitutive KO and Late-cKO mice. a, Spatial pattern of Arc/Arg3.1 expression shows complete ablation in adult KO brain, but residual Arc/Arg3.1 in the DG of Late-cKO mice which is further reduced in the homozygous Late-cKO$_{2xCre}$ mouse indicated by rISH and immunohistochemistry. **b,** Arc/Arg3.1 was not expressed in the medial septum. Residual Arc/Arg3.1 was observed in the lateral septum of Late-cKO mice, and was further ablated in the Late-cKO$_{2xCre}$. Ctx, cortex; Amy, amygdala; LS, lateral septum; MS, medial septum.

Arc/Arg3.1 mRNA and protein were strongly induced in the cortex, hippocampus, amygdala and lateral septum of WT-control mice 2 hours after Kainate-induced seizures.

Surprisingly, Arc/Arg3.1 protein was not expressed in the medial septum at least after seizure induction (Fig. 2.9b). Arc/Arg3.1 mRNA and protein were eliminated in the entire brain of adult KO mice. There was no detectable Arc/Arg3.1 mRNA and protein in the adult KO mice. In Late-cKO mice Arc/Arg3.1 mRNA and protein were also dramatically reduced in the cortex, amygdala complex and hippocampal CA1, but was not completely removed. A relatively high amount of Arc/Arg3.1 was still present in the DG and CA3 regions of the hippocampus (Fig. 2.9a). Some residual Arc/Arg3.1 was also observed in the lateral septum (Fig. 2.9b). In order to achieve stronger ablation of Arc/Arg3.1 in the Late-cKO mice, mice were bred to homozygosity of Cre recombinase. The offspring were termed "Late-cKO$_{2xCre}$". With this strategy, Arc/Arg3.1 ablation was additionally increased. Most of the remaining Arc/Arg3.1 in the DG and CA3 was removed in the Late-cKO$_{2xCre}$ mice (Fig. 2.9a). To better quantify the amount of residual Arc/Arg3.1 protein in the adult Late-cKO mice, western blots were performed on brain lysates from dissected cortex, hippocampi and amygdala complex samples (Fig. 2.10a). Data were normalized to WT-control. Indeed, Arc/Arg3.1 was completely removed in the KO mice. Approximately, 80% of Arc/Arg3.1 protein in the cortex and amygdala complex and 60% in the hippocampi were ablated in the Late-cKO mice (Fig. 2.10b). Residual Arc/Arg3.1 protein was additionally reduced to about 15% in the cortex, 6% in the hippocampus and 7% in the amygdala of Late-cKO$_{2xCre}$ (Fig. 2.10c).

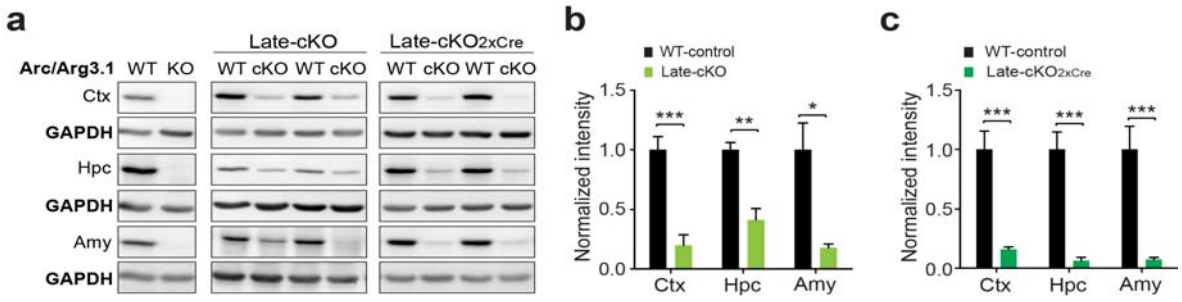

Fig. 2.10 Quantification of Arc/Arg3.1 protein in the adult constitutive KO and Late-cKO mice after Kainate-induced seizures. a, Representative Western blots. **b-c**, Quantification of residual Arc/Arg3.1 protein in Late-cKO (**b**) mice brain lysates normalized to WT-control, Ctx (20.00 ± 8.81%; *n* = 4), Hpc (42.63 ± 6.72%; *n* = 4) and Amy (18.71 ± 5.28%; *n* = 4). Further reduction in Arc/Arg3.1 was observed in Late-cKO$_{2xCre}$ mice (**c**), Ctx (15.92 ± 3.50%; *n* = 4), Hpc (6.38 ± 4.64%; *n* = 4) and Amy (7.27 ± 3.02%; *n* = 4). Bars show mean ± S.E.M. **p* < 0.05, ***p* < 0.01, ****p* < 0.001. Ctx, cortex; Amy, amygdala; Hpc, hippocampus.

2.3.3 Exploratory and anxiety-like behaviors in Arc/Arg3.1 KO and Late-cKO mice

To evaluate the effects of prenatal or late postnatal Arc/Arg3.1 removal on general behaviors, KO and Late-cKO mice were first tested in the open field (Fig. 2.11a). Neither the global Arc/Arg3.1 elimination (KO) nor the late postnatal Arc/Arg3.1 ablation (Late-cKO and Late-cKO$_{2xCre}$) altered animals' performance in the open field test. As both KO and Late-cKO mice (including Late-cKO$_{2xCre}$) spent similar time in the center of the arena (Fig. 2.11b, 2.12a,

d), had comparable velocity (Fig. 2.11c & 2.12b, e) and path length (Fig. 2.11d & 2.12c, f) to WT or WT-control mice, indicating normal exploratory behaviors and locomotion activity.

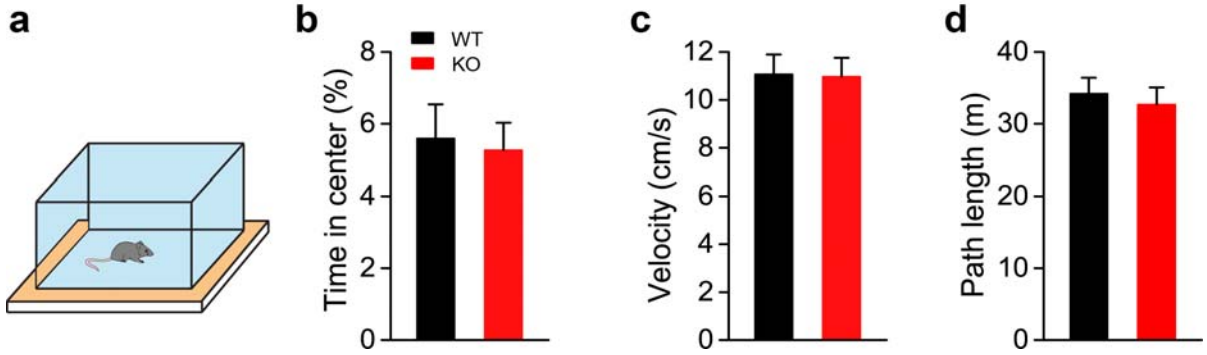

Fig. 2.11 Locomotion activity and exploratory behavior in KO mice. a-d, KO mice showed normal exploratory behavior and locomotion activity like their WT littermates in the open field test **(a)**. **b,** Percent time spent in the center was: WT, 5.60 ± 0.94%, *n* = 10, and KO, 5.27 ± 0.76%, *n* = 9; t_{17} = 0.27, *p* = 0.79, NS. **c,** Velocity was: WT, 11.07 ± 0.82 cm/s, *n* = 10, and KO, 10.98 ± 0.77 cm/s, *n* = 9, t_{17} = 0.08, *p* = 0.94, NS; **d,** Path length was: WT, 34.22 ± 2.19 m, *n* = 10, and 32.72 ± 2.33 m; *n* = 9; t_{17} = 0.47, *p* = 0.64, NS. All error bars show ± S.E.M. Two sample *t*-tests were performed between genotypes.

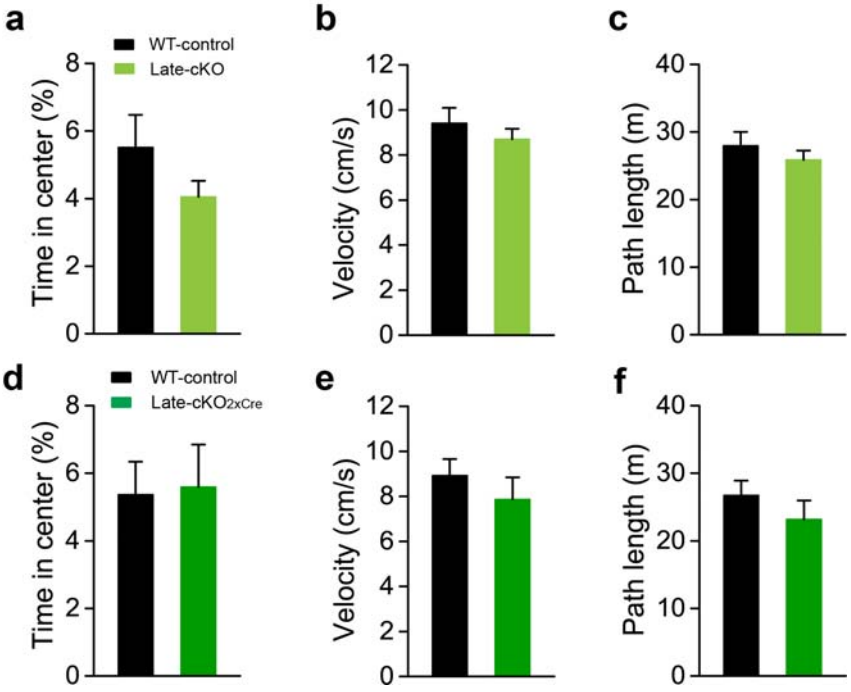

Fig. 2.12 Locomotion activity and exploratory behavior in Late-cKO mice. a-f, Late-cKO **(a-c)** and Late-cKO$_{2xCre}$ (**d-f**) showed comparable exploratory behavior and locomotor activity with WT-control littermates in the open field test. Percent time spent in the center was: **a,** WT-control, 5.52 ± 0.96%, *n* = 11, and Late-cKO, 4.05 ± 0.47%, *n* = 15; t_{24} = 1.49, *p* = 0.15, NS. **d,** WT-control, 5.37 ± 0.97%, *n* = 11, and Late-cKO$_{2xCre,}$ 5.60 ± 1.25%, *n* = 13; t_{22} = -0.15, *p* = 0.89, NS. Velocity was: **b,** WT-control, 9.42 ± 0.67 cm/s, *n* = 10, and Late-cKO, 8.70 ± 0.46 cm/s, *n* = 9, t_{24} = 0.92, *p* = 0.37, NS; **e,** WT-control, 8.93 ± 0.72%, *n* = 11, and Late-cKO$_{2xCre,}$ 7.87 ± 0.97%, *n* = 13; t_{22} = 0.39, *p* = 0.39, NS. Path length was: **c,** WT-control, 27.97 ± 2.03 m; *n* = 11 and Late-cKO, 25.87 ± 1.36 m, *n* = 15; t_{24} = 0.89, *p* = 0.38, NS; **f,** WT-control, 26.75 ± 2.14 m, *n* = 11 and Late-cKO$_{2xCre}$, 23.17 ± 2.80 m, *n* = 13; t_{22} = 1.01, *p* = 0.32, NS. All error bars show ± S.E.M. Two sample *t*-tests were performed between genotypes.

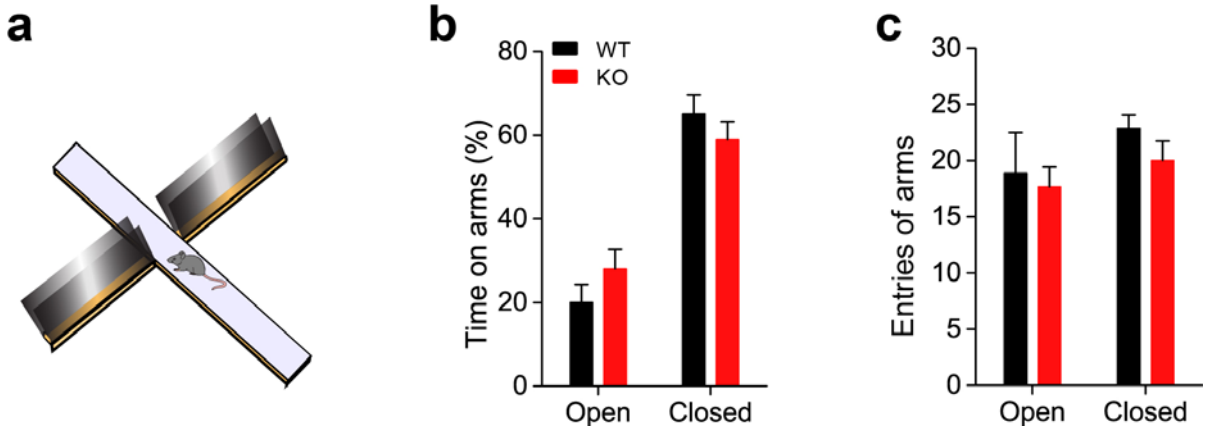

Fig. 2.13 Unaltered anxiety-like behavior in KO mice. a, Schematic of elevated plus maze test **b,** Percent time spent in open arms was: WT, 20.01 ± 4.30%, and KO, 28.01 ± 4.67%; t_{18} = -1.19, p = 0.25, NS; Percent time spent in closed arms was: WT, 65.09 ± 4.58%, and KO, 58.9 ± 4.35%; t_{18} = 0.95, p = 0.36, NS; **c,** Number of entries into the open arms was: WT, 18.88 ± 3.62, and KO, 17.67 ± 1.76; t_{18} = 0.33, p = 0.74, NS; Number of entries into the closed arms was: WT, 22.88 ± 1.16, and KO, 20.00 ± 1.74; t_{18} = 1.23, p = 0.24, NS. WT, n = 8; KO, n = 12. All error bars show ± S.E.M. Two sample t-tests were performed between genotypes.

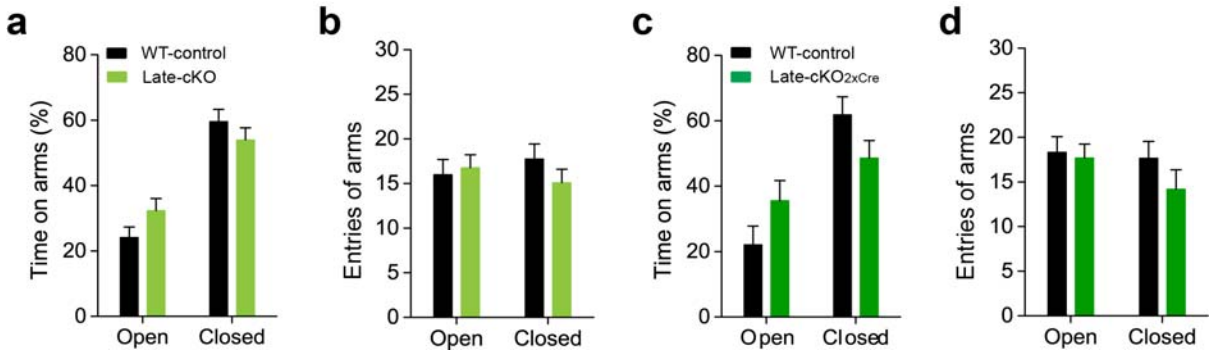

Fig. 2.14 Comparable anxiety-like behavior in Late-cKO and their WT-control littermates. **a,** Percent time spent in open arms was: WT-control, 24.15 ± 3.18%, n = 16, and Late-cKO, 32.35 ± 3.69%, n = 25; t_{39} = -1.55, p = 0.13, NS; **c,** WT-control, 22.06 ± 5.72%, n = 6, and Late-cKO$_{2xCre}$, 35.54 ± 6.16%, n = 10; t_{14} = -1.47, p = 0.16, NS; **a,** Percent time spent in closed arms was: WT-control, 59.58 ± 3.72%, n = 16, and Late-cKO, 53.97 ± 3.71%, n = 25; t_{39} = 1.02, p = 0.32, NS; **c,** WT-control, 61.86 ± 5.43%, n = 6, and Late-cKO$_{2xCre}$, 48.58 ± 5.34%, n = 10; t_{14} = 1.64, p = 0.12, NS. **b,** Entries into open arms was: WT-control, 16.00 ± 1.68, n = 16, and Late-cKO, 16.76 ± 1.46, n = 25; t_{39} = -0.33, p = 0.74, NS; **d,** WT-control, 18.33 ± 1.74, n = 6, and Late-cKO$_{2xCre}$, 17.70 ± 1.55, n = 10; t_{14} = 0.26, p = 0.80, NS; **b,** Entries into closed arms was: WT-control, 17.75 ± 1.67, n = 16, and Late-cKO, 15.08 ± 1.53, n = 25; t_{39} = 1.15, p = 0.26, NS; **d,** WT-control, 17.67 ± 1.87, n = 6, and Late-cKO$_{2xCre}$, 14.20 ± 2.15, n = 10; t_{14} = 1.10, p = 0.29, NS. All error bars show ± S.E.M. Two sample t-tests were performed between genotypes.

Elevated plus maze (Fig. 2.13a) is another general behavioral paradigm for evaluating innate anxiety-like behaviors. In this test, mice were released in the center of the maze facing the open arms and were allowed to explore the arena for 5 min. The natural instinct of mice is to avoid exposed open places and thus they prefer to stay in the wall-protected closed arms. Increased or decreased exploration of non-protected open arms indicates anxiolytic or

anxiogenic behaviors. KO, Late-cKO mice (including Late-cKO$_{2xCre}$) and their WT-control littermates, spent similar time exploring the open and closed arms (Fig. 2.13b; 2.14a, c). KO and Late-cKO also entered open and closed arms as frequently as their WT or WT-control littermates (Fig. 2.13c; 2.14b, d), indicating unaltered innate anxiety-like behaviors.

In summary, neither prenatal nor late postnatal Arc/Arg3.1 ablation affected locomotion activity, exploratory behavior, and innate anxiety-like behavior which is similar to our previously published data from conventional Arc/Arg3.1 KO mice (Plath et al., 2006)

Part II Dependence of spatial learning and explicit memory consolidation on temporal Arc/Arg3.1 expression

2.4 Long-term explicit memories in Arc/Arg3.1 KO and Late-cKO mice

Previously, colleagues from the lab of Dietmar Kuhl reported a profound loss of long-term memory in conventional Arc/Arg3.1 KO mice (Plath et al., 2006). However, whether Arc/Arg3.1 ablation during postnatal development can affect memory consolidation and whether memory consolidation needs lifelong Arc/Arg3.1 expression during adulthood remains unclear. Here, I was trying to address the specificity of Arc/Arg3.1 expression on long-term explicit memory processing by genetically removing Arc/Arg3.1 before or during late postnatal development and tested learning and memory in the adult mice.

2.4.1 Long-term novel object recognition memory in KO and Late-cKO mice

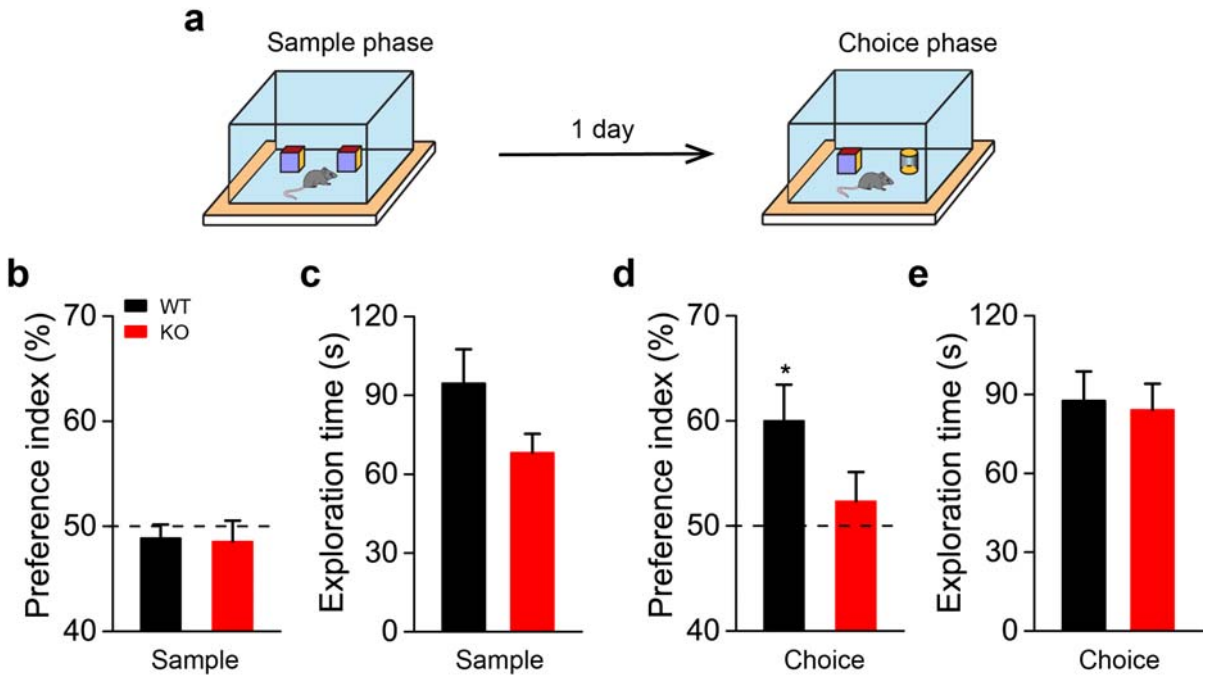

Fig. 2.15 Impaired long-term novel object recognition memory in KO mice. a, Schematic of the novel object recognition (NOR) test. **b,** Both WT and KO showed unbiased exploration of object replica during acquisition phase (WT, 48.87 ± 1.28%, t_9 = -0.88, p = 0.40, NS, and KO, 48.57 ± 1.97%, t_8 = -0.65, p = 0.54, NS); **c,** Nonsignificantly different time of objects exploration in KO and WT mice during sample phase (WT, 94.59 ± 12.90 s, and KO, 68.11 ± 7.24 s, t_{17} = 1.69, p = 0.11, NS); **d,** WT but not KO mice preferentially explored the novel object (WT, 59.99 ± 3.46%, t_9 = 2.89, *p < 0.05, and KO, 52.36% ± 3.08%, t_8 = 0.77, p = 0.47, NS). **e,** WT and KO mice spent similar time in exploring objects during choice phase (WT, 87.71 ± 11.08 s, and KO, 84.18 ± 9.85 s, t_{17} = 0.24, NS). WT, n = 10; KO, n = 9. Bars show mean ± S.E.M. One sample t-tests against chance level (50% of preference) were performed for each group, separately. Two sample t-tests were performed between genotypes.

I first examined the mice in a rapidly acquired explicit memory task relying on a hippocampal-cortical network: novel object recognition (NOR, Fig. 2.15a and 2.16a). During this task, mice were first habituated to an open field arena for 2 days followed by a sample phase during which mice were exposed to two identical objects. One day later, mice were

reintroduced into the same arena with one object replaced by a novel one. Novelty-seeking in normal mice drives mice to explore the novel object more intensely than the familiar one. Hence, preferential exploration of the novel object is taken to indicate memory of the familiar one.

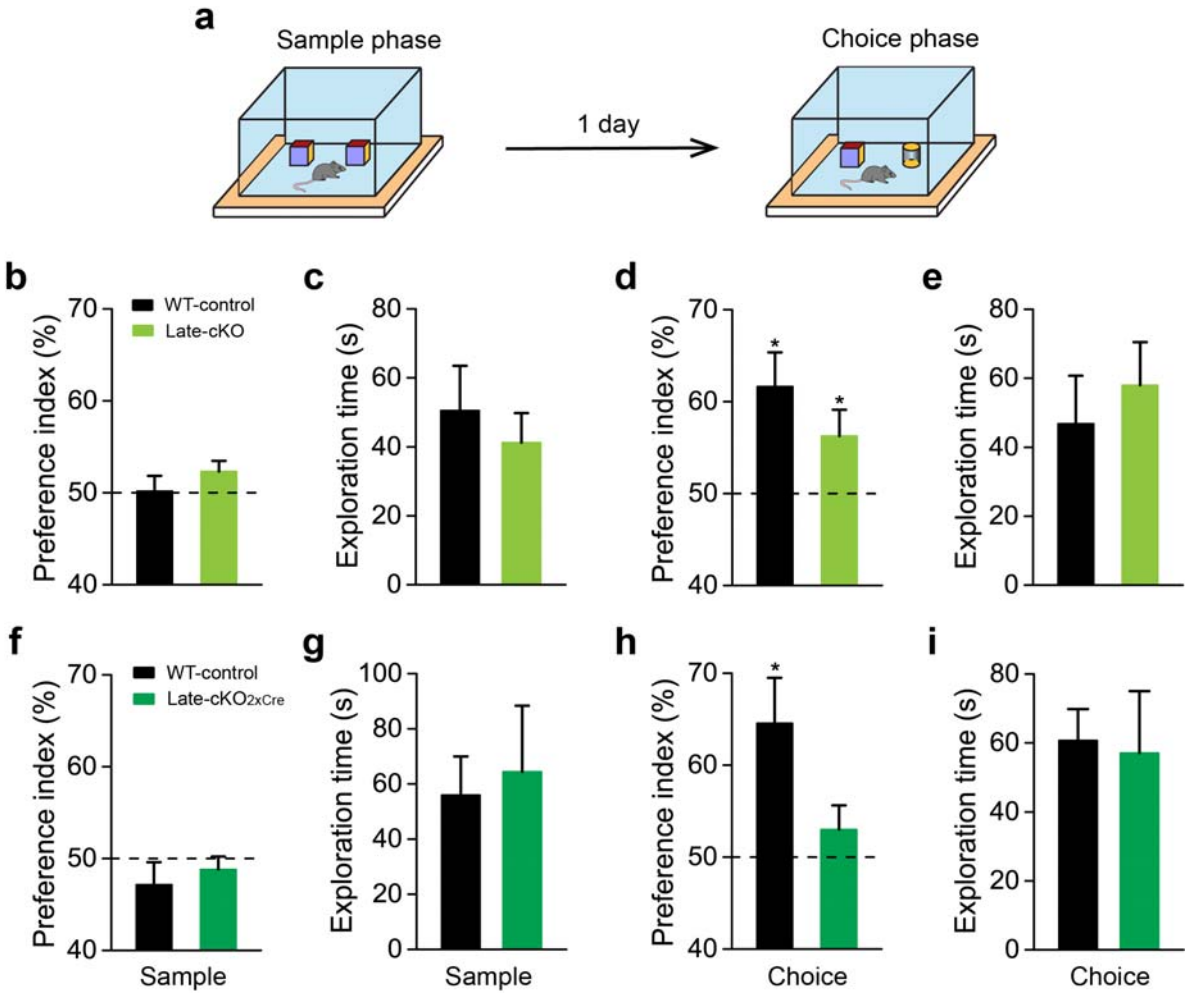

Fig. 2.16 Impaired long-term novel object recognition memory in Late-cKO$_{2xCre}$ mice. a, Schematic of the novel object recognition (NOR) test. Late-cKO **(b)** and Late-cKO$_{2xCre}$ **(f)** showed unbiased exploration of object replica during acquisition phase. Object preference index was: **b,** WT-control, 50.18 ± 1.65%, n = 11, t_{10} = 0.11, p = 0.92, NS and Late-cKO, 52.33 ± 1.14%, n = 15, t_{14} = 2.03, p = 0.06, NS; **f,** WT-Control, 47.17 ± 2.43%, n = 6, t_5 = -1.16, p = 0.30, NS and Late-cKO$_{2xCre}$, 48.82 ± 1.39%, n = 5, t_4 = -0.85, p = 0.44, NS. Non-significantly different time of objects exploration in WT-control and Late-cKO **(c)** and Late-cKO$_{2xCre}$ **(g)** mice during sample phase (**c,** WT-control, 50.53 ± 12.99 s, and Late-cKO, 41.21 ± 8.60 s, t_{24} = 0.62, p = 0.54, NS; **g,** WT-control, 55.98 ± 13.94 s, and Late-cKO$_{2xCre}$, 64.44 ± 23.94 s, t_9 = -0.32, p = 0.76, NS). A non-significant reduction of NOR memory was observed in Late-cKO mice 1 day after acquisition **(d)**, but was significantly impaired in Late-cKO$_{2xCre}$ (**h**) mice. **d,** WT-control and Late-cKO mice preferentially explored the novel object (61.65% ± 3.71%, *p < 0.05, n = 11 and 56.28% ± 2.85%, *p < 0.05, n = 15, respectively). **h,** WT-control but not Late-cKO$_{2xCre}$ mice preferentially explored the novel object (64.57% ± 4.94%, *p < 0.05, n = 6 and 53.02% ± 2.60%, p = 0.31, NS, n = 5). Late-cKO **(e)** and Late-cKO$_{2xCre}$ **(i)** mice spent similar time in exploring objects during choice phase in comparison with WT-controls. (e, WT-control, 46.86 ± 13.85 s, and Late-cKO, 58.00 ± 12.48 s, t_{24} = -0.59, p = 0.56, NS; **i,** WT-control, 60.70 ± 9.11 s, and Late-cKO$_{2xCre}$, 57.12 ± 17.88 s, t_9 = 0.19, p = 0.85, NS). Bars show mean ± S.E.M. One sample t-tests against chance level (50% of preference) were performed for each group, separately. Two-sample t-tests were performed between genotypes.

All WT and WT-control mice preferentially explored the novel object 24 hours after acquisition. However, KO and Late-cKO$_{2xCre}$ mice did not show significant preference for exploring the novel object ($p < 0.05$, one sample *t*-test against 50% chance level), indicating a loss of long-term memory (Fig. 2.15d & Fig. 2.16h). Late-cKO mice, carrying only a single copy of Cre, exhibited reduced yet above chance preference ($p = 0.045$, one sample *t*-test against 50% chance level) for the novel object, implying a non-significant reduction of long-term memory (Fig. 2.16d).

To avoid bias due to spatial location, the position of the two objects was always counter-balanced and the same preference index was calculated for the sample phase as an estimate of place preference. During the sample phase WT, WT-control, KO and Late-cKO mice (including Late-cKO$_{2xCre}$), explored the two identical objects equally, indicating non-place biased exploration (Fig. 2.15b & Fig. 2.16b, f). The total exploration time during both sample and choice phases did not differ between WT and KO or between WT-control and Late-cKO or between WT-control and Late-cKO$_{2xCre}$ mice, excluding the possibility that reduced preference for the novel object in the KO and cKO mice resulted from insufficient exploration (Fig. 2.15c, e & Fig. 2.16c, e, g, i).

2.4.2 Long-term contextual fear memory in KO and Late-cKO mice

To examine later phases of explicit memory, I employed contextual fear conditioning (CFC, Fig. 2.17a and 2.18a) task.

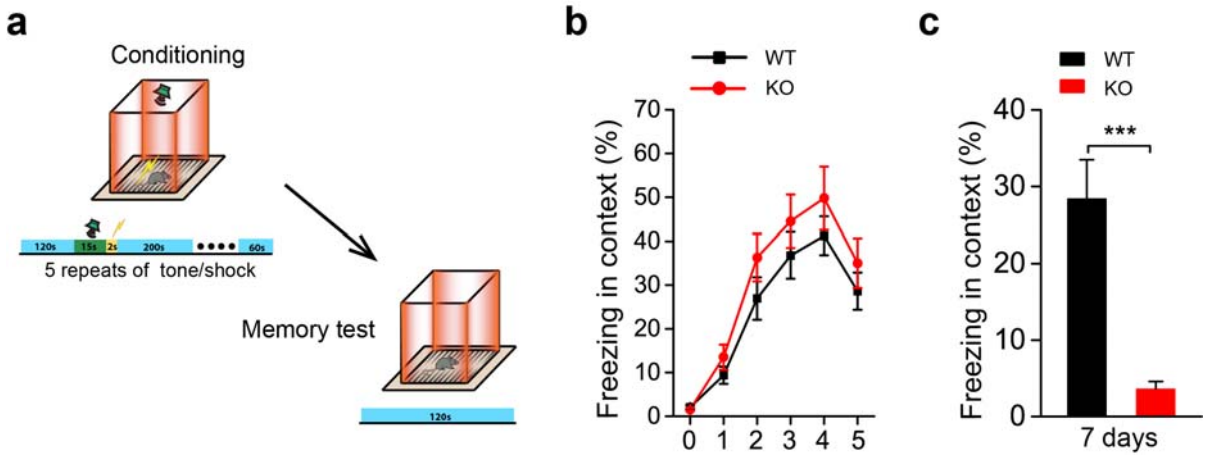

Fig. 2.17 Impaired long-term contextual fear memory in KO mice. a, Schematic of the contextual fear conditioning. **b,** Mean percent freezing during conditioning intervals was similar for WT and KO mice (genotype, $F_{(1, 21)} = 1.41$, $p = 0.25$, NS; Trial, $F_{(5,105)} = 60.77$, $p < 0.001$; interaction, $F_{(5,105)} = 0.70$, $p = 0.63$, NS; WT, $n = 12$; KO, $n = 11$). **c,** KO mice froze significantly less than their WT littermates 7 days after conditioning (WT, 28.38 ± 5.12%; $n = 12$ and KO, 3.59 ± 1.01%; $n = 11$; $t_{21} = 4.55$, ***$p <$ 0.001). Each point in the conditioning curve represents the mean percent freezing during the intervals between delivered shocks. Two-way ANOVA with repeated measurements and *post hoc* Fisher's LSD tests were applied. Bars show mean ± S.E.M. Significance was tested with two-tailed two-sample *t*-tests between genotypes.

CFC is a highly robust form of associative learning in which aversive stimuli (e.g. foot shocks) are administered within a previously neutral context. Re-exposure to the context then elicits a range of defensive behavioral responses (e.g. freezing). Well-conditioned mice will display freezing behaviors when being placed back to the conditioning context. Robust and long-lasting fear memory is generated (Phillips and LeDoux, 1992). During my experiments, mice were fear conditioned in a multiple fear conditioning system (TSE system) by applying mild foot shocks (0.25 mA, 2 s). In order to attract attention of the mice to the context, a neutral tone (2000 Hz, 98 dB, 15 s) was always coupled with foot shocks.

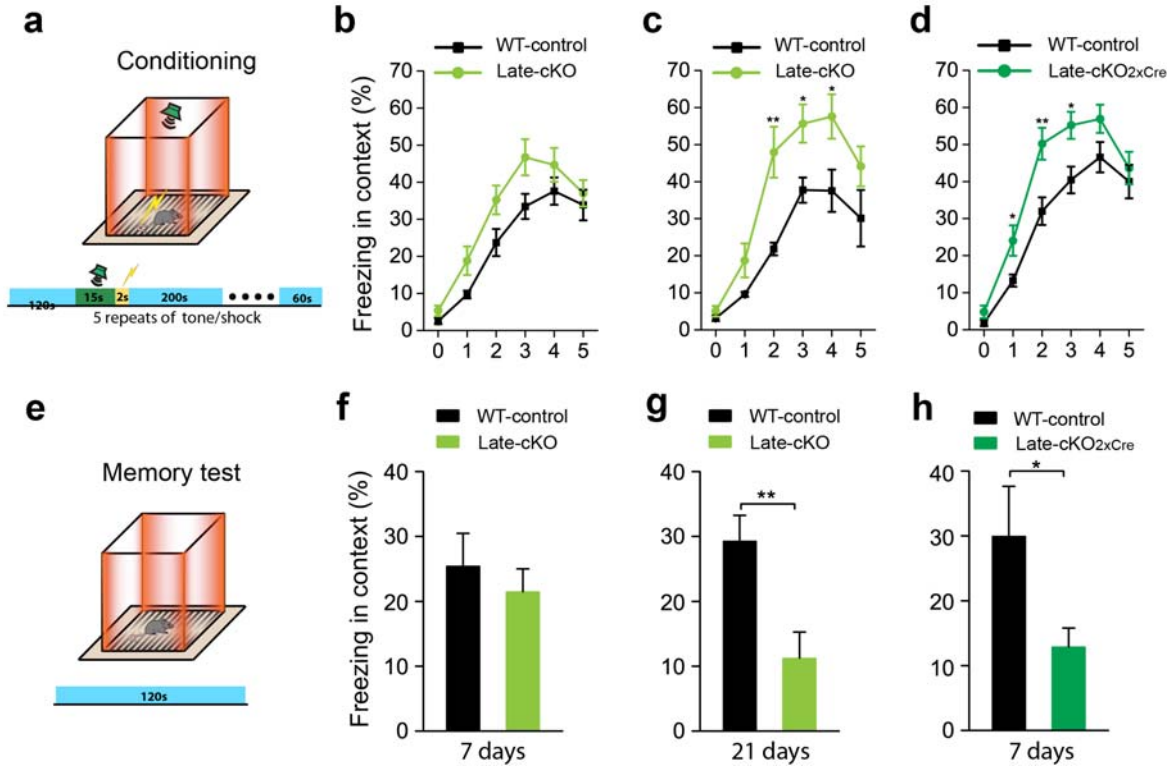

Fig. 2.18 Impaired long-term contextual fear memory in Late-cKO mice. a, Schematic of the contextual fear conditioning test. (**b-d),** Mean percent freezing during conditioning intervals was higher in Late-cKO mice. **b,** 7 days group: (genotype, $F_{(1,28)}$ = 3.05, p = 0.09, NS; Trial, $F_{(5,140)}$ = 65.98, p < 0.001; interaction, $F_{(5,140)}$ = 1.33, p = 0.26, NS; WT-control, n = 11; Late cKO, n = 19). **c,** 21 days group: (genotype, $F_{(1,12)}$ = 9.89, p < 0.01; Trial, $F_{(5,60)}$ = 38.79, p < 0.001; interaction, $F_{(5,60)}$ = 2.23, p = 0.11, NS; WT-control, n = 6; Late cKO, n = 8). **d,** Mean percent freezing during conditioning intervals was higher in Late-cKO$_{2xCre}$ compared with their WT-control littermates (genotype, $F_{(1,20)}$ = 13.19, p < 0.01; Trial, $F_{(5,100)}$ = 57.95, p < 0.001; interaction, $F_{(1,100)}$ = 1.46, p = 0.21, NS; WT-control, n = 9; Late-cKO$_{2xCre}$, n = 13). (**e-g),** Contextual fear memory was impaired in Late-cKO mice within 21 days not 7 days, indicating longer memory persistence. **f,** Similar freezing of WT-control and Late-cKO mice in the context 7 days after conditioning (WT-control, 25.44 ± 5.03%; n = 11 and Late-cKO, 21.46 ± 3.52%; n = 19; t_{28} = 0.66, p = 0.51, NS); **g,** Late-cKO mice froze significantly less than their WT-control littermates 21 days after conditioning (WT-control, 29.28 ± 3.95%; n = 6 and Late-cKO, 11.22 ± 4.04%, n = 8; t_{12} = 3.11, $^{**}p$ < 0.01); **h,** Significantly reduced freezing in the Late-cKO$_{2xCre}$ mice 7 days after conditioning (WT-control, 29.93 ± 7.74%; n = 9 and Late-cKO$_{2xCre}$, 12.87 ± 2.91%, n = 13; t_{20} = 2.34, $^{*}p$ < 0.05). Each point in the conditioning curve represents the mean percent freezing during the intervals between delivered shocks. Two-way ANOVA with repeated measurements and *post hoc* Fisher's LSD tests ($^{*}p$ < 0.05, $^{**}p$ < 0.01) were applied. Bars show mean ± S.E.M. Significance was tested with two-tailed two-sample *t*-tests between genotypes.

Long-term contextual fear memory was assessed either 7 or 21 days later, each time with an independent group of animals. Both KO and Late-cKO mice (including Late-cKO$_{2xCre}$) exhibited strong freezing during the inter-shock intervals. Freezing percentage was even higher in KO and cKO mice compared to WT or WT-control littermates indicating stronger fear memory acquisitions (Fig. 2.17b, Fig. 2.18b-d). Despite being strongly conditioned, KO and all Late-cKO mice had eventually forgotten the conditioning context 7 days and 21 days after conditioning, respectively. However, their WT or WT-control littermates still maintained a strong and stable memory representation of the conditioning context. Significantly reduced levels of freezing were observed in KO (7 days, $p < 0.001$, two-sample *t*-test), Late-cKO (21 days, $p < 0.01$) and Late-cKO$_{2xCre}$ (7 days, $p < 0.05$) mice during memory retrieval compared with WT or WT-controls (Fig. 2.17c, Fig. 2.18g-h). Besides, Late-cKO mice exhibited longer memory persistence and a slower decay of the contextual fear memory. Late-cKO mice lost fear memory within 21 days, while their Late-cKO$_{2xCre}$ siblings within 7 days (Fig. 2.18f-h).

Altogether, results from NOR and CFC show that consolidation of long-term explicit memories in adult KO and Late-cKO mice was strongly impaired in absence of Arc/Arg3.1 irrespective of its presence during prenatal or postnatal development. In contrast, both KO and Late-cKO mice still maintain the ability to acquire these tasks, suggesting that rapid encoding of novelty and fear associations can occur independently from Arc/Arg3.1. Strikingly, Late-cKO mice displayed slower long-term memory decay than their Late-cKO$_{2xCre}$ siblings, indicating that residual Arc/Arg3.1 in the hippocampus of Late-cKO mice can prolong the persistence of long-term explicit memory but does not suffice to maintain its remote phase.

2.5 Spatial learning and memory in KO and Late-cKO mice

Novel object recognition and contextual fear conditioning are behavioral paradigms particularly suited for assessing memories that depend on hippocampal-cortical networks. Although the rapid acquisition of these tasks makes them ideal for testing memory persistence, it does not allow for investigating complex and protracted learning processes. To address this question, I next examined the mice in the Morris water maze (MWM, Fig. 2.19a & Fig. 2.20a), a spatial navigation task that is particularly suited for dissecting hippocampus-dependent learning and memory in rodents. Spatial learning was evaluated in the training phase, during which mice were trained to learn to search for the submerged hidden platform guided by the visual cues being placed around the wall of pool for several days. Escape latency to the hidden platform and total swimming path length were used for evaluating spatial learning ability during training. Spatial memory was assessed as well in the probe tests by removing submerged hidden platform.

2.5.1 Spatial learning and memory in KO mice

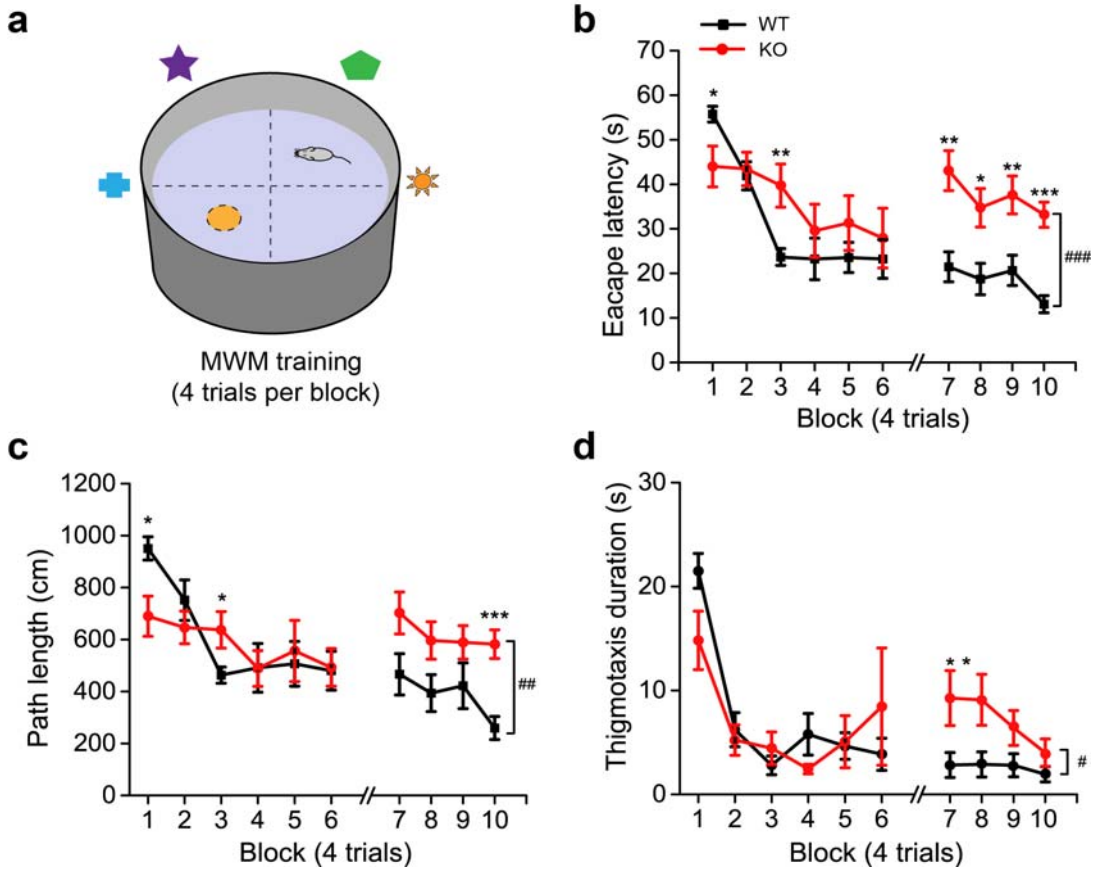

Fig. 2.19 Impaired spatial learning in KO mice. a, Schematic of acquisition phase of Morris water maze (MWM). Spatial learning gauged from the escape latency **(b)** and path length **(c)** to the hidden platform during training. Thigmotactic responses **(d)** were accessed by the duration in a circular zone which is 20 cm away from the edge of the tank. Each point represents the mean ± S.E.M. Significance was assessed with a two-way ANOVA with repeated measures ($^{\#}p < 0.05$, $^{\#\#}p < 0.01$, $^{\#\#\#}p < 0.001$) and with a *post hoc* Fisher LSD test ($*p < 0.05$, $**p < 0.01$, $***p < 0.001$). **b-c,** KO mice displayed significantly longer escape latencies (genotype $F_{(1,14)} = 10.90$, $p < 0.01$; block $F_{(9,126)} = 9.86$, $p < 0.001$; interaction $F_{(9,126)}=3.65$, $^{\#\#\#}p < 0.001$; WT, $n = 8$; KO, $n = 8$) and path length (Genotype $F_{(1,14)} = 3.25$, $p = 0.09$, NS; trial block $F_{(9,126)} = 5.56$, $p < 0.001$; interaction $F_{(9,126)} = 3.07$, $^{\#\#}p < 0.01$; WT, $n = 8$; KO, $n = 8$) to the hidden platform during training when a 7 days break was applied between block 6 and 7. **d,** KO mice showed stronger thigmotactic responses in comparison with their WT littermates after 7 days break (genotype $F_{(1,14)} = 0.78$, $p = 0.39$, NS; block $F_{(9,126)} = 10.84$, $p < 0.001$; interaction $F_{(9,126)} = 2.54$, $^{\#}p < 0.05$; WT, $n = 8$; KO, $n = 8$).

During training phase, WT mice consistently and continuously improved their escape strategy as reflected in shorter escape latencies (Fig. 2.19b) and swimming paths (Fig. 2.19c) following training. In contrast, KO mice exhibited only a minor and insignificant shortening of escape latencies or swim paths with ongoing learning (Block 1 vs. 6, WT Latency and Path length, both $p < 0.05$; KO Latency and Path length, both NS; Paired-*t* test.). The entire learning curve of KO mice was significantly shallower compared to WT mice (Fig. 2.19b-c) (Block1-10: Latency WT vs. KO, $p < 0.001$; Path length WT vs. KO, $p < 0.01$, two-way ANOVA with repeated measures). Notably, after the 7 days pause between blocks 6 and 7,

KO mice spent significantly more time in swimming along the pool walls (a zone which is 20 cm away from the wall), a strategy termed thigmotaxis which commonly reflects inability to perform reference-based navigation (genotype x block, $F_{(9,126)} = 2.54$, $p < 0.05$, two-way ANOVA with repeated measures) (Fig. 2.19d).

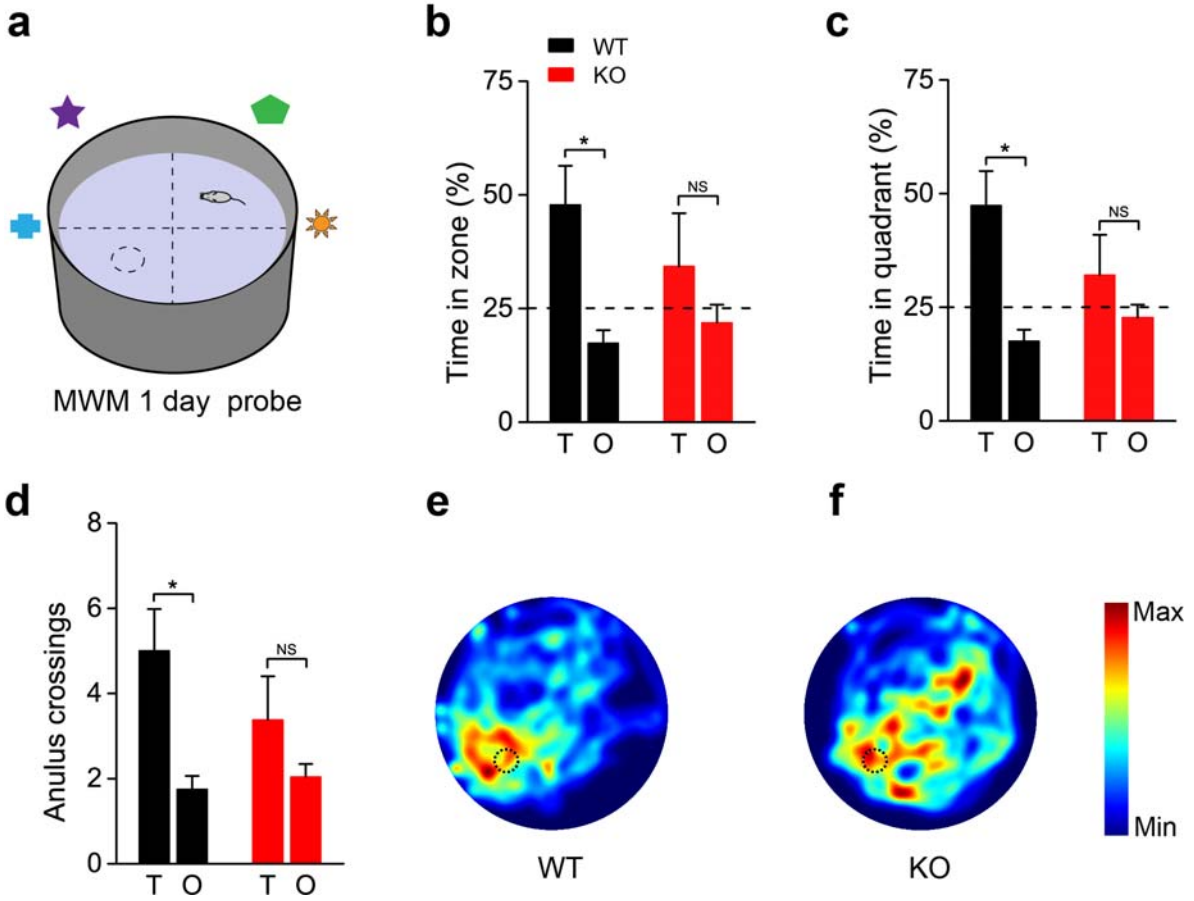

Fig. 2.20 Impaired spatial memory in KO mice 1 day after training. a, Schematic of the spatial memory test in the MWM. One day after the last training session (10th day), spatial memory was assessed in a probe trial in which the platform was removed. Spatial memory was analyzed by calculating percent time spent in target (T) zone or quadrant versus averaged percent time spent in the other (O) three equivalent zones or quadrants during probe test. Spatial memory precision was assessed by determining annulus crossings in target (T) zone versus annulus crossings in other (O) three zones. **b-f,** Spatial memory of KO mice was impaired during 1 day probe test. **b,** WT exhibited a significant preference to the target zone compared to other quadrant zones (T: 47.83 ± 8.58% and O: 17.39 ± 2.86%; respectively, $t_7 = 2.66$, $n = 8$, $^*p < 0.05$,) whereas KO mice did not show significant preference for the target zone (T: 34.28 ± 11.69% and O: 21.91 ± 3.90%, $t_7 = 0.79$, NS, $p = 0.45$, $n = 8$). **c,** Similar results were found from calculations of the time searching within the quadrants (WT, T: 47.39 ± 7.56% and O: 17.54 ± 2.52%; respectively, $t_7 = 2.96$, $n = 8$, $^*p < 0.05$; KO, T: 32.09 ± 8.82% and O: 22.64 ± 2.94%, $t_7 = 0.80$, $p = 0.45$, NS, n=8). **d,** WT mice had precise memory of the platform location as indicated by a significantly higher number of annulus crossings at the target zone compared to other equivalent zones (T: 5.00 ± 0.98 vs O: 1.75 ± 0.31; $t_7 = 2.55$, $^*p < 0.05$, $n = 8$). In contrast, KO mice crossed target and non-target zones similarly often (T: 3.38 ± 1.02 vs O: 2.04 ± 0.31, $t_7 = 1.04$, $p = 0.33$, NS, $n = 8$). **e-f,** Occupancy plots illustrate the search precision of the WT **(e)** and KO **(f)** in the vicinity of the platform zone during 1 day probe test. WT mice displayed precise searching around the hidden platform arena, while KO mice were searching mostly remote from the platforms zone. Data were plotted by mean ± S.E.M. Significance was assessed with a paired two-sample *t*-test. Occupancy plots represent the normalized mean occupancy across the maze area.

One day after the last training session, a probe trial was performed during which the hidden platform was removed. WT mice spent significantly more time searching in the target annulus zone (2 times of the platform size, $p < 0.05$, Paired *t*-test) and target quadrant ($p < 0.05$, Paired *t*-test) compared to the averaged time spent in the other three zones or quadrants. In contrast, KO mice did not spend significantly more time in the target zone ($p = 0.45$) or quadrant ($p = 0.45$), suggesting that KO mice didn't remember clearly where the hidden platform was (Fig. 2.20b-c). This was further confirmed by the non-significant number of crossings ($p = 0.33$, Paired *t*-test) of the target annulus zone (Fig. 2.20d). The occupancy plot representing the normalized mean occupancy across the maze area also showed that KO mice were exploring dispersedly in the maze (Fig. 2.20f), while WT mice formed a precise spatial representation of the platform location, was intensely searching around the platform area and made significantly more crossings ($p < 0.05$) of the target zone (Fig. 2.20d-e).

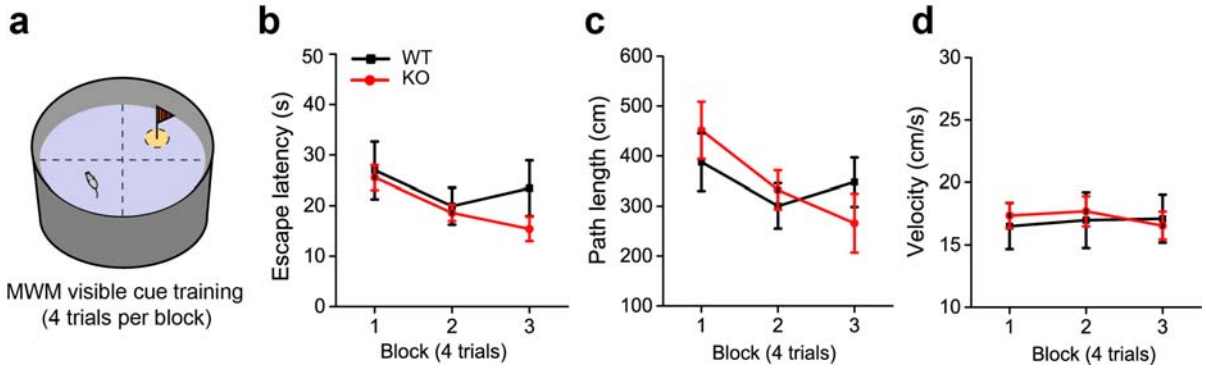

Fig. 2.21 Unaltered spatial cue learning in KO mice. a, Schematic of cue learning in the MWM. After probe test, mice were trained to find a platform cued with a visible flag to test possible motivational, visual or sensory deficits. KO mice did not show any such deficits and can navigate to the cued platform as efficiently as WT littermates which is indicated by escape latency (**b**, genotype $F_{(1,14)} = 0.60$, $p = 0.45$, NS; block $F_{(2,28)} = 5.13$, $p < 0.05$; interaction $F_{(2,28)}=1.19$, $p = 0.32$, NS), path length (**c**, genotype $F_{(1,14)} = 0.01$, $p = 0.92$, NS; block $F_{(2,28)} = 3.18$, $p = 0.06$, NS; interaction $F_{(2,28)}=1.19$, $p = 0.32$, NS) and velocity (**d**, genotype $F_{(1,14)} = 0.03$, $p = 0.88$, NS; block $F_{(2,28)} = 0.24$, $p = 0.79$, NS; interaction $F_{(2,28)}=0.50$, $p = 0.61$, NS). All WT, $n = 8$; KO, $n = 8$. Each point represents the mean ± S.E.M. Significance was assessed with a two-way ANOVA with repeated measures and with a *post hoc* Fisher LSD test.

To exclude the possibility that the observed spatial learning and memory deficits were due to visual or motor disability, a three days long visible platform test was performed after the last probe trial. During this test, spatial cues were removed and a flag was mounted above the submerged platform (Fig. 2.21a). KO mice located the cued platform as efficiently as WT mice, and swam with similar velocity and path length as WT mice (Fig. 2.21b-d; Velocity genotype x block, $p = 0.61$; Path length genotype x block, $p = 0.32$; two-way ANOVA with repeated measures).

In summary, prenatal removal of Arc/Arg3.1 strongly disturbs spatial learning, and impairs long-term spatial memory consolidation, in agreement with previously published findings from conventional KO mice (Plath et al., 2006).

2.5.2 Spatial learning and memory in Late-cKO mice

In parallel to KO mice, I also subjected Late-cKO mice to the same MWM procedures. By strong contrast to the KO mice, Late-cKO mice continuously improved in localizing the hidden platform during training as indicated by gradually reduced escape latency and shortened swim path, indicating acquisition of a precise spatial representation. Learning curve of the Late-cKO mice was indistinguishable (p > 0.05, two-way ANOVA with repeated measures) from their WT-control littermates (Fig. 2.22a-c). Moreover, Late-cKO mice did not display increased thigmotaxis behavior which was different from KO mice (Fig. 2.22d).

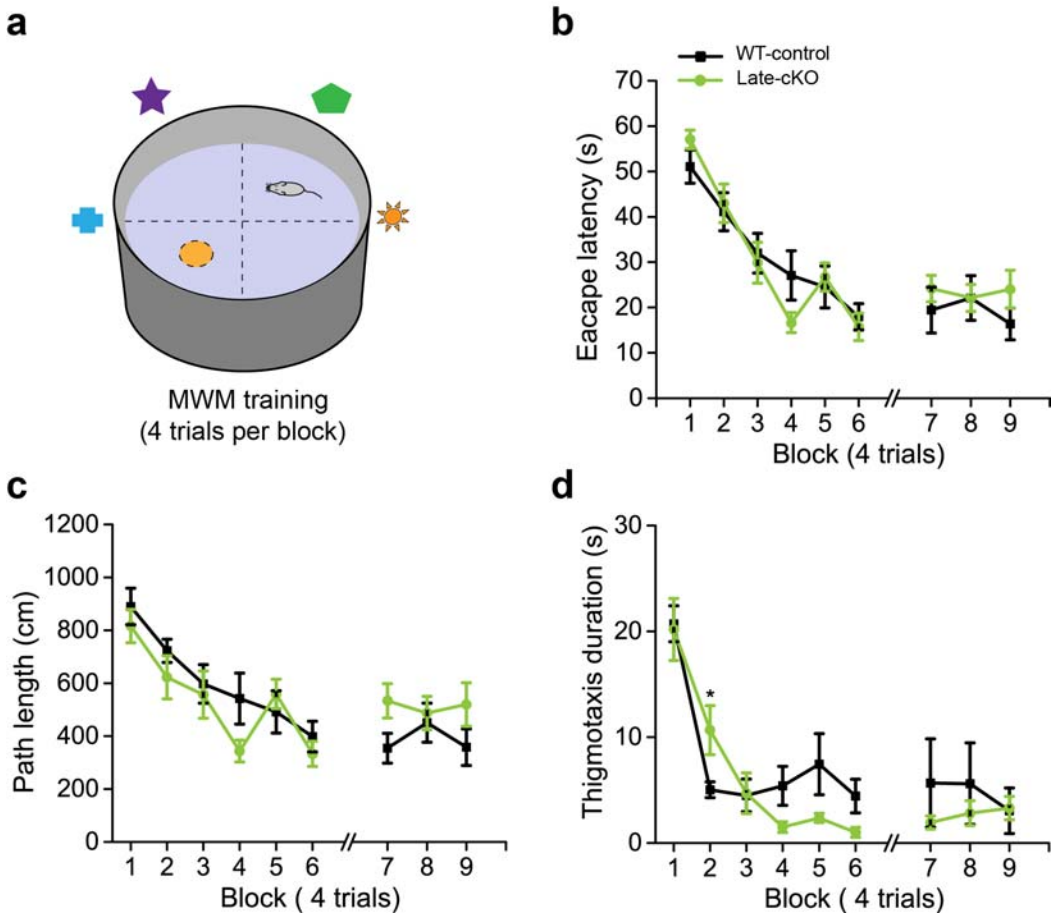

Fig. 2.22 Intact spatial learning in Late-cKO mice. a, Schematic of MWM training. **b-c,** Late-cKO mice display an indistinguishable learning curve from their WT littermates as indicated by escape latency (**b,** genotype $F_{(1, 18)}$ = 0.08, p = 0.78, NS; block $F_{(8, 144)}$ = 24.79, p < 0.001; interaction $F_{(8, 144)}$ = 1.24, p = 0.28, NS) and path length (**c,** Genotype $F_{(1,18)}$ = 0.01, p = 0.95, NS; trial block $F_{(8,144)}$ = 11.53, p < 0.001; interaction $F_{(8,144)}$ = 1.99, p = 0.052, NS) to the hidden platform. **d,** Late-cKO mice showed continuously decreasing thigmotactic swimming similar to their WT littermates (genotype $F_{(1, 18)}$ = 0.55, p = 0.47, NS; block $F_{(8, 144)}$ = 23.58, p < 0.001; interaction $F_{(8, 144)}$ = 2.05, p = 0.044). All WT-control, n = 10; Late-cKO, n = 10. Data represents the mean ± S.E.M. Significance was assessed with a two-way ANOVA with repeated measures and with a *post hoc* Fisher LSD test (*p < 0.05).

A probe test was first performed in Late-cKO mice 1 day after the last training session on day 9 (Fig. 2.23a). Since Late-cKO mice displayed indistinguishable performance during spatial learning, it was not surprising that Late-cKO had an intact 1 day spatial memory. Not only WT-control mice but also Late-cKO mice clearly preferred searching the hidden platform in the target annulus zone or target quadrant (WT-control, $p < 0.001$; Late-cKO, $p < 0.05$, Paired *t*-test, Fig. 2.23b-c). Furthermore, significantly higher crossings of the target zone ($p < 0.05$, Paired *t*-test) demonstrated that Late-cKO mice also formed a precise spatial representation of the platform location (Fig. 2.23e). Just like WT-control mice, Late-cKO mice intensively and locally searched around the platform area as can be seen from the average occupancy heat maps (Fig. 2.23e-f).

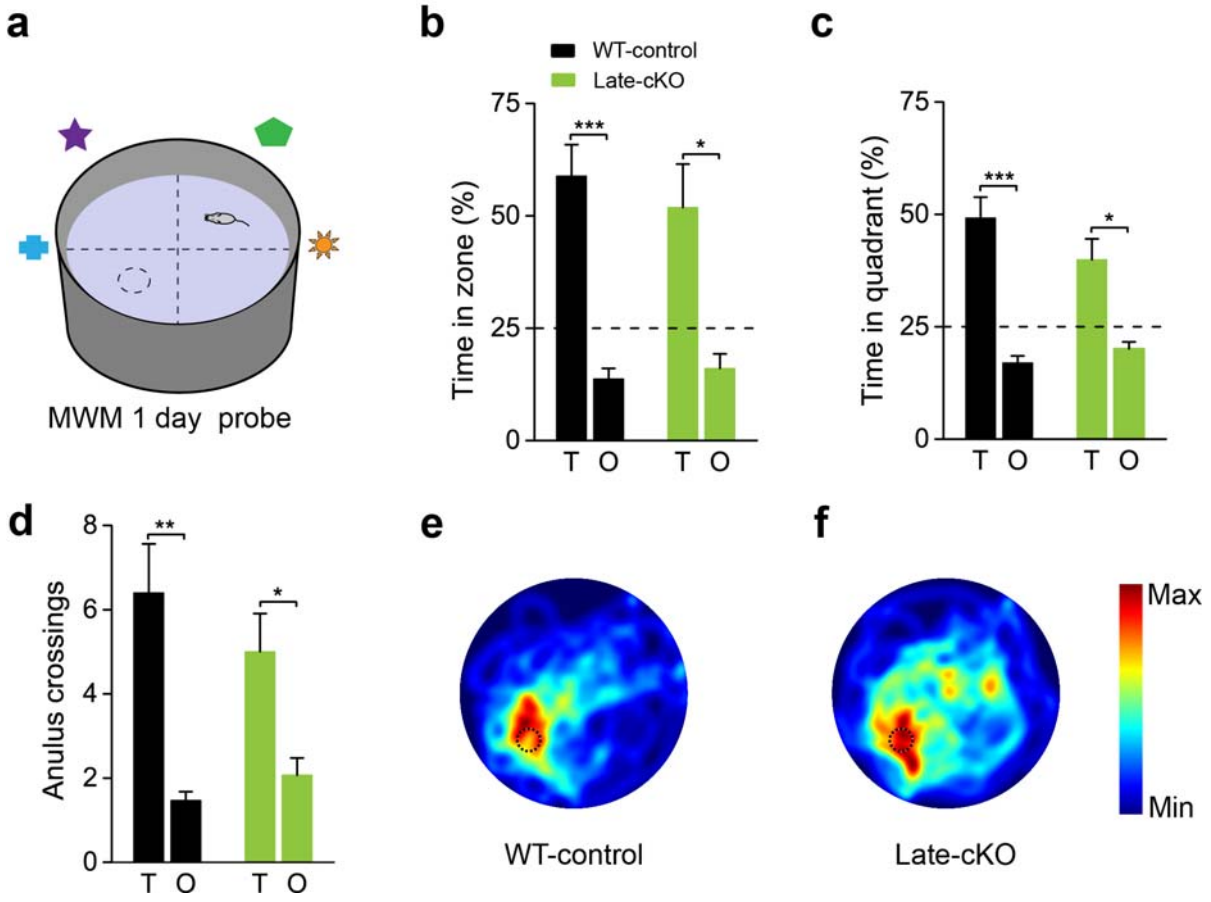

Fig. 2.23 Indistinguishable spatial memory in Late-cKO mice 1 day after training. a-f, 1 day spatial memory was indistinguishable in WT-control and in Late-cKO mice as shown by: **b**, Percent time in zone: (WT-control, T: 58.83 ± 6.99% vs. O: 13.72 ± 2.33%; $t_9 = 4.84$, ***$p < 0.001$; Late-cKO, T: 51.86 ± 9.66% vs. O: 16.05 ± 3.22%, $t_9 = 2.78$, *$p < 0.05$); **c**, Percent time in quadrant: (WT-control, T: 49.18 ± 4.67% vs. O: 16.94 ± 1.56%; $t_9 = 5.18$, ***$p < 0.001$; Late-cKO, T: 39.90 ± 4.68% vs. O: 20.03 ± 1.56%, $t_9 = 3.19$, *$p < 0.05$); **d**, Annulus crossings: (WT-control, T: 6.40 ± 1.16 vs. O: 1.47 ± 0.21; $t_9 = 3.92$, **$p < 0.01$; Late-KO, T: 5.00 ± 0.91 vs. O: 2.07 ± 0.41, $t_9 = 2.48$, *$p < 0.05$). **e-f,** Occupancy plots illustrate comparable search precision of the WT-control and Late-cKO mice in the vicinity of the platform zone. All WT-control, $n = 10$; Late-cKO, $n = 10$. Data were plotted by mean ± S.E.M. Significance was assessed with a paired two-sample *t*-tests. Occupancy plots represent the normalized mean occupancy across the maze area

However, the precise spatial memory observed in the 1 day probe test did not endure. Late-cKO mice forgot the platform location 21 days after training, and did not show preference for the target zone or quadrant ($p > 0.05$). Instead they searched in the entire pool with comparable crossings of the target and the other three zones ($p > 0.05$), indicating impaired remote spatial memory. In contrast, WT-control mice still preferred searching in the target zone ($p < 0.05$) and maintained a relatively precise spatial representation of the platform location 21 days after training (Fig. 2.24).

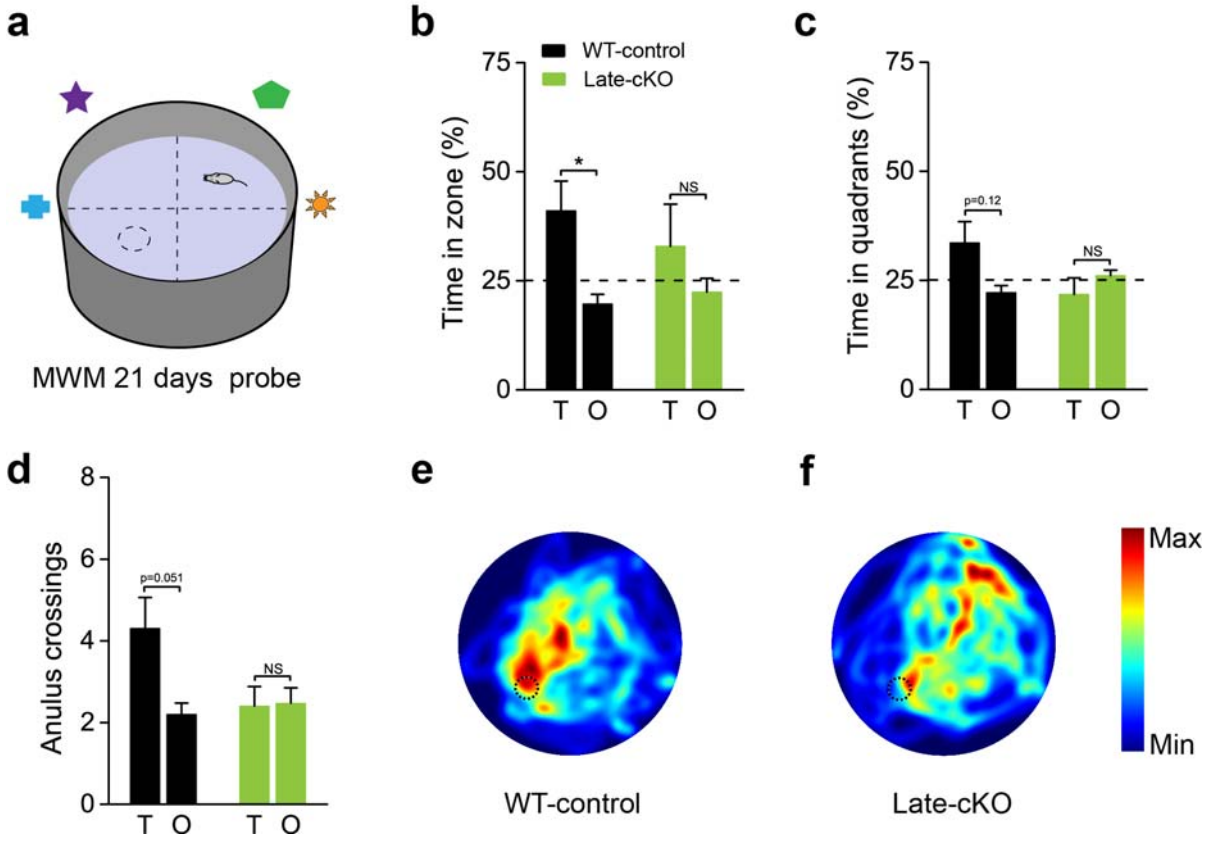

Fig. 2.24 Impaired remote spatial memory in Late-cKO mice 21 days after training. a-f, Remote spatial memory was impaired in Late-cKO mice 21 days after training indicated by: **b**, Percent time in zone: (WT-control, T: 41.04 ± 6.78% vs. O: 19.65 ± 2.26%; $t_9 = 2.37$,*$p < 0.05$; Late-cKO, T: 32.89 ± 9.64% vs. O: 22.37 ± 3.21%, $t_9 = 0.82$, $p = 0.43$, NS); **c**, Percent time in quadrant: (WT-control, T: 33.55 ± 4.92% vs. O: 22.15 ± 1.64%; $t_9 = 1.74$, $p = 0.12$; Late-cKO, T: 21.78 ± 3.75% vs. O: 26.07 ± 1.25%, $t_9 = -0.86$, $p = 0.41$, NS); **d**, Annulus crossings (WT-control, T: 4.30 ± 0.76 vs O: 2.20 ± 0.28; $t_9 = 2.25$, $p = 0.051$; Late-cKO, T: 2.40 ± 0.48 vs O: 2.47 ± 0.38, $t_9 = -0.08$, $p = 0.93$, NS). **e-f**, Occupancy plots illustrate a larger search-area of the Late-cKO mostly remote from the platforms zone, while WT-control mice still kept relatively precise searching around the platform. All WT-control, $n = 10$; Late-cKO, $n = 10$. Data were plotted by mean ± S.E.M. Significance was assessed with a paired two-sample t-test. Occupancy plots represent the normalized mean occupancy across the maze area.

In the cued phase of the MWM test, Late-cKO mice located the flagged-platform with similar latencies ($p > 0.05$) and swim paths ($p > 0.05$) as their WT-control littermates, indicating normal visual and motor functions as well as distance based navigation (Fig. 2.25).

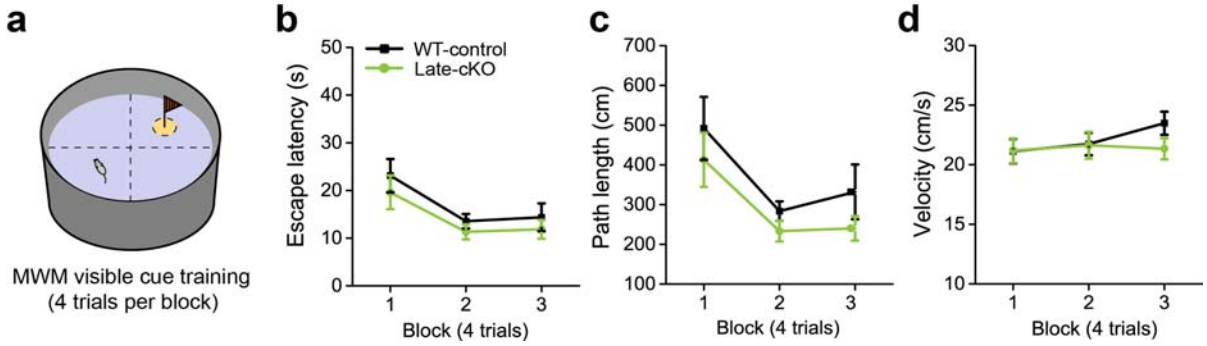

Fig. 2.25 Unaltered spatial cue learning in Late-cKO mice. Intact navigation to a cued platform (**a**) in Late-cKO mice is evident from comparable escape latency (**b,** Genotype $F_{(1,18)} = 1.04$, $p = 0.32$, NS; trial block $F_{(2,36)} = 9.84$, $p < 0.001$; interaction $F_{(2,36)} = 0.04$, $p = 0.96$, NS), path length (**c,** Genotype $F_{(1,18)} = 2.12$, $p = 0.16$, NS; trial block $F_{(2,36)} = 8.59$, $p < 0.001$; interaction $F_{(2,36)} = 0.09$, $p = 0.92$, NS) and velocity (**d,** Genotype $F_{(1,18)} = 0.34$, $p = 0.57$, NS; trial block $F_{(2,36)} = 2.40$, $p = 0{,}11$; interaction $F_{(2,36)} = 2.31$, $p = 0.11$, NS). WT-Control, $n = 10$; Late-cKO, $n = 10$. Each point represents the mean ± S.E.M. Significance was assessed with a two-way ANOVA with repeated measures and with a *post hoc* Fisher LSD test.

To exclude the possibility that the superior learning and intact 1 day spatial memory in the Late-cKO mice were resulted from residual Arc/Arg3.1 expression in the hippocampus, I employed a recombinant adeno-associated virus (rAAV) vector harboring Cre recombinase and a reporter gene Venus (rAAV-CreER^{T2}-2AP-Venus, Fig. 2.26a) to further remove residual Arc/Arg3.1 in the hippocampus. Viral vectors were first tested by unilateral injection in the hippocampus of Arc/Arg3.1$^{f/f}$ mice. A week after the injection (without tamoxifen application) Cre recombinase and Venus were strongly expressed in the injected hippocampus, and Arc/Arg3.1 protein was nearly absent (Fig. 2.26a), showing that leaky (tamoxifen-independent) Cre activity was sufficient for Arc/Arg3.1 ablation. I then injected a second cohort of Late-cKO mice in the hippocampus bilaterally with rAAV-CreER^{T2}-2AP-Venus. The virus diffused broadly and Cre/Venus was widely expressed in the hippocampi without elevating inflammatory responses as shown by Iba-1, a marker for identifying activated microglia (Fig. 2.26b). Immunofluorescence staining demonstrated that Arc/Arg3.1 ablation was evident most prominently in the CA3 and DG of the injected Late-cKO mice (Fig. 2.26c).

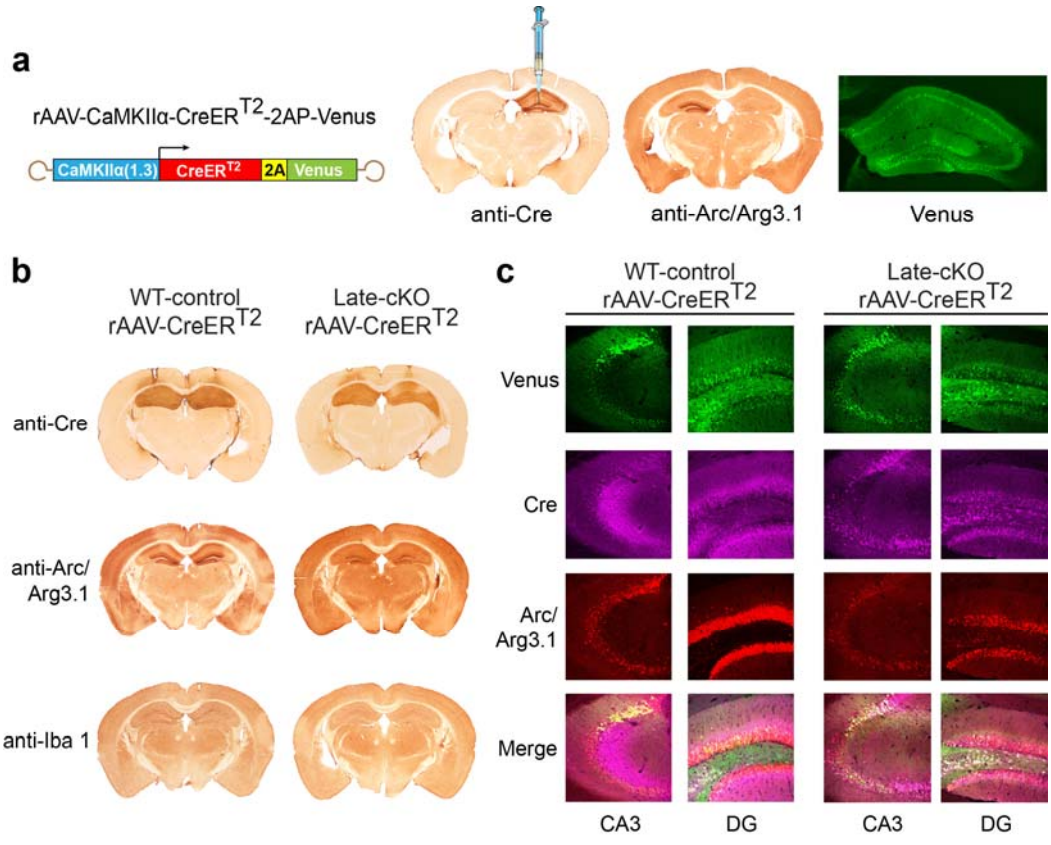

Fig. 2.26 rAAV-CreER^{T2}-Venus mediated acute Arc/Arg3.1 ablation in the hippocampus of Late-cKO mice. a, Unilateral injection of rAAV vectors harboring CreER^{T2} transgene driven by the CaMKIIα promoter in the hippocampus of Arc/Arg3.1$^{f/f}$ mice without tamoxifen application was sufficient for Arc/Arg3.1 ablation. **b,** Immunostaining with DAB against Cre, Arc/Arg3.1, and Iba-1 in mice 5 weeks after injections showed widespread expression of Cre in the injected hippocampi, strong reduction of Arc/Arg3.1 expression in the Late-cKO mouse but not in the WT-control. Lack of toxicity was observed by lacking of microglia activation (Iba-1). **c,** Immunofluorescence of Cre-Ab and genetically expressed Venus in the hippocampal CA3 and DG.

Seven days after virus injection, mice were subjected to MWM. Surprisingly, the injected Late-cKO mice still learned to locate the hidden platform as rapidly as injected WT-control mice. Similar efficient spatial learning curves were obtained in both injected Late-cKO and WT-control mice (Fig. 2.27a-c). Meanwhile, no increased thigmotaxis behavior was observed in the injected mice (Fig. 2.27d). These data suggest that the superior learning observed in the Late-cKO mice was not due to the remaining Arc/Arg3.1 in the hippocampus.

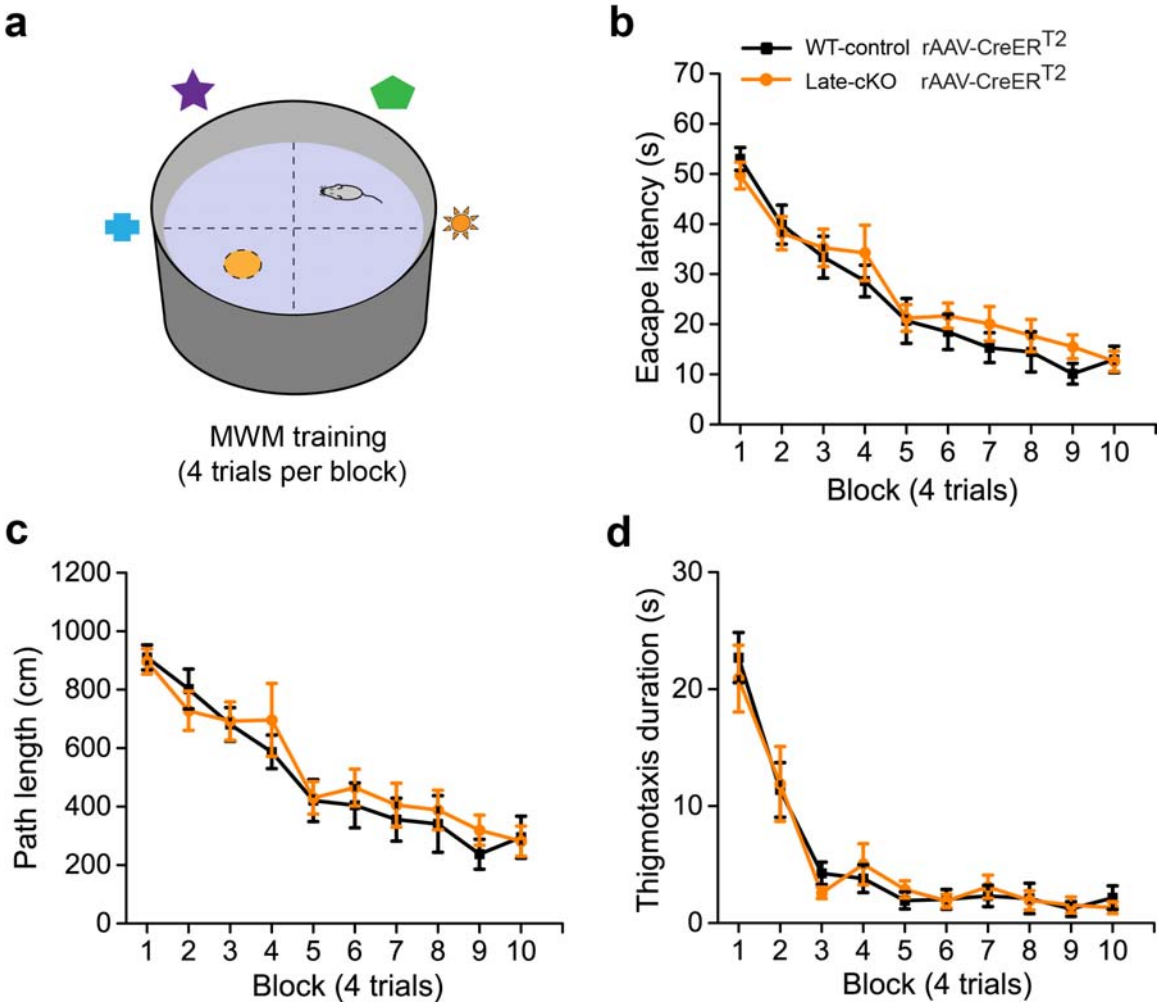

Fig. 2.27 Intact spatial learning in Late-cKO mice injected with rAAV-CreER^{T2}-Venus in the hippocampus. a, Schematic of the MWM training. **b-c,** Spatial learning was normal in WT-control and in Late-cKO mice injected with rAAV-CreER^{T2}-Venus in the hippocampus. **b,** Escape latency (genotype $F_{(1,17)}$ = 1.15, p = 0.30, NS; block $F_{(9,153)}$ = 30.81, p < 0.001; interaction $F_{(9,153)}$ = 0.44, p = 0.91, NS). **c,** Path length (Genotype $F_{(1,17)}$ = 0.65, p = 0.43, NS; trial block $F_{(9,153)}$ = 19.82, p < 0.001; interaction $F_{(9,153)}$ = 0.31, p = 0.97, NS). **d,** rAAV-CreER^{T2} injection did not affect the thigmotactic responses in both WT-control and Late-cKO mice. Thigmotaxis duration (Genotype $F_{(1,17)}$ = 0.01, p = 0.92, NS; trial block $F_{(9,153)}$ = 41.77, p < 0.001; interaction $F_{(9,153)}$ = 0.28, p = 0.98, NS). All WT-control, n = 9; Late-cKO, n = 10. Each point represents the mean ± S.E.M. Significance was assessed with a two-way ANOVA with repeated measures and with a *post hoc* Fisher LSD test.

Notably, like injected WT-control mice, Late-cKO mice spent more time in exploring the target zone (p < 0.01) and quadrant (p < 0.001) with significantly higher annulus crossings (p

< 0.01) of the target zone (Fig. 2.28a-d), suggesting intact 1 day spatial memory. However, the injected Late-cKO mice exhibited a less precise searching map compared to the injected WT-control mice which might indicate the beginning of memory loss (Fig. 2.28e-f).

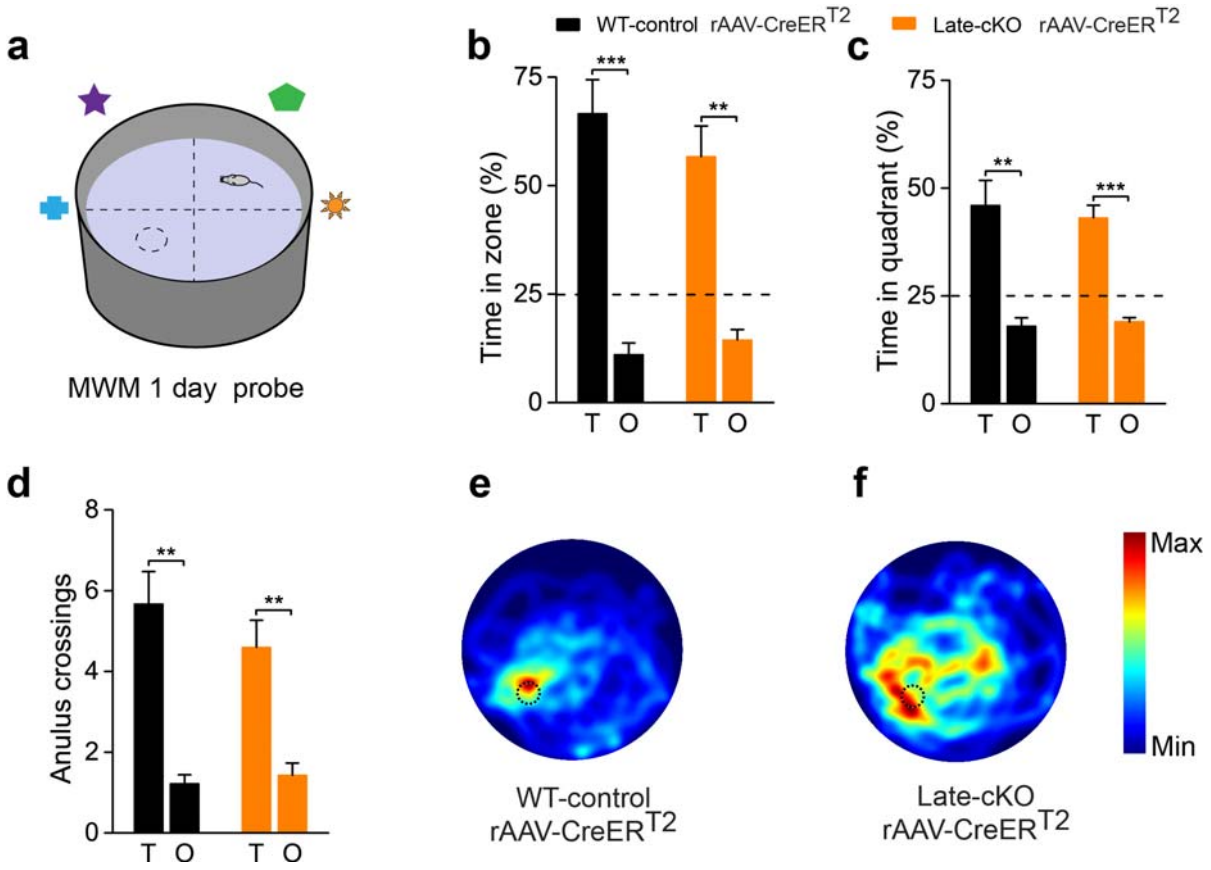

Fig. 2.28 Impaired spatial memory in Late-cKO mice with rAAV-CreER^{T2}-Venus injection in the hippocampus 1 day after training. a, Spatial memory was first assessed in a 1 day probe trial. **b-d**, 1 day spatial memory was intact in WT-control and in Late-cKO mice with rAAV-CreER^{T2}-Venus injection in the hippocampus indicated by: **b,** Percent time in zone (WT-control, T: 66.60 ± 7.80% vs. O: 11.13 ± 2.60%, t_8 = 5.33, ***p < 0.001; Late-cKO, T: 56.65 ± 7.10% vs. O: 14.45 ± 2.37%, t_9 = 4.45, **p < 0.01, respectively). **c,** Percent time in quadrant (WT-control, T: 46.02 ± 5.76% vs. O: 17.99 ± 1.92%, t_8 = 3.65, **p < 0.01; Late-cKO, T: 43.09 ± 2.91% vs O: 18.97 ± 0.97%, t_9 = 6.22, ***p < 0.001, respectively). **d,** Annulus crossings (WT-control, T: 5.67 ± 0.80 vs. O: 1.22 ± 0.22, t_8 = 4.61, **p < 0.01; Late-cKO, T: 4.60 ± 0.67 vs. O: 1.43 ± 0.30, t_9 = 3.85, **p < 0.01). **e-f**, Occupancy plots showed that injected Late-cKO mice developed a less precise searching maps comparing to the injected WT-control mice. All WT-control, n = 9; Late-cKO, n = 10. Data were plotted by mean ± S.E.M. Significance was assessed with a paired two-sample t-test. Occupancy plots represent the normalized mean occupancy across the maze area.

Although injected Late-cKO mice acquired a precise representation of the platform location, memory of this location did not persist and was completely lost one week after training, as indicated by a lack of searching preference for the target zone or quadrant and by non-significant crossings of the target zone (all p > 0.05; Fig. 2.29a-f). Late-cKO mice injected with rAAV-CreER^{T2}-2AP-Venus performed the flagged-platform task as well as their WT littermates, indicating that Arc/Arg3.1 ablation in the hippocampus did not affect visual or motor abilities (Fig. 2.30).

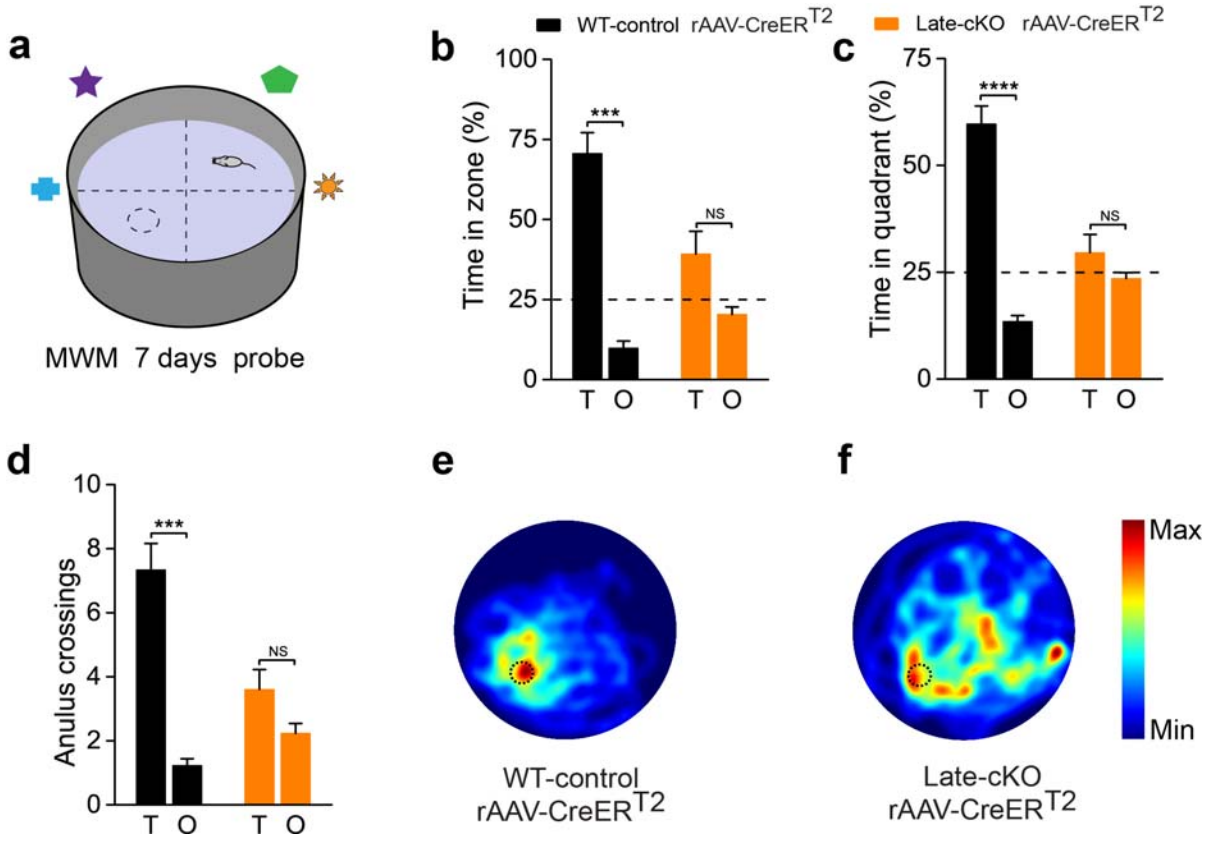

Fig. 2.29 Loss of spatial memory in Late-cKO mice with rAAV-CreER^{T2} injection in the hippocampus 7 days after training. a, Spatial memory was assessed in a 7 days probe trial. **b,** Percent time in zone (WT-control, T: 70.61 ± 6.52% vs. O: 9.80 ± 2.17%, t_8 = 6.99, ***p < 0.001; Late-cKO, T: 39.17 ± 7.11% vs. O: 20.28 ± 2.37%, t_9 = 1.99, p = 0.08, NS). **c,** Percent time in quadrant (WT-control, T: 59.66 ± 4.24% vs. O: 13.44 ± 1.41%, t_8 = 8.17, ****p < 0.0001; Late-cKO, T: 29.57 ± 4.28% vs. O: 23.48 ± 1.43%, t_9 = 1.07, p = 0.31, NS). **d,** Loss of precise spatial memory in the virus injected Late-cKO mice 7 days after training as indicated by similarly low numbers of annulus crossings over the target- and non-target zones (WT-control, T: 7.33 ± 0.83 vs. O: 1.22 ± 0.22, t_8 = 6.29, **p < 0.001; Late-cKO, T: 3.60 ± 0.62 vs. O: 2.23 ± 0.31, t_9 = 2.17, p = 0.06, NS). **e-f,** Occupancy plots confirmed focal search strategy of virus injected WT-control contrasting with entirely diffuse search of the injected Late-cKO mice. All WT-control, n = 9; Late-cKO, n = 10. Data were plotted as mean ± S.E.M. Significance was assessed with a paired two-sample t-test. Occupancy plots represent the normalized mean occupancy across the maze area.

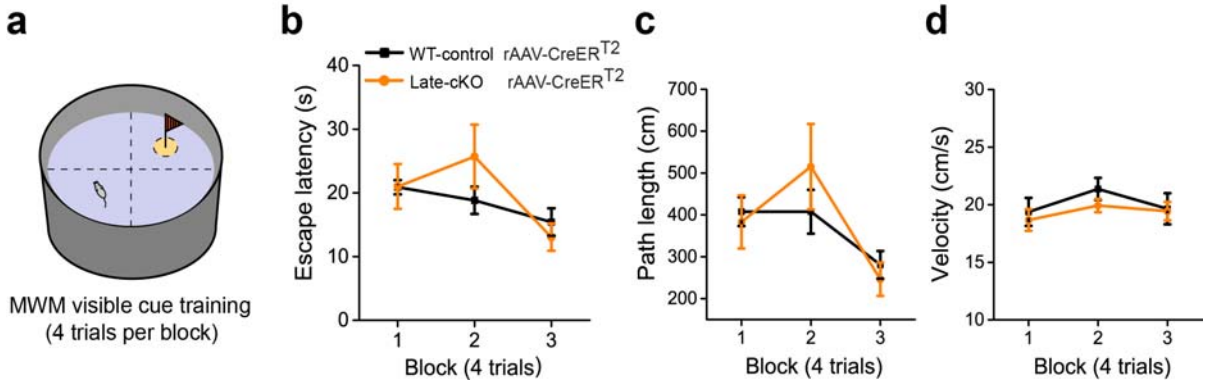

Fig. 2.30 Intact spatial cued navigation in Late-cKO mice with rAAV-CreER^{T2}-Venus injection in the hippocampus. Intact navigation to a cued platform **(a)** in rAAV-CreERT^2 -Venus injected WT-controls and Late-cKO mice was evident from comparable escape latencies (**b,** Genotype $F_{(1,17)}$ = 0.40,

p = 0.54, NS; trial block $F_{(2,34)}$ = 3.85, p < 0.05; interaction $F_{(2,34)}$ = 1.19, p = 0.32, NS), path length (**c,** Genotype $F_{(1,17)}$ = 0.10, p = 0.75, NS; trial block $F_{(2,34)}$ = 0.52, p < 0.01; interaction $F_{(2,34)}$ = 0.85, p = 0.44, NS) and velocity (**d,** Genotype $F_{(1,17)}$ = 0.44, p = 0.52, NS; trial block $F_{(2,34)}$ = 3.69, p < 0.05; interaction $F_{(2,34)}$ = 0.51, p = 0.60, NS). WT-control, n = 9; Late-cKO, n = 10. Each point represents the mean ± S.E.M. Significance was assessed with a two-way ANOVA with repeated measures and with a *post hoc* Fisher LSD test.

Taking all results obtained from the MWM test, I conclude that spatial learning relies on intact Arc/Arg3.1 expression during early development (prenatal or early postnatal). Removal of Arc/Arg3.1 after the third postnatal weeks or in adulthood does not debilitate spatial learning. In contrast, endurance of spatial memory does require the expression of Arc/Arg3.1 in adulthood.

Summing up all of the data from the explicit memory paradigms (NOR, CFC, and MWM), it is faithfully to conclude that either prenatal or postnatal Arc/Arg3.1 ablation impairs explicit memory consolidation in the adult mice. A certain amount of residual Arc/Arg3.1 in the hippocampus of adult mice can protract long-term memory, but is not enough for maintaining its remote phase. In general, Arc/Arg3.1 is essential for long-term explicit memory consolidation. Consolidation of long-term explicit memories requires lifelong Arc/Arg3.1 expression in the adulthood.

2.6 Hippocampal synaptic plasticity in Arc/Arg3.1 KO and Late-cKO mice

Synaptic plasticity refers to the ability of synapses to enhance or weaken their strength in response to increased or decreased activity (Hughes, 1958). LTP is an increase in synaptic response following electrical, chemical or optical stimulation. It can persist for hours, days or even longer and, is widely considered by neuroscientists as a cellular mechanism for memory consolidation. Studies in the last two decades very often correlate episodic memory deficits with impaired LTP in the hippocampus. To assess the synaptic plasticity in the hippocampus after prenatal or late postnatal Arc/Arg3.1 ablation, I recorded LTP in the perforant path-granule cell synapses *in vivo* (Fig. 2.32b).

2.6.1 Long-term potentiation in KO mice

My former colleagues previously demonstrated that LTP in the perforant pathway *in vivo* can be successfully induced in the conventional Arc/Arg3.1 KO mice. Theta-burst stimulation (TBS) of the perforant fibers from the entorhinal cortex induced a surprisingly large early-LTP in the synaptic layer of the granular hippocampal neurons. Most remarkably, this enhanced early-LTP exceeded that of WT-littermates by 50% during the first 60 min, but rapidly declined to baseline after about 90 min (Fig. 2.31). These results indicated that Arc/Arg3.1 is required for consolidation of transient synaptic plasticity into persistent changes which might underlie memory storage.

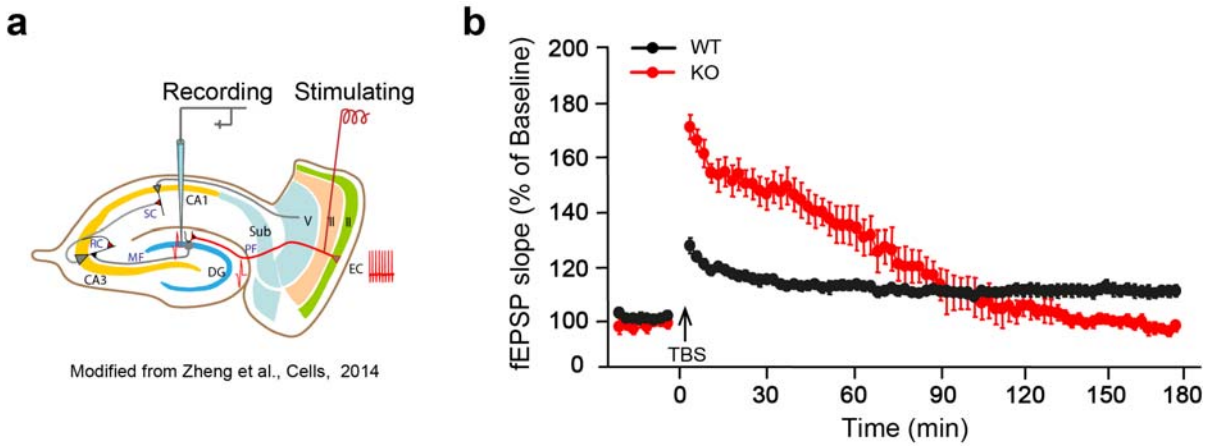

(Modified from Plath, N. *et al*, Neuron, 2006)

Fig. 2.31 Impaired hippocampal LTP consolidation in KO mice. a, Illustration of field recording in the hippocampal DG *in vivo.* **b,** LTP at perforant path/granule cell synapses *in vivo*. Mean normalized fEPSP slope is plotted as a function of time. A theta-burst stimulation (arrow) induced a strongly enhanced early LTP in KO mice (0–5 min: WT, 126.2% ± 2.6%; KO, 169.8% ± 4.2%, $p < 0.0005$) that subsequently decayed to baseline (175–180 min: WT, 111.2% ± 2.0%; KO, 97.5% ± 1.6%, $p < 0.0001$). WT, $n = 5$; KO, $n = 6$. Significance was assessed with Mann-Whitney test between groups. (Plath, N. *et al*, Neuron, 2006)

2.6.2 Long-term potentiation in Late-cKO mice

Previously, it was reported that acute knockdown of Arc/Arg3.1 in the adult hippocampus of rats also impaired LTP in the DG *in vivo* (Guzowski et al., 2000). However, what is the role of Arc/Arg3.1 during late postnatal development in synaptic consolidation, and whether synaptic consolidation requires lifelong Arc/Arg3.1 expression in adulthood remains unclear. To address these questions, perforant path LTP was recorded in the DG of Late-cKO mice. Before LTP induction, input/output (IO) curves were generated by applying stepwise increasing currents to evaluate the effects of late-postnatal Arc/Arg3.1 ablation on basal synaptic transmission (Fig. 2.32c-d).

Field excitatory postsynaptic potential (fEPSP) slope and population spike (PS) amplitude were measured as references for synaptic responses and neuronal excitability, respectively. Baseline IO curves were slightly weaker in Late-cKO mice compared with WT-control mice, though not significantly (Fig. 2.32c). PS amplitude was similar in WT-control and Late-cKO mice over most of the applied current intensities (Fig. 2.32d). Basic synaptic transmission in the Late-cKO mice was not significantly affected by late postnatal Arc/Arg3.1 ablation. In sharp contrast to the conventional KO mice, TBS induced a stable and long-lasting LTP (both fEPSP-LTP and PS-LTP) in the Late-cKO mice which were indistinguishable from WT-littermates. The early phase of this LTP was not enhanced in the Late-cKO nor was the late phase reduced (Fig. 2.32e-f). These results were surprising given that the Late-cKO mice had severe remote memory impairments, just like the conventional

KO mice. A possible explanation is that the residual Arc/Arg3.1 in the DG can protract LTP induction and support synaptic consolidation in the Late-cKO mice over longer time periods.

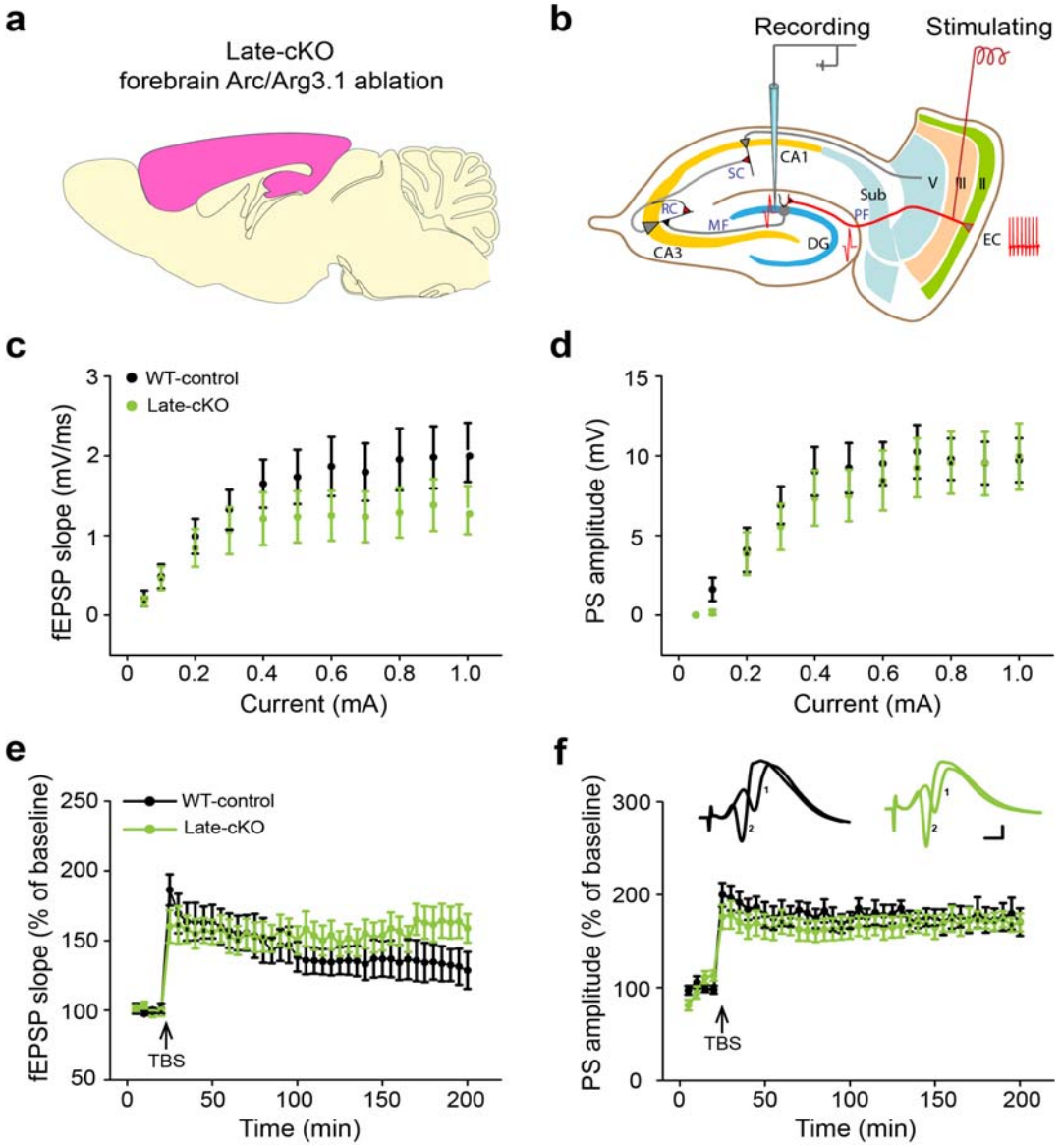

Fig. 2.32 Normal baseline synaptic transmission and hippocampal LTP in Late-cKO mice. a, Schematic diagram of Arc/Arg3.1 ablation in Late-cKO mice (magenta). **b,** Illustration of field recording in the hippocampal DG *in vivo*. **c-d,** Basic synaptic transmission was not significantly different between WT-control and Late-cKO mice as indicated by input/output (I/O) curves of the fEPSP slope and PS amplitude plotted as a function of different stimulus intensities. fEPSP slope (**c,** Genotype $F_{(1,11)} = 1.21$, $p = 0.30$, NS; Current intensity $F_{(10,110)} = 29.50$, $p < 0.0001$; interaction $F_{(10,110)} = 1.87$, $p = 0.06$, NS). PS amplitude (**d,** Genotype $F_{(1,11)} = 0.20$, $p = 0.67$, NS; Current intensity $F_{(10,110)} = 33.53$, $p < 0.0001$; interaction $F_{(10,110)} = 0.35$, $p = 0.97$, NS). **e-f,** LTP at perforant path/granule cell synapses *in vivo* was comparable between WT-control and Late-cKO mice as shown by mean normalized fEPSP slope and PS amplitude plotted as a function of time. fEPSP-LTP (**e,** Genotype $F_{(1,11)} = 0.65$, $p = 0.44$, NS; Time $F_{(35,385)} = 3.10$, $p < 0.0001$; interaction $F_{(35,385)} = 2.98$, NS.). PS-LTP (**f,** Genotype $F_{(1,11)} = 0.56$, $p = 0.47$, NS; Time $F_{(35,385)} = 1.33$, $p = 0.10$, NS; interaction $F_{(35,385)} = 0.74$, $p = 0.86$, NS). Waveforms are averages of consecutive fEPSP traces from a representative experiment, measured before and after theta-burst stimulation (TBS). 1, waveform before TBS; 2, waveform after TBS. Scale bars: vertical bar 2 mV and horizontal bar 2 ms. All WT-control, $n = 6$; Late-cKO, $n = 7$. Significance was assessed with a two-way ANOVA with repeated measures and with a *post hoc* Fisher LSD test.

Taken together, prenatal Arc/Arg3.1 ablation strongly impaired LTP consolidation. Certain amount of Arc/Arg3.1 in the adult hippocampus might protract LTP consolidation which is very well correlated with the prolonged explicit memory persistence in the Late-cKO mice. However, this residual plasticity was not sufficient for maintaining remote memory consolidation. Another possibility is that impaired remote memory consolidation probably was caused by inability of synaptic consolidation in the cortical regions due to broad and large amount of Arc/Arg3.1 ablation in the cortex.

2.7 Oscillatory network activity in Arc/Arg3.1 KO and Late-cKO mice

2.7.1 Local field potential recording *in vivo*

Oscillations in the theta and gamma frequency are considered essential for the function and synchronization of hippocampal-cortical networks during spatial navigation, learning and memory retrieval (Winson, 1978; Buzsaki and Draguhn, 2004; Montgomery and Buzsaki, 2007; Nyhus and Curran, 2010; Buzsaki and Moser, 2013b). High frequency oscillatory events in CA1, termed ripples, are believed to be important for encoding spatial information and for consolidation of memory (Girardeau et al., 2009; Ego-Stengel and Wilson, 2010; Jadhav et al., 2012). I next asked whether the strong deficits in spatial learning and long-term memory consolidation observed in the KO and cKO mice could be related to impairments in any of these network activity patterns. To address this question, simultaneous multichannel depth recordings from the hippocampus (Fig. 2.33a) and prefrontal cortex (Fig. 2.33b) were performed in urethane-anaesthetized mice by my colleague Jasper Grendel. LFPs were measured and analyzed (Fig.2.33c-d).

2.7.2 Oscillatory activity in the hippocampus and prefrontal cortex of KO and Late-cKO mice

Simultaneous multichannel LFP recordings allow us to dissect neuronal activities from different layers from which three major forms of rhythmic activity (theta, gamma and sharp wave ripples) can be identified. In this study theta and gamma activity were detected in the *pyramidal layer* of hippocampal CA1 and prefrontal cortex in urethane anesthetized mice during REM-like phases. WT mice exhibited clear theta (4-6 Hz) accompanied by low gamma (20-50 Hz) oscillations in the CA1 *pyramidal layer* and in the PFC (Fig. 2.34a). Strikingly, KO mice exhibited significantly reduced theta and gamma power in CA1 *pyramidal layer* and PFC ($p < 0.05$ or $p < 0.01$, Mann Whitney test; Fig. 2.34a-c). In stark contrast, Late-cKO mice were WT-like in the measures of theta and gamma network activity in both hippocampus and PFC. The theta and gamma power in the CA1 and PFC were indistinguishable from those of their WT-control littermates (Fig. 2.34a, b, d). These data demonstrate that prenatal Arc/Arg3.1 ablation significantly reduces theta and gamma activity in the hippocampal CA1

and PFC, while late postnatal ablation of Arc/Arg3.1 does not cause obvious changes of these activities.

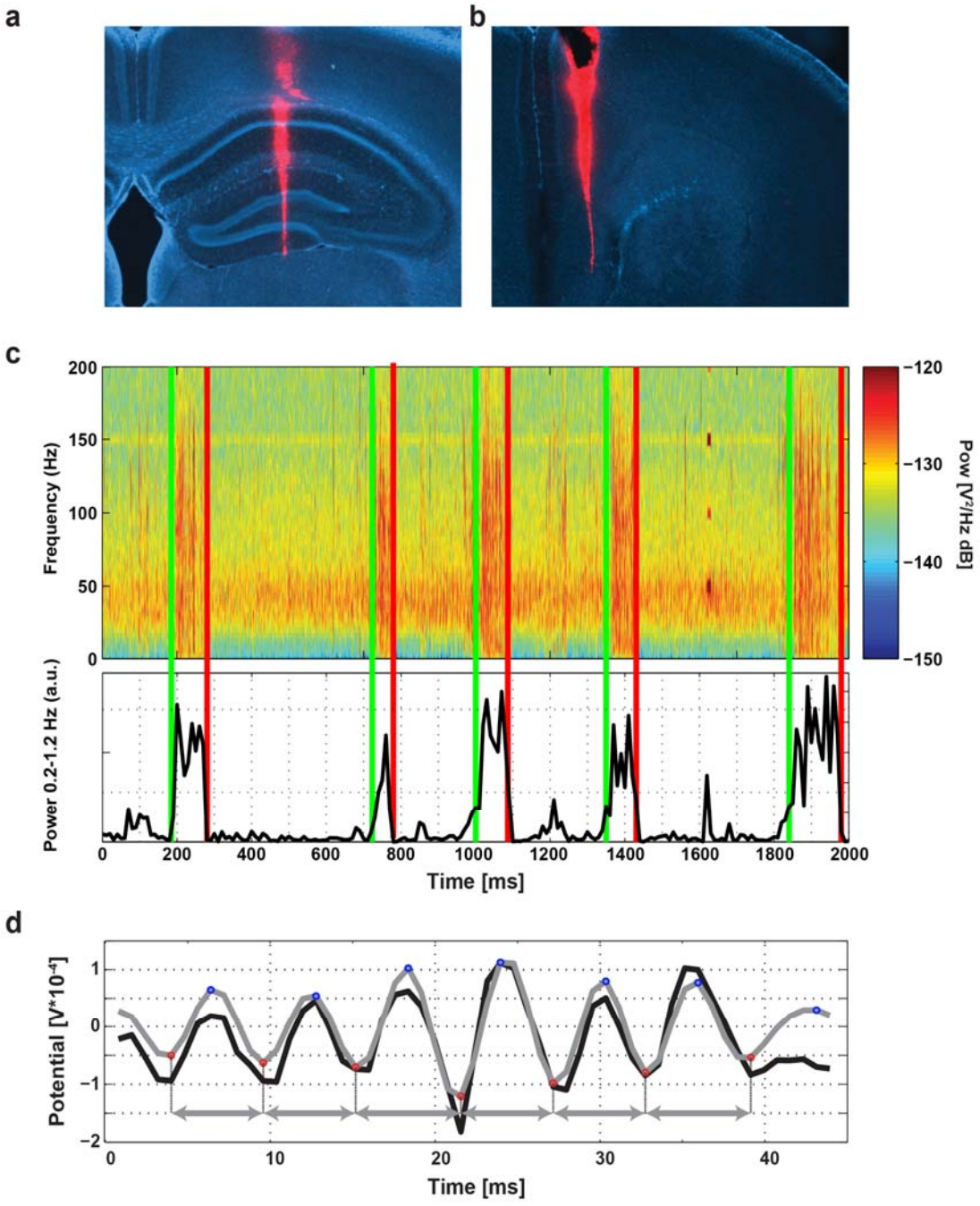

Fig. 2.33 Measurements of local field potentials. a-b, Histological verification of DiI-coated probes for dorsal hippocampus (**a**) and mPFC (**b**) with DAPI staining shown in blue and DiI in magenta. **c,** Spectrogram excerpts from a recording show intermittent high frequency bursts (top). Low frequency (0.2-1.2 Hz) power, indicative for putative SWS epochs, shows an increase in power, during these intermittent bursts (bottom). SWS epochs in this example are marked with start (green) and stop (red) borders. **d,** Parameters from single ripples were calculated as follows. The raw trace (black) was bandpass filtered (Butterworth, 14th order, 100-250 Hz, grey). The ripple amplitude was calculated by subtracting the average voltage of all local minima (red) from the average voltage of all local maxima (blue). The ripple frequency was calculated by taking the average distances between local minima, i.e. the average of all grey arrows. Data was acquired by Jasper Grendel and presented with permission.

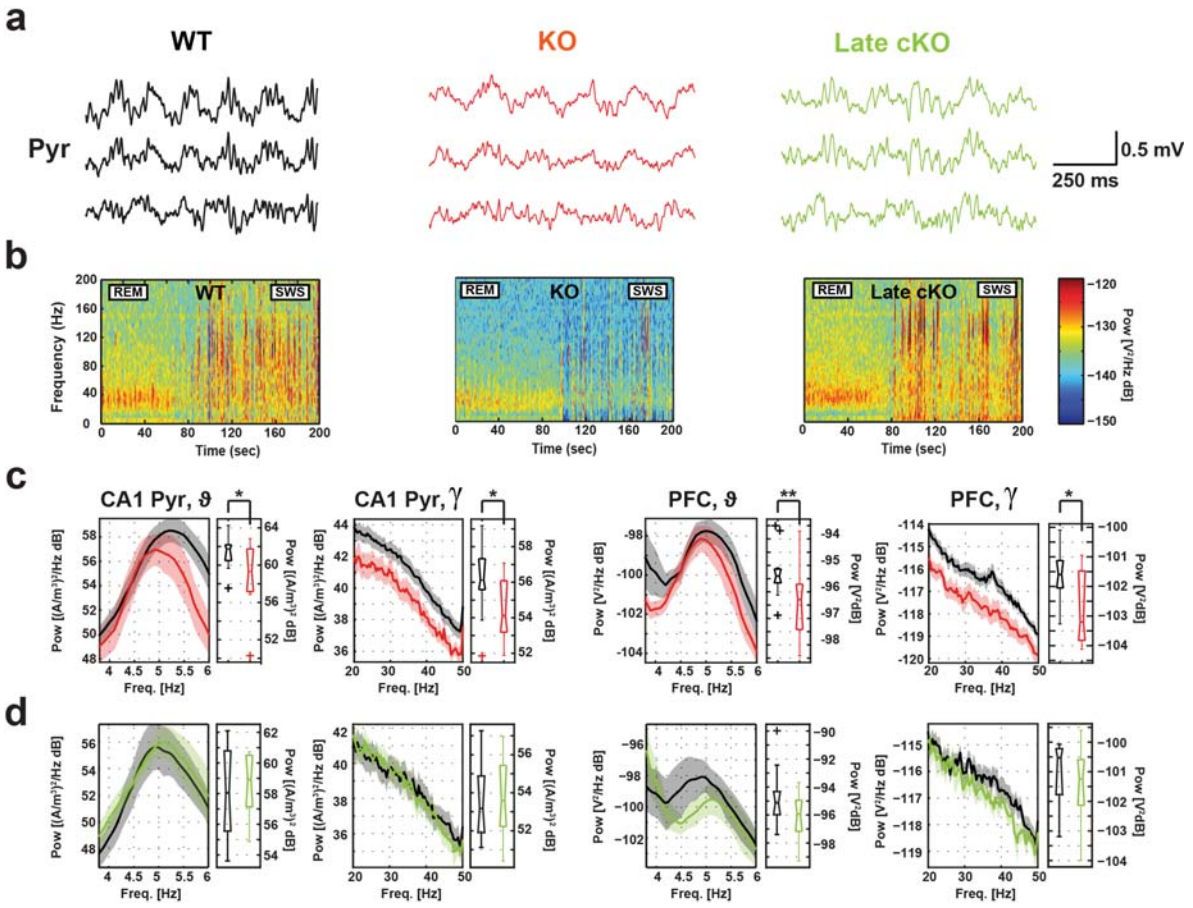

Fig. 2.34 Oscillatory activity in the hippocampus and PFC of KO and Late-cKO mice. a, Exemplary raw traces from hippocampus CA1 str. Pyr (plus one channel above and below) during paradoxical/REM-like sleep state. Oscillations in the theta and gamma frequency band are evident in all three genotypes but are smaller in the KO traces. Genotype is color coded: black: WT-control, red: constitutive KO, green: Late-cKO. **b,** Whitened LFP spectrograms from 200s excerpts of recorded data from str. Pyr, roughly aligned to a transition between a paradoxical sleep and SWS state. Lack of gamma and theta bands is particularly evident in the KO mice. **c-d**, Power spectra from paradoxical REM sleep for both the theta and gamma band in str. Pyr (from the CSD) and PFC (from the LFP) showing mean ± S.E.M., together with their corresponding box plots, showing median, 25th and 75th percentiles (hour glass markers) and outliers (crosses). **c**, All parameters were reduced in the KO (str. Pyr. ϑ, WT 61.8 dB, n = 14, KO 59.3 dB, n = 8 *p < 0.05; str. Pyr γ, WT 56.1 dB, KO 54.1 dB, *p < 0.05; mPFC ϑ, WT -95.4 dB, KO -96.3 dB, **p < 0.01; mPFC γ, WT -101.6 dB, n = 11, KO -103.2 dB, n = 10, *p < 0.05). **d,** Late-cKO exhibit indistinguishable theta and gamma spectra in CA1 str. Pyr and in the mPFC, compared to their WT littermates. (str. Pyr. ϑ, WT-control 58.1 dB, Late-cKO 58.9 dB, p = 0.42; str. Pyr γ, WT-control 53.2 dB, Late-cKO 53.6 dB, p = 0.48, n = 9 and n = 10, for WT-control and Late-cKO, respectively; mPFC ϑ, WT-control -95.1 dB, Late-cKO, -96.0 dB, p = 0.15; mPFC γ, WT-control -101.0 dB, Late-cKO -101.7dB, p = 0.17, n = 10 each for WT-control and Late-cKO). Data was acquired by Jasper Grendel and presented with permission.

2.7.3 Sharp wave activity in the hippocampus of KO and Late-cKO mice

Sharp waves (SPWs) in the CA1 and CA3 regions of the hippocampus *stratum radiatum* accompanied by ripples in the *pyramidal layer* of CA1 are present during immobility and slow-wave sleep (SWS). Sharp wave activities with ripple properties were also determined in urethane anesthetized mice (Fig. 2.35a).

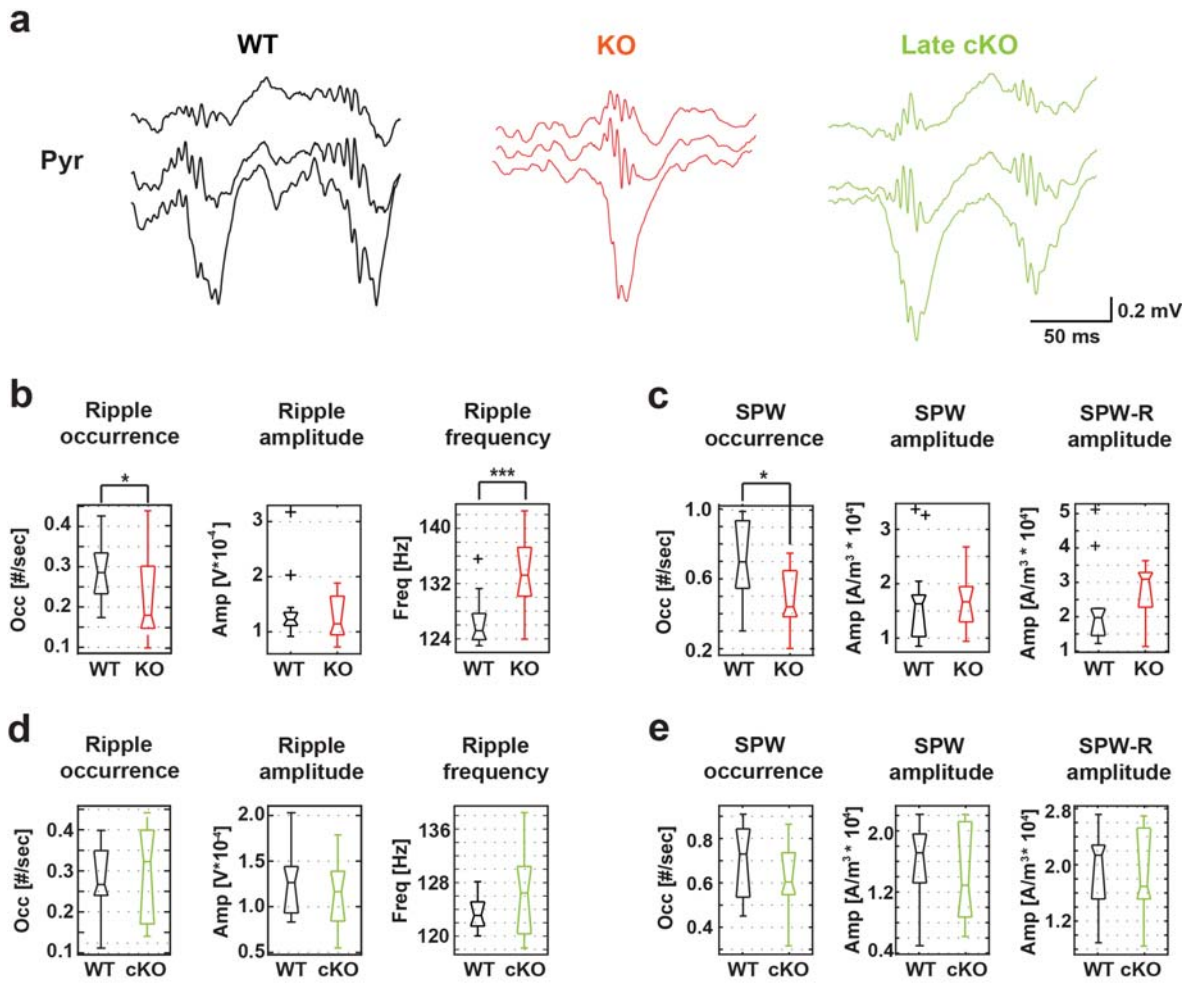

Fig. 2.35 Sharp wave activity in the hippocampus of KO and Late-cKO mice. a, Exemplary raw traces from hippocampus CA1 str. Pyr (plus one channel above and below) during SWS states. Fewer ripples were detected in the KO. Genotype is color coded: black: WT-control, red: constitutive KO, green: Late-cKO. **b-e**, Ripples and SPWs were independently detected and measured from SWS states. Boxplots showing medians, 25th and 75th percentiles (hour glass markers) and outliers (crosses). **b**, KO exhibited reduced ripple occurrence (WT 0.29 s^{-1}, KO 0.18 s^{-1}, *$p < 0.05$), no change in amplitude (WT 1.22 * 10^{-4} V, KO 1.15 * 10^{-4} V, $p = 0.24$) and an increase in frequency (WT 125.2 Hz, KO 133.2 Hz, ***$p < 0.001$). All WT, $n = 14$; KO, $n = 12$. **c,** Occurrence of SPW was reduced (WT 0. 704 s^{-1}, KO 0.44 s^{-1}, *$p < 0.05$) but not their amplitude (WT 1.64 * 10^4 A/m^3, KO 1.67 * 10^4 A/m^3, $p = 0.30$). Amplitudes of SPW co-occurring with ripples (SPW-R) was not significantly changed (WT 1.99 * 10^4 A/m^3, KO 3.10 * 10^4 A/m^3, $p = 0.08$). All WT, $n = 14$; KO, $n = 8$. **d,** In Late-cKO mice ripple occurrence, amplitude and frequency were indistinguishable from WT-control littermates (occurrence, WT-control 0.27 s^{-1}, Late-cKO 0.35 s^{-1}, $p = 0.43$; amplitude, WT-control 1.24 * 10^{-4} V, Late-cKO 1.12 * 10^{-4} V, $p = 0.36$; frequency, WT-control 122.9 Hz, Late-cKO 126.1 Hz). All WT-control, $n = 11$ and Late-cKO, $n = 10$. **e,** Occurrence and amplitudes of SPW and of SPW-R were also similar among WT-control and Late-cKO mice (occurrence, WT-control 0.73 s^{-1}, Late-cKO 0.60 s^{-1}, $p = 0.15$; amplitude, WT-control 1.72 * 10^4 A/m^3, Late-cKO 1.28 * 10^4 A/m^3, $p = 0.44$; SPW-R amplitude, WT-control 2.15 * 10^4 A/m^3, Late-cKO 1.69 * 10^4 A/m^3, $p = 0.35$). Data was acquired by Jasper Grendel and presented with permission.

Significantly fewer ripples and fewer SPWs (occurrence) during SWS phases were observed in the KO mice ($p < 0.05$, Mann Whitney test; Fig. 2.35b-c). In contrast, ripple frequency was significantly increased in the KO mice compared with WT mice ($p < 0.001$, Mann Whitney test; Fig. 2.35b). Remaining ripples and SPWs that were still detected in KO

CA1 *pyramidal layer* and *stratum radiatum*, respectively, were similar in amplitude with their WT counterparts (Fig. 2.35b-c). Consistently, all of the measurements (occurrence, amplitude and frequency) about ripple, SPWs and SPW co-occurring with ripples (SPW-Rs) in the Late-cKO mice were also indistinguishable from those of their WT-control littermates (Fig. 2.35a, d, e), suggesting that Late-cKO can still generate WT-like sharp waves and ripples. Therefore, slow wave activity was disturbed in absence of Arc/Arg3.1 during prenatal development, but was not affected when Arc/Arg3.1 was ablated during late postnatal development.

2.7.4 Oscillatory and sharp wave activity in the hippocampus and prefrontal cortex of Late-cKO$_{2xCre}$ mice

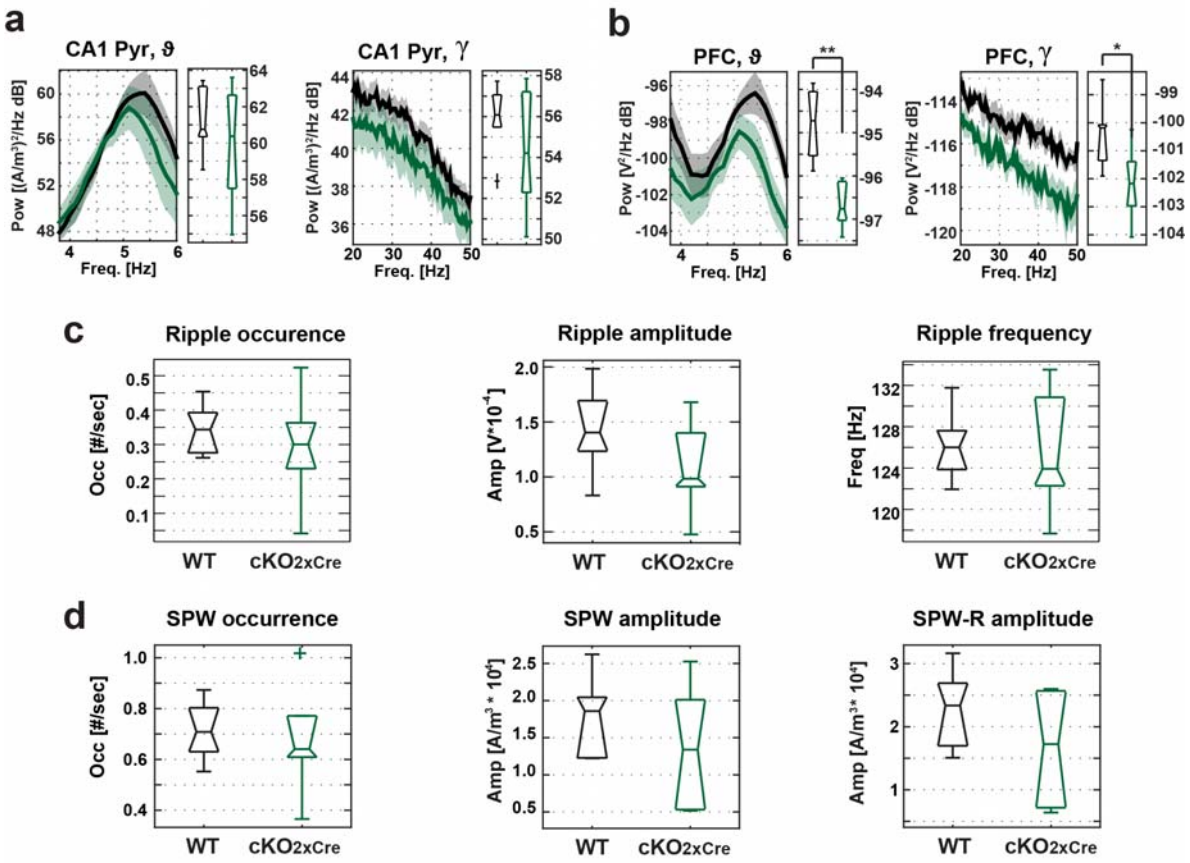

Fig. 2.36 Oscillatory and sharp wave activity in Late-cKO$_{2xCre}$ mice. a, Indistinguishable theta (WT-control 60.8 dB, Late-cKO$_{2xCre}$ 60.4 dB, p = 0.34) and gamma power (WT-control 56.1 dB, Late-cKO$_{2xCre}$ 54.2 dB, p = 0.29) in Str. Pyr of WT-control and Late-cKO$_{2xCre}$ mice. **b,** mPFC oscillations were decreased on both theta (WT-control -94.7 dB, Late-cKO$_{2xCre}$, -96.8 dB, $^{**}p < 0.01$) and gamma power (WT-control -100.2 dB, Late-cKO$_{2xCre}$ -102.2 dB, $^{*}p < 0.05$). **c,** Unchanged ripple occurrence (WT-control 0.34 s^{-1}, Late-cKO$_{2xCre}$ 0.30 s^{-1}, p = 0.24), amplitude (WT-control 1.40 * 10^{-4} V, Late-cKO$_{2xCre}$ 0.98 * 10^{-4} V, p = 0.11) and frequency (WT-control 126.0 Hz, Late-cKO$_{2xCre}$, 123.7 Hz, p = 0.29) in Late-cKO$_{2xCre}$ mice. **d,** Unchanged SPW occurrence (WT-control 0.71 s^{-1}, Late-cKO$_{2xCre}$ 0.64 s^{-1}, p = 0.34) and amplitude (WT-control 1.86 * 10^{4} A/m^{3}, Late-cKO$_{2xCre}$ 1.34 * 10^{4} A/m^{3}, p = 0.15) and SPW-R (WT-control 2.34 * 10^{4} A/m^{3}, Late-cKO$_{2xCre}$ 1.72 * 10^{4} A/m^{3}, p = 0.15) in Late-cKO$_{2xCre}$ mice. Data was acquired by Jasper Grendel and presented with permission.

To exclude the effect of residual Arc/Arg3.1 in adult hippocampus of Late-cKO mice, the same recordings and analysis were performed on Late-cKO$_{2xCre}$ mice. Surprisingly, theta and gamma power in the hippocampal *pyramidal layer* of Late-cKO$_{2xCre}$ mice were still comparable with their WT-control littermates (Fig. 2.36a).

In contrast, significantly reduced theta ($p < 0.01$, Mann Whitney test) and gamma ($p < 0.05$, Mann Whitney test) power were detected in the PFC of Late-cKO$_{2xCre}$ mice (Fig. 2.36b). Meanwhile, the activity events during SWS including ripple occurrence, amplitude and frequency as well as sharp wave properties were indistinguishable between Late-cKO$_{2xCre}$ and WT-control mice (Fig. 2.36c-d). Thus, it further tells us that observed intact hippocampal network activity in the Late-cKO was not due to the protective effects of residual Arc/Arg3.1 in the hippocampus. In general, late postnatal Arc/Arg3.1 ablation does not alter hippocampal network activity. By comparison, dramatically reduced oscillatory activities both in the hippocampus and PFC of KO mice were caused by early Arc/Arg3.1 ablation during early development. Results showed a temporal effect of Arc/Arg3.1 ablation on network activity and indicated Arc/Arg3.1 mediated plasticity plays an essential role in establishing functional neural network during early development. However, reduced oscillatory activities were detected in the PFC of Late-cKO$_{2xCre}$ mice which might also correlate with delayed development of PFC in mice in parallel with delayed Arc/Arg3.1 expression in the PFC compared with that in hippocampus.

Altogether, prenatal ablation of Arc/Arg3.1 significantly reduces oscillatory network activity in the hippocampus and prefrontal cortex, dramatically attenuates hippocampal plasticity and therefore strongly impairs spatial learning and explicit long-term memory consolidation. In stark contrast, late postnatal removal of Arc/Arg3.1 leaves hippocampal oscillatory network activity and spatial learning largely intact, whereas, long-term explicit memories are still significantly impaired. In addition, residual Arc/Arg3.1 in the hippocampus, especially in the DG, protracts long-term synaptic plasticity together with intact hippocampal oscillatory network activity contributes to the prolonged explicit memory persistence. Meanwhile, the observed reduced theta and gamma power in the PFC might be one of the causes of earlier explicit memory deficits in Late-cKO$_{2xCre}$ mice. Collectively, intact hippocampal network activity and spatial learning strictly rely on the presence of Arc/Arg3.1 during early development (prenatal or early postnatal) of the brain. Arc/Arg3.1 expression during late postnatal development is not necessary for establishing and maintaining functional hippocampal network, but is still critical for long-term explicit memory consolidation in adulthood.

Part III Dependence of memory consolidation on spatial Arc/Arg3.1 expression in hippocampal-cortical networks

2.8 Effects of brain region-specific Arc/Arg3.1 ablation on contextual fear memory consolidation and retrieval

It has become clear that close communication between hippocampus and cortex is essential for formation and consolidation of spatial and episodic-like memories. Understanding how this communication leads to memory formation and what the physical equivalents of information storage are, remain a great challenge. Furthermore, so far it is not known whether memory consolidation in the hippocampus is similar in the cortex and if continuous reconsolidation in the hippocampus is essential for LTM even when cortical representations already exist. In the first part of this thesis, I already showed that late postnatal Arc/Arg3.1 ablation in the forebrain (including hippocampus and cortical regions) impaired LTM consolidation in mice, demonstrating the essential role of Arc/Arg3.1 in LTM consolidation in adulthood. To further explore the role of Arc/Arg3.1 mediated synaptic plasticity in specific brain regions in memory formation, consolidation and retrieval, I employed rAAV-Cre mediated local Arc/Arg3.1 ablation by injection in either hippocampus or cortical regions of the Arc/Arg3.1$^{f/f}$ mice. By taking this strategy, I utilize Arc/Arg3.1 as a molecular tool and try to investigate where, when and how memories are encoded, consolidated and stored at various time, and ultimately try to elucidate the dependence of memory consolidation on synaptic consolidation in the hippocampal-cortical networks.

2.8.1 rAAV-Cre mediated Arc/Arg3.1 ablation in mice *in vivo*

To achieve local Arc/Arg3.1 ablation in the brain *in vivo*, a target viral vector in which Cre expression is driven by CaMKIIα promoter (rAAV-CaMKIIα-Cre) was constructed and purified. A rAAV-CaMKIIα-GFP vector was likewise generated and used as sham control to preclude possible side effects which might be induced by over-expression of Cre recombinase in neurons. To test the quality and efficiency of recombination, purified viral vectors were unilaterally injected into the hippocampus of Arc/Arg3.1$^{f/f}$ mice. 7 days after injection, seizures were induced by administrating Kainate to the injected mice. 2 hours after seizure onset, mice were euthanized and perfused with 4% paraformaldehyde (PFA). Brain was removed and sectioned for IHC.

Immunostaining against Cre recombinase and GFP fluorescence revealed that viruses diffused broadly and rAAV carrying genes were nicely expressed in the injected hippocampus. In parallel, Arc/Arg3.1 protein was strongly reduced in the rAAV-CaMKIIα-Cre injected hippocampus. Arc/Arg3.1 expression in the rAAV-CaMKIIα-GFP injected hippocampus was not affected in comparison with the non-injected hemisphere (Fig. 2.37). In order to control for possible cytoxicity induced either by gene over-expression or by rAAV injection, an apoptotic marker, cleaved caspase-3 was detected by antibody. No difference

was observed between injected and non-injected hippocampi, indicating that no clear cytotoxicity was induced in the hippocampus after 7 days of viral infection (Fig. 2.37).

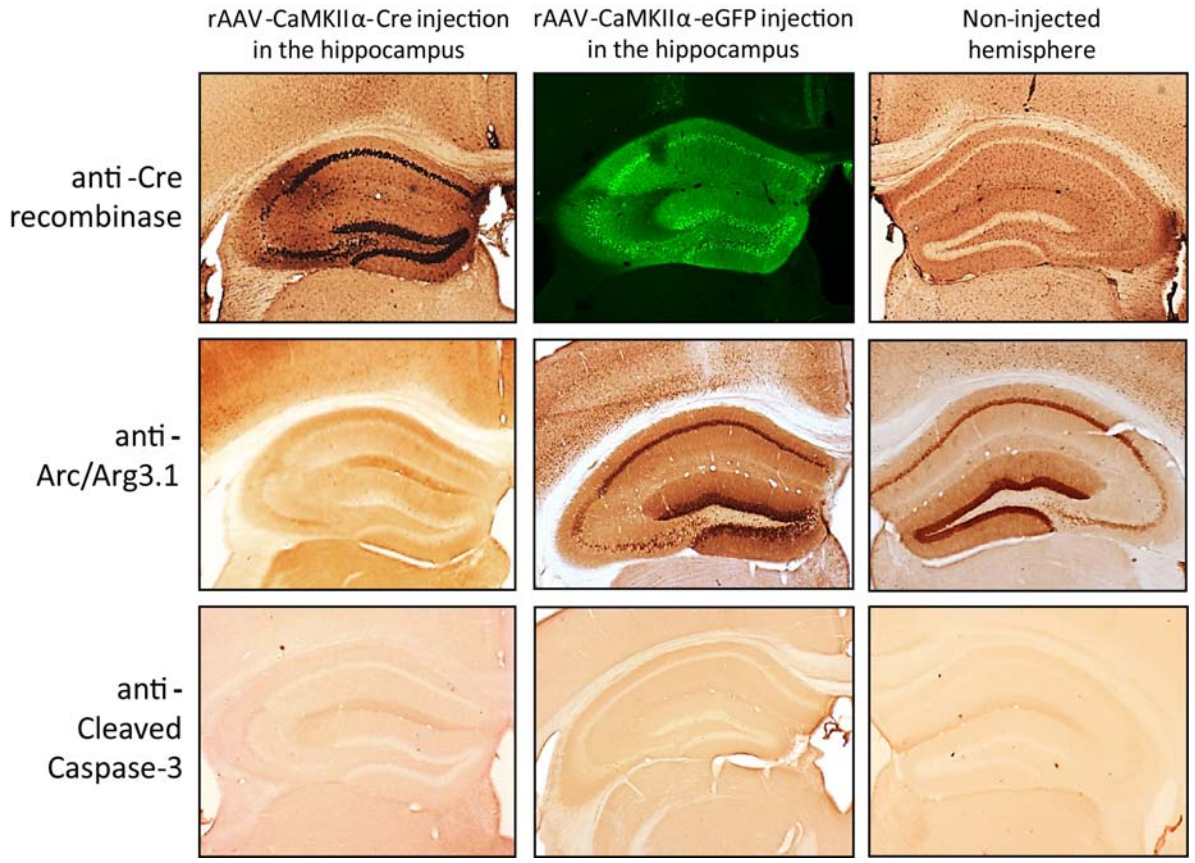

Fig. 2.37 rAAV harbored gene expression and Cre mediated Arc/Arg3.1 ablation in the hippocampus *in vivo*. Upper, rAAV harbored genes (Cre recombinase and GFP) were widely expressed and diffused in the injected hippocampus; **Middle,** Arc/Arg3.1 was well ablated in in the rAAV-Cre injected hippocampus; **Lower,** No clear cytotoxicity was detected as indicated by a cell apoptotic marker Cleaved Caspase-3. Immunohistochemistry was performed on hippocampal slices after Kainate-induced seizures. The non-injected hemisphere was used as negative control.

To examine the time window of rAAV-Cre mediated Arc/Arg3.1 ablation in the mouse brain *in vivo*, a group of mice were injected in the hippocampus unilaterally. Seizures were induced and brains were collected at different time delays after injection and sectioned for IHC. Cre expression and consequent Arc/Arg3.1 ablation started around 3 days after injection, and proceeded within 5 days. Seven days after injection, Cre was highly expressed in the injected hippocampus and Arc/Arg3.1 was nearly absent, in contrast to its strong expression in non-injected regions such as the contralateral hippocampus and the cortex. Importantly, rAAV-Cre mediated Arc/Arg3.1 ablation in adult mouse brain *in vivo* did not induce clear cytotoxicity within 7 days as shown by the apoptotic marker, cleaved caspase-3 (Fig. 2.38). Thus, these two viral vectors were proven to be effective, specific and also non-toxic for the duration of 2 weeks. Since rAAV-Cre mediated Arc/Arg3.1 ablation was already complete within 7 days, all of the following experiments were performed 7 days after injection.

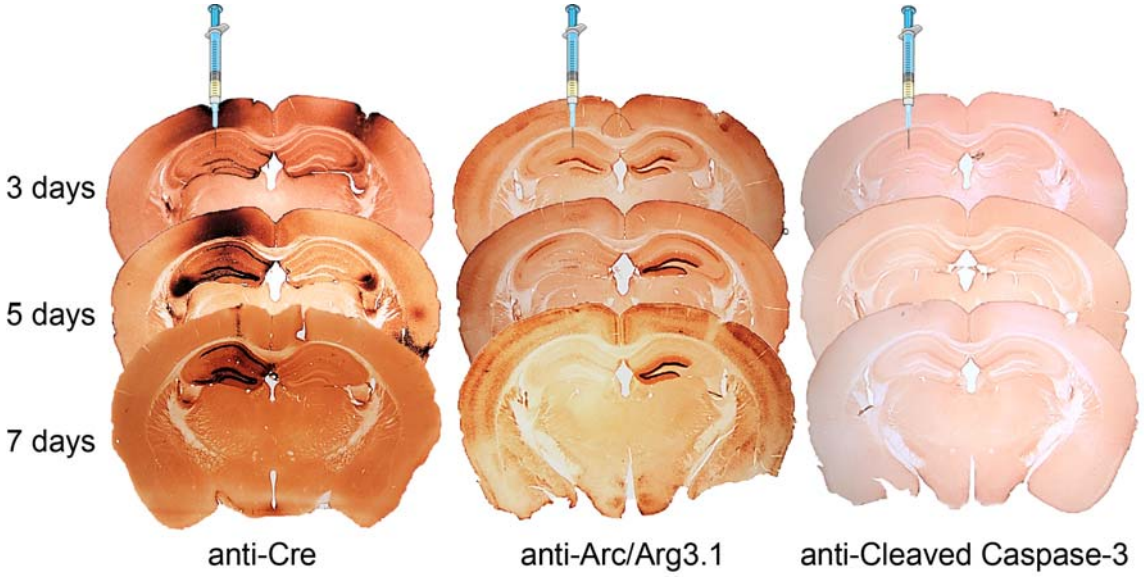

Fig. 2.38 Time window of rAAV-Cre mediated Arc/Arg3.1 ablation in the mouse brain *in vivo*. rAAV-Cre was injected in one hemisphere of the hippocampi. Cre expression, Arc/Arg3.1 ablation and Cleaved Caspase-3 were determined by using anti-Cre, anti-Arc/Arg3.1 and anti-Cleaved Caspse-3 antibody, separately. Immunohistochemistry performed on brain slices after kainate-induced seizures showed that Cre expression and Arc/Arg3.1 ablation already started 3 days after injection and proceeded in 5 days. By day 7, Cre was highly expressed in the injected hippocampus and Arc/Arg3.1 was already strongly reduced in comparison with the non-injected hemisphere of hippocampus and other cortical regions. Cre mediated Arc/Arg3.1 ablation in adult mouse brain *in vivo* did not induced clear cellular toxicity within 7 days as shown by the absence of the apoptotic marker Cleaved Caspase-3.

Furthermore, double staining with anti-Cre/CaMKIIα, anti-Cre/GFAP and anti-Cre/Iba-1 antibodies showed that Cre was specifically expressed in the CaMKIIα positive neurons but not in astrocytes or microglia (Fig. 2.39).

2.8.2 Contextual fear memory after local Arc/Arg3.1 ablation in the hippocampus

Hippocampus is widely considered as one of the most important regions involved in fast formation of memory and in its later consolidation, especially for episodic memories. However, the specific role of the hippocampus in LTM consolidation is still controversial. The standard hypothesis posits a time limited role of the hippocampus in LTM and holds that the hippocampus is not essential for remote memory consolidation (Alvarez and Squire, 1994; McClelland et al., 1995; Squire, 2004; Frankland and Bontempi, 2005). In contrast, a growing number of studies report that hippocampal disruption can affect both recent and remote LTM, indicating that the hippocampus also participates in remote memory processing (Viskontas et al., 2000; Lehmann et al., 2007; Goshen et al., 2011; Winocur et al., 2013). To address these hypotheses, I relied on the specificity and indispensability of Arc/Arg3.1 to memory formation.

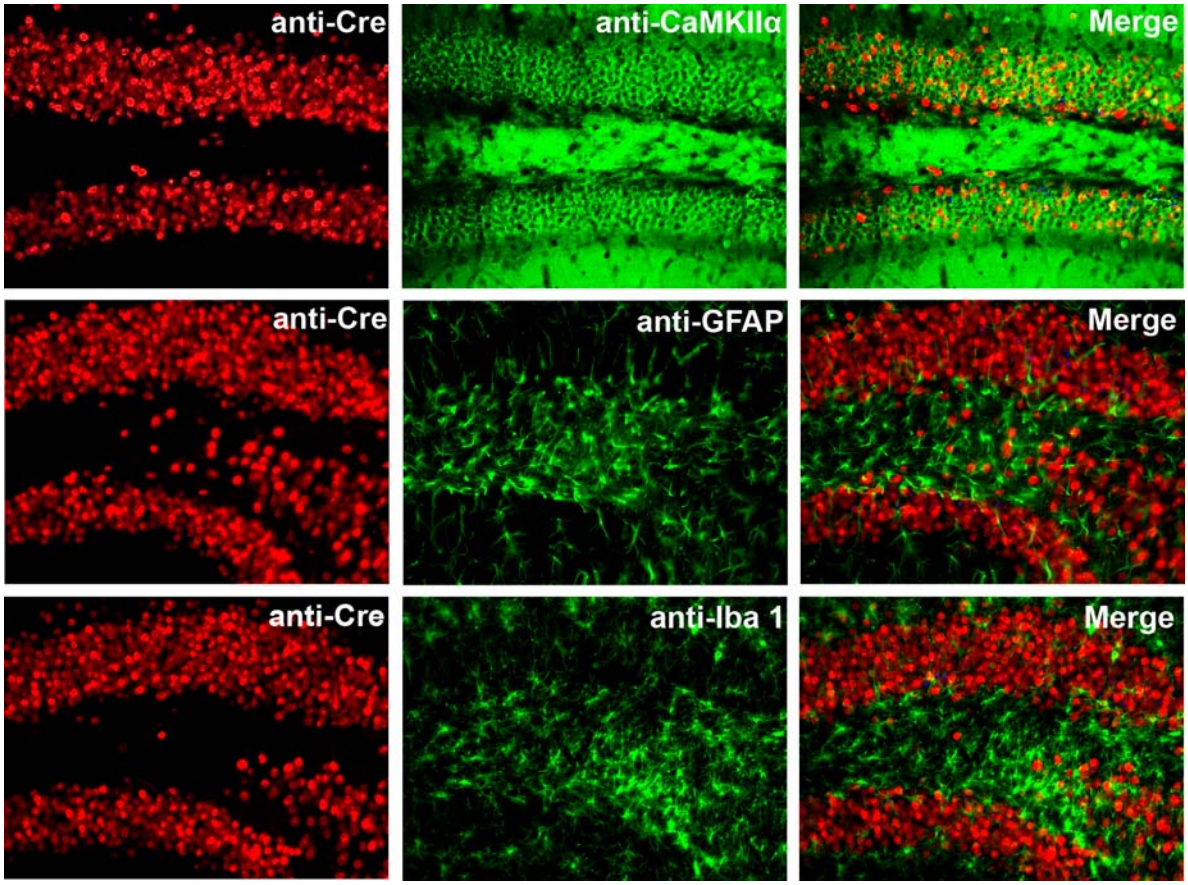

Fig. 2.39 Cell type specific Cre recombinase expression in the hippocampus *in vivo*. Double staining with different cell type markers showed that Cre recombinase expression driven by CaMKIIα promoter was only expressed in the CaMKIIα positive principal neurons (upper) not in astrocytes (GFAP as a marker, middle) or microglia (Iba-1 as a marker, lower). Images were taken under 20X objective.

I bilaterally injected rAAV-Cre in the hippocampus of Arc/Arg3.1$^{f/f}$ and WT mice to locally ablate Arc/Arg3.1 in the hippocampus and explore the role of hippocampus in LTM consolidation. The injected mice were termed “HPC-cKO” and “WT-control”, respectively. As sham control, a group of Arc/Arg3.1$^{f/f}$ mice were injected with rAAV-GFP, termed “GFP-control” (Fig. 2.40a). Seven days after injection, I subjected mice to a fear conditioning stimulus (0.5 mA foot shock) associated with a specific context and tone. Long-term contextual fear memory was assessed at different time delays (Fig. 2.40b, e). All injected mice exhibited strong freezing immediately after foot shocks, indicating successful induction of fear (Fig. 2.40c-d). When tested 3 or 7 days after conditioning, WT-control and GFP-control mice exhibited strong freezing in the conditioning environment, indicating that they properly formed, consolidated and successfully retrieved memory of the context and the shocks. Surprisingly, HPC-cKO mice also showed strong freezing in the context which was comparable to WT-control or GFP-control (Fig. 2.40f-g). No significant difference was observed between groups, indicating successful contextual fear memory retrieval even 7 days after acquisition despite of removal of Arc/Arg3.1 from the hippocampus. Since GFP-

control mice behaved similarly to WT-control mice, this control group was omitted from the second cohort of injection. Independent groups of mice were injected and used for each test time point.

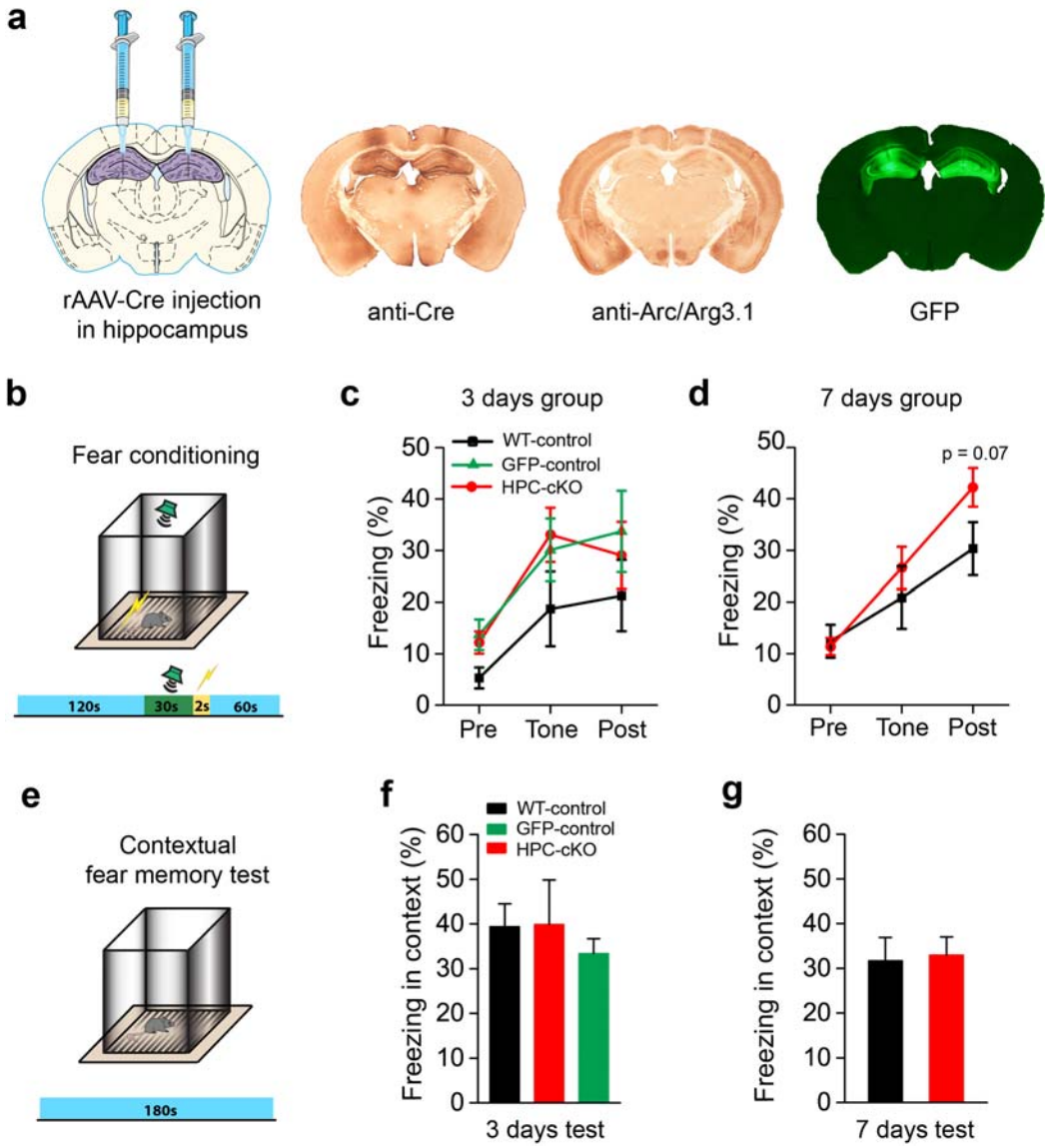

Fig. 2.40 Intact contextual fear memory retrieval after rAAV-Cre mediated Arc/Arg3.1 ablation in the hippocampus. a, rAAV-Cre or rAAV-GFP was injected in the hippocampus. Immunostaining showed that Cre recombinase and GFP were expressed throughout the dorsal hippocampus and Arc/Arg3.1 was completely removed. **b,** Schematic of contextual fear conditioning paradigm and protocol. Mice were conditioned by a pair of mild foot shocks (0.5 mA) applied together with a tone (10k Hz, 70 dB). **c-d,** Average percent freezing during fear acquisition phase. HPC-cKO mice showed non-significantly higher percent freezing immediately after foot shocks. **e,** Schematic of contextual fear memory retrieval paradigm and protocol. Contextual fear memory was tested 3 days and 7 days after conditioning, each time point with a separate group of mice. **f,** Similar freezing of WT-control, GFP-control and HPC-cKO mice in the context 3 days after conditioning (WT-control, 39.41 ± 5.08%; *n* = 6 and HPC-cKO, 39.91 ± 9.9%; *n* = 7; GFP-control, 33.4 ± 3.28%; *n* = 6, One-way ANOVA with a *post hoc* LSD test, NS). **g**, Even 7 days after acquisition WT-control and HPC-cKO mice exhibited similar percent freezing in the context (WT-control, 31.74 ± 5.17%; *n* = 10 and HPC-cKO, 33.01 ± 4.02%; *n* = 14; t_{22} = -0.2, *p* = 0.85, NS). Bars show mean ± S.E.M. Significance was tested with two-tailed two-sample *t*-test between genotypes.

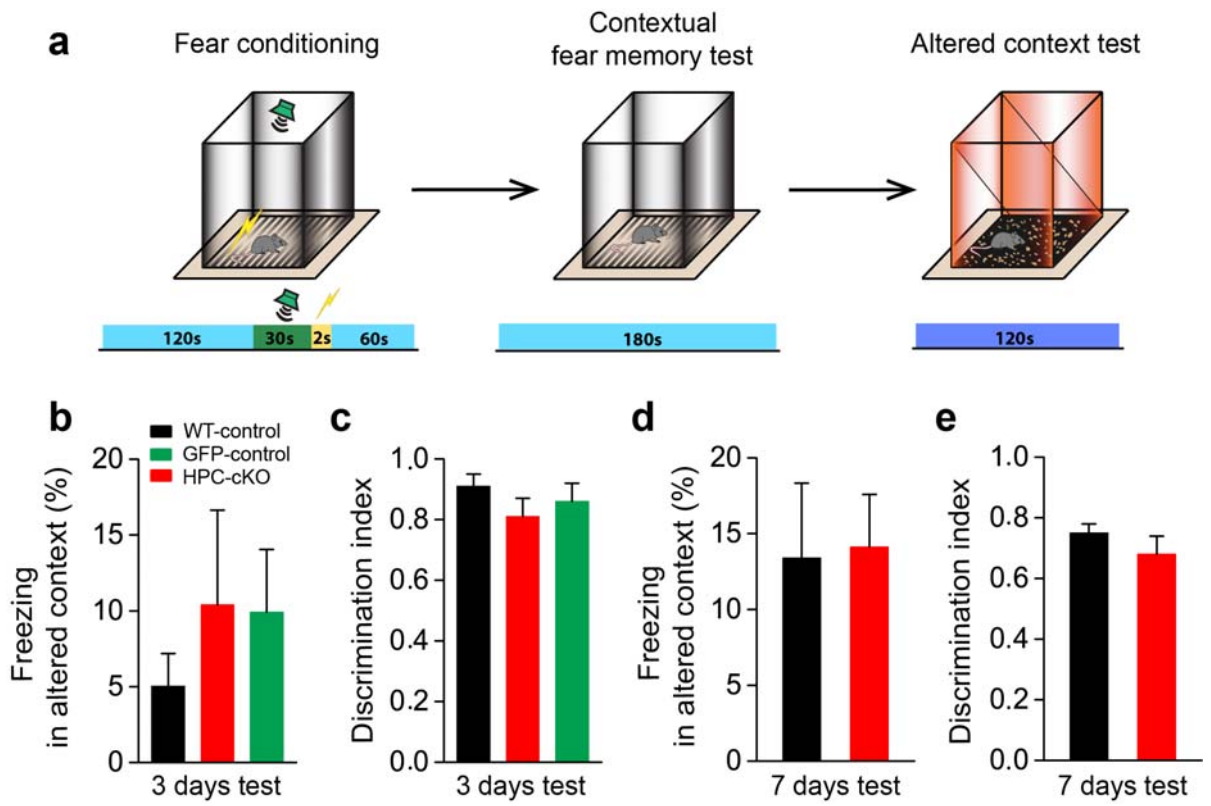

Fig. 2.41 Unaltered specificity of contextual fear memory after rAAV-Cre mediated Arc/Arg3.1 ablation in the hippocampus. a, Schematic of contextual fear conditioning and memory test paradigm. **b-e,** Memory specificity was not altered in HPC-cKOmice within a week after acquisition. **b,** Percent freezing in the altered context 3 days after conditioning was not significantly different between WT-control, GFP-control and HPC-cKO (WT-control, 5.04 ± 2.15%; *n* = 6 and HPC-cKO, 10.40 ± 6.24%; *n* = 7; GFP-control, 9.90 ± 4.15%; *n* = 6, , NS). **c** Similar discrimination index for all mice 3 days after conditioning (WT-control, 0.91 ± 0.04; *n* = 6 and HPC-cKO, 0.86 ± 0.06; *n* = 7; GFP-control, 0.81 ± 0.06; *n* = 6, NS). **d,** Percent freeing in altered context was similar in all groups 7 days after conditioning (WT-control, 13.39 ± 4.94%; *n* = 10 and HPC-cKO, 14.11 ± 3.48%; *n* = 14; t_{22} = -0.12, *p* = 0.90, NS). **e,** Discrimination index for WT-control and HPC-cKO was similar 7 days after conditioning (0.75 ± 0.03; *n* = 10 and 0.68 ± 0.06; *n* = 14; respectively, t_{22} = 0.86, *p* = 0.40, NS). Bars show mean ± S.E.M. Significance was tested with One-way ANOVA with a *post hoc* LSD test between genotypes or with two-tailed two-sample *t*-test when there were only two groups.

To evaluate the quality of the recalled contextual memory, I then assessed memory specificity by placing mice in an altered context which was different in its geometrical, olfactory and visual characteristics from the conditioning context. Mice with intact and precise memory are expected to recognize the differences between the conditioning and altered contexts and do not freeze in the altered context (Fig. 2.41a). Freezing level was calculated and compared between groups. To check whether and how good mice can distinguish the altered context from the conditioning context, a discrimination index was presented as: %context freezing / (%context freezing + %altered context freezing). Not only control mice but also HPC-cKO mice were able to distinguish between the altered and the conditioning contexts, as indicated by comparable percent freezing (Fig. 2.41b, d) and

discrimination index (Fig. 2.41c, e) either 3 days or 7 days after conditioning. This suggests that HPC-cKO not only can retrieve fear memory but also can retrieve it specifically, like WT-control or GFP-control mice. It means that local Arc/Arg3.1 ablation in the adult hippocampus does not affect the specificity of recalled long-term contextual fear memory within 7 days.

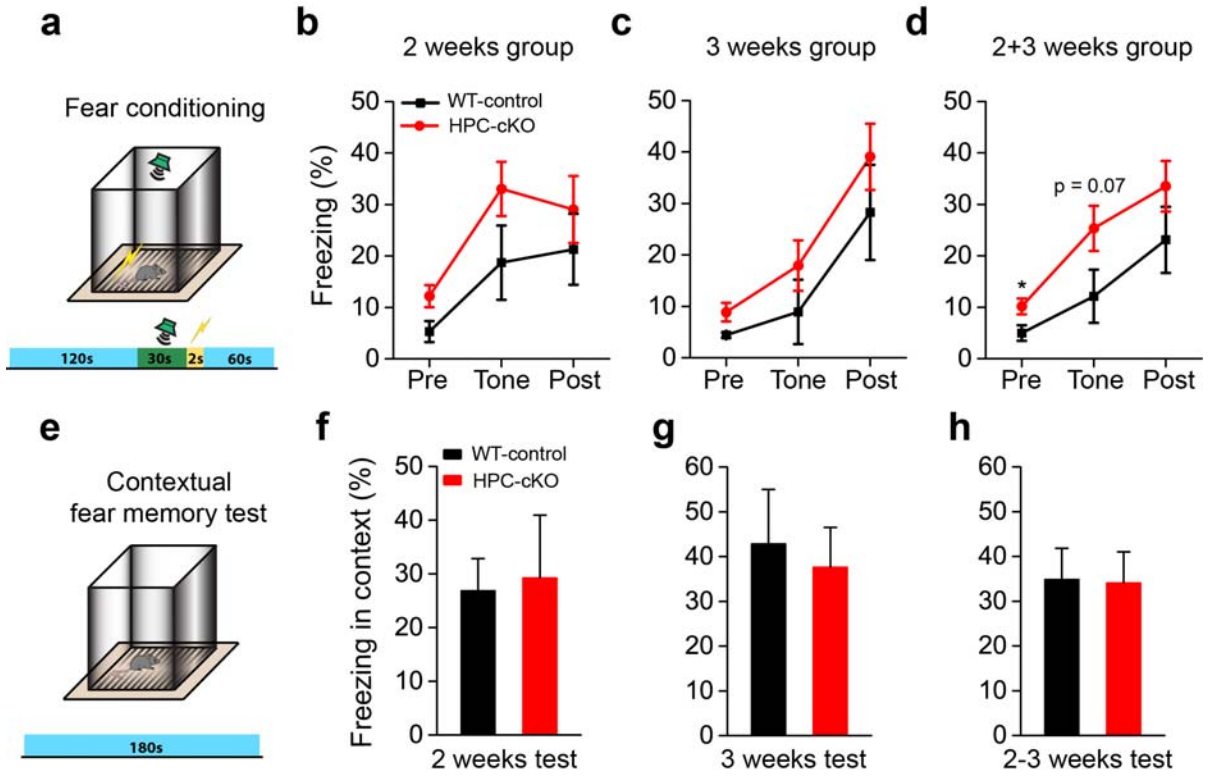

Fig. 2.42 Successful remote contextual fear memory retrieval after rAAV-Cre mediated Arc/Arg3.1 ablation in the hippocampus. a, Schematic of contextual fear conditioning paradigm and tests. **b-d,** Average percent freezing during fear acquisition phase. HPC-cKO mice showed higher but not significant level of freezing after foot shock. **e,** Schematic of contextual fear memory retrieval paradigm and protocol. Remote contextual fear memory was tested 2 or 3 weeks post conditioning. **f-h,** Similar freezing of WT-control and HPC-cKO mice in the context 2 weeks and 3 weeks post conditioning. **f,** 2 weeks context (WT-control, 26.91 ± 5.93%; *n* = 4 and HPC-cKO, 29.30 ± 11.63%; *n* = 5; Mann-Whitney test, *p* = 0.9, NS). **g,** 3 weeks context (WT-control, 42.88 ± 12.12%; *n* = 4 and HPC-cKO, 37.64 ± 8.86%; *n* = 7; Mann-Whitney test, *p* = 0.79, NS). **h,** 2-3 weeks context (WT-control, 34.89 ± 6.94%; *n* = 8 and HPC-cKO, 34.16 ± 6.85%; *n* = 12; t_{18} = 0.07, two-sample *t*-test, *p* = 0.94, NS). Bars show mean ± S.E.M. Significance was tested with Mann-Whitney or two-tailed two-sample *t*-test.

To further test the effects of local Arc/Arg3.1 ablation in adult hippocampus on LTM consolidation and retrieval and to further reveal the role of hippocampus during remote memory consolidation, two additional cohorts of mice were injected and tested 2 weeks or 3 weeks after fear conditioning, respectively. HPC-cKO mice consistently displayed slightly higher but not significant percent freezing after foot shocks during conditioning (Fig. 2.42a-d). Interestingly, HPC-cKO mice showed similar percent freezing compared with WT-control in the context, suggesting successful retrieval of remote memory (Fig. 2.42e-h).

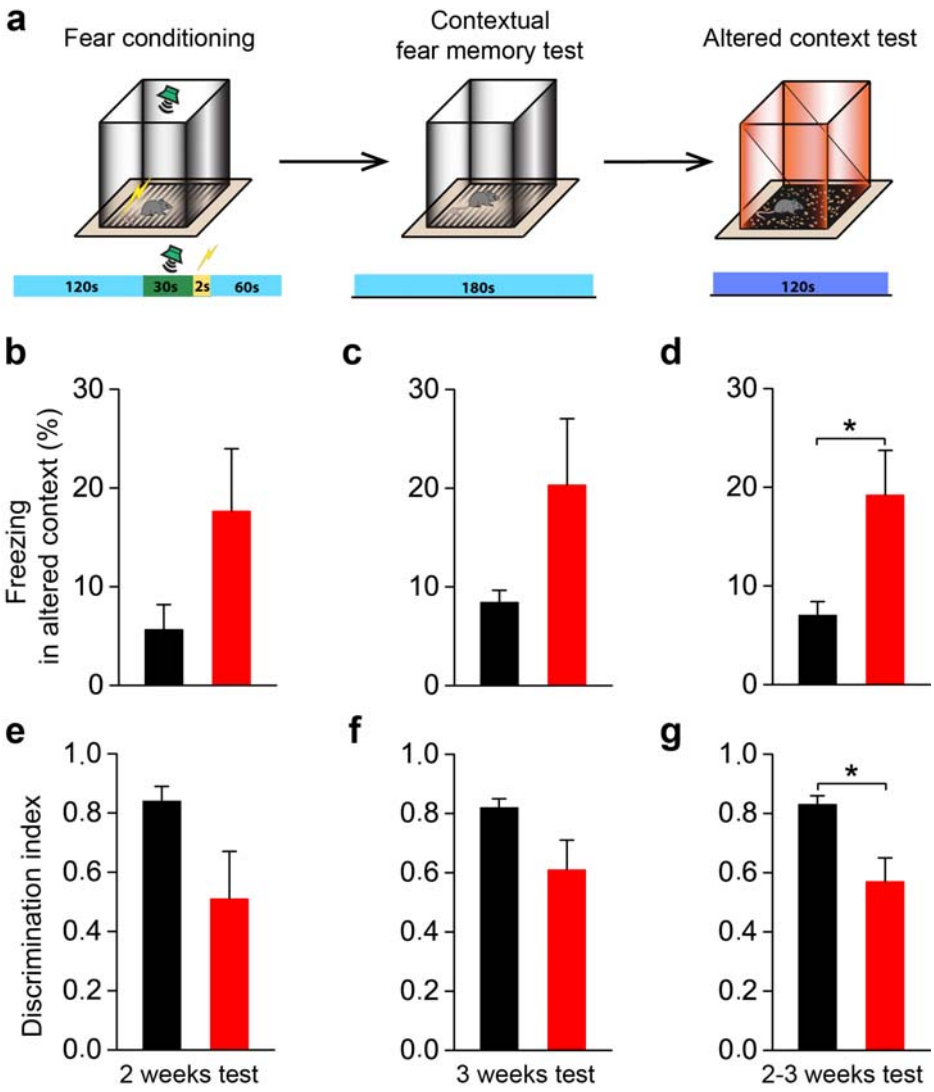

Fig. 2.43 Reduced specificity of remote contextual fear memory after rAAV-Cre mediated Arc/Arg3.1 ablation in the hippocampus. a, Schematic of contextual fear conditioning and memory test paradigm and protocol. **b-g,** HPC-cKO mice displayed progressively reduced memory specificity as indicated by significantly higher freezing in the altered context and lower discrimination index 2-3 weeks after conditioning. **b,** 2 weeks altered context (WT-control, 5.65 ± 2.55%; *n* = 4 and HPC-cKO, 17.65 ± 6.33%; *n* = 5; Mann-Whitney test, *p* = 0.19, NS). **e,** 2 weeks discrimination index (WT-control, 0.84 ± 0.04; *n* = 4 and HPC-cKO, 0.51 ± 0.16; *n* = 5; Mann-Whitney test, *p* = 0.11, NS). **c,** 3 weeks altered context (WT-control, 8.42 ± 1.23%; *n* = 4 and HPC-cKO, 20.31 ± 6.72%; *n* = 7; Mann-Whitney test, *p* = 0.07, NS). **f,** 3 weeks discrimination index (WT-control, 0.82 ± 0.03; *n* = 4 and HPC-cKO, 0.61 ± 0.10; *n* = 7; Mann-Whitney test, *p* = 0.11, NS). **d,** 2-3 weeks altered context (WT-control, 7.03 ± 1.41%; *n* = 8 and HPC-cKO, 19.20 ± 4.54%; *n* = 12; t_{18} = -2.13; two-sample *t*-test, **p* < 0.05). **g,** 2-3 weeks discrimination index (WT-control, 0.83 ± 0.03; *n* = 8 and HPC-cKO, 0.57 ± 0.08; *n* = 12; t_{18} = 2.47, **p* < 0.05). Bars show mean ± S.E.M. Significance was tested with Mann-Whitney or two-tailed two-sample *t*-test.

Remarkably, HPC-cKO mice produced higher levels of freezing in the altered context (2 weeks, *p* = 0.19; 3 weeks, *p* = 0.07; Mann Whitney test; Fig. 2.43b-c) accompanied by lower discrimination index of context and altered context (2 weeks, *p* = 0.11; 3 weeks, *p* = 0.11; Mann Whitney test; Fig. 2.43e-f). These effects became statistically significant when data

from these two cohorts were pooled together to increase the number of the subjects and enhance the statistical test power (freezing level and discrimination index both $p < 0.05$, two-sample *t*-test; Fig. 2.43d, g).

These data indicate that HPC-cKO mice could not well distinguish the altered context from the conditioning context even though they could still to some extent, retrieve acquired fear memory. This implies that ablation of Arc/Arg3.1 in the adult hippocampus reduces specificity of remote contextual fear memory and suggests that detailed information of the contexts characteristics might be still stored in the hippocampus. Arc/Arg3.1 mediated synaptic plasticity in the hippocampus should play an important role in the process of storage.

2.8.3 Hippocampal synaptic plasticity after local Arc/Arg3.1 ablation in the hippocampus

LTP is widely considered as one of the cellular mechanisms underlying memory consolidation. It was impaired in conventional Arc/Arg3.1 KO mice which also exhibited memory deficits. Acutely blocking Arc/Arg3.1 mRNA translation by intrahippocampal infusion of an Arc/Arg3.1 antisense ODNs also attenuated LTP in the adult rats (Guzowski et al., 2000). However, it is still unclear whether genetic removal of Arc/Arg3.1 gene in the adult hippocampus can disturb LTP consolidation or not. It is still not clear whether Arc/Arg3.1 is required for synaptic consolidation in adulthood? To answer this question, I injected a group of mice with rAAV-Cre in the hippocampus (Fig. 2.44a). 7 days after virus injection, *in vivo* field recordings were performed in the hippocampal DG of WT-control and HPC-cKO mice by stimulating perforant path (PP) fibers from the entorhinal cortex. To evaluate the effects of local Arc/Arg3.1 ablation in the adult hippocampus on basic functions of synaptic transmission, IO curves were first generated by applying stepwise increasing currents. Synapses in the PP-DG pathway of HPC-cKO mice generated similar responses to the electrical stimulus compared to WT-control mice as indicated by the overlapping IO curves of the fEPSP slope. Since the fEPSP reflects mostly the number of activated synapses and their strength, these results also implicate similar synaptic numbers and strength in both WT-control and HPC-cKO mice (Fig. 2.44c). Population spike (PS) induced by the synaptic stimulations is the extracellularly recorded field action potentials of the granular neurons. Granule cells in the DG of HPC-cKO or WT-control mice responded similarly to the electrical stimulation. Indistinguishable IO curves of the PS amplitude were generated in both WT-control and HPC-cKO mice, suggesting that comparable numbers of neurons were activated and fired synchronously when the same stimulus was applied (Fig. 2.44d). These data suggest that genetic removal of Arc/Arg3.1 in the hippocampus did not alter basic neural properties or synaptic transmission.

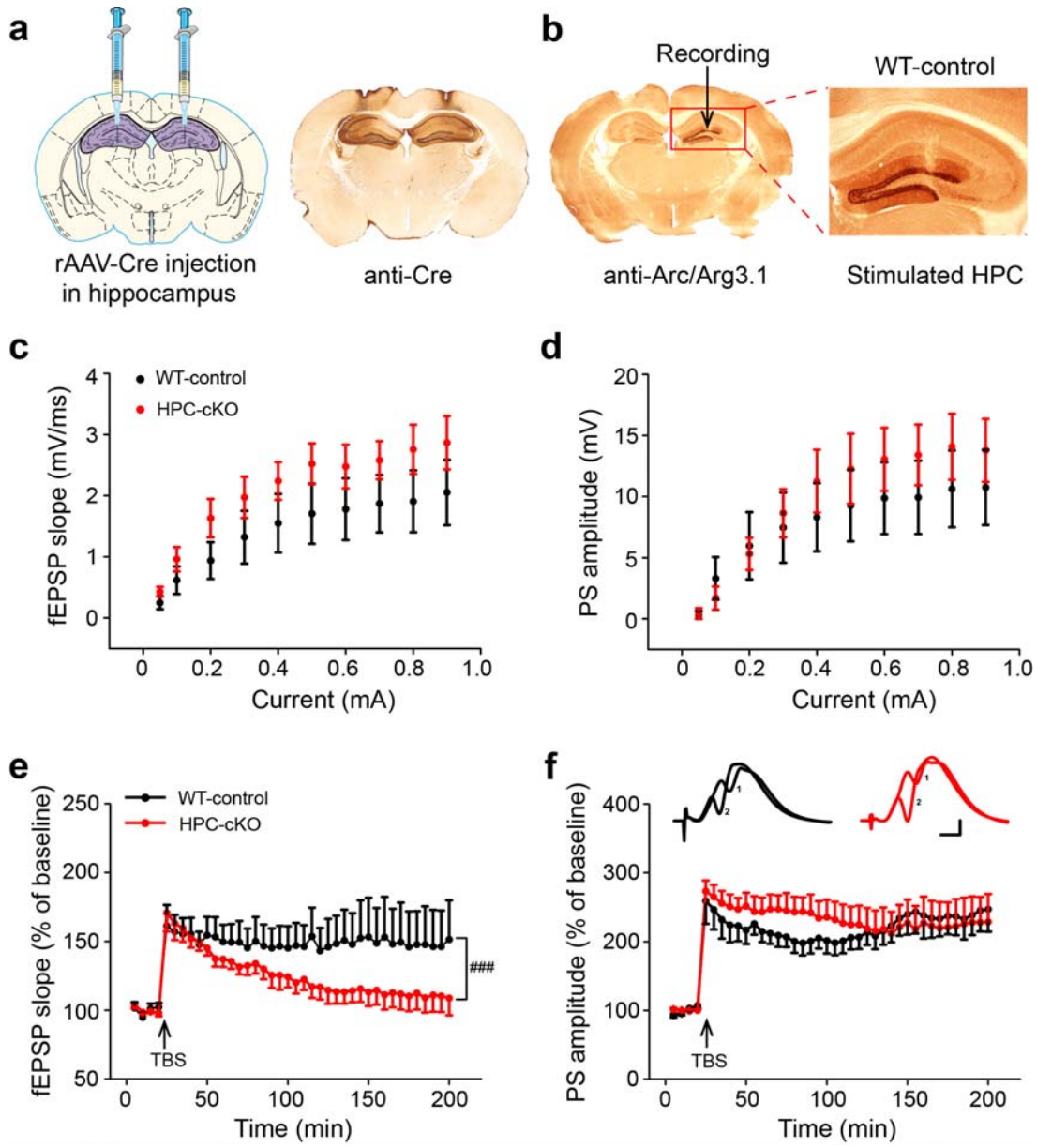

Fig. 2.44 Impaired hippocampal synaptic plasticity after rAAV-Cre mediated Arc/Arg3.1 ablation. **a,** Immunostaining showed that Cre recombinase was very strongly expressed in both injected hippocampi 7 days after injection. **b,** Arc/Arg3.1 protein was highly induced in the stimulated dentate gyrus of a WT-control mouse by stimulating the perforant fibers with theta-burst stimulation in the entorhinal cortex. **c-d,** Basic synaptic transmission was not different between WT-control and HPC-cKO mice as indicated by input/output (I/O) curves of the fEPSP slope and PS amplitude plotted as a function of stimulus intensities. fEPSP slope (**c,** Genotype $F_{(1,10)} = 1.67$, $p = 0.23$, NS; Current intensity $F_{(9, 90)} = 44.35$, $p < 0.0001$; interaction $F_{(9, 90)} = 0.99$, $p = 0.45$, NS). PS amplitude (**d,** Genotype $F_{(1,10)} = 0.34$, $p = 0.57$, NS; Current intensity $F_{(9, 90)} = 27.99$, $p < 0.0001$; interaction $F_{(9, 90)} = 1.37$, $p = 0.22$, NS). **e-f,** LTP at perforant path/granule cell synapses *in vivo* was impaired in HPC-cKO mice as shown by mean normalized fEPSP slope as a function of time. fEPSP-LTP (**e,** Genotype $F_{(1, 11)} = 1.63$, $p = 0.23$, NS; Time $F_{(35, 385)} = 3.57$, $p < 0.0001$; interaction $F_{(35, 385)} = 2.05$, $^{###}p < 0.001$). However, the PS-LTP was slightly but not significantly enhanced during the first 2 hours post TBS in the HPC-cKO mice (**f,** Genotype $F_{(1, 11)} = 0.14$, $p = 0.72$, NS; Time $F_{(35, 385)} = 1.16$, $p = 0.25$, NS; interaction $F_{(35, 385)} = 1.08$, $p = 0.36$, NS). Waveforms are the averaged representative fEPSP traces measured before and after theta-burst stimulation (TBS). 1, waveform before TBS; 2, waveform after TBS. Scale bars: vertical bar 2 mV and horizontal bar 2 ms. All WT-control, $n = 6$; HPC-cKO, $n = 7$. Significance was assessed with a two-way ANOVA with repeated measures and with a *post hoc* Fisher LSD test.

To further check the effects local Arc/Arg3.1 ablation on synaptic consolidation, LTP was induced by applying TBS stimulation in the perforant path fibers. Remarkably, HPC-cKO mice developed a nonstable and gradually declining fEPSP-LTP, while WT-control mice generated a stable and long-lasting fEPSP-LTP. Two-way ANOVA with repeated measures revealed that fEPSP-LTP was significantly impaired in the HPC-cKO mice compared to WT-control mice, suggesting that Arc/Arg3.1 mediated plasticity is still essential for synaptic consolidation in the adult hippocampus (Fig. 2.44e). In contrast, PS-LTP was not significantly altered in the HPC-cKO mice (Fig. 2.44f). Immunostaining with anti-Arc/Arg3.1 antiserum nicely showed that Arc/Arg3.1 protein was clearly induced in the stimulated DG of a WT-control mouse, suggesting that Arc/Arg3.1 up-regulation by LTP-inducing stimulus is necessary for its later consolidation (Fig. 2.44b).

2.8.4 Engram cells reactivation during memory retrieval after local Arc/Arg3.1 ablation in the hippocampus

A number of studies reported that up-regulation of Arc/Arg3.1 is observed during acquisition and retrieval of various memory paradigms (Gusev and Gubin, 2010a; Lonergan et al., 2010; Santini et al., 2011; Chau et al., 2013). These observations had accredited Arc/Arg3.1 as a reliable molecular marker for tracing memory engrams in the brain. To identify specific brain regions in which Arc/Arg3.1 mediated plasticity could possibly contribute to memory retrieval and specificity, I extracted mice brains 90 min after fear memory retrieval and stained them against Arc/Arg3.1. HPC-cKO mice together with WT-control and GFP-control mice were perfused with 4% PFA. GFP-control mice sacrificed immediately after memory retrieval were used as non-retrieval controls. Arc/Arg3.1 positive neurons in the DG, mPFC and BLA were counted. Cell numbers were normalized to the area of each measured region. As expected, numbers of Arc/Arg3.1 positive neurons in the DG, mPFC and BLA of GFP-control and WT-control mice 90 min after memory retrieval were clearly increased in comparison with GFP-control mice immediately after memory retrieval (Fig. 2.45a). Surprisingly, I observed significantly less Arc/Arg3.1 positive neurons in the mPFC and BLA of HPC-cKO mice compared with WT-control mice ($p < 0.05$, Kruskal-Wallis test with Dunn's multiple comparison), suggesting that mPFC and BLA were not highly reactivated during contextual fear memory retrieval after local ablation of Arc/Arg3.1 in the hippocampus (Fig. 2.45c-d). As expected, the number of Arc/Arg3.1 positive neurons was very low in the DG of HPC-cKO mice, demonstrating the completeness of rAAV-Cre mediated Arc/Arg3.1 ablation there (Fig. 2.45b). These data suggest that cortical representations which are required for consolidating and stabilizing long-term contextual fear memories cannot be reactivated during memory retrieval in absence of Arc/Arg3.1 mediated synaptic plasticity in the hippocampus.

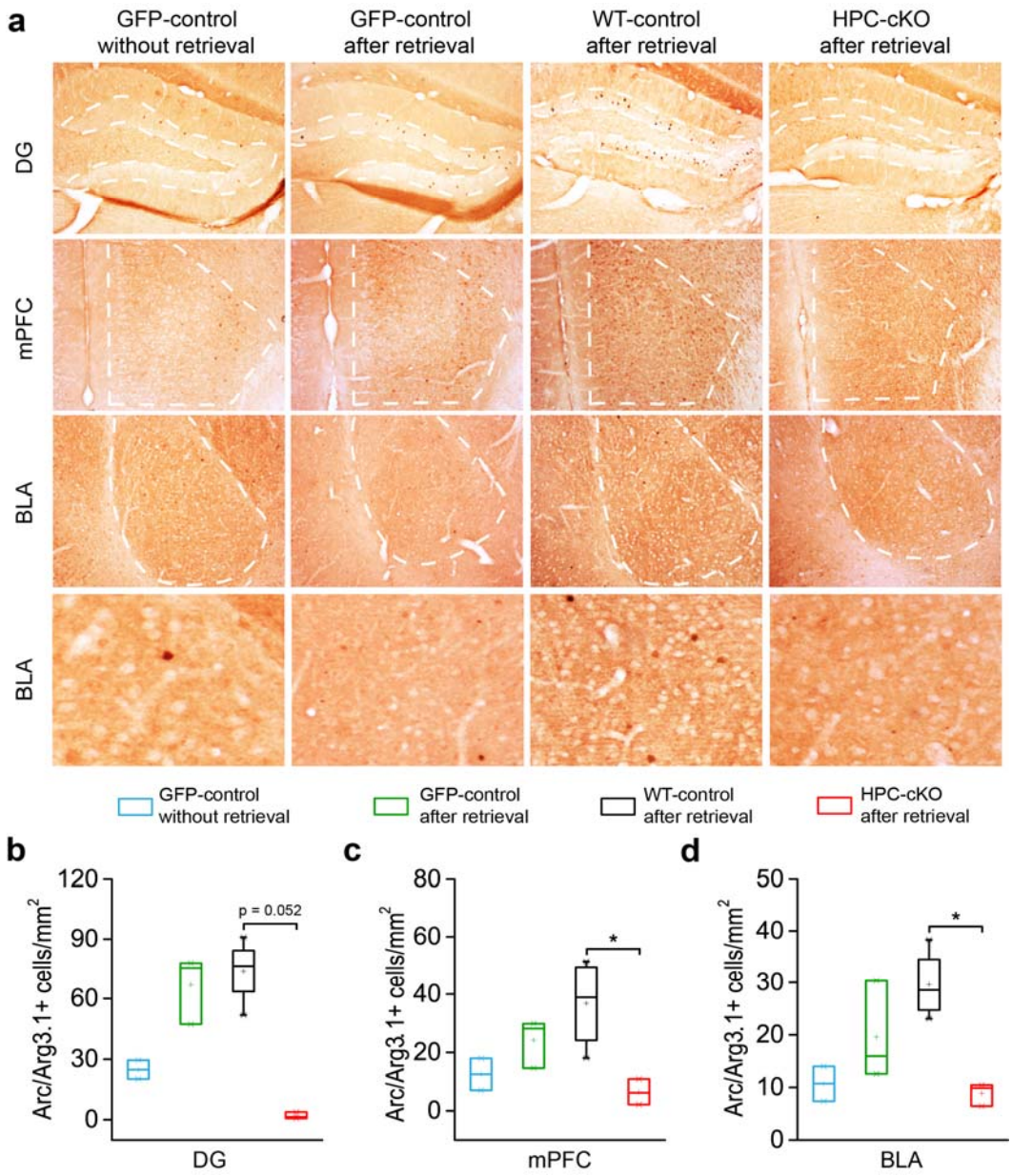

Fig. 2.45 Engram cells reactivation during memory retrieval after rAAV-Cre mediated Arc/Arg3.1 ablation in the hippocampus. a, Immunostaining showed that number of Arc/Arg3.1 positive neurons was increased in the DG, mPFC and BLA of GFP-control and WT-control mice 90 min after contextual fear memory retrieval in comparison with GFP-control mice immediately after memory retrieval (GFP-control without retrieval). Almost no Arc/Arg3.1 positive neuron was visible in the related region of HPC-cKO mice. **b,** The number of Arc/Arg3.1 positive neurons was strongly reduced (p=0.052) in the DG of HPC-cKO mice, indicating efficient rAAV-mediated Arc/Arg3.1 ablation (Median: GFP-control without retrieval, 24.82; GFP-control after retrieval, 75.36; WT-control after retrieval, 76.31; HPC-cKO after retrieval, 1.45). **c,** Number of Arc/Arg3.1 positive neurons was significantly lower in the mPFC of HPC-cKO mice compared to WT-control mice after memory retrieval (Median: GFP-control without retrieval, 12.54; GFP-control after retrieval, 28.14; WT-control after retrieval, 38.85; HPC-cKO after retrieval, 6.17). **d,** Number of Arc/Arg3.1 positive neurons was significantly lower in the BLA of HPC-cKO mice comparing to WT-control mice after memory retrieval (Median: GFP-control without retrieval, 10.69; GFP-control after retrieval, 15.97; WT-control after retrieval, 28.53; HPC-cKO after retrieval, 9.85). GFP-control without retrieval, *n* = 2; GFP-control after retrieval, *n* = 3; WT-control after retrieval, *n* = 4; HPC-cKO after retrieval, *n* = 3. Box plots show median (-), 25th and 75th percentiles, mean (+) and outliers (×). Kruskal-Wallis test with Dunn's multiple comparison was performed between genotypes, **p* < 0.05. DG, dentate gyrus; mPFC, medial prefrontal cortex; BLA, basolateral amygdala.

Together, ablation of Arc/Arg3.1 in adult hippocampus ostensibly seems to leave the ability of recalling long-term contextual fear memory intact, but reduces the specificity of remote memory. Meanwhile, Arc/Arg3.1 mediated synaptic plasticity was dramatically reduced in the ablated hippocampus and also in memory relevant regions it directly targets, such as mPFC and BLA. Collectively, these observations demonstrate that hippocampus is always essential for both recent and remote LTM consolidation and for precise memory retrieval.

2.8.5 Contextual fear memory after local Arc/Arg3.1 ablation in the medial prefrontal cortex

Arc/Arg3.1 ablation in the adult hippocampus does not affect remote contextual fear memory retrieval, but reduces remote memory specificity. One hypothesis is that the absence of Arc/Arg3.1 mediated synaptic plasticity in the hippocampus can be compensated by Arc/Arg3.1 mediated synaptic plasticity in cortical regions involved in memory encoding and retrieval. mPFC is considered to play a pivotal role in learning and memory. Inhibition or lesions of this region result in dysfunctional cognitive and memory performance (Beeman et al., 2013; Zelikowsky et al., 2013; Chao et al., 2016).

I hypothesized that ablation of Arc/Arg3.1 in the adult mPFC would affect remote memory performance. To test this hypothesis, I injected two groups of mice with rAAV-Cre targeting mPFC (Fig. 2.46a). Arc/Arg3.1$^{f/f}$ mice injected with rAAV-Cre were termed “mPFC-cKO”. “WT-control” and “GFP-control” were injected with rAAV-Cre and rAAV-GFP, respectively. Mice were fear conditioned 7 days after injection. Memory retrieval was assessed either 1 day or 2 weeks later (Fig. 2.46b, e). During conditioning, all mice developed a similar fear response (Fig. 2.46c-d). However, in contrary to my prediction, mPFC mice generated comparable level of freezing to WT-controls and GFP-controls during memory retrieve test. No difference was observed both in the recent LTM (1 day, Fig. 2.46f) and in the remote LTM retrieval (2 weeks, Fig. 2.46g).

Moreover, mPFC-cKO mice cannot only successfully retrieve fear memory but also can recall the memory as precisely as control mice, because mPFC-cKO mice can also distinguish altered context from the fearful conditioning context as indicated by low percent freezing in the altered context and high discrimination index. Similar levels of freezing in the altered context (Fig. 2.47b, d) and indistinguishable contexts discrimination index (Fig. 2.47c, e) suggest that contextual fear memory specificity was not altered with absence of Arc/Arg3.1 in the mPFC of adult mice.

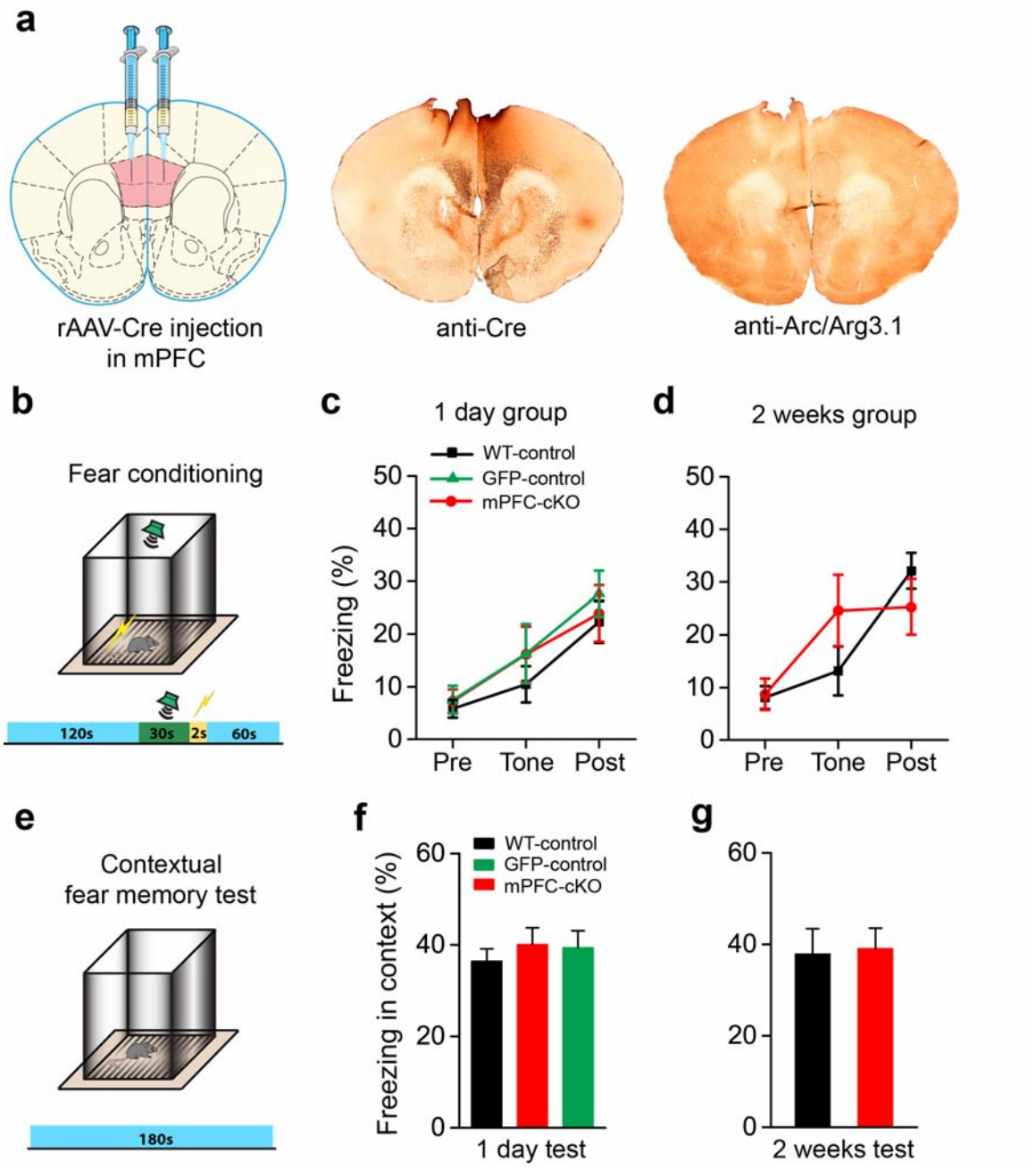

Fig. 2.46 Intact contextual fear memory retrieval after rAAV-Cre mediated Arc/Arg3.1 ablation in the mPFC. a, Immunostaining showed that Cre recombinase was strongly expressed in the mPFC, and Arc/Arg3.1 was efficiently ablated. **b,** Schematic of the contextual fear conditioning **c-d,** Average percent freezing during fear acquisition. mPFC-cKO mice showed comparable level of freezing after foot shocks comparing to WT-control mice. **e,** Schematic of the contextual fear memory retrieval test. Contextual fear memory was tested 1 day and 2 weeks after conditioning with independent groups of mice. **f,** Similar freezing of WT-control and mPFC-cKO mice in the context 1 day and 2 weeks after conditioning. GFP-control mice showed comparable percent freezing to WT-control and to mPFC-cKO mice 1 day after conditioning (WT-control, 36.50 ± 2.64%; *n* = 12 and mPFC-cKO, 40.12 ± 3.60%; *n* = 14; GFP-control, 39.44 ± 3.63%; *n* = 14, One-way ANOVA with a *post hoc* LSD test, NS). **g**, Similar freezing in the context was observed for all groups 2 weeks after conditioning (WT-control, 37.92 ± 5.51%; *n* = 8 and mPFC-cKO, 39.09 ± 4.44%; *n* = 10; t_{16} = -0.17, *p* = 0.87, NS). Bars show mean ± S.E.M. Significance between two genotypes was tested with One-way ANOVA with a *post hoc* LSD test or with two-tailed two-sample *t*-test when there were only two groups.

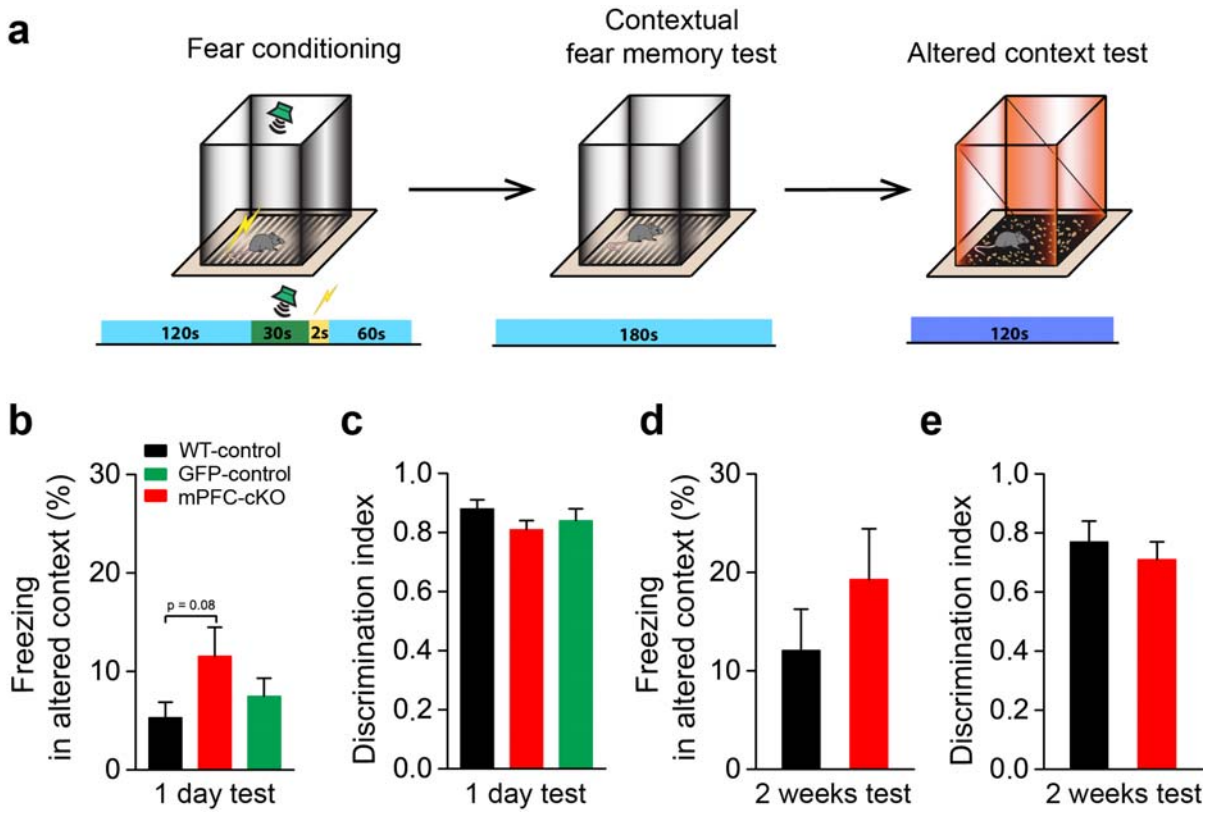

Fig. 2.47 Unaltered memory specificity after rAAV-Cre mediated Arc/Arg3.1 ablation in the mPFC. a, Schematic of contextual fear conditioning and memory test paradigm and protocol. **b-e,** mPFC-cKO mice displayed comparable memory specificity in comparison with WT-control and GFP-control mice as indicated by freezing level in the altered context and discrimination index of two contexts. **b,** 1 day altered context (WT-control, 5.32 ± 1.55%; *n* = 12 and mPFC-cKO, 11.56 ± 2.91%; *n* = 14; GFP-control, 7.49 ± 1.83%; *n* = 14, One-way ANOVA with a *post hoc* LSD test, NS; WT-control vs. mPFC-cKO, two-sample t-test, *p* = 0.08). **f,** 1 day discrimination index (WT-control, 0.88 ± 0.03; *n* = 12 and mPFC-cKO, 0.81 ± 0.03; *n* = 14; GFP-control, 0.84 ± 0.04; *n* = 14, One-way ANOVA with a *post hoc* LSD test, NS). **i,** 2 weeks altered context (WT-control, 12.07 ± 4.2%; *n* = 8 and mPFC-cKO, 19.27 ± 5.16%; *n* = 10; t_{16} = -1.04, *p* = 0.31, NS). **j,** 2 weeks discrimination index (WT-control, 0.77 ± 0.07; *n* = 8 and mPFC-cKO, 0.71 ± 0.06; *n* = 10; t_{16} = 0.68, *p* = 0.51, NS). Bars show mean ± S.E.M. Significance between two genotypes was tested with One-way ANOVA with a *post hoc* LSD test or with two-tailed two-sample *t*-test when there were only two groups.

2.8.6 Cortical synaptic plasticity after local Arc/Arg3.1 ablation in the medial prefrontal cortex

Cortical plasticity is also important for memory consolidation, especially for remote memory (Frankland et al., 2001; Zhao et al., 2005). Arc/Arg3.1 mediated synaptic plasticity in the mPFC was evaluated with LTP induction in the injected mice (Fig. 2.48a) by applying HFS into ventral CA1 and recording in the prelimbic layer of mPFC. Clearly, Arc/Arg3.1 protein expression was upregulated in the mPFC of WT-control mice after LTP recordings (Fig. 2.48b). Comparable IO curves were generated from mPFC-cKO and WT-control mice by applying stepwise increasing currents, indicating that local Arc/Arg3.1 ablation in the mPFC did not affect basic neuronal transmission (Fig. 2.48c-d).

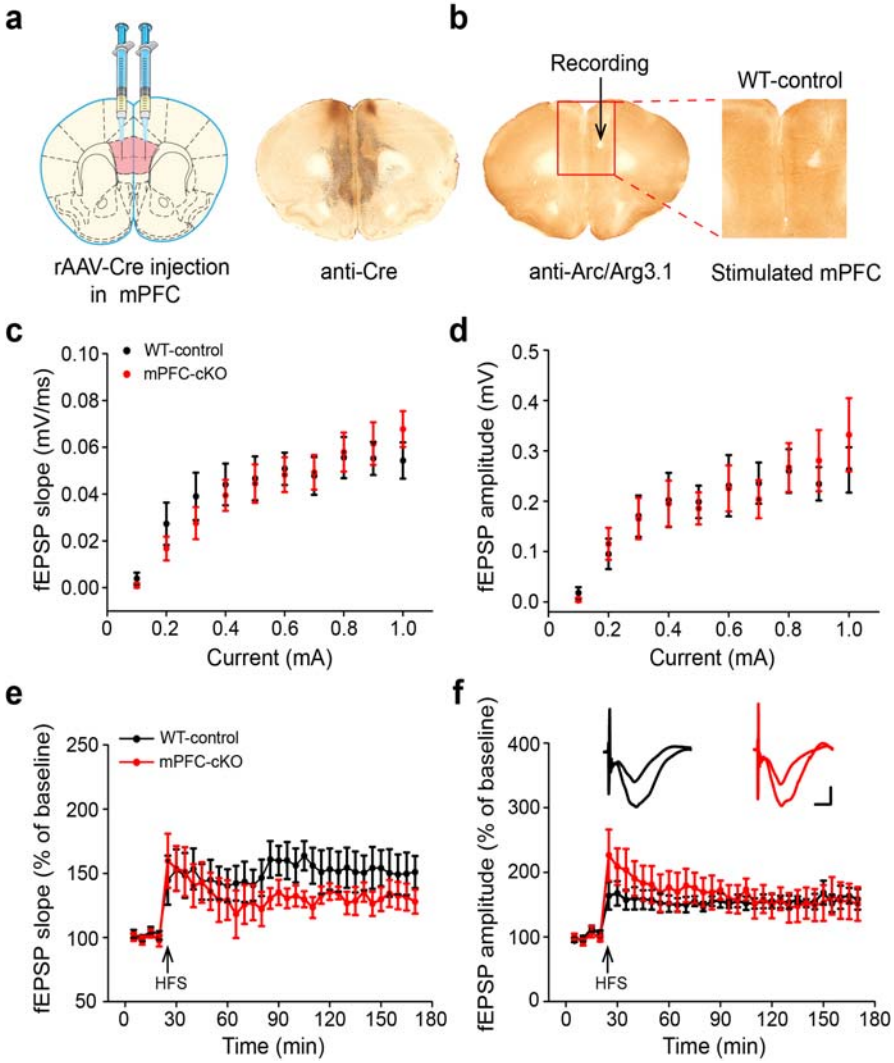

Fig. 2.48 Non-significantly reduced long-term potentiation after rAAV-Cre mediated Arc/Arg3.1 ablation in the mPFC. a, Immunostaining showed that Cre recombinase was strongly expressed in the mPFC 7 days after injection. **b,** Arc/Arg3.1 protein was induced in the mPFC of a WT-control mouse following ipsilateral high-frequency stimulation of the CA1 afferents. **c-d,** Basic synaptic transmission was not significantly different between WT-control and mPFC-cKO mice as indicated by input/output (I/O) curves of the fEPSP slope and PS amplitude plotted as a function of stimulus intensities. fEPSP slope (**c,** Genotype $F_{(1,10)} = 0.01$, $p = 0.91$, NS; Current intensity $F_{(9,90)} = 42.22$, $p < 0.0001$; interaction $F_{(9,90)} = 1.77$, $p = 0.09$, NS). PS amplitude (**d,** Genotype $F_{(1,10)} = 0.02$, $p = 0.89$, NS; Current intensity $F_{(9,90)} = 17.62$, $p < 0.0001$; interaction $F_{(9,90)} = 0.59$, $p = 0.80$, NS). **e-f,** LTP at perforant path/granule cell synapses *in vivo* was reduced in mPFC-cKO mice but not significantly different from WT-control mice as shown by mean normalized fEPSP slope as a function of time (**e,** Genotype $F_{(1,10)} = 1.09$, $p = 0.32$, NS; Time $F_{(29,290)} = 1.16$, $p = 0.26$, NS; interaction $F_{(29,290)} = 1.24$, $p = 0.19$, NS). While the fEPSP-amplitude potentiation was enhanced during the first hour post HFS (**f,** Genotype $F_{(1,10)} = 0.23$, $p = 0.65$, NS; Time $F_{(29,290)} = 3.66$, $p < 0.0001$; interaction $F_{(29,290)} = 2.73$, $p = 0.043$). Waveforms are the averaged representative traces measured before and after high frequency stimulation (HFS). 1. Waveform before HFS; 2. Waveform after HFS. Scale bars: vertical bar 0.1 mV and horizontal bar 5 ms. All WT-control, $n = 6$; mPFC-cKO, $n = 6$. Significance was assessed with a two-way ANOVA with repeated measures and with a *post hoc* Fisher LSD test.

However, I observed a non-significantly reduced potentiation of synaptic responses in the mPFC-cKO compared with WT-control mice (Fig. 2.48e), suggesting that local Arc/Arg3.1 ablation in the adult mPFC does not remarkably change long-term synaptic plasticity neither

on the level of the single synapse strength nor on the level of synaptic synchronization, as indicated by normalized fEPSP amplitudes (Fig. 2.48f).

2.8.7 Engram cells reactivation during memory retrieval after local Arc/Arg3.1 ablation in the medial prefrontal cortex

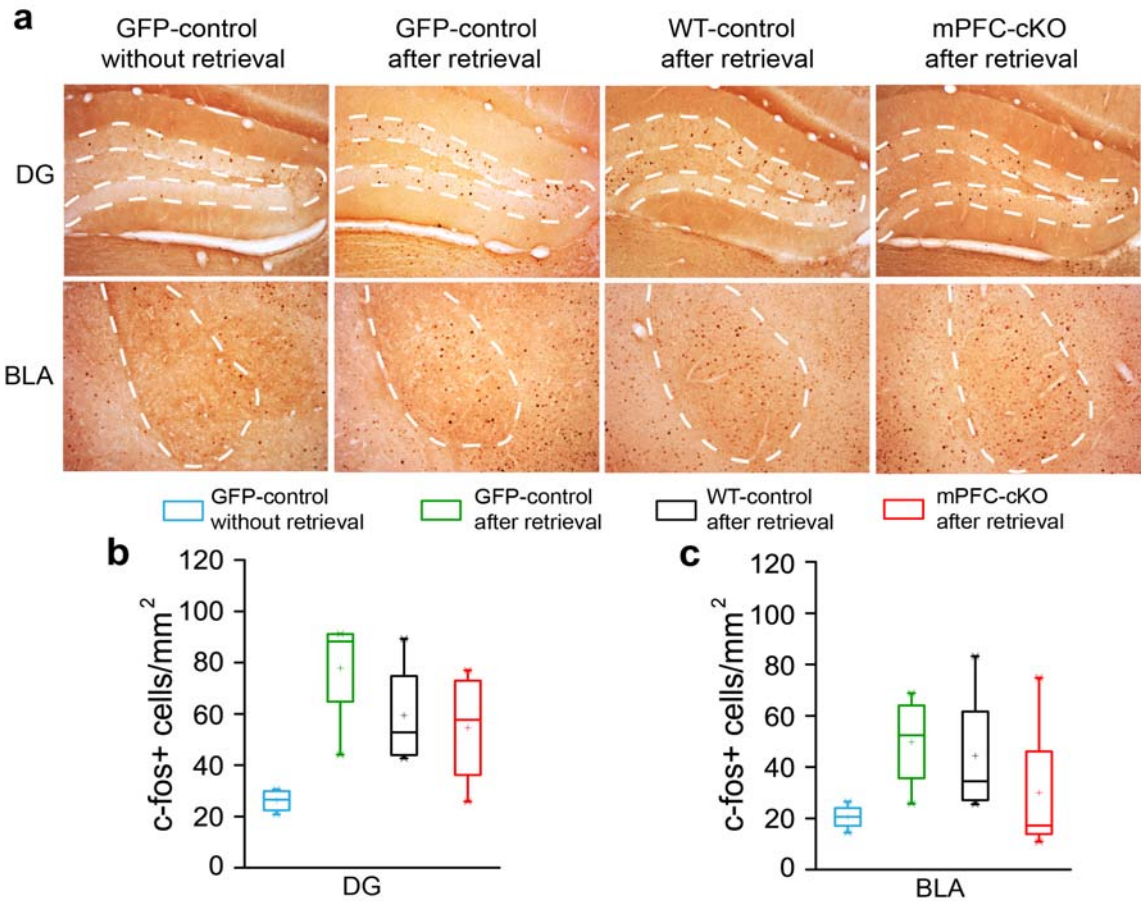

Fig. 2.49 Neuronal activity after rAAV-Cre mediated Arc/Arg3.1 ablation in the mPFC. a, Immunohistochemistry showed number of c-fos positive neurons was increased in the DG and BLA of GFP-control; WT-control and mPFC-cKO mice 90 min after contextual fear memory retrieval in comparison with GFP-control mice immediately after memory retrieval (GFP-control without retrieval). **b,** Numbers of c-fos positive neurons were increased in the DG of mice after memory retrieval in comparison with GFP-control mice immediately after memory retrieval (Median: GFP-control without retrieval, 26.59; GFP-control after retrieval, 88.19; WT-control after retrieval, 52.77; mPFC-cKO after retrieval, 57.75, NS). **c,** Numbers of c-fos positive neurons were comparably increased in the BLA of mice 90 min after memory retrieval in comparison with GFP-control mice without memory retrieval (Median: GFP-control without retrieval, 20.63; GFP-control after retrieval, 52.38; WT-control after retrieval, 34.41; mPFC-cKO after retrieval, 17.14, NS). GFP-control without retrieval, *n* = 4; GFP-control after retrieval, *n* = 4; WT-control after retrieval, *n* = 4; mPFC-cKO after retrieval, *n* = 4. Box plots show median (-), 25th and 75th percentiles, mean (+) and outliers (×). Kruskal-Wallis test with Dunn's multiple comparison was performed between genotypes. DG, dentate gyrus; BLA, basolateral amygdala.

To investigate the effects of local Arc/Arg3.1 ablation in the mPFC on local neuronal activity and engram cells reactivation in the DG and BLA during memory retrieval, c-fos positive neurons (Fig. 2.49a) and Arc/Arg3.1 positive neurons (Fig. 2.50a) were counted in

these areas. Brains were extracted and fixed 90 min after contextual fear memory retrieval. GFP-control mice sacrificed immediately after memory retrieval served as non-retrieval controls.

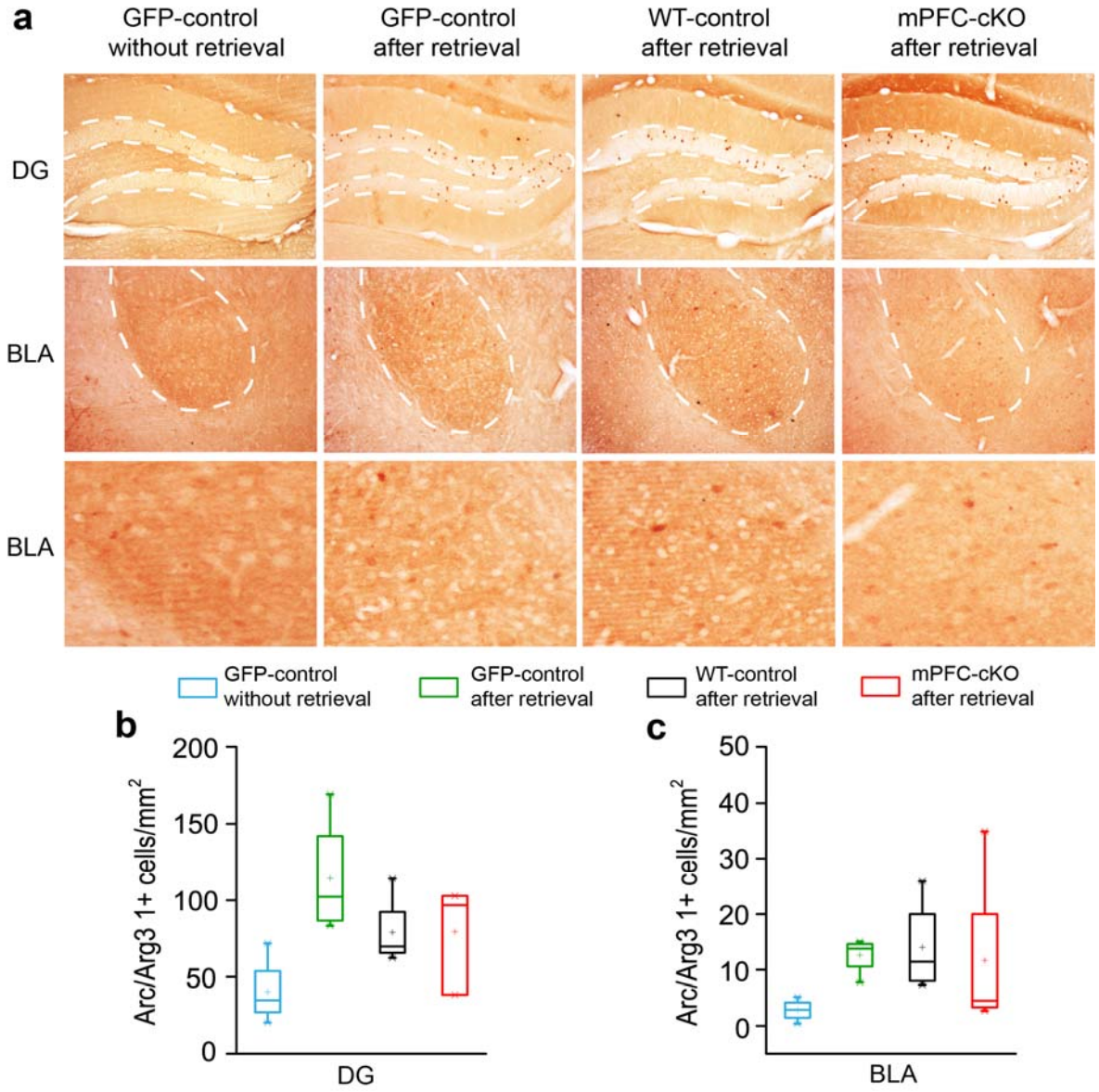

Fig. 2.50 Engram cells reactivation after rAAV-Cre mediated Arc/Arg3.1 ablation in the mPFC. a, Immunohistochemistry showed number of Arc/Arg3.1 positive neurons was increased in the DG and BLA of GFP-control, WT-control and mPFC-cKO mice 90 min after contextual fear memory retrieval in comparison with GFP-control mice immediately after memory retrieval (GFP-control without retrieval). **b,** Numbers of Arc/Arg3.1 positive neurons were increased in the DG of mice after memory retrieval in comparison with GFP-control mice without retrieval (Median: GFP-control without retrieval, 34.77; GFP-control after retrieval, 102.3; WT-control after retrieval, 69.71; mPFC-cKO after retrieval, 96.70, NS). **c,** Numbers of Arc/Arg3.1 positive neurons were comparably increased in the BLA of mice 90 min after memory retrieval in comparison with GFP-control mice without memory retrieval (Median: GFP-control without retrieval, 2.85; GFP-control after retrieval, 13.79; WT-control after retrieval, 11.43; mPFC-cKO after retrieval, 4.50, NS). GFP-control without retrieval, n = 4; GFP-control after retrieval, n = 4; WT-control after retrieval, n = 4; mPFC-cKO after retrieval, n = 4. Box plots show median (-), 25th and 75th percentiles, mean (+) and outliers (×). Kruskal-Wallis test with Dunn's multiple comparison was performed between genotypes. DG, dentate gyrus; BLA, basolateral amygdala.

Numbers of c-fos and Arc/Arg3.1 positive neurons in the DG and BLA of GFP-control, WT-control and mPFC-cKO mice after memory retrieval were clearly increased 90 min after memory retrieval compared with non-retrieval controls (Fig. 2.49a & 2.50a). However, the increment in the DG and BLA of mPFC-cKO mice did not significantly differ from that of WT-control and GFP-control mice. Especially, the number of Arc/Arg3.1 positive cells was comparable between WT-control and mPFC-cKO mice (Fig. 2.50b-c), suggesting indistinguishable size of engram cells population. Similar number of c-fos positive neurons was also observed in the DG and BLA of all groups of mice 90 min after memory retrieval (Fig. 2.49a-c), indicating comparable neuronal activity. Therefore, Arc/Arg3.1 ablation in the adult mPFC does not affect neuronal activity and engram cells reactivation in the DG and BLA during memory retrieval (Fig. 2.49-2.50).

Together, local ablation of Arc/Arg3.1 in the adult mPFC does not affect long-term contextual fear memory performance, neither retrieval nor specificity. Meanwhile, synaptic plasticity was not remarkably changed and neuronal activity and plasticity evoked by memory retrieval was not altered in the regions connected with mPFC such that engram cells could still be effectively reactivated in the DG and BLA in absence of Arc/Arg3.1 in the mPFC.

2.8.8 Contextual fear memory after local Arc/Arg.3.1 ablation in the anterior cingulate cortex and retrosplenial cortex

In light of the dispensability of the mPFC, I next ask which regions in the cortex are important for long-term storage of memory. Anterior cinglulate cortex (ACC) and retrosplenial cortex (RSC) were suggested to play a role in memory encoding, consolidation and spatial information representation. Both of these regions are highly activated during memory acquisition and retrieval as indicated by elevated expression of the activity marker, c-fos and the plasticity marker, Arc/Arg3.1 (Gusev and Gubin, 2010a; Tayler et al., 2013; Vousden et al., 2015). Inactivation or lesions of these regions caused profound memory impairments, and especially disrupted remote memory recall (Goshen et al., 2011; Czajkowski et al., 2014).

To further detect in which neocortical regions Arc/Arg3.1 mediated plasticity supports memory formation, consolidation and retrieval, I bilaterally injected another two cohorts of mice with rAAV-Cre either in the ACC (Fig. 2.51a) or in the RSC (Fig. 2.53a). I also termed the injected Arc/Arg3.1 floxed mice “ACC-cKO” and “RSC-cKO”, respectively. I conditioned the injected mice 7 days after injection in a multiple fear conditioning system. Compared with WT-control mice, ACC-cKO mice generated significantly higher level of freezing (Fig. 2.51b-c), indicating robust and even stronger fear acquisition. Contextual fear memory retrieval was tested 7 days and 14 days after conditioning. ACC-cKO and WT-control mice exhibited

similar percent freezing in the conditioning context, implying intact retrieval of both recent and remote long-term memory (Fig. 2.51d-f).

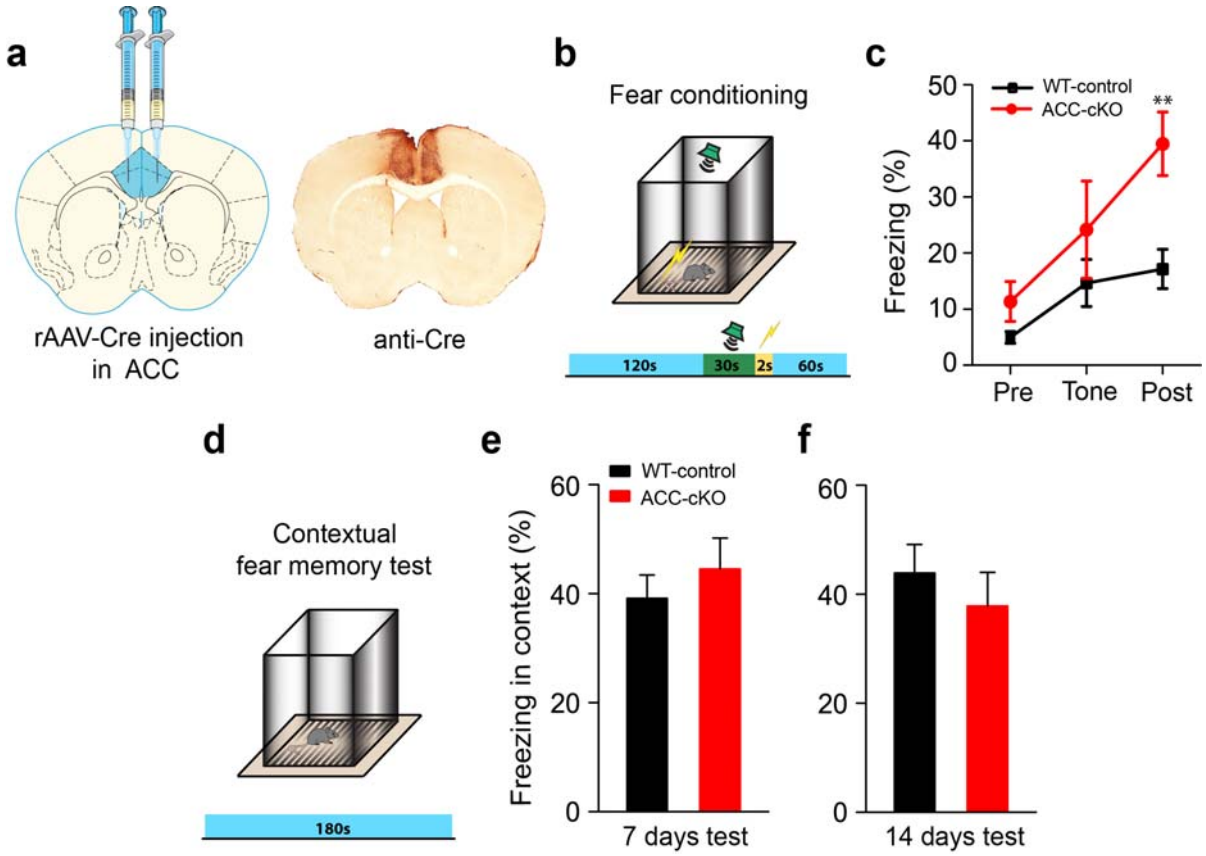

Fig. 2.51 Intact memory retrieval after rAAV-Cre mediated Arc/Arg3.1 ablation in the ACC. a, Virus injection and Cre expression in the ACC. **b,** Schematic of contextual fear conditioning paradigm and protocol. **c,** Averaged percentage of freezing during fear acquisition phase. ACC-cKO mice developed higher level of freezing post foot shock compared with WT-control mice (WT-control, 17.15 ± 3.51%; *n* = 11 and ACC-cKO, 39.46 ± 5.67%; *n* = 9; t_{18}= -3.47, $^{**}p < 0.01$). **d,** Schematic of contextual fear memory retrieval paradigm and protocol. Contextual fear memory was tested at 7 days and 14 days delay after conditioning. **e-f,** Similar levels of freezing of WT-control and ACC-cKO mice in the context 7 days and 14 days after conditioning. 7 days context (**e,** WT-control, 39.15 ± 4.25%; *n* = 11 and ACC-cKO, 44.51 ± 5.66%; *n* = 9; t_{18} = -0.77, *p* = 0.45, NS). 14 days context (**f,** WT-control, 43.92 ± 5.19%; *n* = 11 and ACC-cKO, 37.84 ± 6.14%; *n* = 9; t_{18}= 0.76, *p* = 0.46, NS). Bars show mean ± S.E.M. Significance between two genotypes was tested with two-tailed two-sample *t*-test.

The specificity of the retrieved memory was evaluated by comparing freezing levels in an altered context with conditioning context (Fig. 2.52a). ACC-cKO mice, like WT-control mice, showed low percent freezing in the altered context 7 days after conditioning and a slightly higher freezing after 14 days (Fig. 2.52b, d). Indistinguishable contexts discrimination index between WT-control and ACC-cKO mice suggested the intact memory retrieval in the ACC-cKO mice was also context specific (Fig. 2.52c, e). This reveals that ablation of Arc/Arg3.1 in the adult ACC also did not affect long-term fear memory retrieval or its specificity.

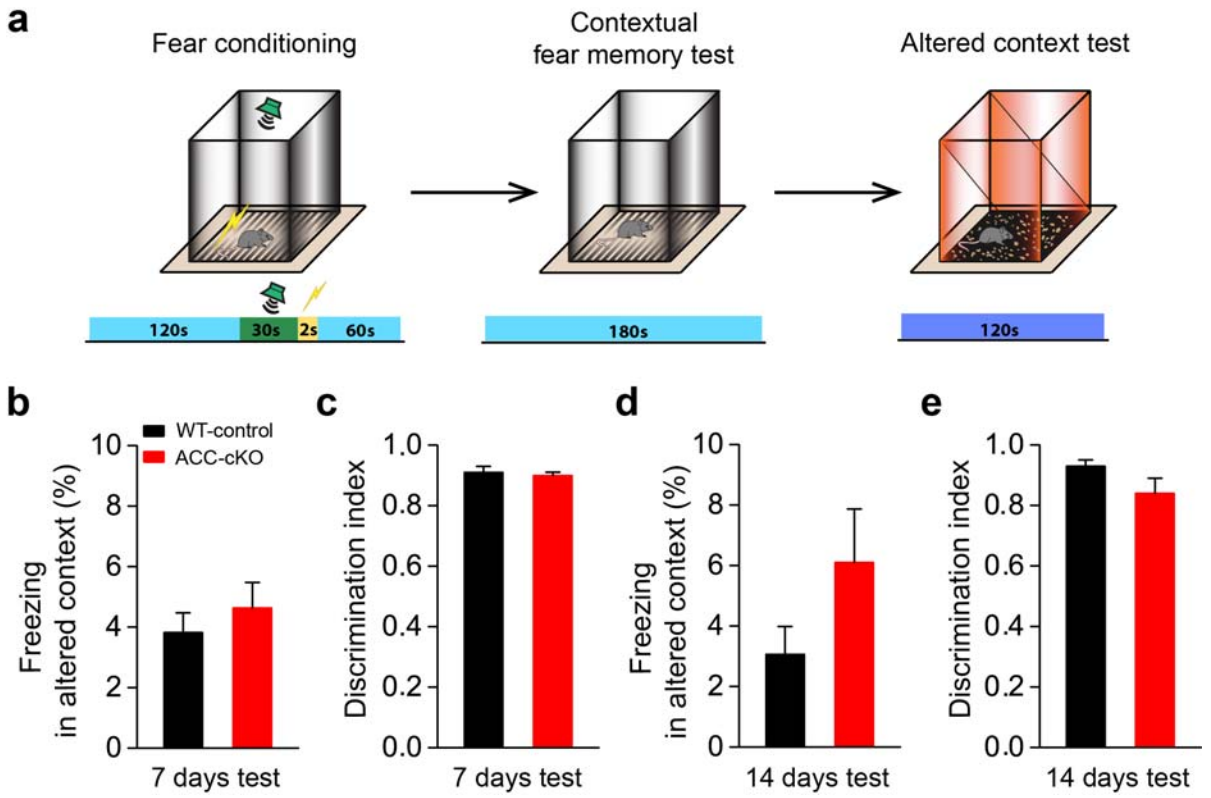

Fig. 2.52 Unaltered memory specificity after rAAV-Cre mediated Arc/Arg3.1 ablation in the ACC. **a,** Schematic of fear conditioning and memory tests paradigm and protocol. **b-e,** ACC-cKO mice displayed comparable memory specificity in comparison with WT-control and GFP-control mice as indicated by freezing levels in the altered context and discrimination index of two contexts. **b,** 7 days altered context (WT-control, 3.82 ± 0.65%; n = 11 and ACC-cKO, 4.63 ± 0.85%; n = 9; t_{18} = -0.77, p =0.45 , NS). **c,** 7 days discrimination index (WT-control, 0.91 ± 0.02; n = 11 and ACC-cKO, 0.90 ± 0.01; n = 9; t_{18} = 0.23, p = 0.82, NS). **d,** 14 days altered context (WT-control, 3.07 ± 0.91%; n = 11 and ACC-cKO, 6.10 ± 1.77%; n = 9; t_{18} = -1.61, p = 0.12, NS). **e,** 14 days discrimination index (WT-control, 0.93 ± 0.02; n = 11 and ACC-cKO, 0.84 ± 0.05; n = 9; t_{18} = 1.92, p = 0.07, NS). Bars show mean ± S.E.M. Significance between two genotypes was tested with two-tailed two-sample t-test.

Very similar to what I found in the mPFC-cKO and ACC-cKO mice, RSC-cKO mice could also successfully retrieve long-term fear memory at 7 days and 14 days delay (Fig. 2.53d-f), and RSC-cKO mice distinguished the conditioning context from the altered context, demonstrating precise memory (Fig. 2.54). I did not observe any significant difference between WT-control and RSC-cKO mice neither during conditioning nor during memory retrieval (Fig. 2.53 and 2.54).

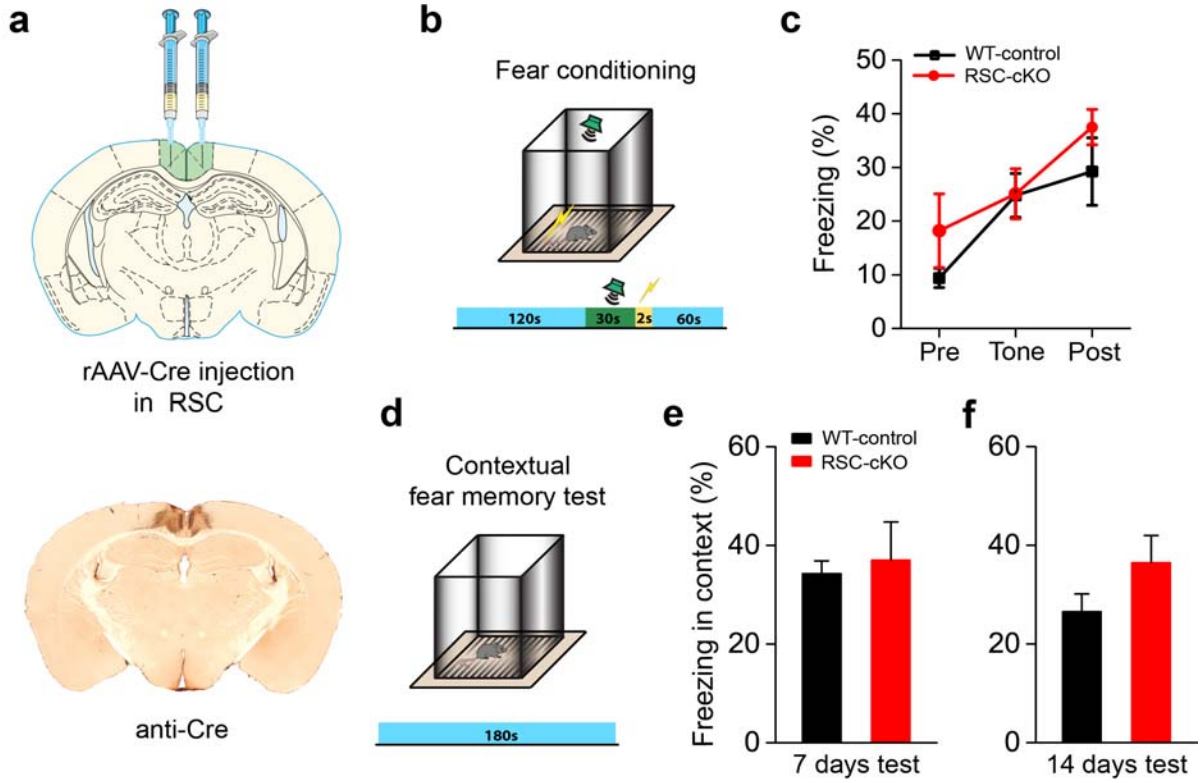

Fig. 2.53 Intact memory retrieval after rAAV-Cre mediated Arc/Arg3.1 ablation in the RSC. a, Virus injection and Cre expression in the RSC. **b,** Schematic of contextual fear conditioning paradigm **c,** Average percent freezing during fear acquisition. Similar percent freezing in RSC-cKO and WT-control mice immediately after foot shocks. **d,** Schematic of contextual fear memory retrieval tests. Contextual fear memory was tested 7 and 14 days after conditioning. **e,** Comparable levels of freezing of WT-control and RSC-cKO mice in the context 7 days (WT-control, 34.29 ± 2.57%; n = 5 and RSC-cKO, 37.04 ± 7.69%; n = 8; t_{11} = -0.27, p = 0.79, NS). **f,** Comparable levels of freezing of WT-control and RSC-cKO mice in the context 14 days after conditioning (WT-control, 26.57 ± 3.59%; n = 5 and RSC-cKO, 36.50 ± 5.47%; n = 6; t_9 = -1.45, p = 0.18, NS). Bars show mean ± S.E.M. Significance between two genotypes was tested with two-tailed two-sample t-test.

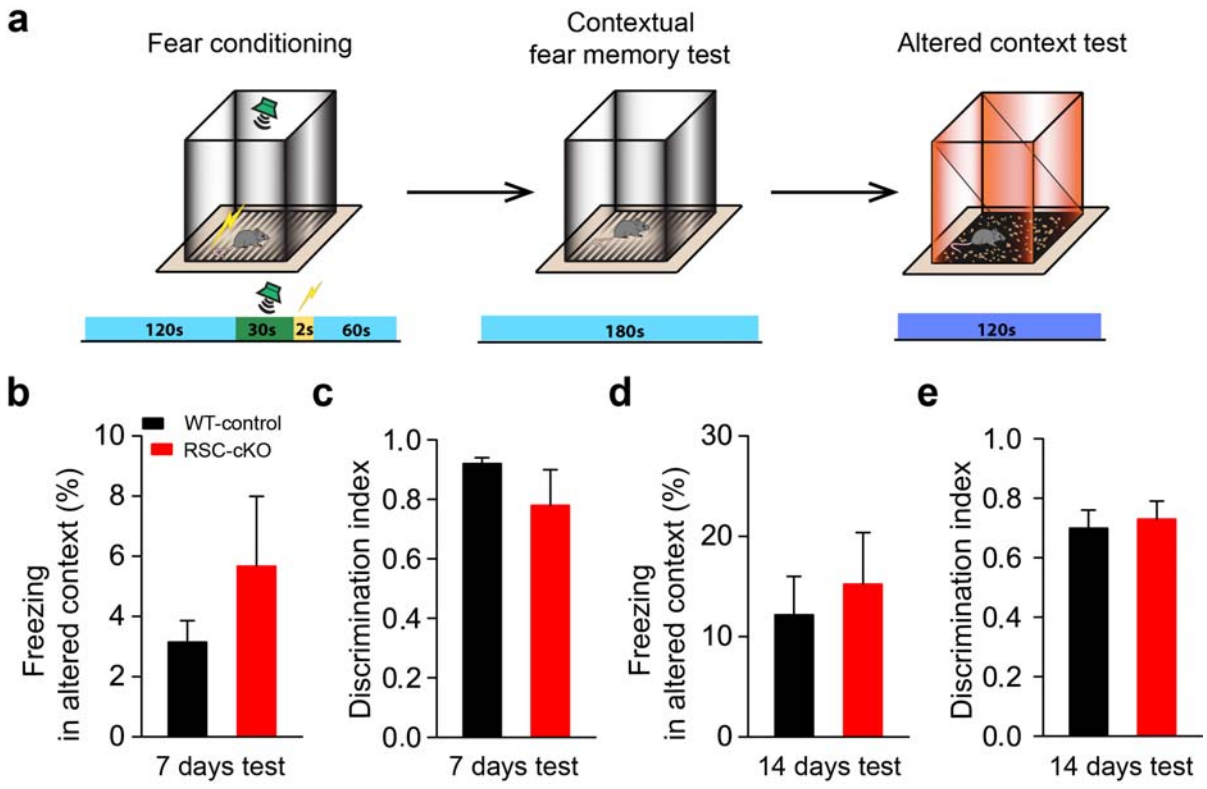

Fig. 2.54 Unaltered memory specificity after rAAV-Cre mediated Arc/Arg3.1 ablation in the RSC. **a,** Schematic of fear conditioning and memory tests paradigm and protocol. **b-e,** RSC-cKO mice displayed comparable memory specificity in comparison with WT-control and GFP-control mice as indicated by freezing levels in the altered context and discrimination index of two contexts. **b,** 7 days altered context (WT-control, 3.15 ± 0.71%; n = 5 and RSC-cKO, 5.67 ± 2.32%; n = 8; t_{11} = -0.83, p = 0.42, NS). **c,** 7 days discrimination index (WT-control, 0.92 ± 0.02; n = 5 and RSC-cKO, 0.76 ± 0.12; n = 8; t_{11} = 0.91, p = 0.38, NS). **d,** 14 days altered context (WT-control, 12.20 ± 3.81%; n = 5 and RSC-cKO, 15.22 ± 5.15%; n = 6; t_9 = -0.45, p = 0.66, NS). **e,** 14 days discrimination index (WT-control, 0.70 ± 0.06; n = 5 and RSC-cKO, 0.73 ± 0.06; n = 6; t_9 = -0.29, p = 0.78, NS). Bars show mean ± S.E.M. Two-tailed two-sample t-test was applied between genotypes.

So far, I have chosen three regions (mPFC, ACC and RSC) in the cortex which are believed to be important for memory formation and consolidation, especially for long-term storage of stable memory traces. However, I surprisingly found that removal of Arc/Arg3.1 in each of these regions alone did not disturb long-term contextual fear memory retrieval and specificity. These data strongly imply that contextual fear memory can be encoded, consolidated and precisely retrieved with the help of other mnemonic regions when plasticity was removed from any single cortical region.

2.8.9 Contextual fear memory after local Arc/Arg3.1 ablation in the basolateral amygdala

Basolateral amygdala (BLA) has been traditionally described as an essential structure in fear generation and also as a region for generating the association between co-occurring

aversive and neutral stimuli such as the foot shocks with the tone presented during fear conditioning (Herry and Johansen, 2014). It might also be an essential hub for encoding and storing contextual fear information. Therefore, I hypothesized that removal of Arc/Arg3.1 mediated plasticity from the BLA might affect fear memory encoding, consolidation or retrieval.

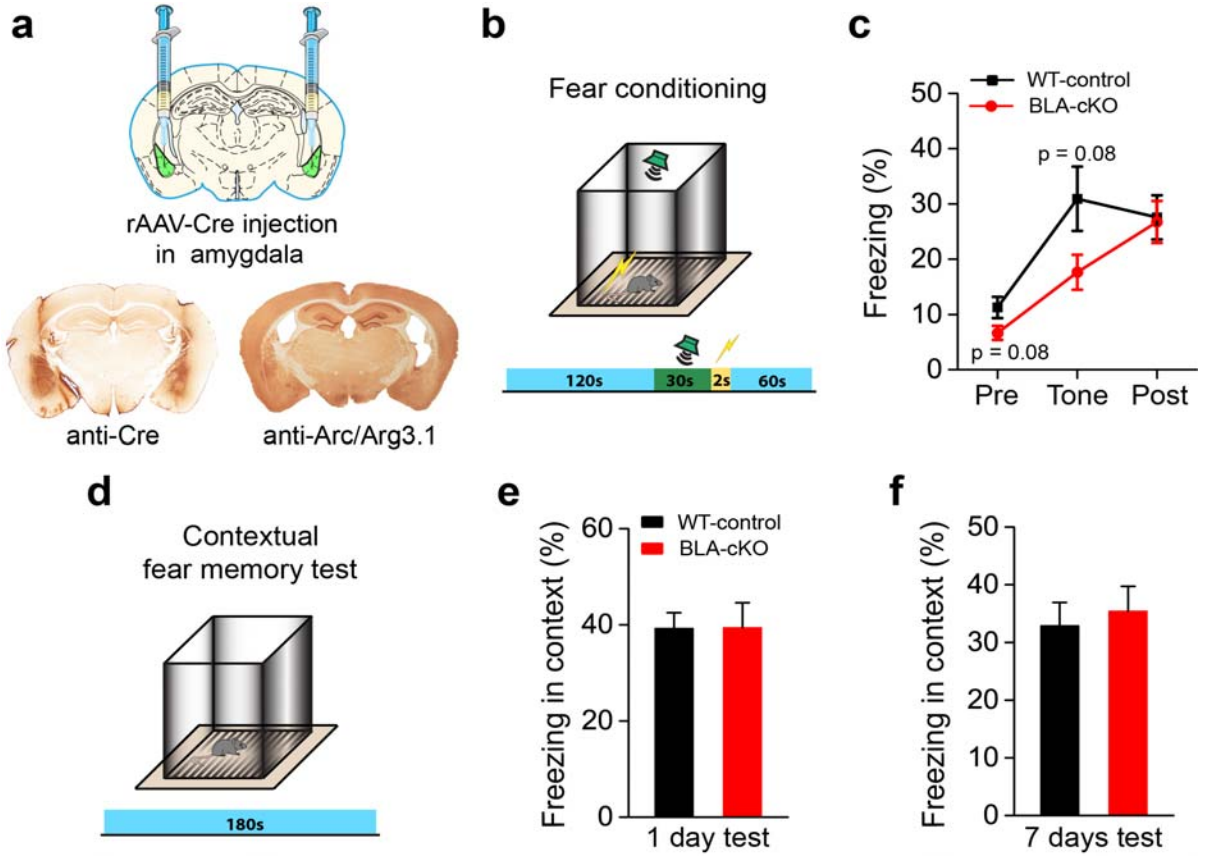

Fig. 2.55 Intact memory retrieval after rAAV-Cre mediated Arc/Arg3.1 ablation in the BLA. a, Immunohistochemistry showed that Cre recombinase was very well expressed in the BLA, and Arc/Arg3.1 was well ablated in the brain injected with rAAV-Cre, in parallels. **b,** Schematic of contextual fear conditioning paradigm and protocol. **c,** Averaged percentage of freezing during fear acquisition phase. BLA-cKO mice showed lower level of freezing before foot shocks (Pre) and comparable level of freezing after foot shock (Post). **d,** Schematic of contextual fear memory retrieval paradigm and protocol. Contextual fear memory was tested at 1 day and 7 days delay. **e,** WT-control and BLA-cKO mice displayed comparable level of freezing in the context 1 after conditioning (WT-control, 39.25 ± 3.27%; n = 16 and BLA-cKO, 39.40 ± 5.19%; n = 12; t_{26} = -0.02, p = 0.98, NS). **f,** WT-control and BLA-cKO mice displayed comparable level of freezing in the context 7 days after conditioning (WT-control, 32.88 ± 4.04%; n = 16 and BLA-cKO, 35.43 ± 4.29%; n = 12; t_{26} = -0.43, p = 0.67, NS). Bars show mean ± S.E.M. Significance was tested with two-tailed two-sample t-test.

To test this hypothesis, I bilaterally injected a group of mice with rAAV-Cre targeting the BLA (Fig. 2.55a). The injected Arc/Arg3.1$^{f/f}$ and WT mice were termed “BLA-cKO” and “WT-control”, respectively. A generic fear conditioning protocol and conditions were applied to the injected mice. Long-term contextual fear memory was assessed either 1 or 7 days later (Fig. 2.55b, d). BLA-cKO mice displayed non-significantly lower baseline freezing in the context

prior to and during conditioning (Fig. 2.55c), perhaps due to a BLA-mediated reduction in autonomous freezing. However, normal freezing immediately following the shocks, indicates intact fear generation in response to aversive stimuli (Fig. 2.55c). When placed in the context a day or a week after acquisition, BLA-cKO mice exhibited strong freezing, indistinguishable from WT-controls (Fig. 2.55e-f), indicating intact long-term contextual fear memory. In addition, BLA-cKO mice exhibited lower freezing in the altered context and a higher context discrimination index, demonstrating a context-specific memory consolidation in the absence of Arc/Arg3.1 in the BLA (Fig. 2.56).

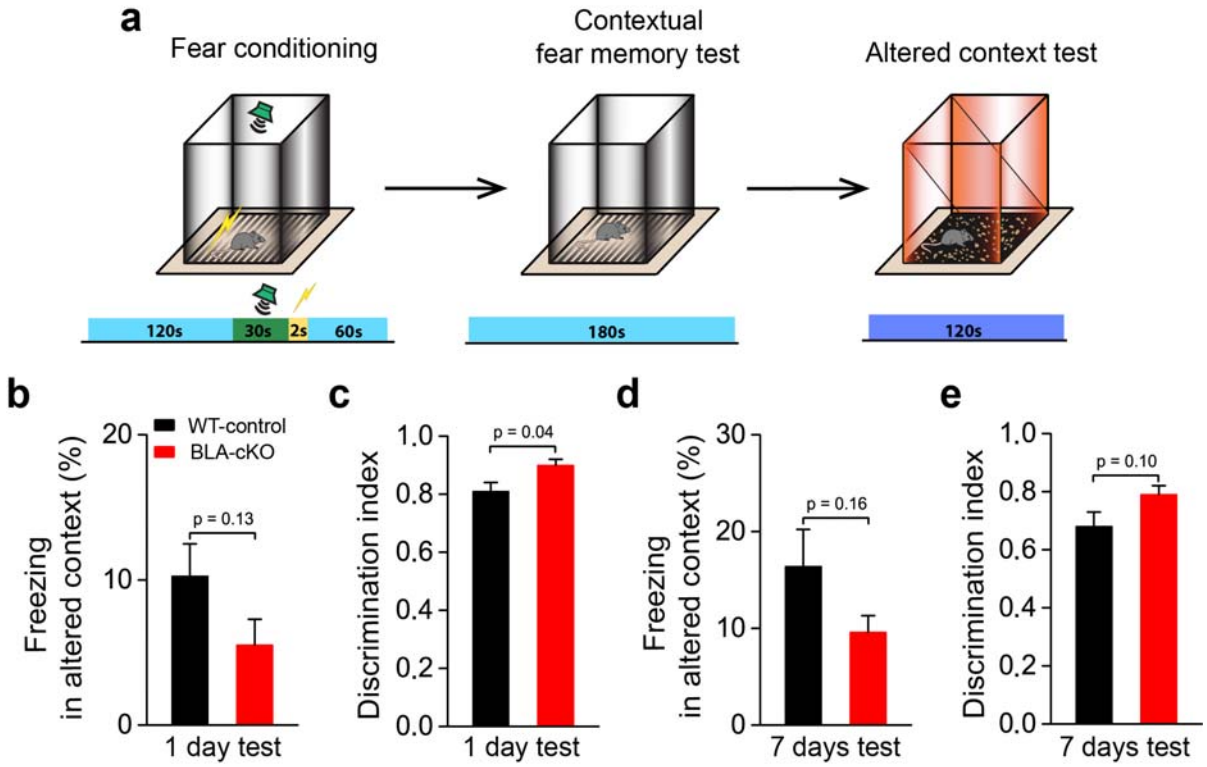

Fig. 2.56 Reduced fear generalization after rAAV-Cre mediated Arc/Arg3.1 ablation in the BLA. a, Schematic of fear conditioning and memory test paradigm and protocol. BLA-cKO showed lower level of freezing in the altered context (**b,** WT-control, 10.26 ± 2.22%; *n* = 16 and BLA-cKO, 5.52 ± 1.77%; *n* = 12; t_{26} = 1.58, *p* = 0.13, NS) and higher discrimination index (**c,** WT-control, 0.81 ± 0.03; *n* = 16 and BLA-cKO, 0.90 ± 0.02; *n* = 12; t_{26} = -2.11, *p* = 0.04) in comparison with WT-control mice 1 day after conditioning. BLA-cKO showed lower level of freezing in the altered context (**d,** WT-control, 16.41 ± 3.80%; *n* = 16 and BLA-cKO, 9.60 ± 1.71%; *n* = 12; t_{26} = 1.46, *p* = 0.16, NS) and higher discrimination index (**e,** WT-control, 0.68 ± 0.05; *n* = 16 and BLA-cKO, 0.79 ± 0.03; *n* = 12; t_{26} = -1.69, *p* = 0.10) 7 days after conditioning. Bars show mean ± S.E.M. Significance was tested with two-tailed two-sample *t*-test.

Altogether, not consistent with the presumed role of Arc/Arg3.1 in the BLA, long-term contextual fear memory retrieval can also succeed in absence of Arc/Arg3.1 mediated plasticity. Thus, BLA does not function as a unique hub for long-term storage of contextual fear information.

2.8.10 Contextual fear memory after local Arc/Arg3.1 ablation in both hippocampus and medial prefrontal cortex

It has been reported that the hippocampus and the mPFC functionally interact during memory acquisition and retrieval, partially via a direct efferent connection from CA1 to the mPFC (Jin and Maren, 2015). These interactions might work in a circuitry that could eventually compensate the damage or loss of functionality in either region. To address the possibility that Arc/Arg3.1 ablation in one of these regions could be compensated by the remaining one, a group of mice were injected with rAAV-Cre both in the dorsal hippocampus and the mPFC bilaterally (Fig. 2.57a).

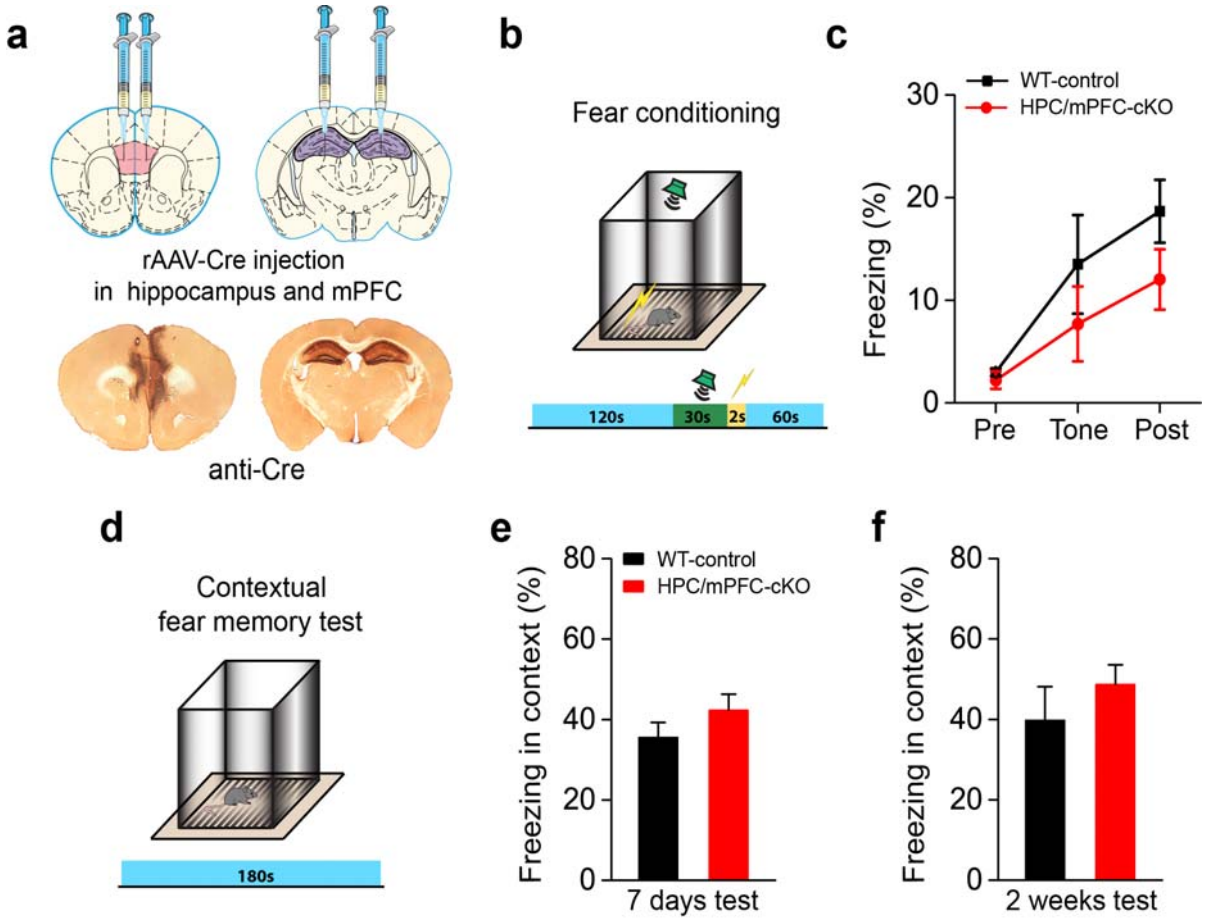

Fig. 2.57 Intact memory retrieval after rAAV-Cre mediated Arc/Arg3.1 ablation in both hippocampus and mPFC. a, Virus injection and Cre recombinase expression in dorsal HPC and mPFC. **b,** Schematic of fear conditioning paradigm and protocol. **c,** Averaged percentage of freezing during fear acquisition phase. HPC/mPFC-cKO mice showed comparable level of freezing after foot shock compared with WT-control mice. **d,** Schematic of fear memory retrieval paradigm and protocol. Contextual fear memory was tested at 7 days and 2 weeks after conditioning. **e,** WT-control and HPC/mPFC-cKO mice showed similar level of freezing in the context 7 days after conditioning (WT-control, 35.58 ± 3.66%; n = 5 and HPC/mPFC-cKO, 42.30 ± 4.01%; n = 7; t_{10} = -1.18, p = 0.26, NS). **f,** WT-control and HPC/mPFC-cKO mice showed similar level of freezing in the context 2 weeks after conditioning (WT-control, 39.83 ± 8.29%; n = 5 and HPC/mPFC-cKO, 48.69 ± 4.89%; n = 7; t_{10} = -0.98, p = 0.35, NS). Bars show mean ± S.E.M. Significance was tested with two-tailed two-sample t-test.

The injected Arc/Arg3.1$^{f/f}$ and WT mice were termed “HPC/mPFC-cKO” and “WT-control”, respectively. Following injections, mice were conditioned at day 7 and long-term fear memory retrieval and specificity were tested either 7 days or 2 weeks later (Fig. 2.57 and 2.58). HPC/mPFC-cKO mice exhibited comparable freezing immediately post foot shocks (Fig. 2.57c), and also perfectly intact retrieval of long-term contextual fear memory 7 days and 2 weeks after conditioning. No significant difference was observed between WT-control and HPC/mPFC-cKO mice in percent freezing in the conditioning context (Fig. 2.57d-f).

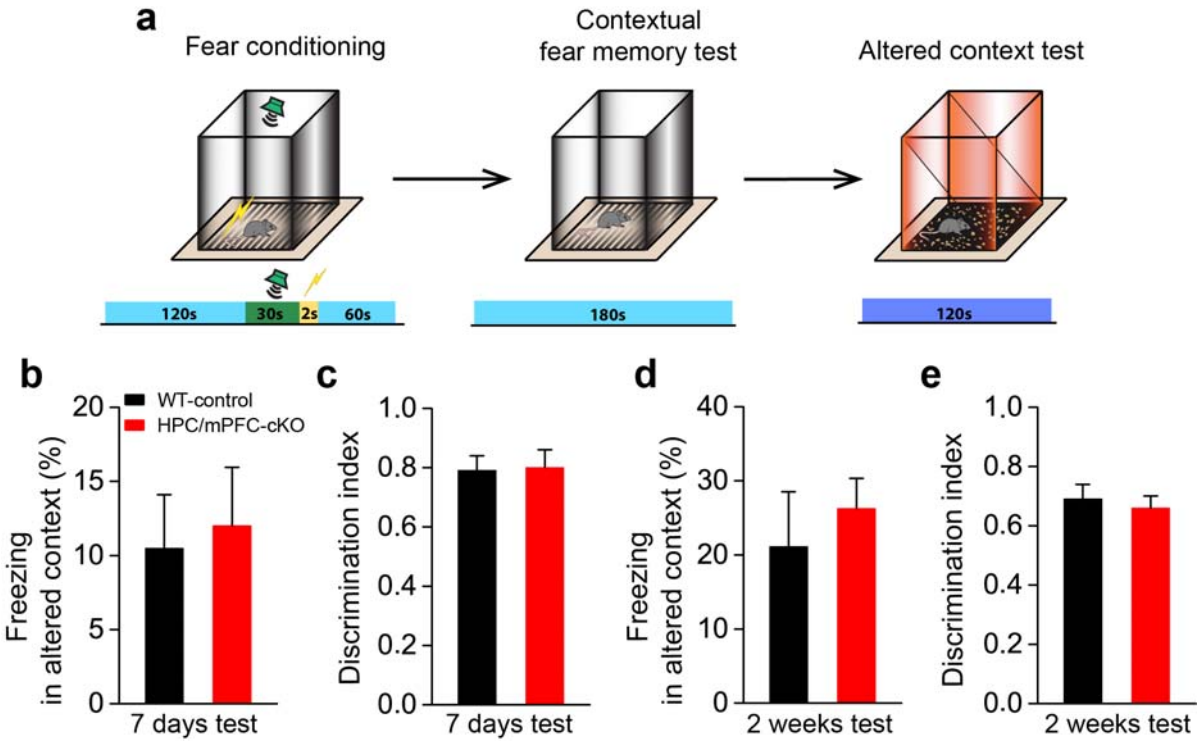

Fig. 2.58 Unaltered memory specificity after rAAV-Cre mediated Arc/Arg3.1 ablation in both hippocampus and mPFC. a, Schematic of fear conditioning and memory test paradigm and protocol. **b-e,** HPC/mPFC-cKO mice displayed comparable memory specificity in comparison with WT-control mice as indicated by freezing level in the altered context and discrimination index of two contexts. 7 days altered context (**b,** WT-control, 10.47 ± 3.63%; *n* = 5 and HPC/mPFC-cKO, 12.00 ± 3.95%; *n* = 7; t_{10} = -0.27, *p* = 0.79, NS). 7 days discrimination index (**c,** WT-control, 0.79 ± 0.05; *n* = 5 and HPC/mPFC-cKO, 0.80 ± 0.06; *n* = 7; t_{10} = -0.13, *p* = 0.90, NS). 2 weeks altered context (**d,** WT-control, 21.13 ± 7.37%; *n* = 5 and HPC/mPFC-cKO, 26.24 ± 4.09%; *n* = 7; t_{10} = -0.65, *p* = 0.53, NS). 2 weeks discrimination index (**e,** WT-control, 0.69 ± 0.05; *n* = 5 and HPC/mPFC-cKO, 0.66 ± 0.04; n = 7; t_{10} = 0.49, *p* = 0.64, NS). Bars show mean ± S.E.M. Significance was tested with two-tailed two-sample *t*-test.

Memory specificity was tested 7 days after conditioning (Fig. 2.58a). HPC/mPFC-cKO, like WT-control mice, exhibited low freezing in the altered context and a high discrimination index (Fig. 2.58b-c). However, 14 days post conditioning the same mice were placed into a second altered context (Home cage arena with fresh beddings). Both WT-control and HPC/mPFC-cKO mice exhibited stronger freezing compared to the first altered context,

indicating stronger generalization and weaker context specificity of retrieved memory (Fig. 2.58d-e). Because the retest induced generalization also existed in the WT-control mice, it will be necessary in the future to inject another independent group of mice for assessing memory specificity at 14 days or even longer time point. Despite of this, it was clearly shown that, ablation of Arc/Arg3.1 in both hippocampus and mPFC still did not disrupt retrieval of long-term contextual fear memory. These data, to some extent, intimate that there must be other traces of the contextual fear memory generated through Arc/Arg3.1 mediated plasticity in broader brain regions. Mutual plasticity compensation among these mnemonic regions occurs in a general and comprehensive way.

2.8.11 Contextual fear memory in Late-cKO mice with Arc/Arg3.1 ablation in forebrain

Local ablation of Arc/Arg3.1 in the hippocampus, mPFC, ACC, RSC and BLA alone or in the hippocampus and mPFC together did not affect the ability of long-term contextual fear memory retrieval, which might be explained by the hypothesis that memory is encoded by multiple engrams in a broadly distributed hippocampal-cortical network. In this network, contextual fear memory could be preserved even when one or more engrams were confounded. If this is true, then removal of Arc/Arg3.1 from even more brain regions would induce the expected loss of contextual fear memory.

By utilizing Late-cKO mice, I could achieve broad ablation of Arc/Arg3.1 in the forebrain including hippocampus and most cortical regions. In order to make a fair comparison with locally Arc/Arg3.1 ablated mice, I subjected independent groups of Late-cKO and their WT-control littermates to the same fear conditioning protocol and procedure. Contextual fear memory was tested 7 and 21 days after conditioning. Post foot shocks, Late-cKO produced slightly stronger fear responses with higher percent freezing compared to WT-control mice (7 days group, $p = 0.09$; Fig. 2.59b-c). 7 days after conditioning Late-cKO mice had intact contextual fear memory retrieval, however, they displayed significantly impaired remote memory retrieval after 21 days (7 days, $p = 0.71$; 21 days, $p < 0.001$, two-sample *t*-test; Fig. 2.59d-f). Percent freezing was dramatically lower in the Late-cKO mice compared with WT-control mice ($p < 0.001$, two-sample *t*-test; Fig. 2.59f). Memory persistence was even shorter when residual Arc/Arg3.1 in the hippocampus was further removed by rAAV-CreER^{T2}-Venus injection. One day after conditioning, memory retrieval was already impaired in the injected Late-cKO mice as shown by significantly lower freezing ($p < 0.05$, two-sample *t*-test; Fig. 2.60d).

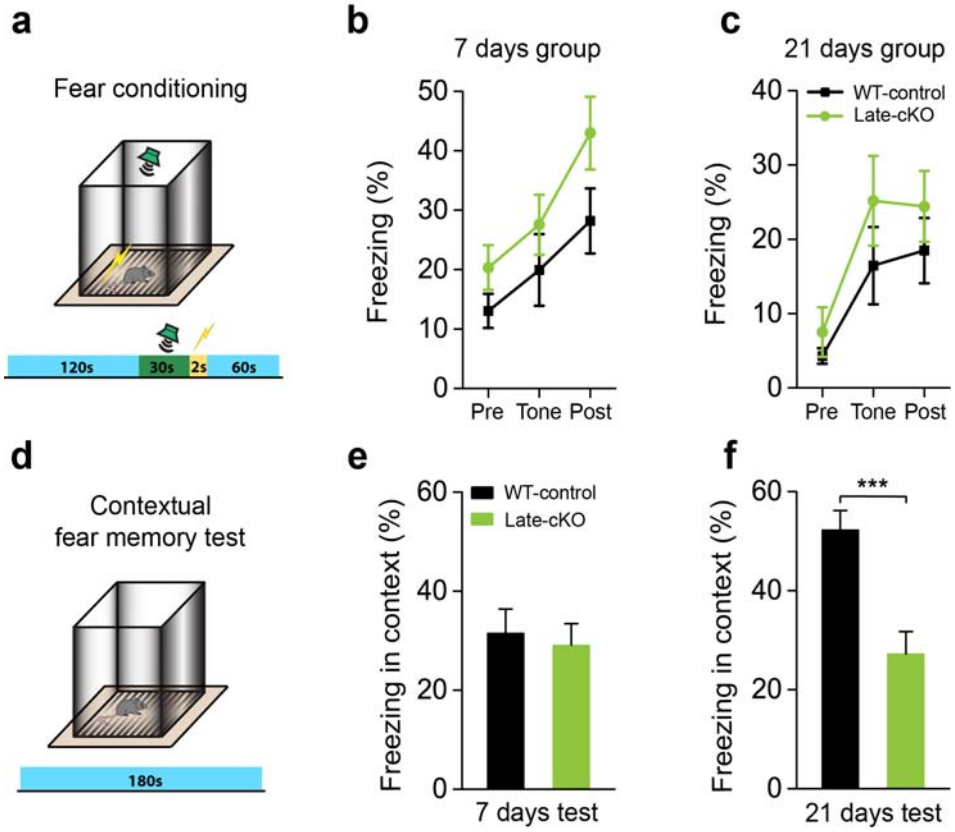

Fig. 2.59 Impaired remote contextual fear memory in mice with forebrain Arc/Arg3.1 ablation. a, Schematic of fear conditioning paradigm and protocol. Contextual fear memory was tested at 7 days or 21 days delay after conditioning. **b-c,** Averaged percentage of freezing during fear acquisition phase. **d,** Schematic of fear memory test paradigm and protocol. **e,** WT-control and Late-cKO mice displayed similar level of freezing in the context 7 days after conditioning. Context (WT-control, 31.51 ± 4.87%; n = 10 and Late-cKO, 29.05 ± 4.38%; n = 9; t_{17} = 0.37, p = 0.71, NS). **f,** Remote contextual fear memory was significantly impaired in Late-cKO mice 21 days after conditioning (WT-control, 52.27 ± 3.91%; n = 10 and Late-cKO, 27.18 ± 4.56%; n = 10; t_{18} = 4.18, ***p < 0.001). Bars show mean ± S.E.M. Significance was tested with two-tailed two-sample t-test.

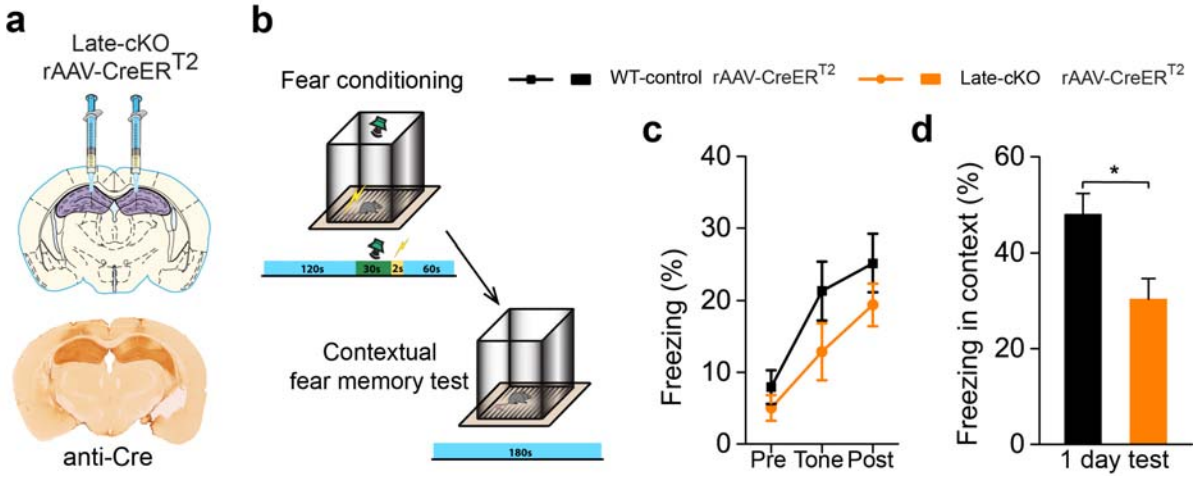

Fig. 2.60 Earlier contextual fear memory deficits after rAAV-CreER^{T2} mediated Arc/Arg3.1 ablation in the hippocampus of Late-cKO mice. a, Schematic of fear conditioning and memory test paradigm and protocol. **b,** Cre expression in the hippocampus of Late-cKO mice with rAAV-CreER^{T2} injection. **c,** Similar levels of freezing during conditioning. **d,** Residual Arc/Arg3.1 ablation in the hippocampus of Late-cKO mice caused earlier memory deficit. 1 day context (WT-control rAAV-CreER^{T2}, 47.97 ± 4.34%; n = 7 and Late-cKO rAAV-CreER^{T2}, 30.34 ± 4.31%; n = 8; t_{13} = 2.87, *p < 0.05). Bars show mean ± S.E.M. Significance was tested with two-tailed two-sample t-test.

However, despite successful memory retrieval at 7 days delay, Late-cKO mice were confounded in the altered context and exhibited significantly higher freezing compared to WT-control mice (p < 0.001, two-sample t-test; Fig. 2.61b). A strongly reduced context discrimination index in the Late-cKO mice further confirmed their loss of memory specificity (p < 0.001, two-sample t-test; Fig. 2.61c). Memory specificity was not assessed at 21 days delay for the Late-cKO or at 1 day delay for the injected Late-cKO mice due to loss of context memory.

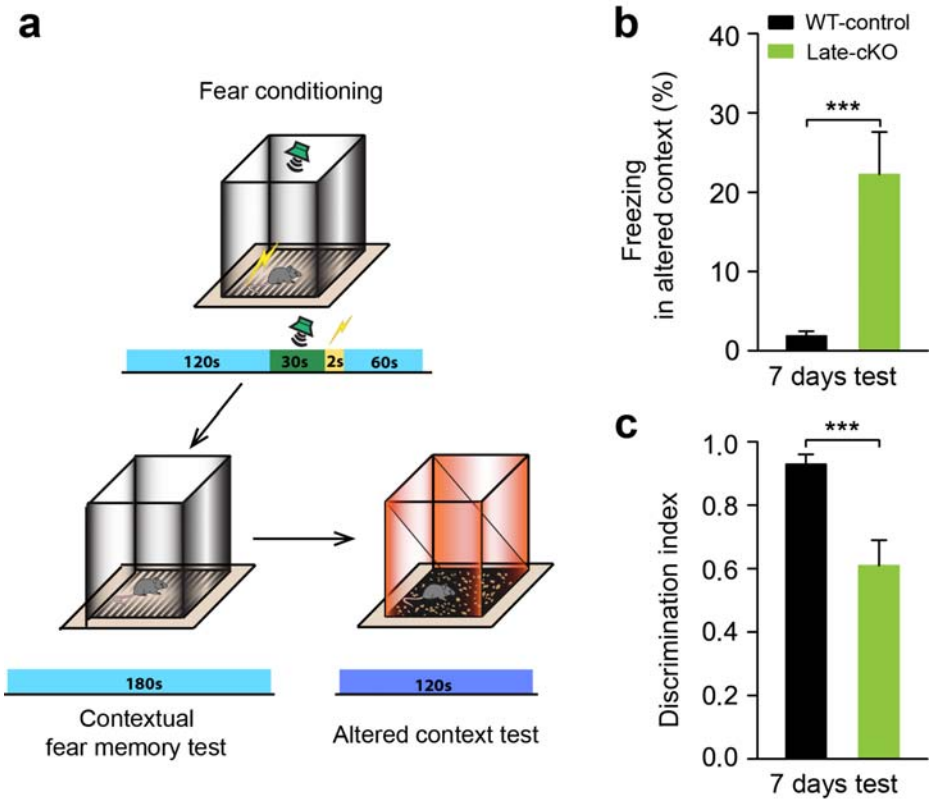

Fig. 2.61 Loss of memory specificity in the mice with forebrain Arc/Arg3.1 ablation. a, Schematic of fear conditioning and memory test paradigm and protocol. **b,** Late-cKO mice showed significantly higher freezing level in the altered context 7 days after conditioning (WT-control, 1.87 ± 0.57%; n = 10 and Late-cKO, 22.26 ± 5.34%; n = 9; t_{17} = -4.01, ***p < 0.001). **c,** Late-cKO mice showed significantly lower discrimination index of two contexts 7 days after conditioning (WT-control, 0.93 ± 0.03; n = 10 and Late-cKO, 0.61 ± 0.08; n = 9; t_{17} = 4.08, ***p < 0.001). Bars show mean ± S.E.M. Significance was tested with two-tailed two-sample t-test.

Taken together, data from local and forebrain Arc/Arg3.1 ablation complemented each other and proved that even a single brain region (e.g. hippocampus) containing sufficient number of Arc/Arg3.1 expressing neurons, could protract long-term contextual fear memory. In contrast, removal of Arc/Arg3.1 in one or two mnemonic regions cannot significantly block contextual fear memory retrieval. However, ablation of Arc/Arg3.1 in the adult hippocampus impaired synaptic plasticity and thereby possibly caused reduced memory specificity which demonstrates that either critical details of contextual information are permanently stored in the hippocampus for achieving precise memory retrieval or precise memory retrieval relies

on functional hippocampus communicating with relevant mnemonic regions. Collectively, Arc/Arg3.1 mediated synaptic plasticity in broadly distributed hippocampal-cortical networks is essential for memory consolidation and retrieval in adulthood. Notably, precise remote memory retrieval cannot be achieved independent of plastic and functional hippocampus.

Part IV Dependence of long-term implicit memory consolidation on spatiotemporal Arc/Arg3.1 expression

2.9 Long-term implicit memories in Arc/Arg3.1 KO and Late-cKO mice

Implicit memory may be the only type of memory observed in lower invertebrates which demonstrates its early phylogenetical origin, extreme necessity and importance in life. Unlike explicit memories, the recall of implicit memories is always unconscious. A very good example of the differences between explicit and implicit memory is the famous case of the patient H.M. H.M. had strong memory deficits when his medial temporal lobe was resected bilaterally (Scoville and Milner, 1957; Penfield and Milner, 1958). Surprisingly, scientists found that lesion induced-memory impairments in H.M. were mainly limited to explicit memories. He still demonstrated the ability to store implicit long-term memories in a procedural learning experiment (Squire and Wixted, 2011). This research indicates that implicit and explicit memories are represented by different neurological systems (Dew and Cabeza, 2011; Squire and Dede, 2015).

In the above chapters of this thesis, I investigated the role of Arc/Arg3.1 in formation and consolidation of explicit memories. I revealed that long-term explicit memory consolidation required lifelong Arc/Arg3.1 expression in the adult brain which was distributed in a large hippocampal-cortical network. In the following chapter, I addressed the contribution of Arc/Arg3.1 during development to implicit memory formation and investigated the circuitry within which it is stored. The implicit memory paradigms I employed were auditory fear conditioning and conditioned taste aversion.

2.9.1 Tone fear memory in KO and Late-cKO mice

Auditory fear conditioning is a form of learning in which an aversive unconditional stimulus (US, e.g. electrical shock) is associated with a particular neutral conditional stimulus (CS, e.g. a tone). Eventually, after conditioning the neutral stimulus alone can elicit the state of fear. In this study tone fear memory was first tested in KO and Late-cKO mice. I placed mice in a conditioning arena and subjected them to 5 pairs of tones / foot shocks stimuli. Tone fear memory was assessed by placing mice into a novel arena with different visual, tactile, geometrical and olfactory characteristics from the conditioning environment (Fig. 2.62a). The same neutral tone that was paired with the CS shocks and was replayed in the novel context to isolate the tone fear memory. Consistent with previous reports from conventional Arc/Arg3.1 KO mice, re-derived constitutive Arc/Arg3.1 KO mice exhibited lower percent freezing to the tone compared to their WT littermates, when tested 7 days after conditioning ($p < 0.05$, two-sample *t*-test; Fig. 2.62b), implying a loss of tone fear memory. In strong contrast, Late-cKO mice exhibited similar percent freezing as their WT-control littermates when tested 7 or even 21 days after conditioning (Fig. 2.62c-d). Since residual low amount of Arc/Arg3.1 in the brains of Late-cKO mice might be sufficient to support

implicit memory, I tested tone fear memory in their siblings (Late-cKO$_{2xCre}$) which carry double amount of Cre and consequently even less Arc/Arg3.1. Surprisingly, unlike in contextual fear conditioning, Late-cKO$_{2xCre}$ mice still froze very much to the CS tone when being tested 7 days after conditioning, suggesting intact tone fear memory (Fig. 2.62e).

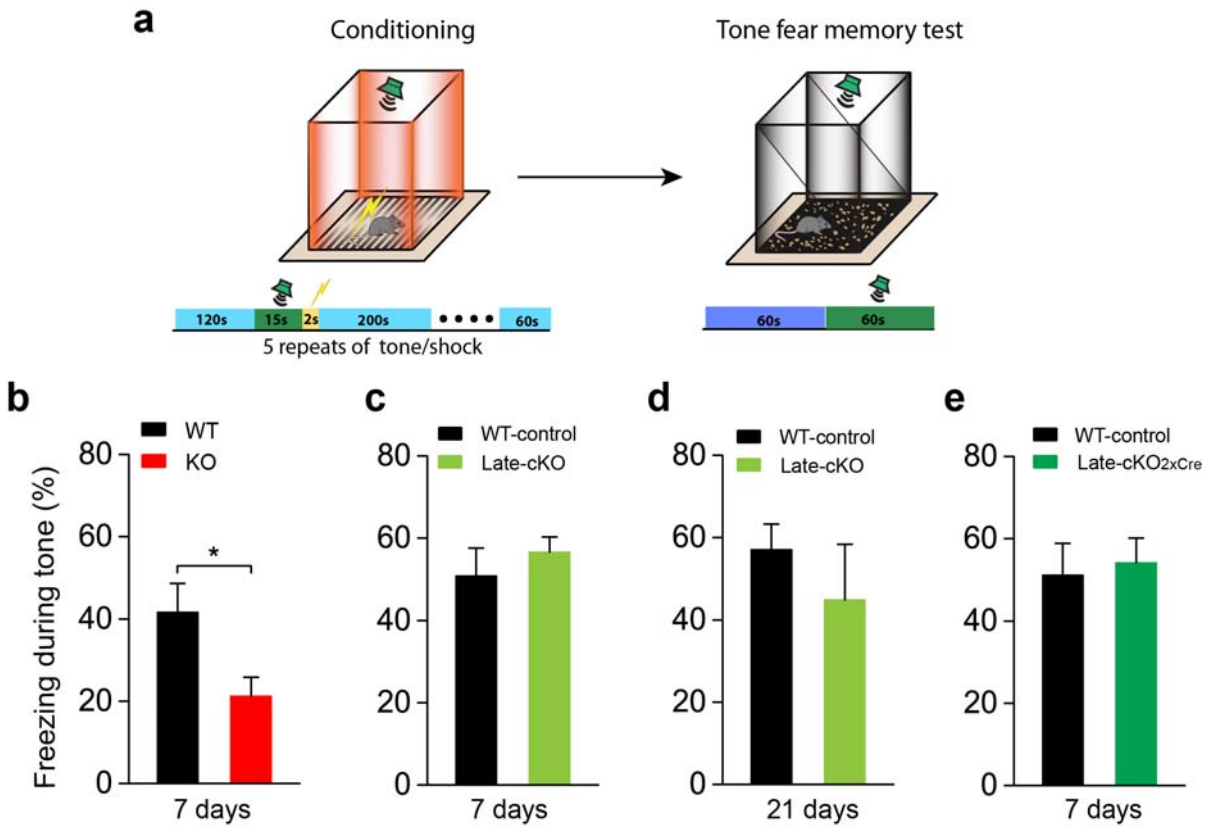

Fig. 2.62 Impaired tone fear memory in KO but not in Late-cKO mice. a, Schematic of tone fear conditioning with 5CS-US. **b,** KO mice froze significantly less to the conditioning stimulus (CS) tone than their WT littermates 7 days after conditioning (WT, 41.65 ± 6.99%; n = 12 and KO, 21.27 ± 4.53%; n = 11; t_{21} = 2.40, *p < 0.05). **c,** Similar freezing of WT-control and Late-cKO mice during the CS tone presentation 7 days after conditioning (WT-control, 50.88 ± 6.69%; n = 11 and Late-cKO, 56.58 ± 3.72%; n = 19; t_{28} = -0.81, p = 0.42, NS). **d,** After 21 days**,** Late-cKO mice still froze similarly as control littermates (WT-control, 57.11 ± 6.18%; n = 6 and Late-cKO, 44.88 ± 13.48%, n = 8; t_{12} = 0.74, p = 0.47, NS). **e,** No significant difference of freezing during the CS tone was observed between WT-control Late-cKO$_{2xCre}$ 7 days after conditioning (WT-control, 51.22 ± 7.65%; n = 9 and Late-cKO$_{2xCre}$, 54.20 ± 5.93%, n = 13; t_{20} = -0.31, p = 0.76, NS). Bars show mean ± S.E.M. Significance was tested with two-tailed two-sample t-test.

In these tests I used 5 pairs of CS-US with high tone intensity (98 dB), which might either saturate fear responses or be themselves aversive and hence obscure detection of differences between WT and Late-cKO mice. To rule out this possibility, I next conditioned Late-cKO mice with a milder protocol in which only one pair of tone/shock association was applied and the tone intensity was reduced (Fig. 2.63a). Remarkably, Late-cKO mice still showed successful tone fear memory retrieval even 21 days after acquisition (Fig. 2.63b-c). Hence, genetically removal of Arc/Arg3.1 during late postnatal development does not

significantly impair tone fear memory consolidation, at least, up to 21 days. Therefore, I conclude that prenatal Arc/Arg3.1 ablation significantly impairs tone fear memory retrieval, whereas, late postnatal Arc/Arg3.1 ablation in the forebrain does not clearly affect it. It also implies a weaker dependence of tone fear memory on Arc/Arg3.1 expression in the forebrain, and possibly a stronger dependence on Arc/Arg3.1 expression in the subcortical areas, such as amygdala and thalamus.

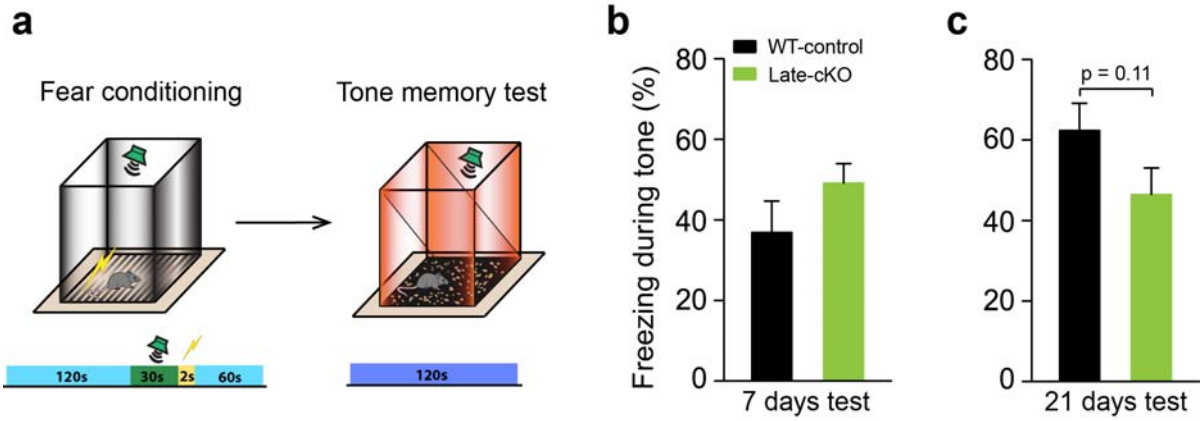

Fig. 2.63 Intact tone fear memory in Late-cKO mice. a, Schematic of tone fear conditioning with 1 CS-US. **b,** Similar level of freezing of WT-control and Late-cKO mice during the CS tone presentation 7 days after conditioning (WT-control, 36.91 ± 7.77%; n = 10 and Late-cKO, 49.14 ± 4.85%; n = 9; t_{17} = -1.30, p = 0.21, NS). **c,** Nonsignificant reduction of freezing in Late-cKO mice at 21 days delay (WT-control, 62.4 ± 6.7%; n = 10 and Late-cKO, 46.44 ± 6.59%, n = 10; t_{18} = 1.70, p = 0.11, NS). Bars show mean ± S.E.M. Significance was tested with two-tailed two-sample t-test.

2.9.2 Tone fear memory after local Arc/Arg3.1 ablation in the hippocampus or basolateral amygdala

To further explore in which brain regions Arc/Arg3.1 mediated plasticity contribute to tone fear memory formation, consolidation and retrieval, I selectively targeted hippocampus and BLA for local rAAV-Cre mediated Arc/Arg3.1 ablation. Fear responses to various stimuli require intact amygdala which receives converging inputs from sensory cortical regions (e.g. auditory cortex), thalamic nuclei and brainstem autonomic nuclei (e.g. periaqueductal gray, PAG). Converging information (CS Tone) is believed to be associated and stored locally in the amygdala (Romanski and LeDoux, 1992; Herry and Johansen, 2014). Lesions of amygdala prevent both encoding and expression of learned fear (Gale et al., 2004). Hippocampus is also thought to mediate some types of fear conditioning (e.g. contextual and trace fear conditioning) by receiving affective impulses from the amygdala and integrating them with previously existing information to make it meaningful. Therefore, I hypothesized that Arc/Arg3.1 mediated plasticity in the amygdala (here refers to BLA) should be essential for implicit tone fear memory, while Arc/Arg3.1 mediated plasticity in the hippocampus might not be necessary. To test this hypothesis, I first bilaterally injected rAAV-Cre into the hippocampus of the Arc/Arg3.1$^{f/f}$ mice and then subjected them to mild tone fear conditioning

(1 paired CS-US with 10k Hz, 70 dB Tone). Tone fear memory was tested at different time points with independent groups of animals (Fig. 2.64a-b).

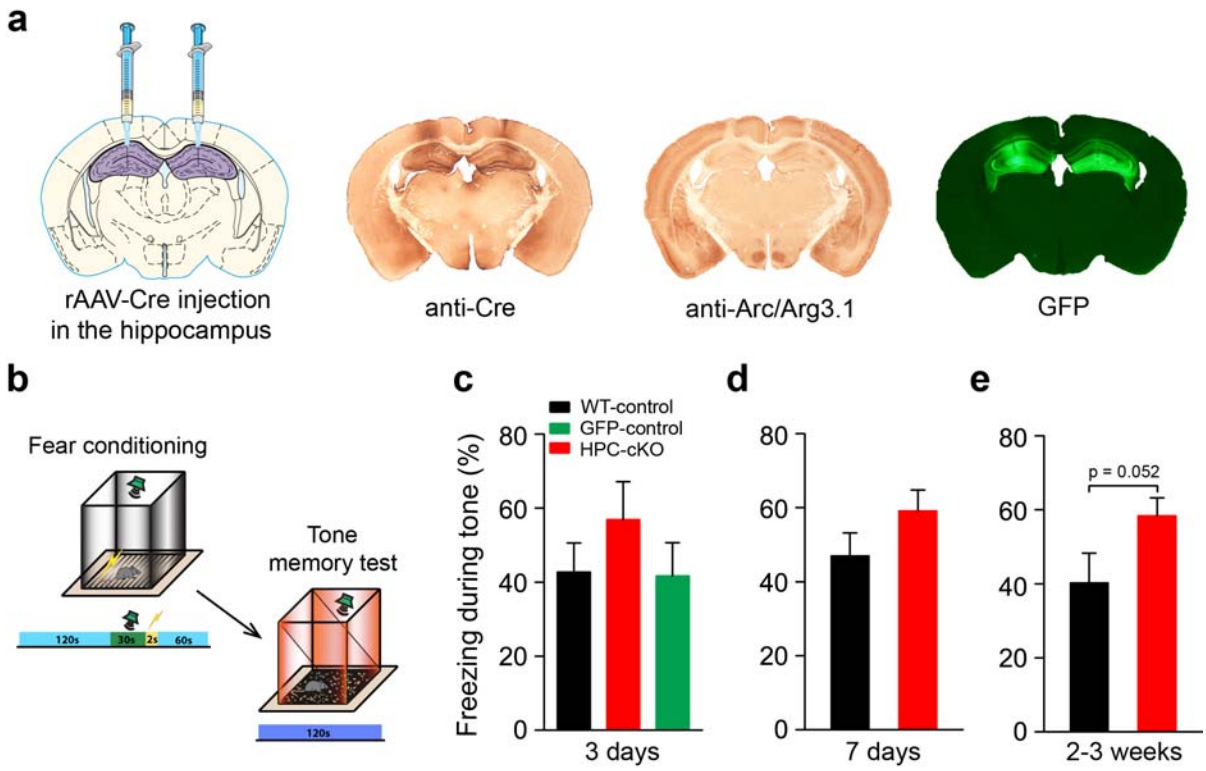

Fig. 2.64 Intact tone fear memory after rAAV-Cre mediated Arc/Arg3.1 ablation in the hippocampus. a, rAAV-Cre or rAAV-GFP was injected bilaterally in the hippocampus. Immunohistochemistry showed that Cre and GFP were well expressed, and Arc/Arg3.1 was well ablated in both hippocampi. **b,** Schematic of tone fear conditioning paradigm and protocol. Mice were conditioned by applying a pair of mild foot shock (0.5 mA) with a neutral tone (10k Hz, 70 dB). **c-e,** Tone fear memory was tested at 3 days, 7 days and 2-3 weeks delay after conditioning with independent groups of mice. **c,** Slightly higher level of freezing in HPC-cKO mice, but no significant difference was observed among WT-control, GFP-control and HPC-cKO mice during 3 days memory retrieval test (WT-control, 42.71 ± 7.84%; n = 6 and HPC-cKO, 56.86 ± 10.25%; n = 7; GFP-control, 41.70 ± 8.95%; n = 6, One-way ANOVA with a *post hoc* LSD test, NS). **d,** Intact tone fear memory retrieval in HPC-cKO mice at 7 days delay (WT-control, 46.97 ± 6.19%; n = 10 and HPC-cKO, 59.18 ± 5.59%; n = 14; t_{22}= -1.45, p = 0.16, NS). **e,** Higher level of freezing in HPC-cKO mice at 2-3 weeks days delay (WT-control, 40.26 ± 7.99%; n = 8 and HPC-cKO, 58.41 ± 4.78%; n = 12; t_{18} = -2.08, p = 0.052, NS). Bars show mean ± S.E.M. Significance was tested with One-way ANOVA with a *post hoc* LSD test or with two-tailed two-sample *t*-test when there were only two groups.

As predicted, when subjected to the CS tone in a novel environment, HPC-cKO mice consistently exhibited strong freezing (Fig. 2.64c-d). An almost significant difference (p = 0.052) was observed when mice were tested 2-3 weeks after conditioning (Fig. 2.64e). However, it must be noted that this does not necessarily indicate enhanced tone fear memory in HPC-cKO mice, because these mice also showed significantly higher percent freezing (about 20%) before replaying CS tone in the same context (Fig. 2.43). In general, local Arc/Arg3.1 ablation in the hippocampus does not affect long-term implicit tone fear

memory retrieval. I next tested tone fear memory in the BLA injected mice (BLA-cKO) in the same conditions with identical stimulation. When tested 1 day after conditioning, BLA-cKO exhibited significantly lower percent freezing compared with WT-control mice, revealing significant loss of tone fear memory ($p < 0.01$, two-sample *t*-test; Fig. 2.65). These findings support the hypothesis that tone fear memory primarily relies on the BLA where Arc/Arg3.1 mediated plasticity plays an essential role. In contrast, tone fear memory formation, consolidation and retrieval does not need the participation of hippocampal plasticity.

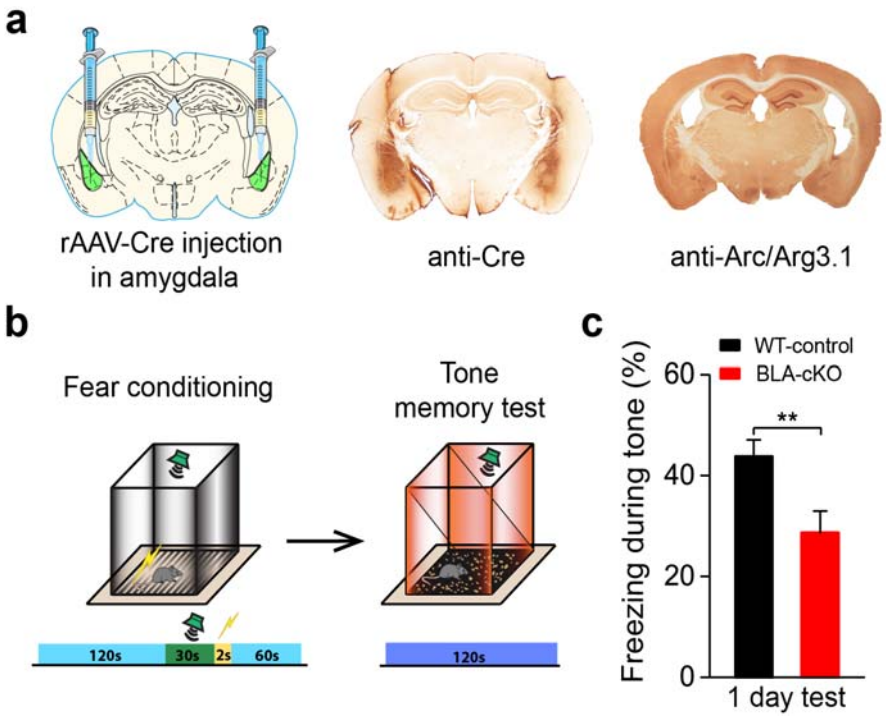

Fig. 2.65 Impaired tone fear memory after rAAV-Cre mediated Arc/Arg3.1 ablation in the BLA. **a,** Schematic of contextual fear conditioning and tone fear memory test paradigm and protocol. **b,** BLA-cKO displayed significantly lower freezing to the tone presentation comparing to WT-control mice, indicating implicit tone fear memory impairment (WT-control, 43.78 ± 3.30%; $n = 16$ and BLA-cKO, 28.66 ± 4.31%; $n = 12$; $t_{26} = 2.83$, $^{**}p < 0.01$). Bars show mean ± S.E.M. Significance was tested with two-tailed two-sample *t*-test.

2.9.3 Conditioned taste aversion memory in KO and Late-cKO mice

Next, I investigated the spatiotemporal role of Arc/Arg3.1 expression in a second implicit memory paradigm: conditioned taste aversion (CTA). In this test, mice were housed in single cage with 3 days water restriction through the pipettes and then were exposed to a novel taste (saccharin) followed by transient gastrointestinal malaise (Fig. 2.66a) induced by intraperitoneal injection of Lithium Chloride (LiCl). Conditioned WT mice strongly and rapidly associate the saccharin with the gastrointestinal malaise, and subsequently avoid it. This association is long-lasting with fast acquisition and moderate extinction (Welzl et al., 2001b). CTA memory was tested at different time delays (Fig. 2.66b). Data were presented by an aversion index: water volume / (water + saccharin volume).

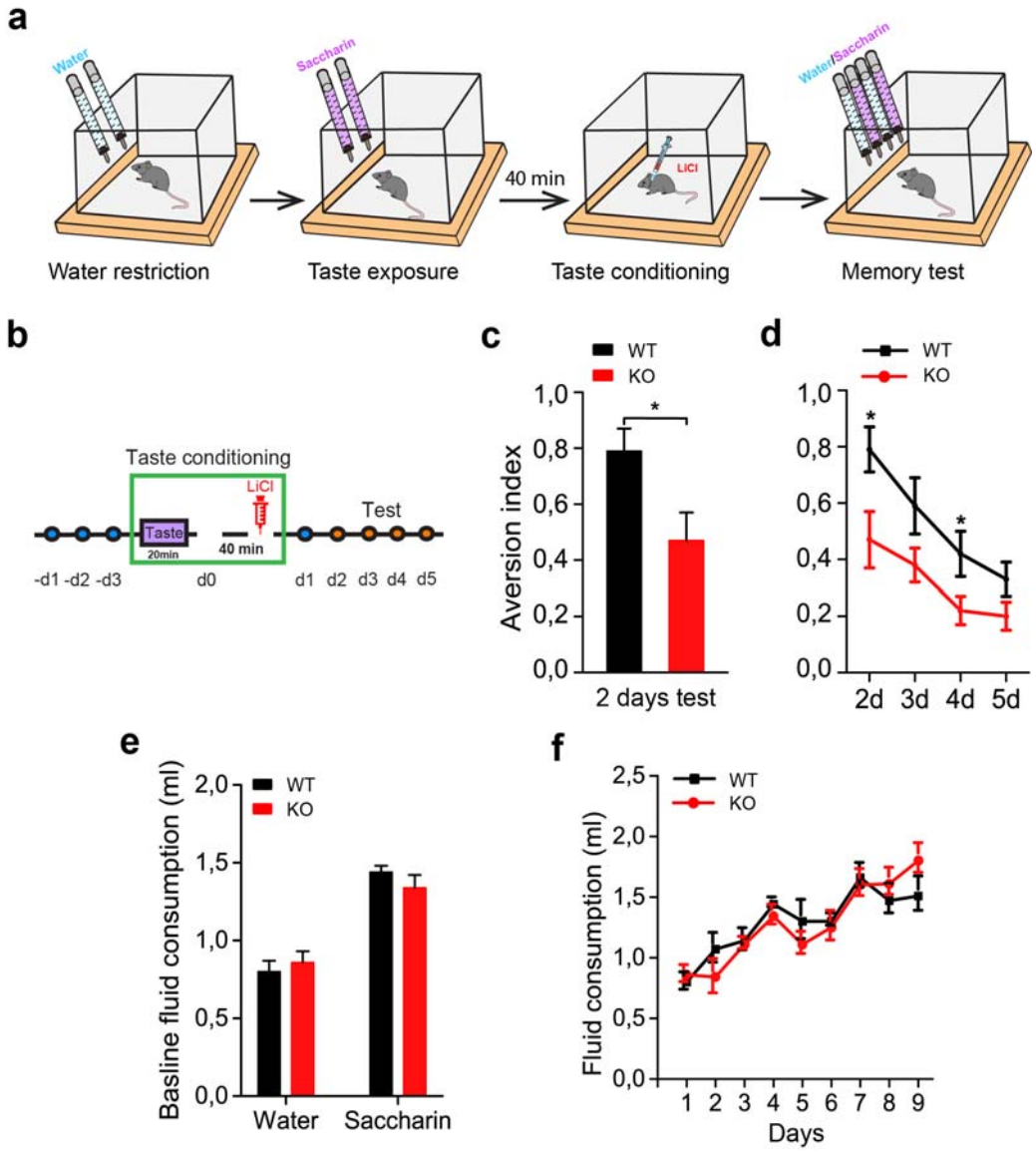

Fig. 2.66 Impaired long-term memory of conditioned taste aversion in KO mice. a-b, Schematic of conditioned taste aversion (CTA) test. Experiment started with a 3 days water restriction regime followed with saccharin exposure and LiCl induced malaise (taste conditioning) on day 4. Implicit taste aversion memory was tested 2-5 days after conditioning. **c**, Two days after conditioning, taste aversion memory was significantly impaired in the KO mice compared to their WT littermates as indicated by lower aversion index (WT, 0.79 ± 0.08 and KO, 0.47 ± 0.10; $t_{13} = 2.38$, $^*p < 0.05$). **d,** Both WT and KO mice showed similar extinction rates of CTA memory (Genotype $F_{(1,13)} = 6.77$, $p < 0.05$; trial block $F_{(3,39)} = 19.72$, $p < 0.0001$; interaction $F_{(3,39)} = 1.01$, $p = 0.40$, NS). **e,** Baseline level of water and saccharin consumption were indistinguishable between WT and KO mice. Water (WT, 0.80 ± 0.07 ml and KO, 0.86 ± 0.07 ml; $t_{13} = -0.62$, $p = 0.55$, NS); Saccharin (WT, 1.44 ± 0.04 ml and KO, 1.34 ± 0.08 ml; $t_{13} = 1.14$, $p = 0.28$, NS). **f,** Both WT and KO mice consumed similar liquid volumes daily during the entire experiment (Genotype $F_{(1,13)} = 0.08$, NS; trial block $F_{(8,104)} = 18.20$, $p < 0.0001$; interaction $F_{(8,104)} = 1.40$, $p = 0.20$, NS). All WT, $n = 7$; KO $n = 8$. Bars show mean ± S.E.M. Significance was assessed with a two-way ANOVA with repeated measures and with a post hoc Fisher LSD test ($^*p < 0.05$) for the memory extinction and daily fluid consumption. Two-tailed two-sample *t*-test was applied between genotypes.

Two days after conditioning, WT mice drunk much more water and avoided drinking from the pipettes containing saccharin as shown by high aversion index, implying that WT

mice formed and consolidated CTA memory. In striking contrast to WT, KO mice did not remember the discomfort induced by LiCl after saccharin consumption and still preferred to drink more saccharin than water with a significantly lower aversion index, suggesting that long-term CTA memory was either not formed or already impaired within 2 days ($p < 0.05$, two-sample *t*-test; Fig. 2.66c).

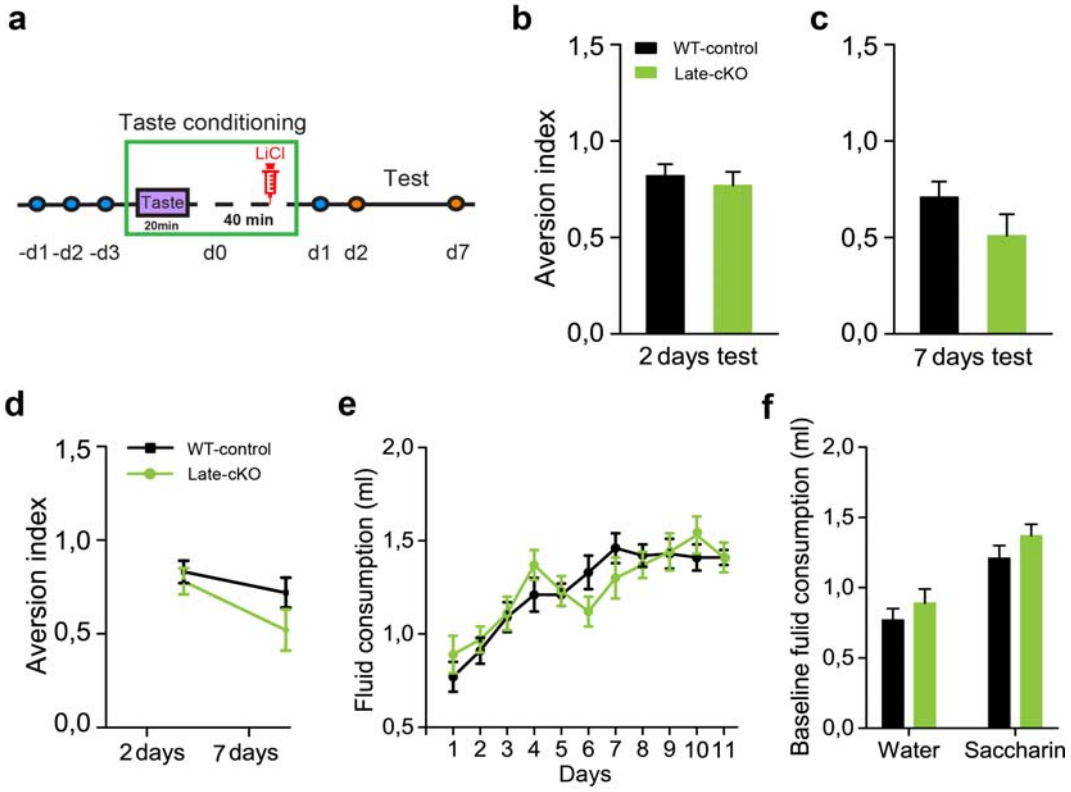

Fig. 2.67 Intact long-term memory of conditioned taste aversion in Late-cKO mice. a, Experiment started with 3 days water restriction following with taste conditioning on day 4. Implicit taste aversion memory was tested 2 days and 7 days after conditioning. **b-d,** Taste aversion memory was not impaired in the Late-cKO mice in comparison with WT-control mice neither 2 days nor 7 days post conditioning as indicated by aversion index: 2 days (WT-control, 0.82 ± 0.06 and Late-cKO, 0.77 ± 0.07; $t_{17} = 0.55$, $p = 0.59$, NS); 7 days (WT-control, 0.71 ± 0.08 and Late-cKO, 0.51 ± 0.11; $t_{17} = 1.43$, $p = 0.17$, NS). **e,** Both WT-control and Late-cKO mice consumed similar amount of fluid every day during the entire experimental process (Genotype $F_{(1,17)} = 0.02$, NS; trial block $F_{(10,170)} = 19.59$, $p < 0.0001$; interaction $F_{(10,170)} = 1.42$, $p = 0.18$, NS). Significance was assessed with a two-way ANOVA with repeated measures and with a *post hoc* Fisher LSD test. **f,** Baseline level of water and saccharin consumption were indistinguishable between WT-control and Late-cKO mice. Water (WT-control, 0.77 ± 0.08 ml and Late-cKO, 0.89 ± 0.10 ml; $t_{17} = -0.93$, $p = 0.37$, NS). Saccharin (WT-control, 1.21 ± 0.09 ml and Late-cKO, 1.37 ± 0.08 ml; $t_{17} = -1.32$, $p = 0.20$, NS). All WT-control, $n = 10$; Late-cKO, $n = 9$. Bars show mean ± S.E.M. Significance was tested with two-tailed two-sample *t*-test between genotypes.

To further test memory extinction, mice were tested again on day 3, 4 and 5. Over time, WT mice learned to uncouple gastrointestinal malaise from saccharin consumption and the response to avoidance of drinking saccharin gradually diminished as indicated by continuously reduced aversion index. KO mice always showed a lower aversion index, but

were nonetheless capable of CTA extinction with a rate similar to WT-littermates (Fig. 2.66d). The innate preference for water and saccharin was similar in WT and KO mice as indicated by similar consumption of water and saccharin prior to the conditioning. These findings indicate that genetic Arc/Arg3.1 deletion did not induce neophobia or hydrophobia (Fig. 2.66e). Thus, the increased saccharin consumption in the KO mice reflects specific CTA memory deficit. Over the entire duration of the CTA test, both WT and KO mice showed gradually increased fluid consumption, but no difference was observed for the total daily fluid consumption, indicating normal fluid uptake and restriction induced drinking pressure (Fig. 2.66f). In strong contrast to the KO mice, Late-cKO mice formed an intact CTA memory that persisted up to 7 days post conditioning, as shown by a clear water/saccharin preference (Fig. 2.67a-d). To test the remote CTA memory, I conditioned a second group of Late-cKO mice and tested them 21 days later (Fig. 2.68a). Surprisingly, Late-cKO mice still exhibited an intact remote CTA memory revealed by their high and WT-like aversion index (Fig. 2.68b).

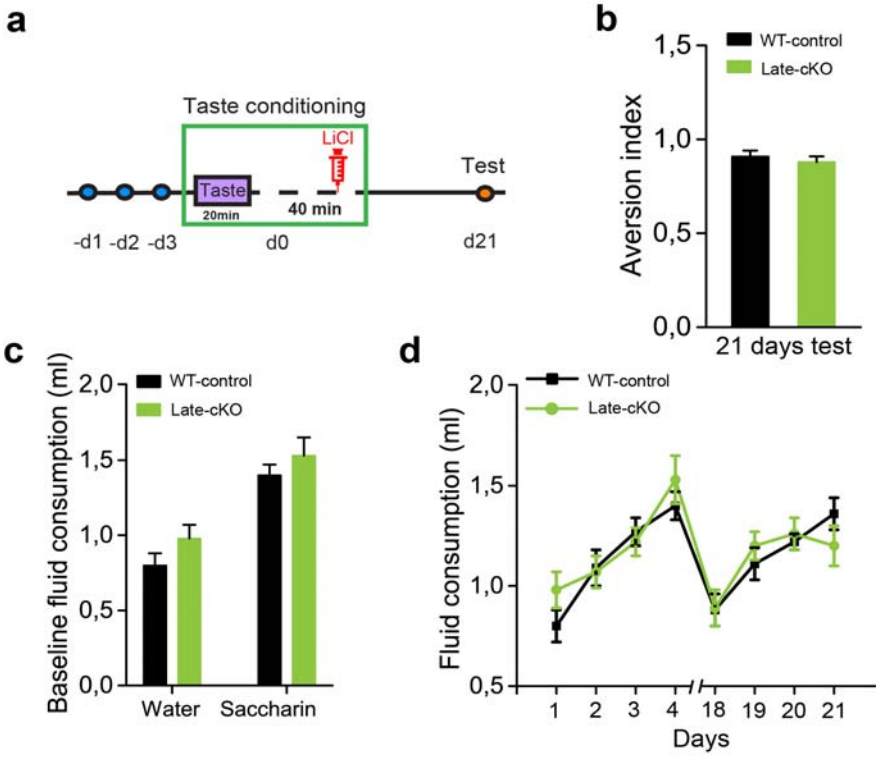

Fig. 2.68 Intact remote memory of conditioned taste aversion in Late-cKO mice. a, Experiment was starting with 3 days water restriction following with taste conditioning on day 4. Remote implicit taste aversion memory was tested 21 days after conditioning. **b,** Remote taste aversion memory was not impaired in the Late-cKO mice in comparison with WT-control mice as indicated by aversion index: (WT-control, 0.91 ± 0.03 and Late-cKO, 0.88 ± 0.03; t_{16} = 0.55, p = 0.59, NS). **c,** Baseline level of water and saccharin consumption were indistinguishable between WT-control and Late-cKO mice. Water (WT-control, 0.80 ± 0.08 ml and Late-cKO, 0.98 ± 0.09 ml; t_{16} = -1.47, p = 0.16, NS). Saccharin (WT-control, 1.40 ± 0.07 ml and Late-cKO, 1.53 ± 0.12 ml; t_{16} = -0.96, p = 0.35, NS). **d,** Both WT-control and Late-cKO mice consumed similar amount of fluid every day during the entire experimental process (Genotype $F_{(1,16)}$ = 0.12, p = 0.74, NS; trial block $F_{(7,112)}$ = 19.44, p < 0.0001; interaction $F_{(7,112)}$ = 1.38, p = 0.22, NS). Significance was assessed with a two-way ANOVA with repeated measurements and with a post hoc Fisher LSD test. All WT-control, n = 9; Late-cKO, n = 9. Bars show mean ± S.E.M. Significance was tested with two-tailed two-sample t-test between genotypes.

Furthermore, long-term CTA memory was also indistinguishable among Late-cKO$_{2xCre}$ and their WT-control littermates 2 and 7 days post conditioning, excluding the possibility that the intact CTA memory in the Late-cKO mice was protracted by the residual Arc/Arg3.1 in the cortex or hippocampus (Fig. 2.69b-d). Besides, late postnatal Arc/Arg3.1 ablation also did not induce neophobia or hydrophobia, and did not affect daily fluid consumption neither in Late-cKO (Fig. 2.67e-f & Fig. 2.68c-d) nor Late-cKO$_{2xCre}$ mice (Fig. 2.69e-f).

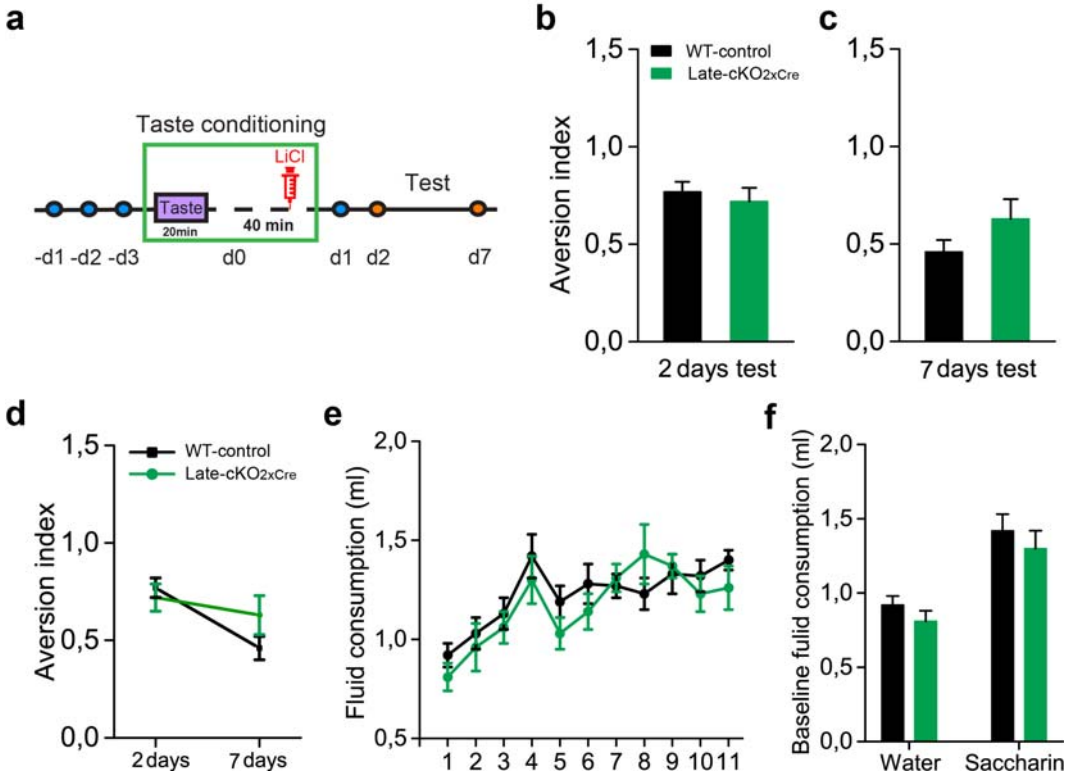

Fig. 2.69 Intact long-term memory of conditioned taste aversion in Late-cKO$_{2xCre}$ mice. a, Experiment was starting with 3 days water restriction following with taste conditioning on day 4. Implicit taste aversion memory was tested 2 days and 7 days after conditioning. **b-d,** Conditioned taste aversion memory was not impaired in the Late-cKO$_{2xCre}$ mice in comparison with WT-control mice neither 2 days nor 7 days post conditioning as indicated by aversion index: 2 days (WT-control, 0.77 ± 0.05 and Late-cKO$_{2xCre}$, 0.72 ± 0.07; t_{17} = 0.55, p = 0.59, NS). 7 days (WT-control, 0.46 ± 0.06 and Late-cKO$_{2xCre}$, 0.63 ± 0.10; t_{17} = -1.42, p = 0.17, NS). **e,** Both WT-control and Late-cKO$_{2xCre}$ mice consumed similar amount of fluid every day during the entire experimental process (Genotype $F_{(1,17)}$ = 0.66, p = 0.43, NS; trial block $F_{(10,170)}$ = 8.49, p < 0.0001; interaction $F_{(10,170)}$ = 0.92, p = 0.52, NS). Significance was assessed with a two-way ANOVA with repeated measures and with a *post hoc* Fisher LSD test. **f,** Baseline level of water and saccharin consumption were indistinguishable between WT-control and Late-cKO$_{2xCre}$ mice. Water (WT-control, 0.92 ± 0.06 ml and Late-cKO$_{2xCre}$, 0.81 ± 0.07 ml; t_{17} = 1.25, p = 0.23, NS). Saccharin (WT-control, 1.42 ± 0.11 ml and Late-cKO$_{2xCre}$, 1.30 ± 0.12 ml; t_{17} = 0.75, p = 0.46, NS). All WT-control, n = 9; Late-cKO$_{2xCre}$, n = 10. Bars show mean ± S.E.M. Significance was tested with two-tailed two-sample t-test between genotypes.

In summary, CTA memory was remarkably impaired as a result of prenatal Arc/Arg3.1 ablation, whereas, late postnatal ablation of Arc/Arg3.1 in the forebrain did not affect CTA memory. One explanation might be that CTA memory formation, consolidation and retrieval do not depend on Arc/Arg3.1 mediated plasticity in the adult. Alternatively, implicit taste

aversion memories rely on specific subcortical regions (e.g. hypothalamus and parabrachial nucleus) (Reilly, 1999; Yamamoto, 2007; Dayawansa et al., 2014) in which Arc/Arg3.1 might not be ablated in the Late-cKO mice and thereby CTA memory could also be protracted with the presence of Arc/Arg3.1 in these areas.

Taken together, intact long-term implicit memories (both tone fear memory & CTA memory) highly rely on Arc/Arg3.1 presence during early development and less depend on Arc/Arg3.1 expression in the adult forebrain. The dependence of implicit memories on Arc/Arg3.1 expression in the subcortical regions should be further explored in the future.

3 Discussion

3.1 Effects of Arc/Arg3.1 gene modification

To achieve spatiotemporally controlled Arc/Arg3.1 ablation, floxed Arc/Arg3.1 mice were generated by Dietmar Kuhl and colleagues (Dammermann, 1999; Bick-Sander, 2002; Plath et al., 2006) through insertion of two loxP sites in the endogenous Arc/Arg3.1 allele. One loxP site is located in the promoter region of Arc/Arg3.1 gene and the second one within the second intron. Any genetic modification can bring unpredictable effects on natural gene expression and behaviors. Especially, here one loxP site was placed in the promoter region which includes sequences for binding RNA transcription factors, synaptic activity response element (SARE) and other regulatory sequences (Fig. 1.4). It might potentially affect RNA transcription efficiency and responses to synaptic activity. I found that Arc/Arg3.1 mRNA and protein can still be induced in Arc/Arg3.1 floxed mice after Kainate-incuded seizures with similar spatial expression, layering pattern and temporal dynamics to WT mice. Nissl staining also indicated normal brain morphology (Fig. 2.3). These results indicate that the strategy used for generating Arc/Arg3.1 floxed mice did not obviously affect baseline and activity-regulated gene expression. In order to serve as a good mouse model for spatiotemporal removal of Arc/Arg3.1, recombination efficacy must be granted. An important factor is the position of and distance between these two loxP sites (~5000 bp in our case). It was previously reported that efficacy of Cre mediated recombination decreases with increasing distance between the loxP sites (Zheng et al., 2000). I found that Cre recombinase driven either by CMV or CaMKIIα promoter efficiently removed Arc/Arg3.1 during development or in adulthood, demonstrating high recombination efficacy (Fig.2.9). Further experiments confirmed that exploratory behavior, locomotor activity, anxiety-like behavior, risk assessment ability, pain sensitivity and fear memory capacity in the Arc/Arg3.1$^{f/f}$ mice were comparable to WT mice (Fig. 2.4-2.7). All of these controls ascertain that Arc/Arg3.1$^{f/f}$ mice behaved exactly like WT mice.

3.2 Cre recombinase mediated Arc/Arg3.1 ablation

Cre-loxP system was designed as a site-specific recombination approach (Sauer, 1987; Sauer and Henderson, 1988). With this approach, it allows researchers to manipulate gene expression in specific cell types (Tsien et al., 1996; Ito-Ishida et al., 2015; Rudenko et al., 2015; Tang et al., 2015) or at specific time points (Erdmann et al., 2007).

Here by employing Cre recombinase transgenic mice or rAAV-Cre injections together with our Arc/Arg3.1 floxed mice, I accomplished Arc/Arg3.1 gene ablation during early embryonic development in the germ cells (by CMV-Cre) or during late postnatal development in the forebrain principal neurons (by CaMKIIα-Cre) or in specific brain regions of adult mice (by rAAV-Cre). This allowed me to explore the role of Arc/Arg3.1 mediated plasticity in

memory consolidation during different developmental stages and to further investigate the spatial dependence of memory consolidation on synaptic consolidation in the hippocampal-cortical network in the adult mice. Cre recombinase under the transcriptional control of a human cytomegalovirus minimal promoter (CMV) mediates Arc/Arg3.1 gene deletion in all cell types, including germ cells (Schwenk et al., 1995). My data showed that Arc/Arg3.1 gene was completely removed. There was no Arc/Arg3.1 mRNA or protein expression in the adult KO brain, just like our conventional KO mice (Fig. 2.9). However, it was reported that Cre gene in the CMV-Cre line appeared to be X-chromosome linked (Schwenk et al., 1995). In my preliminary experiments, WT-controls exhibited memory deficits resulting from the Cre transgene. Thus, to exclude side effects, Cre transgene was crossed out by breeding Arc/Arg3.1$^{f/f,\ Cre+}$ mice with C57Bl/6J WT mice. With this strategy, I successfully re-derived Arc/Arg3.1 KO mice. In order to generate postnatal Arc/Arg3.1 conditional KO mice, CaMKIIα (8.5kb)-Cre mice, in which Cre was expressed in forebrain principal neurons postnatally (Tsien et al., 1996), were crossed with Arc-Arg3.1 floxed mice. This strategy enables a late gene ablation and reduces the risk of abnormal brain development (Tsien et al., 1996). By crossing CaMKIIα-Cre with a ROSA26-LacZ reporter line (Soriano, 1999), Cre activity was detected around P21 in the forebrain but not only in CA1 as originally reported (Tsien et al., 1996). Possibly, CA1 restricted specificity was lost with passage of time and generations. Recent publications and my own data show that this Cre line can now be used as a forebrain specific deleter line.

Nowadays, thanks to the development of viral vectors, local gene ablation in specific cell types and brain regions can also be achieved by injecting rAAV-Cre vectors with cell type specific promoters into gene floxed mice. In my study, I chose rAAV-CaMKIIα-Cre to ablate Arc/Arg3.1 mainly in principal neurons of hippocampus or cortex. I found that Cre expression and Arc/Arg3.1 ablation were very efficient both in the hippocampus and cortex. However, long-term genotoxicity induced by accumulated Cre in the cells was observed to be a function of dosage and time. Preliminary data showed that high level of Cre expression induced apoptosis and significantly increased inflammatory responses indicated by large amount of microglia activation. To circumvent these problems, I reduced the final titer of the virus and restricted the experimental duration to three weeks during which no clear toxicity was detected. Interestingly, leveraging on the leaky activity of rAAV-CaMKIIα-CreER^{T2}-Venus virus, I could ablate Arc/Arg3.1 without genotoxicity for even longer periods of time. Cre-induced toxicity was also reported for some Cre transgenic lines (Forni et al., 2006; Hameyer et al., 2007). Fortunately, I did not observe any clear toxic effect in the brains of the two Cre-carrying mouse lines used in this thesis. The presence of Cre recombinase together with Arc/Arg3.1 ablation does not affect brain development and anatomy. In summary, by

employing Cre-loxP system and Arc/Arg3.1 floxed mice, I reliably achieved spatiotemporally specific Arc/Arg3.1 ablation in the mouse brain thereby addressing the questions at the heart of my thesis.

3.3 Spatiotemporally restricted Arc/Arg3.1 ablation does not affect exploratory and anxiety-like behaviors

Previously published data from our lab revealed that constitutive Arc/Arg3.1 KO mice did not display altered exploratory and emotional behaviors in the open field and elevated plus maze test (Plath et al., 2006). However, some studies demonstrated that cell type specific or brain region specific removal of plasticity related genes (e.g. Bdnf, Cdk5 and Creb) mediated by Cre recombinase lead to hyperactivity (Rios et al., 2001) and increased (Vogt et al., 2014) or decreased (Mishiba et al., 2014; Rudenko et al., 2015) anxiety-like behaviors in the adult conditional KO mice. Thus, I examined whether postnatal ablation of Arc/Arg3.1 in forebrain specific CaMKIIα positive principal neurons (Late-cKO) affected exploratory and anxiety-like behaviors and compared them with the newly re-derived KO mice. I did not observe hyperactive or altered anxiety-like behaviors in the KO or in Late-cKO mice, implying that the re-derived KO mice were similar to the conventional KO and late postnatal removal of Arc/Arg3.1 in the forebrain principal neurons did not adversely alter exploratory or anxiety-like behaviors. Therefore, Arc/Arg3.1 may either play a nonessential role in supporting or regulating these behaviors in adulthood or consequences of its absence could be compensated for by post developmental mechanisms.

3.4 Explicit memory consolidation requires lifelong Arc/Arg3.1 expression in adulthood

Memories are commonly considered to be consolidated on synaptic and system levels termed “synaptic consolidation” and “system consolidation” (Frankland and Bontempi, 2005; Katche et al., 2013a; Dudai et al., 2015), respectively. It was previously reported that Arc/Arg3.1 is involved in both synaptic and system memory consolidation processes. For example, Arc/Arg3.1 was reported to regulate synaptic efficacy and remodeling (Chowdhury et al., 2006; Plath et al., 2006; Rial Verde et al., 2006; Shepherd et al., 2006; Peebles et al., 2010). Moreover, Arc/Arg3.1 KO mice exhibit impaired consolidation of explicit memories (Plath et al., 2006; Peebles et al., 2010; Yamada, 2011). However, these data were acquired from KO mice in which Arc/Arg3.1 was absent starting from embryogenesis. So far, it remains unclear whether explicit memory consolidation needs lifelong Arc/Arg3.1 expression in the adulthood. In this study, by employing Cre/LoxP system I genetically removed Arc/Arg3.1 during late postnatal development (Late-cKO). I consistently observed that adult Late-cKO mice (including Late-cKO_{2xCre} mice) showed impaired long-term explicit memories, including novel object recognition memory (Fig. 2.16), contextual fear memory (Fig. 2.18)

and spatial memory (Fig. 2.24). Notably, Late-cKO mice displayed prolonged memory persistence compared to their Late-cKO$_{2xCre}$ siblings. As in KO mice, memories were impaired within 7 days in Late-cKO$_{2xCre}$ mice, but within 21 days in Late-cKO mice. These findings suggest that explicit memories were impaired no matter when Arc/Arg3.1 was ablated, pre- or postnatally. Moreover, residual Arc/Arg3.1 in the brain, mainly in the hippocampus of Late-cKO mice, can prolong maintenance of long-term explicit memories. In contrast, local ablation of Arc/Arg3.1 in the adult hippocampus reduces memory specificity (Fig. 2.43), and ablation of Arc/Arg3.1 in the BLA of adult mice remarkably impairs tone fear memory (Fig. 2.65). All of these observations indicate that memory consolidation always requires Arc/Arg3.1 expression in the adult brain. These findings further expand our knowledge about the role of Arc/Arg3.1 in memory processing.

3.5 Arc/Arg3.1 mediated plasticity in the hippocampus contributes to controlling of memory specificity

Although Late-cKO mice successfully retrieved contextual fear memory 7 days after conditioning, the specificity of this memory was dramatically reduced (Fig. 2.61), suggesting an essential role of Arc/Arg3.1 in precise long-term explicit memory retrieval in adulthood. Similar phenomenon was observed in the HPC-cKO mice. However, how Arc/Arg3.1 contributes to control of memory specificity is still not clear. A possible explanation is that in absence of Arc/Arg3.1 mediated synaptic plasticity, details of the encoded memory information could not be fully reorganized and stabilized in the activated synapses and were thereafter lost. Although the underlying mechanisms are not wet resolved, a link between Arc/Arg3.1 expression during memory retrieval, neural and synaptic plasticity, had been previously made. Number of published studies demonstrated that cognitive behavioral training activates a relevant population of neurons that are tagged by expression of plasticity markers, such as Arc/Arg3.1, in mnemonic brain regions of adult WT rodents (Gusev et al., 2005; Gusev and Gubin, 2010a, b; Robinson et al., 2012; Chau et al., 2013; Chia and Otto, 2013; Vousden et al., 2015). These Arc/Arg3.1 tagged neurons have notably different properties and are preferentially recruited and integrated into memory engrams compared with non-tagged neurons. For example, studies showed that behavioral training increases Arc/Arg3.1 some excitatory neurons (Arc/Arg3.1 tagged) which exhibit persistent firing in contrast to Arc/Arg3.1 negative neurons from the same mice or neurons from untrained adult mice (Ren et al., 2014) and behavioral learning can integrate Arc/Arg3.1 tagged neurons into active memory ensembles (Cao et al., 2015). A recent observation interestingly stated that Arc/Arg3.1 can also accumulate in inactive synapses and inversely tag them for downregulation of synaptic strength so as to increase the contrast between inactive and active synapses participating in memory encoding and consolidation (Okuno et al., 2012). Therefore, absence of Arc/Arg3.1 expression might lead to imprecise memory related

synaptic tagging or inverse synaptic tagging, degrade memory reorganization and stabilization and eventually lead to loss of memory specificity.

3.6 Arc/Arg3.1 is essential for synaptic consolidation and is critical for establishing learning and memory networks during early development

Why lifelong expression of Arc/Arg3.1 is so important for memory consolidation? How does Arc/Arg3.1 function to modulate memory? Several lines of evidence show that Arc/Arg3.1 plays a critical role in synaptic plasticity which is linked to memory consolidation and retrieval. Colleagues from our and other labs consistently showed that both LTP (also see Fig. 2.31) and LTD were impaired in the Arc/Arg3.1 KO mice (Guzowski et al., 2000; Plath et al., 2006; Park et al., 2008; Waung et al., 2008) accompanied by long-term memory deficits (Guzowski et al., 2000; Plath et al., 2006; Yamada, 2011; Moser et al., 2014). Interestingly, in adult Late-cKO mice LTP was preserved in the hippocampus DG, which is also the area still expressing appreciable amount of Arc/Arg3.1 (Fig. 2.32). This finding implies that Arc/Arg3.1 can support synaptic plasticity locally in isolated neuronal populations even when absent in the projecting or target neurons. This preserved DG plasticity might also explain the intact recent long-term spatial (1 day) and contextual fear memory (7 days) observed in Late-cKO mice. Whereas, remote memory deficits (21 days) in the Late-cKO mice could result from impaired synaptic consolidation in cortical regions lacking Arc/Arg3.1, because insufficient cortical plasticity is more often correlated with remote memory impairment (Frankland et al., 2001; Zhao et al., 2005). An alternative explanation of the preserved DG-LTP could be that the capacity to undergo plasticity depends on the presence of Arc/Arg3.1 in the developing brain and hence is intact in the Late-cKO mice. To address this possibility, future experiments should asses LTP in the DG and cortex of Late-cKO$_{2xCre}$ mice which are largely devoid of Arc/Arg3.1. In addition, hebbian plasticity, homeostatic plasticity and metaplasticity are also involved in memory consolidation. It has been reported that cultured Arc/Arg3.1 KO neurons could not perform homeostatic AMPAR scaling when neuronal activity was artificially manipulated (Shepherd et al., 2006) and Arc/Arg3.1 KO mice exhibited inability of synaptic scaling when sensory deprivation was applied (McCurry et al., 2010), indicating a role of Arc/Arg3.1 in homeostatic plasticity. Meanwhile, Arc/Arg3.1 was suggested to be a modulator in metaplasticity (Shepherd and Bear, 2011) and actually it has been reported that experience induced Arc/Arg3.1 facilitates LTD induction in the CA1 pyramidal neurons (Jakkamsetti et al., 2013). All of these forms of plasticity should also be examined in the Late-cKO mice in the future.

Apart from synaptic plasticity, oscillations in the theta and gamma frequency as well as high frequency oscillatory events in CA1, termed ripples, are believed to be important for memory encoding and consolidation (Winson, 1978; Buzsaki and Draguhn, 2004;

Montgomery and Buzsaki, 2007; Girardeau et al., 2009; Nyhus and Curran, 2010; Jadhav et al., 2012; Boyce et al., 2016). Interestingly, we also found that theta and gamma oscillatory network activity as well as sharp wave activity were dramatically reduced in the hippocampus and prefrontal cortex of KO mice (Fig. 2.34-35) which can be another explanation for the observed long-term memory deficits. A recent report of altered network activity in Arc/Arg3.1 KO mice during running, underscores the relevance of our findings to behavior (Malkki et al., 2016). Additionally, Mizunuma et al. reported that Arc/Arg3.1 positive neurons participated more frequently in sharp wave activity than the Arc/Arg3.1 negative neurons which further enhances the correlation between adult Arc/Arg3.1 expression and memory consolidation related network activity (Mizunuma et al., 2014). However, these network activities were not clearly altered in the Late-cKO mice (Fig. 2.34-35) (with the exception of theta and gamma power in the prefrontal cortex of Late-cKO$_{2xCre}$ mice, Fig. 2.36), despite a profound loss of long-term memory consolidation. These findings suggest that Arc/Arg3.1 is continuously required for linking network activity patterns to memory consolidation. Arc/Arg3.1 might accomplish this task by modifying hippocampal-cortical network architecture via mechanisms similar to those proposed to underlie Arc/Arg3.1's contribution to homeostatic synaptic scaling and plasticity (Shepherd et al., 2006; Messaoudi et al., 2007b; Okuno et al., 2012).

Why network activity was dramatically reduced in the hippocampus and PFC of KO mice, but was only affected in the PFC of Late-cKO$_{2xCre}$ mice? What caused the difference? Studies reported that oscillatory network activity in the rodent hippocampus develops postnatally starting with a sharp increase in gamma oscillations around P7 (Lahtinen et al., 2002), followed by an increase in theta power at P8-9 (Leblanc and Bland, 1979) and the emergence of ripples in CA1 at P10-P12 (Buhl and Buzsaki, 2005). Sharp waves, presumably originating from CA3, emerge as the earliest synchronized hippocampal events at P4-6 (Leinekugel et al., 2002). In parallel with the process of network activity ontogeny, we also observed that Arc/Arg3.1 mRNA was detectable starting at P7, increased dramatically between P14 and P33 and subsequently decreased to a lower baseline level in adulthood (Fig. 2.1a). Hippocampus and mPFC, two major mnemonic regions, exhibited strong up-regulation of Arc/Arg3.1 during early postnatal development (Fig. 2.1b). Therefore, Arc/Arg3.1 expression during early postnatal development parallels the development of network activity. Absence of Arc/Arg3.1 during this period in the KO mice caused strongly attenuated network activity, directly demonstrating that Arc/Arg3.1, indeed, involves in the ontogeny of oscillatory network activity. In stark contrast to KO mice, Arc/Arg3.1 was still present in Late-cKO mice during the first three postnatal weeks and we did not observe significant alteration in the hippocampal network activity of Late-cKO mice (including Late-cKO$_{2xCre}$), indicating that Arc/Arg3.1 presence during early postnatal development protracts

network oscillation ontogeny. Later absence of Arc/Arg3.1 during late postnatal development (after the third postnatal week) does not affect development of network activity. However, I did observe significantly reduced theta and gamma power in the PFC of Late-cKO$_{2xCre}$ mice (Fig. 2.36). One possible explanation is that temporal expression pattern of Arc/Arg3.1 mRNA differed in the hippocampus and PFC. Up-regulation started earlier in areas CA1 and CA3 of the hippocampus and was later in the PFC (Fig. 2.1). The delayed expression of Arc/Arg3.1 in the PFC (at P21) parallels the late development of this brain region (van Eden et al., 1990). If Arc/Arg3.1 ablation starts earlier in the Late-cKO$_{2xCre}$ mice than that in Late-cKO mice, it might explain why PFC theta/gamma oscillations were impaired in the Late-cKO$_{2xCre}$ mice but not in the Late-cKO mice and also probably explains earlier long-term memory deficits (within 7 days not 21 days) in the Late-cKO$_{2xCre}$ mice. An alternative explanation is that a more complete removal of Arc/Arg3.1 in the hippocampus of Late-cKO$_{2xCre}$ mice compared with the Late-cKO, strongly weakened functional interactions between the hippocampus and its target cortical areas, such as PFC, and thereby potentially reduces the oscillatory activity in the PFC.

In summary, Arc/Arg3.1 is essential for establishing, refining and modulating brain network activity during early development, thereby establishing a necessary basis for encoding of memory and spatial information. Given intact neural network, lifelong Arc/Arg3.1 expression in adulthood is still critical for consolidation of synaptic plasticity and of long-term memory.

3.7 Spatial learning highly relies on Arc/Arg3.1 expression during early but not late postnatal development

Spatial learning is a process of generating cognitive maps for locating specific places or positions by using spatial cues (Floresco, 2014). It highly depends on the hippocampus and its adjacent regions in the temporal lobe. In rodents, one of the most commonly used paradigms for assessing spatial learning is the Morris water maze (da Silva et al., 2014). In this study, I investigated the effects of Arc/Arg3.1 ablation during early (KO mice) and late postnatal development (Late-cKO mice) on spatial learning. I found that re-derived Arc/Arg3.1 KO mice displayed a retarded spatial learning curve during the acquisition phase of water maze, indicating a significantly slower process for spatial information acquisition (Fig. 2.19). In contrast to KO mice, Late-cKO mice acquired spatial information as efficiently as WT-control mice, suggesting an intact spatial learning (Fig. 2.22). The intact spatial learning is not a protraction effect of residual Arc/Arg3.1 in the hippocampus, because it was still intact when Arc/Arg3.1 was additionally removed by Cre mediated ablation (Fig. 2.27). These findings are in close agreement with my hypothesis that spatial learning highly relies on Arc/Arg3.1 expression during early development but not later in life.

Spatial learning refers to “on-line” information processing that allows animals to encode spatial information and facilitates subsequent navigation. During performance of spatial tasks, theta rhythm in the hippocampus invariably accompanies “orienting” and “exploratory” behaviors (Vanderwolf, 1969) and theta oscillations represent the “on-line” state of the hippocampus (Buzsaki, 2002). A large body of evidence exists for the importance of theta rhythm to spatial learning and navigation (Buzsaki, 2005), also in the MWM (Olvera-Cortes et al., 2002). Elimination of hippocampal theta rhythm induced by lesions of the medial septal nucleus impaired the performance in spatial learning experiment (Winson, 1978). Therefore, defective online hippocampal theta activity usually parallels insufficient online hippocampus dependent spatial learning. In line with this theory, we observed a strong reduction of theta power in the hippocampus of KO mice that also showed retarded spatial learning, while Late-cKO mice (including Late-cKO$_{2xCre}$) exhibited normal hippocampal theta oscillations (Fig. 2.34-2.36) and intact spatial learning (Fig. 2.22).

Arc/Arg3.1 ablation in the Late-cKO mice mainly occurs in the forebrain, and sparsely in subcortical areas, some of which can also modulate theta oscillations. In particular, the medial septum nucleus is thought to be the main pacemaker of hippocampal theta rhythm (Stumpf et al., 1962; Stewart and Fox, 1990; Buzsaki, 2002). In theory, it is possible that remaining Arc/Arg3.1 in the septum can preserve theta oscillation in the hippocampus. However, I have not observed Arc/Arg3.1 expression in the medial septum nucleus, but instead in the lateral septum nucleus (Fig. 2.9b) which has been reported to modulate hippocampal theta rhythms (Vinogradova, 1995; Pedemonte et al., 1998; Chee et al., 2015). I did find some residual Arc/Arg3.1 in the lateral septal nucleus of Late-cKO mice, but it was strongly ablated in the Late-cKO$_{2xCre}$ mice (Fig. 2.9b). In either case, hippocampal theta activity was intact in both Late-cKO and Late-cKO$_{2xCre}$ mice, excluding the possibility that residual Arc/Arg3.1 in the lateral septum preserves hippocampal theta generation and therefore protracts spatial learning.

It has been reported that during the positive peak of theta oscillations, the postsynaptic membrane potential is depolarized and NMDA channels are opened to allow large calcium influx that is essential for synaptic plasticity, and presumably memory formation and consolidation (Huerta and Lisman, 1995). It is also well established that stimulating perforant fibers from the entorhinal cortex is optimal for LTP induction in the DG and CA1 of hippocampus. Long-term synaptic plasticity in the PP-DG pathway contributes to spatial learning and memory. In line with this hypothesis, TBS-induced LTP in the DG of conventional KO mice (Plath et al.) and spatial learning are both severely impaired. In contrast, Late-cKO mice maintain TBS-induced DG-LTP which could contribute to their

superior spatial learning. In comparison with theta oscillation related “on-line” information processing, sharp-wave ripples (SWRs) occurring mainly during slow wave sleep are thought to involve “off-line” information processing contributing to memory consolidation. Several studies reported that disrupting neuronal activity during ripple events impairs spatial learning (Ego-Stengel and Wilson, 2010). Interestingly, we also observed fewer ripples in the KO mice, together with an increase of the frequency of the remaining ripples (Fig. 2.35). Again we did not observe any significant alteration of SWRs in Late-cKO mice (including Late-cKO_{2xCre} mice, Fig. 2.35-2.36). Thus, absence of Arc/Arg3.1 during early development affects hippocampal SWRs activity which can also lead to impaired spatial learning. In addition, in studies where activity of single neurons was monitored, it was reported that hippocampal neurons frequently replay firing sequences previously acquired while rodents were performing spatial learning (Karlsson and Frank, 2009). It was also reported that awake SWRs are necessary for awake replay of memory related information that support spatial learning (Jadhav et al., 2012). The LFP recordings presented in this thesis were performed under anesthesia and hence may not accurately reflect awake activity. That whether awake SWRs are impaired in the Arc/Arg3.1 KO and Late-cKO mice remains to be examined.

In conclusion, Arc/Arg3.1 expression during early development is critical for establishing functional theta oscillation, mature ripple activity and constructing plastic synapses for supporting efficient spatial learning.

3.8 Compensation for brain region-specific Arc/Arg3.1 ablation in long-term contextual fear memory

Numerous studies have shown that consolidation and recalling of contextual fear memory require the participation of specific cortical regions and the hippocampus, and essentially depend on their interactions. Artificial manipulations of specific brain regions in the network, including lesions, inactivation or activation, proved the involvement of hippocampus, mPFC, ACC, RSC and amygdala in the contextual fear memory encoding, consolidation and retrieval (Maren, 1999; Anagnostaras et al., 2001; Poulos et al., 2009; Goshen et al., 2011; Tse et al., 2011; Einarsson and Nader, 2012; Katche et al., 2013b; Bero et al., 2014; Czajkowski et al., 2014; Denny et al., 2014). In this study, I employed Arc/Arg3.1 as a molecular tool to investigate the dependence of contextual fear memory on synaptic consolidation in the hippocampal-cortical network by using rAAV-Cre mediated specific Arc/Arg3.1 ablation in those mnemonic regions. Surprisingly, I found that local ablation of Arc/Arg3.1 in the hippocampus, amygdala or in any one of the tested cortical regions (mPFC, ACC or RSC) before fear conditioning, did not affect long-term contextual fear memory retrieval (Fig. 3.1). A possible explanation is that loss of synaptic plasticity in one region can be compensated by recruiting other plasticity-intact regions. Fanselow and his colleagues

reported that plasticity through recruitment of alternate structures, especially mPFC, is required for contextual fear memory acquisition and consolidation following damage to the hippocampus (Zelikowsky et al., 2013). Similar compensatory plasticity was found in the bed nuclei of the stria terminalis (BNST) when lesions were performed in the BLA (Poulos et al., 2010). However, under our experimental conditions, mice could still retrieve long-term contextual memory even when Arc/Arg3.1 was removed, simultaneously, in both hippocampus and mPFC (Fig. 2.57), suggesting broader compensatory circuits exist. The observation that forebrain Arc/Arg3.1 ablation in the Late-cKO mice significantly impaired long-term contextual fear memory (Fig. 2.59) suggest that these regions are located within the cortex. These findings support the hypothesis that contextual fear memory can be encoded and stored in parallel by distributed hippocampal-cortical circuits. When one circuit element is prevented from storing the information, another one or more elements can take over such that memory consolidation and retrieval are sustained.

However, other studies reported that lesions or inhibition (optogenetically or pharmacologically) of the hippocampus (Anagnostaras et al., 2001; Goshen et al., 2011; Denny et al., 2014), mPFC (Tse et al., 2011; Bero et al., 2014), ACC (Teixeira et al., 2006; Goshen et al., 2011; Einarsson and Nader, 2012), RSC (Keene and Bucci, 2008; Corcoran et al., 2011; Robinson et al., 2012; Katche et al., 2013b; Czajkowski et al., 2014) or amygdala (Maren, 1999; Gale et al., 2004; Ponnusamy et al., 2007; Han et al., 2009; Poulos et al., 2009) impaired long-term explicit memory formation or retrieval. In contrast, I did not observe any deficits in fear memory acquisition and retrieval in all Arc/Arg3.1 ablated groups. My observations are also inconsistent with previously published data based on local infusion of Arc/Arg3.1 antisense ODNs to acutely block novel protein synthesis (Guzowski et al., 2000; Ploski et al., 2008; Czerniawski et al., 2011; Holloway and McIntyre, 2011; Maddox and Schafe, 2011; Nakayama et al., 2015; Nakayama et al., 2016). Key to understand these differences might be the time point and duration of these artificial manipulations. It has been often reported that post-training hippocampal lesions induce severe retrograde amnesia, while pre-training lesions cause mild anterograde amnesia or nothing, implying that compensation usually occurs before training if enough time is given. In my experiments rAAV-Cre mediated Arc/Arg3.1 ablation proceeded at least 7 days before fear conditioning, thus reflecting a pre-training manipulation. Compared with pre-training lesion results, it is not surprising that fear memory retrieval was still intact. Since I only removed Arc/Arg3.1 mediated plasticity in the specific brain regions, unlike lesions which abrogate local information processing and plasticity as well as their transfer to other target regions. Functional compensation in the memory circuit might be easier and faster under my experimental conditions.

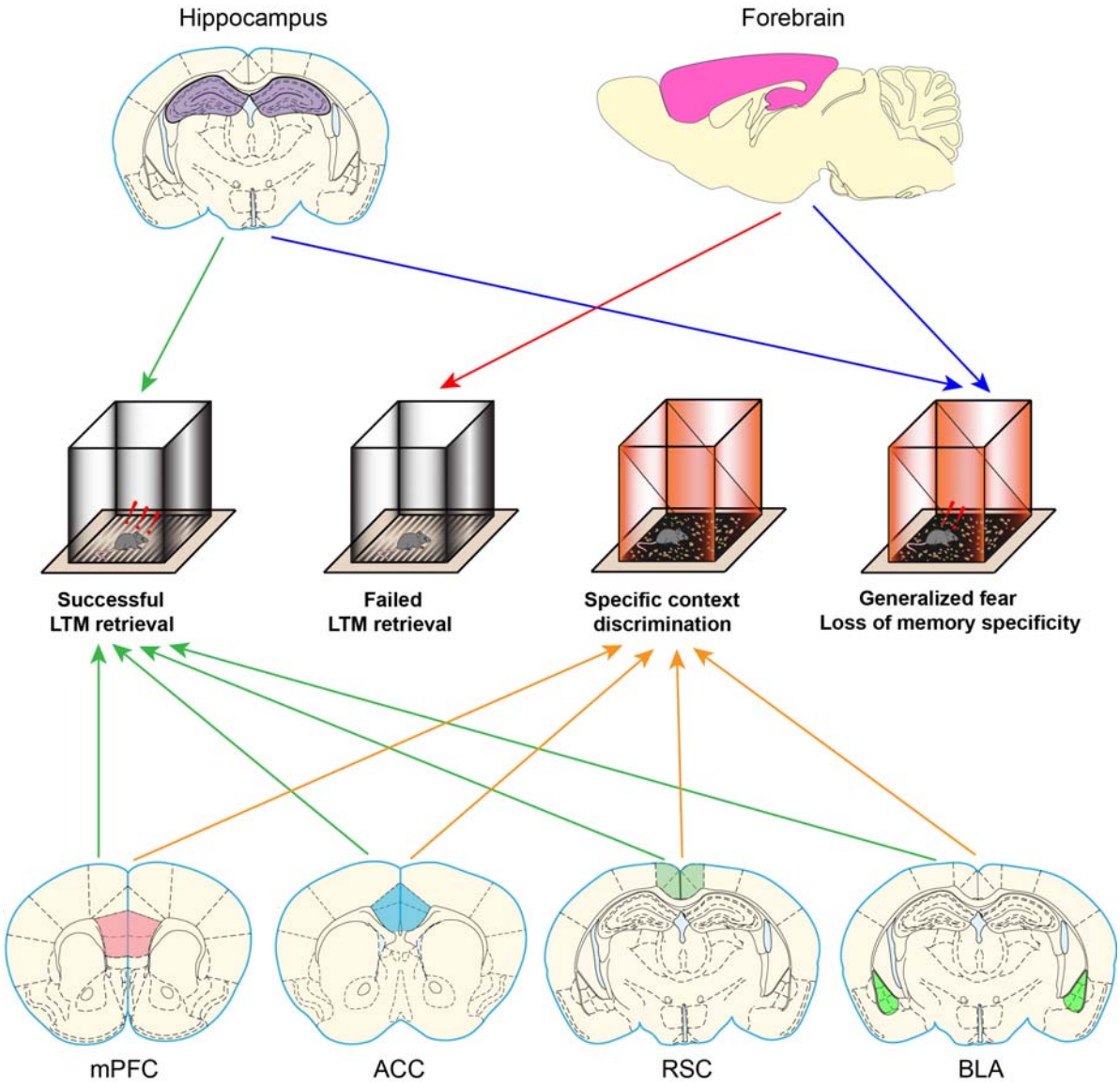

Fig. 3.1 Effects of specific Arc/Arg3.1 ablation in different brain regions on contextual fear memory. Local Arc/Arg3.1 ablation in the hippocampus reduced specificity of remote long-term memory (LTM). Arc/Arg3.1 deletion in single cortical region did not affect LTM retrieval and its specificity. Forebrain Arc/Arg3.1 ablation reduced specificity of early phase of LTM and impaired LTM. ACC, anterior cingulate cortex; BLA, basolateral amygdala; mPFC, medial prefrontal cortex; RSC, retrosplenial cortex.

Temporary inactivation through suppression of synaptic activity in specific brain regions or neurons often induce memory impairments, regardless of whether inhibition was performed pre-training, during training, or post-training. Antisense ODNs acutely blocking novel Arc/Arg3.1 protein synthesis operate similarly to inhibition. Due to the short time course of inhibition and ODNs blockade (from seconds to hours), not enough time is available for functional compensation in the memory circuitry. Therefore, these strategies might potentially mask homeostatic regulation mechanisms underlying acute blockage of novel protein synthesis. In comparison with lesions or acute local inhibition or ODNs blockage, pre-training

plasticity related gene ablation, such as Arc/Arg3.1, only removes an important portion of plasticity in a neuronal circuit leaving synaptic structure and activity largely intact, and this could very well unmask compensation mechanism and allow for more rigorous interpretations. All of these features make it an ideal strategy for investigating the essential components of the memory storage circuitry in the brain.

3.9 The hippocampus interacts with mnemonic cortical regions for detailed memory consolidation

The standard memory consolidation model holds that memory consolidation and retrieval can be achieved independent of the hippocampus as memory aging (Frankland and Bontempi, 2005). A number of studies support this model and revealed that hippocampal lesions or inactivation impair newly acquired contextual fear memory without affecting remote LTM (Kim and Fanselow, 1992; Anagnostaras et al., 1999; Winocur et al., 2009; Wiltgen et al., 2010). Meanwhile, a growing body of literatures reports that hippocampal disruption can affect both recent and remote LTM (Lehmann et al., 2007; Goshen et al., 2011; Winocur et al., 2013).

Therefore, scientists, so far, haven't reached a consensus about whether the hippocampus participates in remote LTM processing or not. In the current study, I observed that mice with local Arc/Arg3.1 ablation in the hippocampus (HPC-cKO mice) could successfully retrieve both recent (3 days) and remote (3 weeks) contextual fear memory (Fig. 2.40 & 2.42), suggesting certain ability to recall recent and remote memories. However, HPC-cKO mice were not capable of distinguishing the conditioning context from an altered one, indicating a loss of memory specificity. These findings demonstrate that the hippocampus, indeed, plays an essential role in remote LTM consolidation and preservation of memory quality (Fig. 2.43). These results are in line with the observations from Frankland and Wiltgen that proper context discrimination requires the involvement of dorsal hippocampus (Frankland et al., 1998) and hippocampus is critical for recalling the details of contextual memories (Wiltgen et al., 2010).

To study the underlying mechanisms, I performed *in vivo* recordings in the DG and observed that TBS-induced fEPSP-LTP was dramatically impaired in the HPC-cKO mice, while basic synaptic transmission was mostly unaffected (Fig. 2.44). I propose that lack of plasticity could affect both local hippocampal network dynamics and communication between the hippocampus and the cortex. Several reports suggested that replay of activity patterns by the hippocampus to the neocortex during sleep contributes to memory consolidation (Nadel et al., 2012; Dudai et al., 2015).

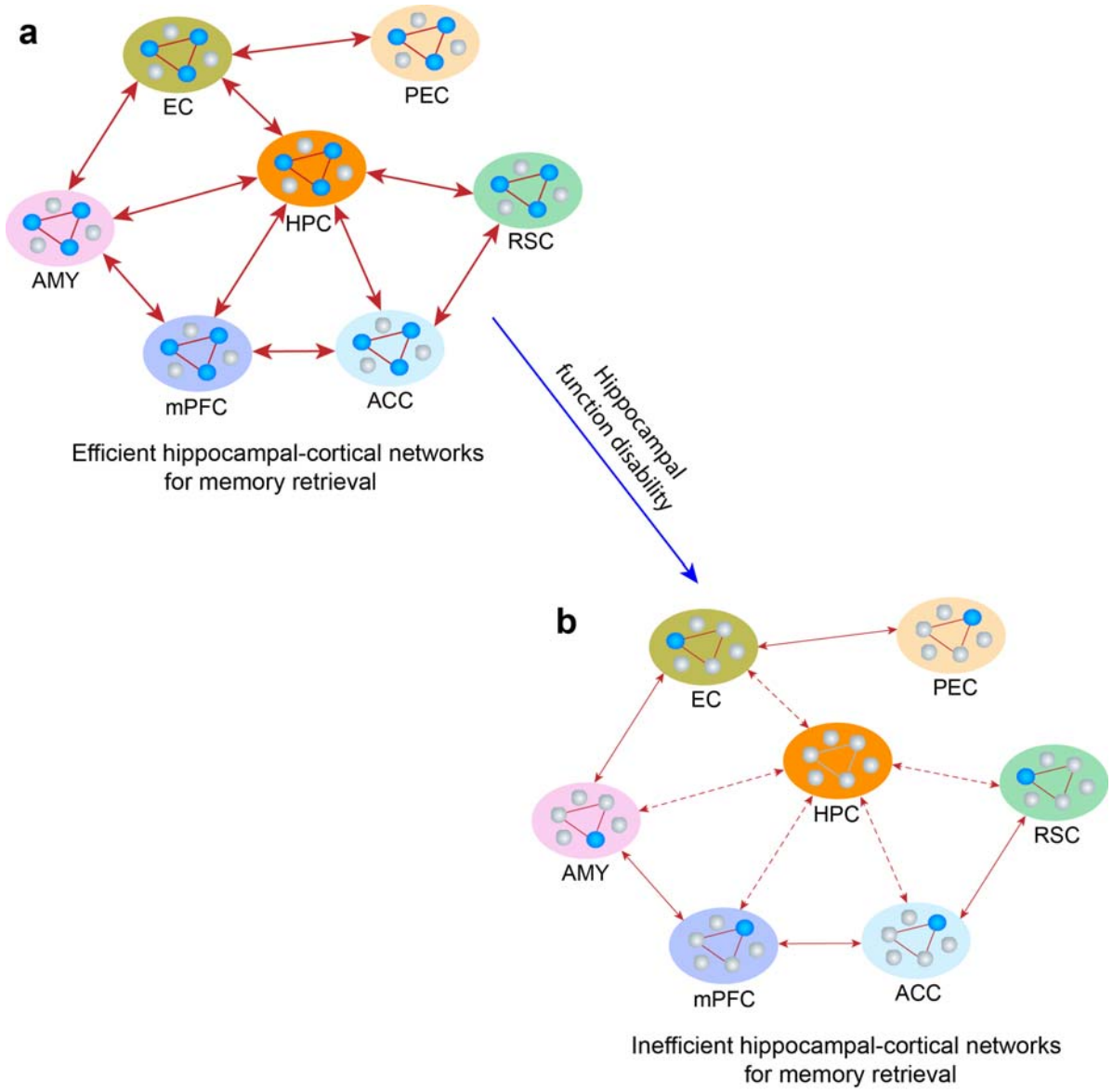

Fig. 3.2 Hippocampal-cortical networks for contextual memory retrieval. a, Efficient communication between hippocampus and cortical regions serves precise contextual memory retrieval. **b,** Hippocampal function disability caused by lesions, inhibition or gene ablation degrades information processing and storage within the hippocampus and disturbs the functional dialog between hippocampus and cortical regions, leading to inefficient reactivation of cortical representations and to reduced accuracy of memory engrams during memory retrieval. ACC, anterior cingulate cortex; AMY, amygdala; EC; entorhinal cortex; HPC, hippocampus; mPFC, medial prefrontal cortex; PEC; perirhinal cortex; RSC, retrosplenial cortex. Solid lines represent strong functional connections; dash lines represent disrupted connections. Line thicknesses represent the strength of the connections.

Due to the lack of plasticity in HPC-cKO mice, the hippocampus can neither efficiently consolidate encoded context memory information in the local hippocampal network nor replay this information correctly to the cortex during memory transformation such that details of the encoded memory are gradually lost. A more likely mechanism is that precise remote LTM retrieval needs functional hippocampus to reactivate specific representations in the cortex. In agreement with this hypothesis, I observed significantly less Arc/Arg3.1 positive

neurons in the mPFC and BLA of HPC-cKO mice after contextual fear memory retrieval (Fig. 2.45 and 3.2), directly suggesting the necessity of functional hippocampus for formation and reactivation of cortical representations. Similarly, Wiltgen and his colleagues recently reported that when CA1 neurons were optogenetically silenced, representations in the EC, RSC, perirhinal cortex (PEC) and amygdala could not be reactivated (Tanaka et al., 2014). Kubik et al. also detected that bilateral pharmacological inactivation of hippocampus resulted in loss of behavior-induced Arc/Arg3.1 expression in RSC (Kubik et al., 2012). In line with these studies, I conclude that loss of Arc/Arg3.1 mediated plasticity in the hippocampus disrupts the interplay between the hippocampus and cortex, degrades information processing and storage within the hippocampus and reduces the accuracy of memory engrams during retrieval.

3.10 Contextual memory encoding, consolidation and retrieval model

So far, neuroscientists have not reached a consensus unifying theory of system memory consolidation. The bone of contention is the questions where memory is encoded and stored, and how it is reorganized and transformed into stable states. The standard consolidation theory (SCT) holds that declarative memories are initially encoded in the hippocampus and then replayed to the neocortex to promote reorganization of cortical representation. Finally, memory is predominantly stored in the cortex independent of the hippocampus (Alvarez and Squire, 1994; McClelland et al., 1995). However, I observed that cortical regions are also activated after fear conditioning indicated by up-regulated Arc/Arg3.1 protein which is similar to other published findings (Tse et al., 2011; Bero et al., 2014; Czajkowski et al., 2014). These observations suggest that not only hippocampus but also neocortex are involved in memory encoding. This was further supported by experiments in which the hippocampus was lesioned yet animals could still encode memory (Anagnostaras et al., 2001; Wiltgen et al., 2006; Zelikowsky et al., 2012). In this study, I also did not observe deficits in memory acquisition when Arc/Arg3.1 mediated plasticity was removed from both hippocampi. A second point of contention in debate about memory storage is about the role of hippocampus in consolidation of LTM. I found that remote LTM specificity was reduced when Arc/Arg3.1 mediated plasticity was prevented in the hippocampus, suggesting a critical role of hippocampus in remote LTM processing which is consistent with some previously published findings (Lehmann et al., 2007; Goshen et al., 2011; Winocur et al., 2013). A third point is whether long-term declarative memory is stored, in unique regions or in distributed networks. What I observed is that ablation of Arc/Arg3.1 mediated plasticity in one or two proposed mnemonic regions, including hippocampus, mPFC, ACC and RSC did not affect contextual fear memory retrieval. Contextual fear memory was significantly impaired only when broad Arc/Arg3.1 ablation was achieved in forebrain principal neurons (Fig. 2.59), strongly suggesting that there are multiple copies of

memory traces that are stored simultaneously in distributed hippocampal-cortical networks. When memory traces in one or two regions are compromised, alternative traces in other regions can compensate and thereby maintain the memory retrieval. Currently, evidence tends to support the multiple trace theory (MTT) of system memory consolidation (Nadel and Moscovitch, 1997; Frankland and Bontempi, 2005). However, Nadel and Moscovitch also proposed in this theory that the extent of hippocampal lesions determines the severity of memory loss. Complete hippocampal lesions should abolish all episodic memories, regardless of their age. My observations and some other published literatures do not support this point as memory can still be encoded and retrieved when hippocampi were completely compromised (Anagnostaras et al., 2001; Wiltgen et al., 2006; Zelikowsky et al., 2012). Based on my observations and published evidence, I propose a parallel encoding and compensation theory for system memory consolidation which, to some extent share similarities with the theory proposed by Fanselow, Wiltgen and Tanaka (Fanselow, 2010; Wiltgen and Tanaka, 2013), but evidence don't support their hypothesis that competitive pathways existing in the hippocampus dominate memory encoding because post-training inhibition of a certain cortical region, such as mPFC or RSC, also impair recent memories (Katche et al., 2013b; Bero et al., 2014), suggesting that there are really functional multiple memory traces which are generated similarly and might have equal competition weight, in parallel, in both hippocampus and cortex.

Taken together, the main points of my proposed model are: during acquisition, declarative memory is encoded simultaneously in both hippocampus and cortical areas by recruiting neurons with high intrinsic excitability and plasticity, such as Arc/Arg3.1 positive (Nonaka et al., 2014; Gouty-Colomer et al., 2015) or CREB positive neurons (Yiu et al., 2014). Meanwhile, multiple traces are generated in distributed regions, and local networks for memory storage are constructed in both hippocampus and cortex. During the consolidation phase, connections between these networks are strengthened to promote efficient memory consolidation and retrieval. Certain connections with the hippocampus must be continuously maintained for controlling precise memory retrieval. When one or two mnemonic regions are compromised, functional traces in other areas can compensate and facilitate memory retrieval. Importantly, hippocampus plays a critical role in precise remote memory retrieval. Details of memory are likely stored in the hippocampus permanently. Once hippocampus function is compromised (activity inhibition or plasticity removal), synaptic consolidation in the hippocampus is abolished, leading to inefficient communications in the hippocampal-cortical networks, defective information replay to the cortex, inability to reactivate certain cortical representations (as what I observed in the IEG mapping experiments) and loss of memory specificity (Fig. 3.3). The detailed information for memory stored in the hippocampus can be reactivated and picked up by self-activating of hippocampus and/or top-down controlling by

activating cortex (Rajasethupathy et al., 2015). Precise remote memory retrieval needs the involvement of both functional hippocampus and cortex.

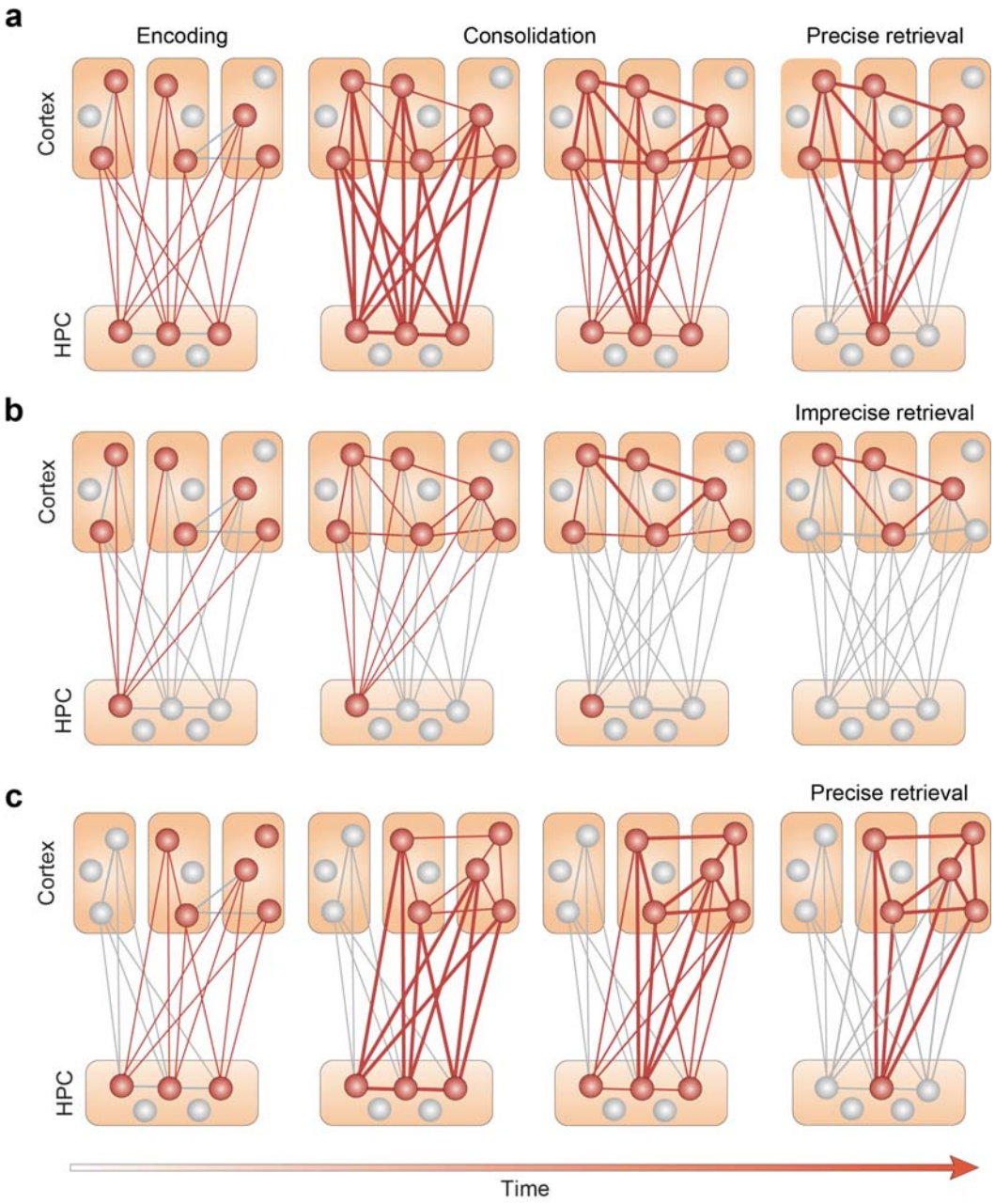

Fig. 3.3 Contextual memory encoding, consolidation and retrieval model. a, Hippocampus and cortex undergo parallel encoding during memory acquisition. Local and functional hippocampal-cortical connections are established and strengthened during memory consolidation. Long-lasting cortical representations are formed due to efficient dialog between hippocampus and cortical regions. Precise memory retrieval needs the involvement of both hippocampus and cortex. The detailed information for memory stored in the hippocampus can be reactivated and picked up by self-activating and/or top-down controlling by activating cortex **b,** Hippocampus disability (induced by lesions, inhibition or plasticity related gene ablation) leads to inefficient communications in the hippocampal-cortical networks and defected information replaying to the cortex during memory consolidation, and finally cause an inability to reactivate certain cortical representations and loss of memory specificity during memory retrieval. **c,** When one cortical regions lose functionality, some other regions compensate it by strengthening local network and hippocampal-cortical connections to achieve precise memory retrieval.

In order to further investigate the precise role of hippocampus and cortex in system consolidation, additional experiments utilizing optogenetic tools can be performed, for example, by selectively expressing light sensitive opsins (Channelrhodopsin or Harlorhodopsin) driven by the Arc/Arg3.1 promoter in either hippocampus or cortical regions.

3.11 Dependence of implicit memory on Arc/Arg3.1 mediated plasticity

Implicit memory, sometime termed non-declarative memory, refers to the ability to retrieve previous experience without involving conscious thought. Brain structures involved in organizing implicit memory (e.g. amygdala) undergo an earlier maturation process during ontogenic development (Joseph, 1996) compared with those supporting explicit memory (e.g. hippocampus) in infants (Joseph, 1996; Siegel, 1999), reflecting their early phylogenetic origin. Actually, people rely on implicit memory in daily life. For example, you can ride your bike, play guitar or tie your shoelace without consciously thinking about them. Strikingly, unlike a strong decline in explicit memories with aging, implicit memories do not decline at all (Roediger, 1990). It means that implicit memories can be persistently maintained and only demand low cognitive function. Therefore, I hypothesized that implicit memory may display weaker plasticity dependence in adulthood. To test this hypothesis, I employed two classical conditioning models, tone fear conditioning and CTA, to test the dependence of implicit memory on Arc/Arg3.1 mediated plasticity. I found that long-term tone fear memory and CTA memory were strongly impaired in KO mice, but both recent and remote implicit memories were not clearly altered in Late-cKO mice including Late-cKO$_{2xCre}$ mice (Fig. 2.62, 2.63, 2.66-69), although cKO mice also showed explicit memory deficits. These findings are consistent with previous observations that amnesic patients (e.g. H.M.) who showed unimpaired ability to acquire implicit memories (Squire and Wixted, 2011), and classical conditioning was intact in amnesia (Clark and Squire, 1998). Together, these data seem to support my hypothesis that implicit memories, unlike explicit memories, do not need lifelong Arc/Arg3.1 mediated plasticity in the adulthood, while highly rely on Arc/Arg3.1 expression during early development in order to establish functional neuronal networks for maintaining efficient memory acquisition, consolidation and retrieval.

However, it also should be noted that formation and consolidation of implicit memories also require activation of subcortical areas, which may still express high levels of Arc/Arg3.1 in the Late-cKO mice. Remaining Arc/Arg3.1 expression in some essential subcortical regions could possibly protract implicit memories. In line with this suggestion, I observed seizure-induced Arc/Arg3.1 expression in the central nucleus and intercalated cells of the amygdala of the Late-cKO mice, which might contribute to their intact tone fear memory. Remaining Arc/Arg3.1 was also observed in the hypothalamus where it could support CTA memory, since hypothalamus also plays an important role in CTA learning and memory

(Dayawansa et al., 2014). Additional regions that support implicit memories are the BNST, nucleus accumbens (NAcc) and parabrachial nucleus (PBN) of the pons. The BNST can also compensate the loss of function of amygdala in consolidation of fear memory (Poulos et al., 2010). PBN, as the second center relay of taste in rodents, is essential for CTA memory acquisition and consolidation. Lesions of PBN completely abolished CTA acquisition (Grigson et al., 1998; Sakai and Yamamoto, 1998; Reilly, 1999). Besides, NAcc is also thought to involve CTA memory processing, because it is connected with brain structures important for CTA memory, such as amygdala, insular cortex, PBN, and nucleus of the solitary tract areas (Ramirez-Lugo et al., 2007). It is currently not clear whether Arc/Arg3.1 is expressed in these regions during consolidation and retrieval of implicit memory and whether it is preserved in the Late-cKO mice. Future examination of this expression pattern would help resolve the role of adult Arc/Arg3.1 in implicit memory formation.

Besides, to investigate the dependence of tone fear memory on spatial Arc/Arg3.1 expression, I bilaterally injected rAAV-Cre in the hippocampus and amygdala of Arc/Arg3.1 floxed mice (termed HPC-cKO and BLA-cKO) and found that tone fear memory was not affected when Arc/Arg3.1 was ablated in the hippocampus, revealing that Arc/Arg3.1 mediated plasticity in the hippocampus is not essential for tone fear memory formation and consolidation which is consistent with the proposed role of hippocampus. Surprisingly, tone fear memory was significantly impaired when Arc/Arg3.1 was ablated in the amygdala which showed an opposite effect compared with Late-cKO mice (including Late-cKO$_{2xCre}$). I propose that acute loss of Arc/Arg3.1 in the adult amygdala cannot be easily compensated because amygdala is the primary region for storing tone fear memory (Herry and Johansen, 2014) and because the time for compensation after ablation is limited compared to the long postnatal developmental period available for compensation in the Late-cKO mice.

3.12 Summary of main findings

In summary, findings reported in this thesis provide first evidence that the capacity for learning and implicit memory is established during early development by Arc/Arg3.1 dependent plasticity mechanisms, while memory consolidation always requires Arc/Arg3.1 expression in the adult brain. These findings further expand our knowledge on the role of Arc/Arg3.1 in memory processing and shed a new light on the development of learning and memory networks that will initiate a novel approach for investigating normal and maladaptive development of these brain functions.

Furthermore, findings presented here support a new model of memory consolidation in which different aspects of information are stored as complementary memory traces in a broad hippocampal-cortical network of brain regions. Interactions between these regions

contribute to memory consolidation and stability in the face of ongoing time and local damage. This study provides new insights into mechanisms underlying system memory consolidation and complements the existing theories that will contribute to the investigations on memory disorder, such as post-traumatic amnesia and Alzheimer's disease.

4 Materials & methods

4.1 Animals

C57BL/6J mice aged between 3 and 6 months were kept in a vivarium with an inverted 12:12 light/dark cycle (8:00–20:00 dark period) under standard housing conditions (23 ± 1°C, 40-50% humidity, food and water *ad libitum*). One week prior to behavioral or electrophysiological experiments animals were housed individually. All the experiments were conducted in accordance with the German and European Community laws on protection of experimental animals and approved by the local authorities of the City of Hamburg. Experimenters were blind to the mice genotype until conclusion of experiments and analysis.

4.2 Generation of Arc/Arg3.1$^{f/f}$ mice

The generation of floxed Arc/Arg3.1 mice (Arc/Arg3.1$^{f/f}$) went along with the generation of conventional KO mice in our lab as described previously (Plath et al., 2006): "Genomic fragments of Arc/Arg3.1 were isolated from λ phage genomic library (AB-1) prepared from 129/Sv (ev) embryonic stem (ES) cells. A 4 kb fragment encompassing the promoter and 5'UTR was subcloned into pBLUESCRIPT (Stratagene), and a 3.7 Kb fragment covering the whole ORF and 3'UTR was subcloned into pZErO-1 (Invitrogen). The Arc/Arg3.1 ORF was flanked by inserting a loxP site at position -1720. A neomycin resistance cassette, flanked by two loxP sites, was inserted at position +2690 into the second intron. The targeting vector was linearized at a unique NotI site and electroporated into R1 ES cells. Positive clones were identified by Southern blot analysis and one targeted ES cell clone was transiently transfected with Cre recombinase. The resulting recombination types were identified by Southern blot. A type II recombination clone was injected into C57Bl/6J blastocytes. Male chimeras were backcrossed into C57Bl/6J. For Southern blot analysis, purified DNA from cell clones and tails was digested with NheI, separated on agarose gels, transferred to duralose membranes (Stratagene) and detected with 5´ and 3´ external probes. Mice were genotyped by Southern blot and PCR analysis. Arc/Arg3.1 loxP flanked mice (Arc/Arg3.1$^{f/f}$) were normal and fertile. The F1 generation of Arc/Arg3.1$^{f/f}$ was backcrossed into C57Bl/6J for at least ten generations to establish a standard inbred congenic line before starting experiments" (Conference on Genetic Background in Mice) (1997).

4.3 Mice breeding and genotyping

Ablation of Arc/Arg3.1 gene prenatally or late postnatally in the brain was accomplished by breeding the Arc/Arg3.1$^{f/f}$ mice with Cre recombinase transgenic mice: 1. Tg(CMV-cre) (Schwenk et al., 1995) to re-derive germ line KO mice; 2. Tg(CaMKIIα-cre)T29-1Stl (Tsien et al., 1996) to obtain Late-cKO mice. Breeding schemes was: in generation F1 Arc/Arg3.1$^{f/f}$ mice were crossed with Arc/Arg3.1$^{+/+,Cre+}$ mice. In generation F2 Arc/Arg3.1$^{f/+,Cre+}$ were crossed with Arc/Arg3.1$^{f/+}$ to obtain Late-cKO mice heterozygous for Cre or with

Arc/Arg3.1$^{f/+,Cre+}$ to obtain the Late-cKO$_{2xCre}$. F3 progeny with genotypes Arc/Arg3.1$^{+/+,\ Cre+}$ and Arc/Arg3.1$^{f/f,\ Cre+}$ were used for all experiments as WT-controls and Late-cKO, respectively. Late-cKO$_{2xCre}$ mice with genotypes Arc/Arg3.1$^{f/f,\ Cre+/Cre+}$ were used in some experiments and WT-controls were their littermates with genotype Arc/Arg3.1$^{+/+,Cre+/Cre+}$. Germ-line KO was bred identically up to the F3 generation, however, in this line WT controls exhibited memory deficits resulting from the Cre transgene. Therefore, Arc/Arg3.1$^{f/f,\ Cre+}$ was back-crossed with C57Bl/6J to obtain Arc/Arg3.1$^{+/-}$ offspring that were crossed with each other in F5 to obtain WT and KO mice for experiments. With this strategy, conventional KO mice were re-derived from the floxed mouse line, these mice were similar in all measures to the conventional KO mice (Plath et al., 2006) , confirming that compensation or drift did not affect the latter. Germ-line derived and conventional KO mice were used in experiments and their results pooled together. Mice were genotyped by PCR for Arc/Arg3.1 and by qPCR based Copy Number Variation (CNV) analysis for Cre. The primers used for genotyping and regenotyping are listed below:

Gene PCR	Primer name	from 5' to 3'
Arc/Arg3.1	TDA	AAG GGC TAC TGG TGG CAT GTG TGC A
Arc/Arg3.1	TDB	CAC TGC AGG GAG GGG AAA CAA GCA G
Arc/Arg3.1	TDC	TCA CCT TCA GCT CTC CGG CTG AGC T
Cre	Cre3	AAA CGT TGA TGC CGG TGA ACG TGC
Cre	Cre4	TAA CAT TCT CCC ACC GTC AGT ACG

Notes: Primer TDA and TDB can identify either Arc/Arg3.1 WT (~220bp amplified fragment) or Arc/Arg3.1$^{f/f}$ (~300bp amplified fragment) mice; TDA and TDC can identify Arc/Arg3.1 KO (~410bp amplified fragment) mice. Primer Cre3 and Cre4 are used to identify Cre+ mice.

4.4 X-gal staining

To examine Cre-mediated recombination in the brain, Tg(CaMKIIα-cre)T29-1Stl mice were crossed with ROSA26-lacZ reporter mice (Soriano, 1999) and Arc/Arg3.1$^{f/f}$ mice. Brains obtained from offspring with genotype Arc/Arg3.1$^{f/f,\ Cre+,LacZ}$ were processed for X-gal staining. Briefly, brains were rapidly removed and frozen in liquid nitrogen and kept at -80°C until further processing. Sagittal brain sections (14 µm) were prepared with a cryostat and mounted on slides (Superfrost plus, Thermo). Slides were air dried and stored at -80°C until use. Sections were fixed (0.2% glutaraldehyde), washed with 1x PBS (8g NaCl, 0.2g KCl, 1.44g Na_2HPO_4, 0.24g KH_2PO_4 in 1L H_2O, PH7.4) and then stained by incubation in X-gal staining solution (1x PBS, 2 mM $MgCl_2$, 0.02% igepal, 0.01% sodium deoxycholate, 5 mM

potassium ferrocyanide, 5 mM potassium ferricyanide, and 1mg/ml 5-bromo-4-chloro-3-indolyl-beta-D galactopyranoside) at 37°C for 12-19 h. Subsequently, sections were fixed in 4%PFA for 10 min, washed twice with PBS, dehydrated in ethanol, dried and mounted in Entellan (Meck Millipore).

4.5 Nissl staining

Coronal brain slices (40 µm) were obtained from PFA-fixed brains, using Leica VT1000S vibratone and mounted on positive charged slides (ROTH) with air dried overnight. Slides were placed directly into 1:1 ethanol /chloroform solution overnight for dehydration and then were rehydrated step through 100% and 95% ethanol to distilled water. And then slices were stained in 0.1% cresyl violet solution for 5-10 minutes. After that the slides were rinsed quickly in distilled water and differentiated in 95% ethanol for 2-30 minutes and controlled under the microscopy for getting ideal image. In the end, slices were dehydrated in 100% ethanol for 2 x 5 min, cleared in xylene 2 x 5 min and mounted with permanent mounting medium (Fluka).

4.6 Kainate-induced seizures and brain perfusion

To maximize Arc/Arg3.1 expression and better quantify its ablation, mice were subjected to Kainate-induced seizures. Adult mice (20-30 g, 3 to 6 months of age) were injected with Kainic acid (Abcam) intraperitoneally (14.8 mg/kg body weight) prepared in PBS. Seizures were scored as generalized if mice exhibited bilateral forelimb tonic and clonic activity; with loss of postural tone. 90-120 min after onset of generalized seizures, mice were deeply anaesthetized with 15% urethane (1.5 mg/g b.w., Sigma) prepared in 0.9% saline, and intracardially perfused with ice cold PBS followed by 4% PFA. Brains were removed into 4% PFA until used.

4.7 Western blots

Mice subjected to Kainate-induced seizures were euthanized with isoflurane (Abbott) and decapitated. Brains were removed and transferred on ice. Hippocampus, cortex, amygdaloid complex and cerebellum were dissected, quick-frozen on dry ice and stored at -80°C until used. Dissected tissues were homogenized with lysis buffer containing 5 mM EDTA, 5 mM EGTA, 50 mM NaF, 1 mM Na_3VO_4, 1% Triton-X100, 1 mM PMSF, Aprotinin 4 µg/ml, Leupeptin 1 µg/ml and Pepstatin A 200 ng/ml in PBS. Protein concentrations were accessed using BCA assay (Thermo, Pierce). Equal amounts of protein were electrophoresed on 12% SDS polyacrylamide gels and transferred to PVDF membranes. Western blots were blocked in 5% nonfat milk in PBS with 0.01% Tween and incubated over night with a polyclonal anti-Arc/Arg3.1 antibody (1:300000, Synaptic Systems), or monoclonal anti-GAPDH antibody (1:500000, Millipore). After secondary antibody incubation,

bands were visualized using Super Signal chemiluminescence reagent (Thermo, Pierce). Immunopositive signals were detected by ImageQuant LAS 4000 (Fuji film) and analyzed using ImageJ (NIH).

4.8 Immunohistochemistry

Mice were anesthetized and intracardiacally perfused with 4% PFA. Brains were removed and post-fixed in PFA overnight. 40 µm coronal slices were obtained using a Leica VT1000S vibratome. Slices first were incubated in 0.31% H_2O_2 (Sigma) for 30 min and then were blocked in blocking solution including 10% horse serum (GBICO), 0.2% BSA (Sigma) and 0.3% TritonX (Sigma) in PBS for 1h and then incubated over night with primary antibody in carrier solution including 1% horse serum, 0.2% BSA and 0.3% TritonX-100 in 1x PBS. Slices were then incubated either with biotinylated HRP-complex conjugated secondary antibody (Vector Labs) in carrier solution containing for 2 hours for DAB staining or with Alexa Fluor® 488 or 555 conjugated secondary antibody (Invitrogen) for immunofluorescence staining. Immunoreactivities for DAB staining were detected using a VECTASTAIN ABC Kit (A, B solution 1:500 in PBS, Vector Labs) and 3, 3-diaminobenzidine (Sigma-Aldrich) as chromogen.

Used antibodies are listed here: primary antibody: anti-Arc/Arg3.1 rabbit polyclonal antiserum (1:1500, Kuhl lab, 5904), anti-Arc/Arg3.1 mouse monoclonal antibody (C7, 1:150, Santa Cruz, sc-17839), anti-c-fos rabbit polyclonal antibody (1:1000, Santa Cruz, sc-52), anti-Cre recombinase mouse monoclonal antibody (1:2000, Millipore, MAB3120), anti-cleaved caspase 3 rabbit polyclonal antibody (1:1000, Cell Signaling, 9661S), anti-CaMKII rabbit monoclonal antibody (1:200, Abcam, EP1829Y), anti-Iba 1 rabbit polyclonal antibody (1:1500, Wako, 019-19741), anti-GFAP rabbit polyclonal antiserum (1:1000, Synaptic Systems, 173002), anti-GFAP Guinea Pigs polyclonal antibody (1:500, Synaptic Systems, 173004). Secondary antibody: Biotinylated HRP-complex conjugated goat anti-rabbit antibody and horse anti-mouse antibody (1:1000, Vector Labs, BA-1000/BA-2000); Alexa Fluor® 488 conjugated goat anti-rabbit or goat anti-mouse or goat anti-Guinea Pigs secondary antibody (1:1000, Invitrogen, A-11008/A-11001/A-11073); Alexa Fluor® 555 conjugated goat anti-rabbit or goat anti-mouse secondary antibody (1:1000, Invitrogen, A-21428/A-21422).

4.9 Cell counting

Arc/Arg3.1 or c-fos positive neurons in the DG, amygdala, or mPFC were counted after fear memory retrieval based on coronal slices from hippocampus or mPFC injected mice with DAB staining. For each experiment, selected mice were divided into four groups: GFP-control perfused with 4% PFA immediately after contextual fear memory retrieval to prevent

gene expression were used as non-retrieval group (GFP-control non-retrieval); GFP-control and WT-control perfused 90 min after contextual fear memory retrieval were termed “GFP-control retrieval” and “WT-control retrieval” group; HPC-cKO or mPFC-cKO perfused 90 min after contextual fear memory retrieval were termed “HPC-cKO retrieval” or “mPFC-cKO retrieval”, respectively. Slices from -0.94 mm to -2.30 mm posterior to bregma were selected based on Allen Brain Mouse Atlas for dorsal DG, from -2.70 mm to -3.80 mm for ventral DG , and slices from -0.82 mm to -2.18 mm posterior to bregma were selected for amygdala and slices from -0.82 mm to -2.18 mm anterior to bregma were selected for mPFC. For each group 2-4 mice and 5 slices per mouse were used for the final analysis. The quantification of Arc/Arg3.1 or c-fos positive cells was done for both hemispheres in all slices. Cell counting was performed manually by using Neurolucida software (MicroBrightField, Williston, VT) under an Olympus BX51 microscope (MBF bioscience) with a digital camera (mbf bioscience CX 9000). Region of interest was first located under a 2.5x objective and then target area was outlined precisely under a 10x objective. Cell counting was limited within outlined region in which area (in mm^2) was calculated. Final data were presented as: total cell number from both hemisphere/total counted area (number # / mm^2). Positive cells were divided into three types based on the color intensity of staining: dark, brown, and weak. Due to the staining intensity, all of these three types of cells were considered for Arc/Arg3.1 positive cells analysis, while only dark and brown cells were considered in c-fos positive cells analysis.

4.10 Radioactive *in situ* hybridization

Mice were anesthetized and brains were fleshly frozen using liquid nitrogen and stored at −80°C until cryosectioning. Coronal or sagittal brain slices (14 µm) were prepared using a cryostat and mounted on slides (Superfrost plus, Thermo Scientific). *In situ* hybridization was performed as described before (Hermey et al., 2013). A fragment corresponding to nucleotides 2342-2923 of the Arc/Arg3.1 3’ UTR was used as a probe and specificity of signals was verified by comparing to KO control. Probes labeled with [α-35S]-UTP were generated according to the manufacturer's instructions (Promega). Transcribed probes were cleaned using G-50 mini columns (GE Healthcare) and diluted in hybridization buffer (4x SSC, 50% formamid, 1 M denhardts, 10% dextransulfat, 0.5 mg/ml salmon sperm DNA, 0.25 mg/ml yeast t-RNA) to a concentration of 5000 cpm/µl. Cryosections of brains were fixed in 4% PFA-PBS, acetylated, dehydrated and hybridized at 55°C overnight. Ribonuclease A treatment was performed for 30 min at 37°C. Following a high stringency wash in 0.1x saline sodium citrate buffer at 55°C, slides were exposed to X-ray films (Kodak Biomax MR; Amersham Bioscience) for 72 h to 44 days.

Quantification of Arc/Arg3.1 mRNA was performed based on rISH images from mouse brains with different ages. Briefly, WT mice were sacrificed at P0, P7, P14, P21 and P28 (3

mice per time point). Brains were cryo-sectioned coronally and subjected to rISH in 3 series. Each series contained a single WT brain per time point (total of 5 brains) and a single adult KO brain as a negative control. Following rISH, series of sections were exposed together with an autoradiographic ^{14}C microscales (GE Healthcare) to Storage Phosphor Screen films (BAS-IP MS 2025, Fujifilm, Tokyo, Japan) during 5 days and subsequently scanned with FLA-900 image scanner (Fujifilm, Tokyo, Japan). 16-bit digitalized images were subjected to densitometry analysis of each region of interest (ROI) using ImageJ – NIH freeware (Washington DC, USA). Measured mean gray levels were converted into approximated nanoCuries per gram (nCi/g) of tissue. Average values for each ROI were pooled from 2 to 3 consecutive brain sections in each time point.

4.11 Plasmid constructs

The pAAV-CaMKIIα-Cre (Cloned by Steffen Schuster) was constructed by inserting Cre recombinase sequence to pAAV-CK(1.3)-EGFP (gift from Dr. Pavel Ostenz, Addgene plasmid # 27227) (Dittgen et al., 2004) in the place of EGFP sequence. The CreERT^2 transgene was amplified from pCAG-CreERT^2 (gift from Dr. Connie Cepko, Addgene plasmid # 14797) (Matsuda and Cepko, 2007) by PCR using the primers Kpn-CreERT^2 (Forward): CCG TGG TAC CAC CAT GTC CAA TTT ACT G, CreERT2-Eco-oS (Reverse): CAA TGA ATT CAG CTG TGG CAG GGA AAC CC; and the product was inserted by 5'-KpnI and 3'-EcoRI restriction and ligation into pAAV-CaMKIIα(1.3)-EGFP in the place of EGFP. 2A peptide-Venus was amplified from pAAV-Syn-iCre2A-Venus (gift from Prof. Rolf Sprengel and Dr. Wannan Tang) (Tang et al., 2009) using the primers: Eco-2AP-Venus (Forward): CCG TGA ATT CGA GGG CAG AGG AAG TCT TC and 2AP-Venus-Eco (Reverse): CAA TGA ATT CTT ACT TGT ACA GCT CGT CC; and inserted by 5'-blunt and 3'-EcoRI restriction and ligation into pAAV-CaMKIIα(1.3)-CreERT^2 and generated pAAV-CaMKIIα(1.3)-CreERT^2-2AP-Venus. The plasmids were sequenced after cloning with the help of the core facility in ZMNH.

pAAV-CaMKIIα(1.3)-CreERT^2-2AP-Venus expression was first tested in the hippocampus of Arc/Arg3.1$^{f/f}$ mice *in vivo*. In absence of 4-OH-Tamoxifen, Arc/Arg3.1 ablation is still efficient (See Fig. 2.26). I utilized this leaky activity to infect mice with the rAAV-CreERT^2 and obtained effective Arc/Arg3.1 ablation for particularly long periods of time (3-6 weeks) avoiding genotoxicity caused by high constitutive Cre recombinase activity.

4.12 Plasmid amplification and purification

To start preparation, Eppi-tubes were first pre-chilled on ice and SOC medium was pre-heated to 37°C. Competent cells were thawed on ice gently and then 50 µl of cell suspensions were dispensed into each of the pre-chilled Eppi-tubes. 0.5 µg of the

experimental DNA were applied to each tube and the mixture was incubated on ice. 30 min later, mixture was heat-shocked in 37°C water bath for 3 minutes and then incubated on ice again shortly for 2 minutes. An then 0.5 ml of preheated (37°C) SOC medium were added into the tubes and incubated the at 37°C for 45 minutes with shaking at 225-250 rpm. After that less than 200 µl of the transformed mixture was scribble in LB agar plates containing the appropriate antibiotic, and incubated at 37°C overnight. On the next day, single clone was picked with pipette tips and transferred to a glass tube containing 2 ml DYT medium with 2 µl antibiotic (100 µg/µl), and incubated at 37°C with shaking at 225-250 rpm. Several hours later, cultures were transferred into big flasks containing 250 ml DYT medium and 250 µl antibiotics (100 µg/µl) and incubated at 37°C with shaking at 225-250 rpm overnight. Next day, cultures were transferred into centrifuge bottle, and centrifuged around 4500-6000 g at 4°C for 15 min. Plasmids were extracted from the precipitates and purified following the procedures from an endotoxin-free plasmid DNA purification kit (NucleoBond® Xtra Midi EF, Macherey-Nagel). Finally, purified plasmids were dissolved in endotoxin-free water, diluted to 1 µg/µl and stored at -20 °C.

4.13 Viral vectors production and stereotaxic delivery *in vivo*

Fig. 4.1 Stereotaxic virus injection system

Viral vectors were produced and purified by HEXT vector facility at the University Medical Center Hamburg-Eppendorf (UKE). The viral vectors were purified by affinity chromatography using AVB Sepharose HP HiTrap columns (GE Healthcare) and tittered by qPCR. rAAV serotype 1/2 with a final titer 5-8 x 10^{11} vg/ml was used for the injection. Mice were anesthetized with 5% isoflurane (Abbott) mixed with 99.8% oxygen (0.5 l/min) during induction and then placed into a stereotaxic frame with 1.5-2% isoflurane for maintenance of anesthesia during the entire surgery and injection process (Fig. 4.1). Body temperature was maintained at 37 °C using a homeothermic heating pad (WPI) throughout the experiment. A midline skin incision was made on the top of the skull. Small craniotomies were drilled under

stereomicroscope (Olympus) above target regions unilaterally or bilaterally based on measured coordinates of the hippocampus (dorsal: 2.0 mm posterior to bregma, 1.65 mm lateral to the midline, 1.4 mm and 1.8 mm in depth corresponding to CA1 and DG; ventral: 3.2 mm posterior to bregma, 3.2 mm lateral to the midline, 3.2 mm and 2.2 mm in depth); medial prefrontal cortex (1.4 mm anterior to bregma, 0.30 mm lateral to the midline, 1.8 mm and 1.4 mm in depth); basolateral amygdala (1.33 mm posterior to bregma, 3.38 mm lateral to the midline, 4.6 mm in depth); anterior cingulate cortex (1.0 mm anterior to bregma, 0.35 mm lateral to the midline, 1.6 mm and 1.3 mm in depth), retrosplenial cortex (1.8 mm posterior to bregma, 0.40 mm lateral to the midline, 0.7 mm and 0.5 mm in depth). Injections were made with a Neurosyringe (Hamilton) driven by a piezo pump (Neurostar) at a speed of 0.15 µl /min. The final injected volume in each hemisphere was 0.4 µl and 0.6 µl in the DG and CA1 of the dorsal hippocampus, each of 0.5 µl in CA1 and DG of the ventral hippocampus, 0.8 µl in the medial prefrontal cortex, 0.7 µl in the basolateral amygdala, 1.0 µl in the anterior cingulate cortex, and 0.8 µl in the retrosplenial cortex. The syringe was left in the place 5-10 min after each injection. Following injections, head skin was closed with tissue adhesive (3M Vetbond) and carprofen (5 mg/kg b.w.) and 0.9% saline were administered subcutaneously for analgesia and hydration, respectively. Mice were placed on a warm mat until fully recovered from anesthesia. Soft food was applied during the recovery days. In the end of the designed experiment, all injected mice were sacrificed and brains were removed for *post hoc* immunohistochemistry. Only the mice with ideal virus injection, good Arc/Arg3.1 ablation and without clear immune responses and cellular toxicity were considered in the final data analysis.

4.14 Open field

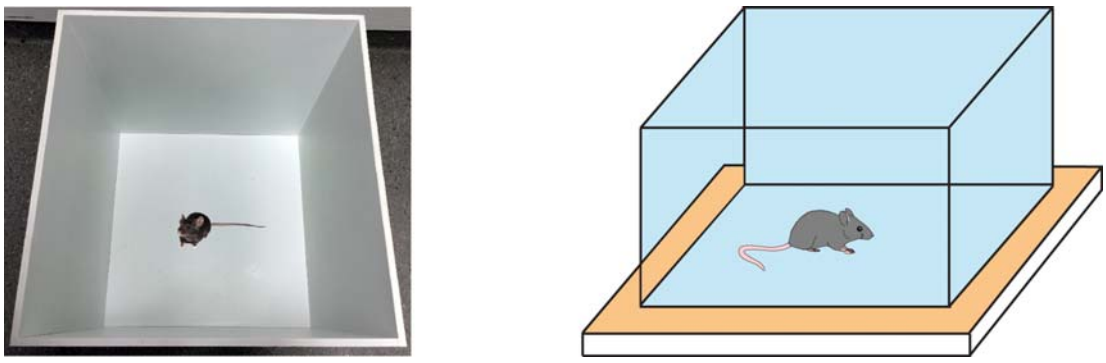

Fig. 4.2 Open field apparatus and schematic diagram

Spontaneous exploration and locomotor activity were evaluated in an open field arena (Fig. 4.2, 50 cm x 50 cm x 50 cm) constructed from opaque white forex plates equipped with a video-based system under dim indirect illumination (40 Lux). Mice activity was video-

recorded for 5 or 10 min using Ethovision XT video-tracking program (Noldus Information Technology). The path length, velocity and time spent in the center were calculated. The box was cleaned with 70% ethanol between subjects.

4.15 Elevated zero maze

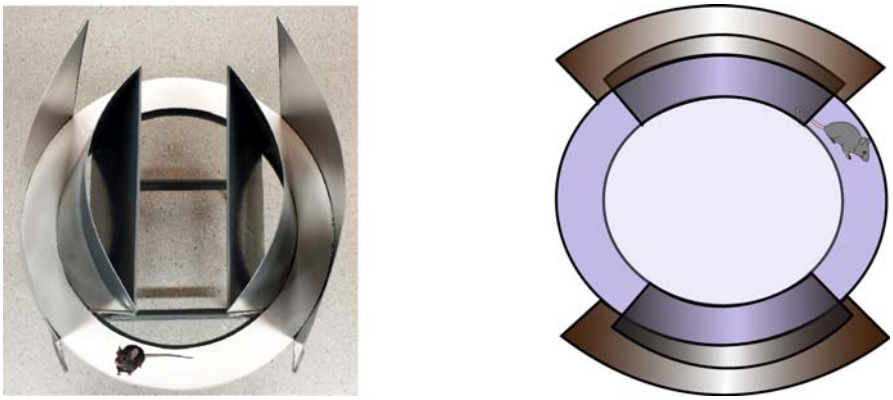

Fig. 4.3 Elevated zero maze apparatus and schematic diagram

Anxiety-like behaviors and risk assessment ability of Arc/Arg3.1$^{f/f}$ mice were evaluated in the elevated zero maze (Fig. 4.3) which has an annular runway (diameter 46 cm, width 5.5 cm). Two opposing 90° sectors of the runway are protected by an inner and outer wall of grey polyvinyl-chloride (height 16 cm). The two remaining sectors are unprotected. The apparatus is mounted 40 cm above the ground and exposed to dim indirect illumination (40 Lux). Each mouse was placed into the wall protected sector and allowed to explore the maze for 10 min. Time spent in the open sectors and head dips to the open sectors were recorded and counted by Ethovision XT video-tracking program (Noldus Information Technology). 70% ethanol was used for cleaning between subjects.

4.16 Elevated plus maze

Fig. 4.4 Elevated plus maze apparatus and schematic diagram

Anxiety-like behaviors of Arc/Arg3.1 KO and Late-cKO mice were assessed in the elevated plus maze (Fig. 4.4) comprising two opposite open (5 cm x 30 cm) and closed arms (5 cm x 30 cm) with 15 cm walls and was elevated to 70 cm above the ground. The arms were connected by a central square (5 cm x 5 cm). Each mouse was placed on the central square heading to the open arm and allowed to explore the maze for 5 min. Time spent in the open and closed arms, and numbers of arm entries were recorded and counted by Ethovision XT video-tracking program (Noldus Information Technology). Mice were tested under dim indirect illumination (40 Lux). 70% ethanol was used to clean maze between subjects.

4.17 Novel object recognition

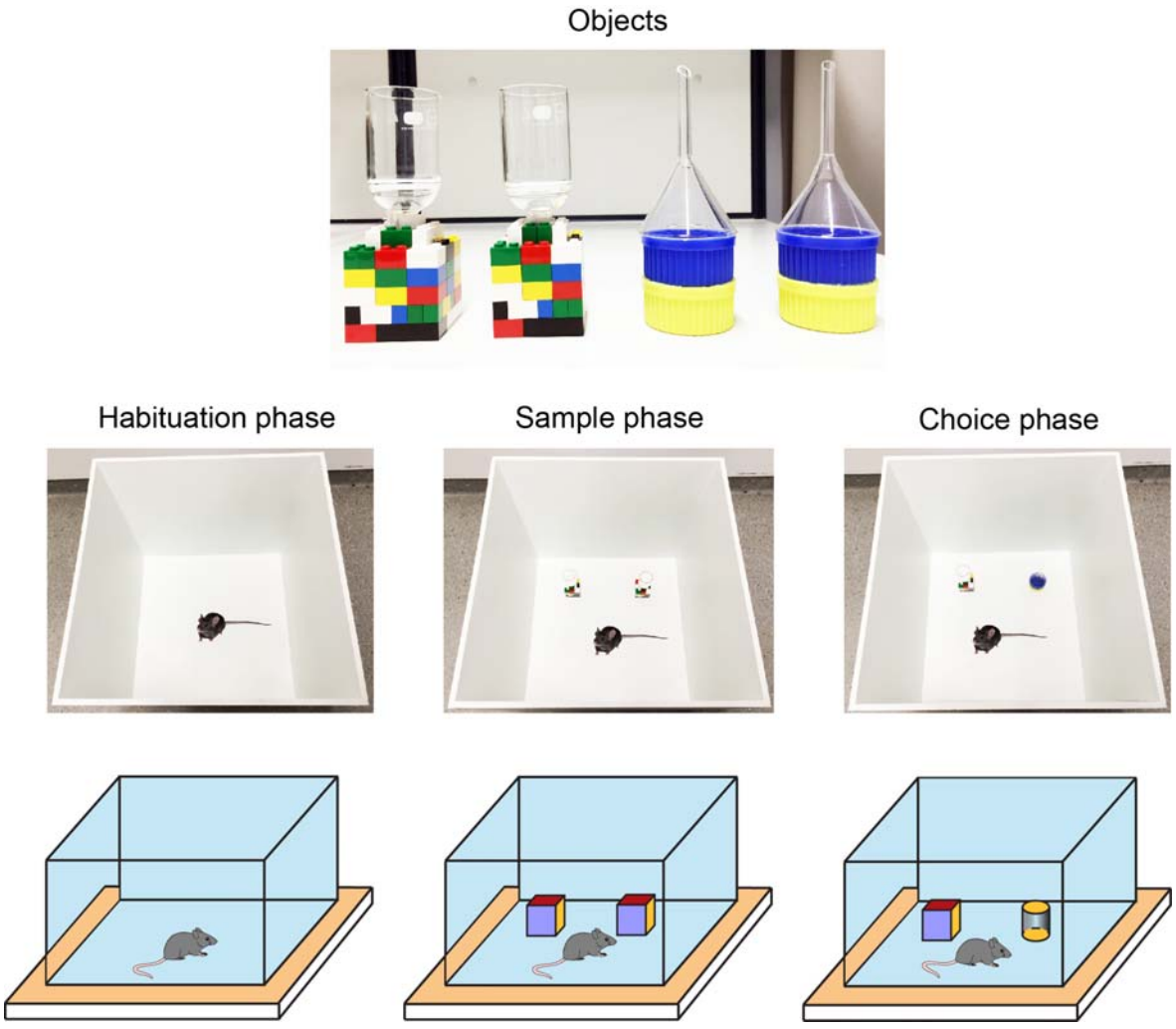

Fig. 4.5 Novel object recognition apparatus and schematic diagram

Novel object recognition (Fig. 4.5) relies on a hippocampal-cortical network for acquisition and storage of information (Warburton and Brown, 2010; Blaser and Heyser, 2015). Mice were trained and tested in the open field arena (50 cm × 50 cm × 50 cm). During the habituation phase, mice were habituated to the open field arena 10 min per day for 2

days. On the following day mice were allowed to freely explore two identical objects in the same arena for 10 min. Objects were positioned equidistantly from the wall of the arena. Memory retention was tested 24 h later by placing mice back into the arena with an identical copy of the familiar object and a novel object. To avoid possible object and place preference, the identity and location of the training and novel objects were swapped in a counterbalanced regime between subjects. Objects and arena were cleaned carefully between tests with 70% ethanol to remove all olfactory cues. Discrimination index was calculated as time spent exploring the novel object / (time spent exploring familiar object + novel object). Experiments were performed under dim indirect illumination (40 Lux). Video was recorded and mice activity was analyzed by Ethovision XT program (Noldus Information Technology).

4.18 Flinch-jump threshold test

Flinch-jump thresholds of Arc/Arg3.1$^{f/f}$ mice were tested in a Multi-Conditioning System (Fig. 4.6, TSE Systems). Mice were placed into a transparent arena with a grid-floor that could deliver electric shocks. Thirty seconds after the mouse was placed into the arena, a train of consecutive 0.5 s long foot shocks with 30 s intervals was administered stepwise from 0.1 mA to maximally 1.0 mA in steps of 0.1 mA. Behavioral responses (no response, flinch or jump) were recorded at each step of intensity. The lowest current intensity eliciting flinch and／or jump was considered as threshold values.

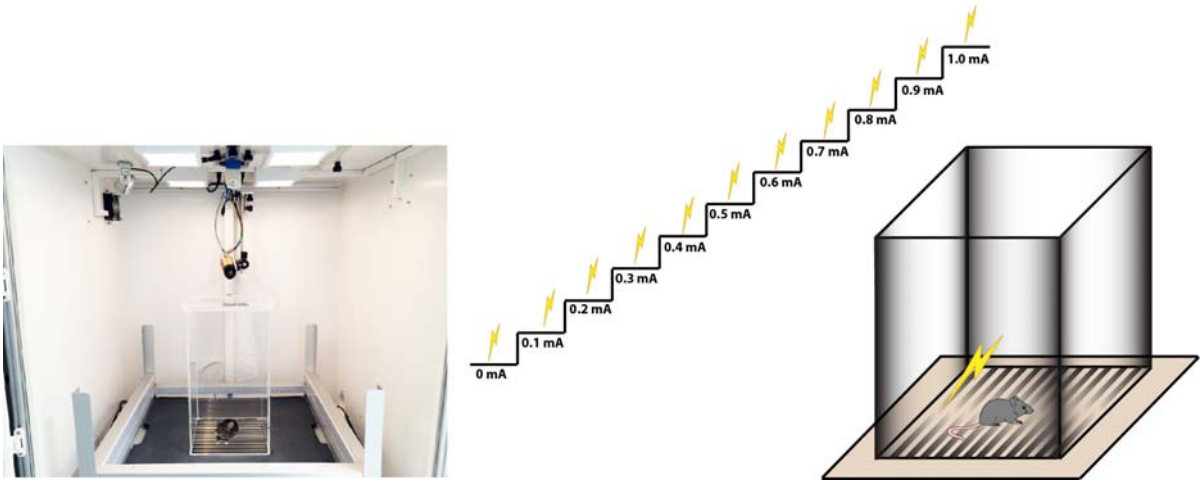

Fig. 4.6 Fear conditioning apparatus and schematic diagram of flinch-jump threshold test

4.19 Fear conditioning (5 CS-US)

Fear conditioning is a rapidly and robustly acquired memory task requiring cortical and hippocampal activation (Maren et al., 2013). I performed it as described previously (Plath et al., 2006) by using an automated conditioning system (Fig. 4.7, TSE Multi-Conditioning

System). Following 3 days handling, mice were placed into the conditioning chamber (Context A, a square arena with opaque walls, placed over a metal grid floor and lit with a dim red light at 5 Lux). Mice were allowed to explore the chamber for 2 min, and then received five subsequent parings of temporally overlapping tone (15 s, 2000 Hz, 98 dB)/shock (2 s, 0.25 mA) with 215 s intervals. After the last pair of tone/shock stimuli, animals remained in the chamber for another 1 min and then were placed back to their home cages. Contextual fear memory was assessed at different delay by placing mice back to the conditioning chamber (Context A) for 2 min and measuring their freezing responses. 70% ethanol was used to clean the chambers between subjects. In order to assess the memory specificity and cued memory, animals were placed into a new chamber (Context B, an arena with transparent walls exposed under 40 Lux white light). The metallic grids for the current delivery were covered with a plastic plate. Fresh bedding was applied into the arena and some distal cues were pasted up on the walls of the chamber. Background noise in the chamber was switched off. Mice were first allowed to explore the new transparent arena (Context B) for 1 min, and then tone fear memory was tested by applying the same tone used during conditioning for another 1 min. Percent freezing during each phase was calculated. A discrimination index (DI = %Freezing in Context A / (%Freezing in Context A + %Freezing in Context B) was used to evaluate the levels of generalization and memory specificity. 1% acetic acid was used to clean the chambers between subjects. All freezing was defined as complete lack of mobility for at least 1s.

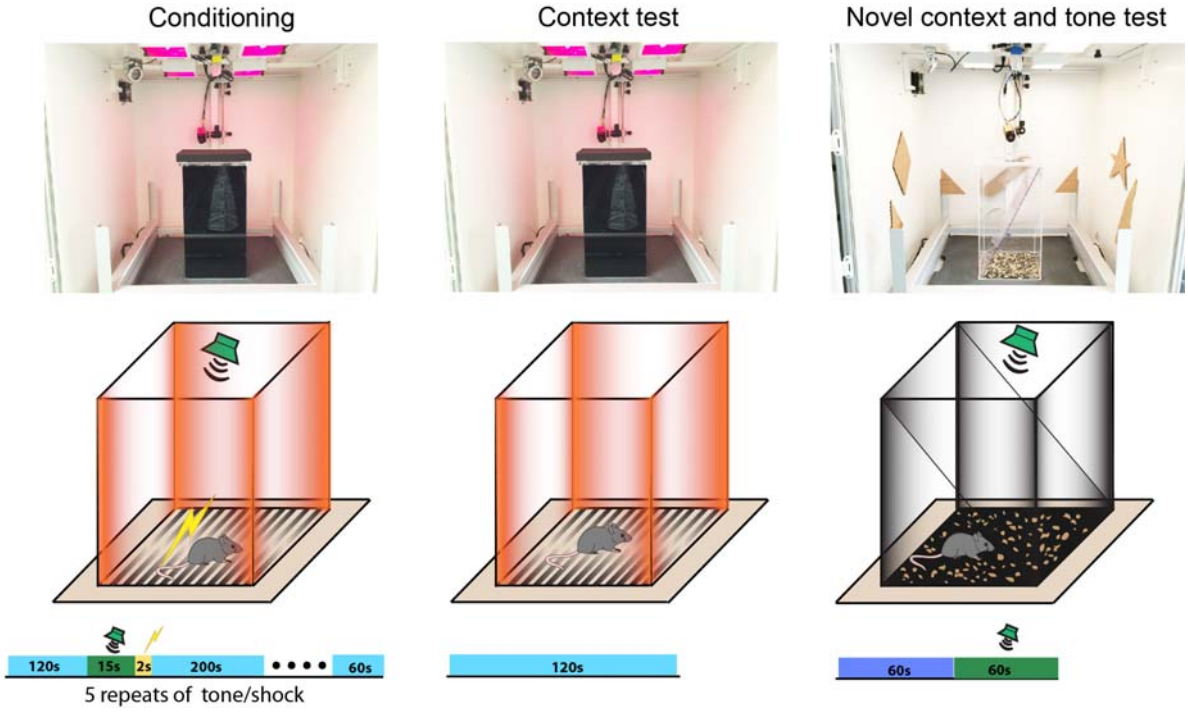

Fig. 4.7 Fear conditioning apparatus and schematic diagram (5 CS-US)

4.20 Fear conditioning (1 CS-US)

Fear conditioning was performed by using TSE Multi-Conditioning System (Fig. 4.8, TSE Systems). Following 3 days handling mice were placed into the conditioning chamber (Context A, an transparent arena with walls exposed under white light ~40 Lux) and allowed to explore the chamber for 2 min, and then received one temporally overlapping tone (30 s, 10K Hz, 70 dB)/shock (2 s, 0.5 mA) pairing. After that mice remained in the chamber for another 1 min and then were placed back to their home cages. Contextual fear memory was assessed at different time delay by placing mice back to the conditioning chamber (Context A) for 3 min. 70% ethanol was used to clean the chambers between subjects. In order to assess the memory specificity and cued memory, mice were placed into a new chamber (Context B, an arena with opaque walls exposed under dim red light < 5 lux). The metallic grids for the current delivery were covered with a plastic plate. Fresh bedding was applied into the arena and some distal cues were pasted up on the walls of the chamber. Background noise in the chamber was switched off. Mice were first allowed to explore the new arena (Context B) for 2 min to test the memory specificity following by tone fear memory test by applying the same tone used during conditioning continuously for another 2 min. Freezing percentage during each phase was calculated. A discrimination index (DI = %Freezing in Context A / (%Freezing in Context A + %Freezing in Context B) was used to evaluate the level of generalization and memory specificity. 1% acetic acid was used to clean the chambers between subjects. All freezing was defined as complete lack of mobility for at least 1s.

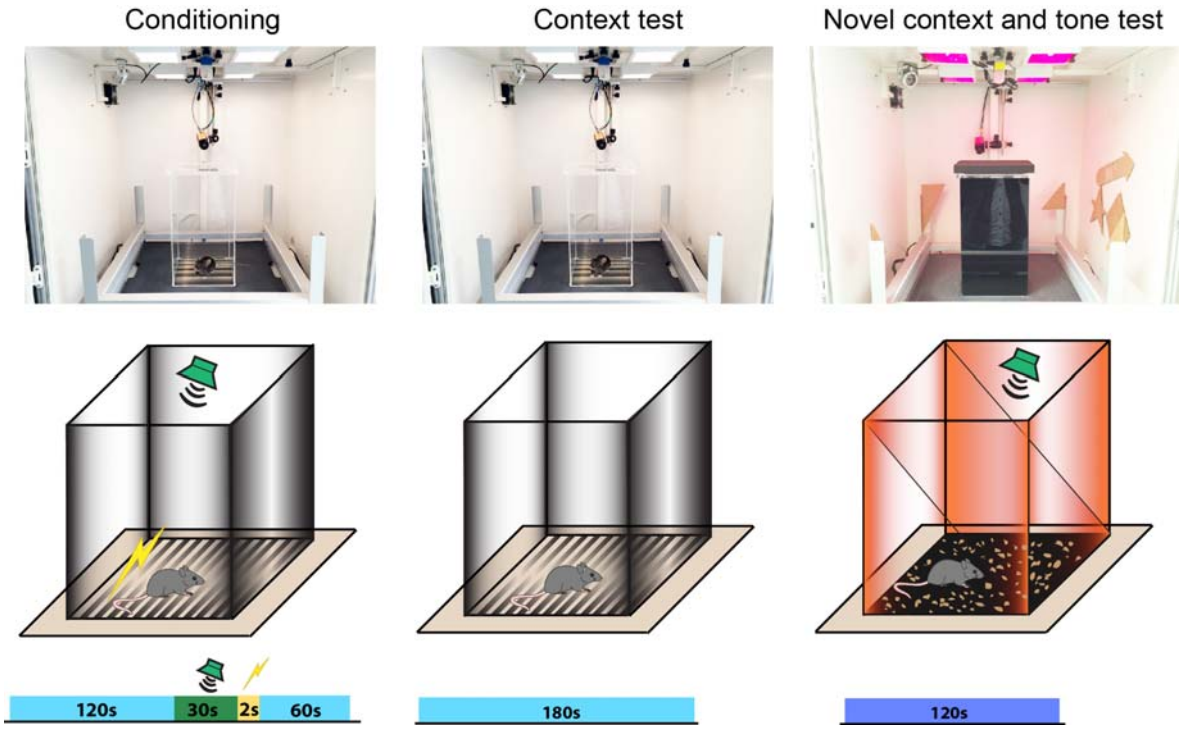

Fig. 4.8 Fear conditioning apparatus and schematic diagram (1 CS-US)

4.21 Conditioned taste aversion

Conditioned taste aversion (CTA, Fig. 4.9) was performed as described previously (Rosenblum et al., 1993; Chinnakkaruppan et al., 2014) to test implicit taste aversion memory. Briefly, mice were restricted to water access for 3 days during which they were habituated to obtain their daily water ration once per day for 20 min from two pipettes, each containing 10 ml of water. On the fourth day (conditioning day), mice were allowed to drink 0.5% sodium saccharin (Sigma) solution from two similar pipettes for 20 min. 40 min later mice were injected with lithium chloride (LiCl, 0.14 M, 2% b.w., Sigma) intraperitoneally. Mice were given 20 min access to the water on days 5 for the recovery. On day 6 (2 days after the conditioning), mice were subjected to a multiple-choice test involving two pipettes each with 10 ml conditioned taste solution (saccharin) and two with 10 ml water. The order of the pipettes was counterbalanced and the volume of fluid consumed from each pipette was recorded. Data are expressed as aversion index (AI): the volume of water consumed divided by the total fluid consumed (ml water/ml water plus ml saccharin). In order to overcome the time effect of water restriction, water or saccharin was given to the mice at the same time every day during the entire procedure.

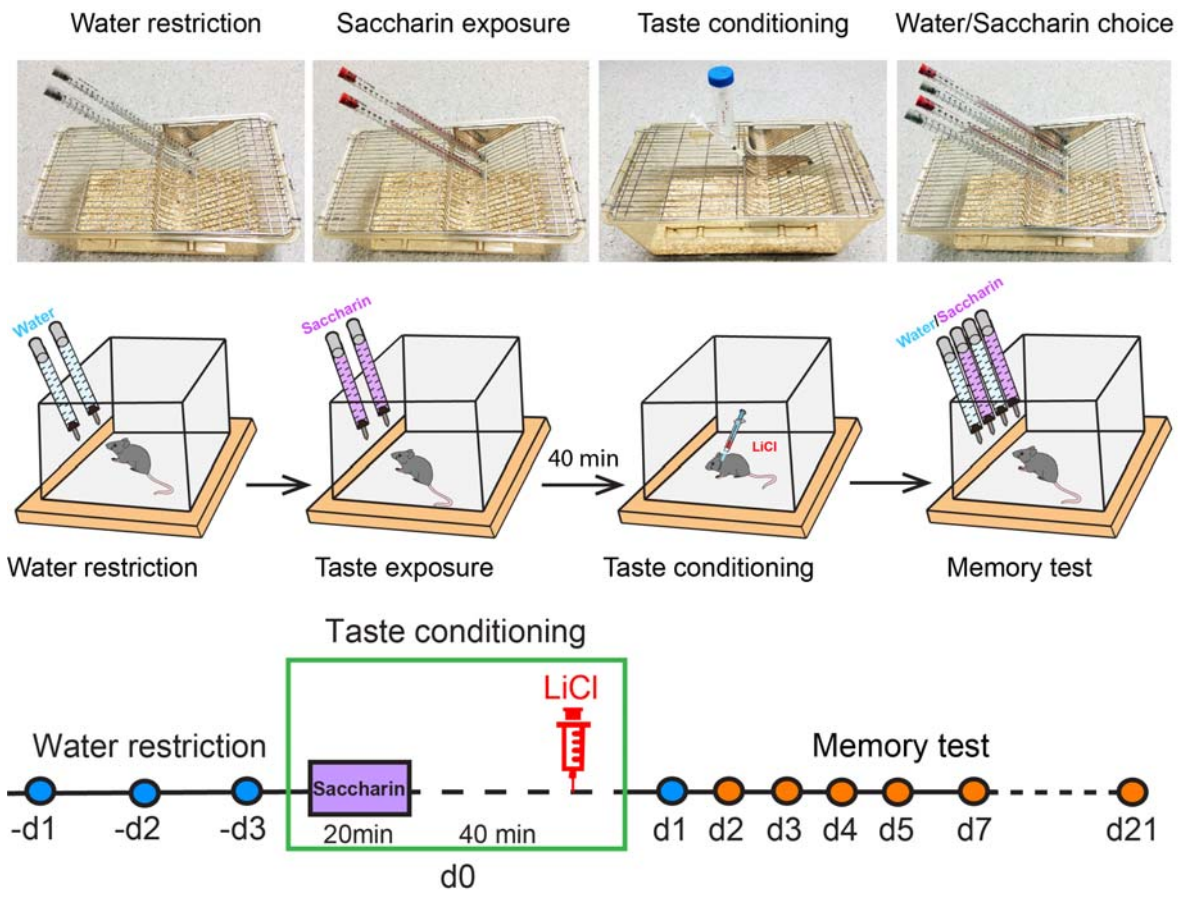

Fig. 4.9 Conditioned taste aversion apparatus and schematic diagram

4.22 Morris water maze

Spatial learning and memory was evaluated in the Morris water maze (Fig. 4.10) (Morris et al., 1982; da Silva et al., 2014) according to previously published routines (Vorhees and Williams, 2006). Briefly, the maze consisted of a circular tank (1.5 m in diameter) filled with water (21 ± 1°C) made opaque with a white non-toxic soluble paint. A submerged circular platform (14 cm in diameter) was placed 1.0 cm below the water surface. Four large reference cues were attached to the wall of the tank at unequal distances from each other. The entire maze was isolated by white curtains and experiment was done under indirect diffused light conditions (40 Lux). During the acquisition phase, mice were trained to learn how to find the hidden platform

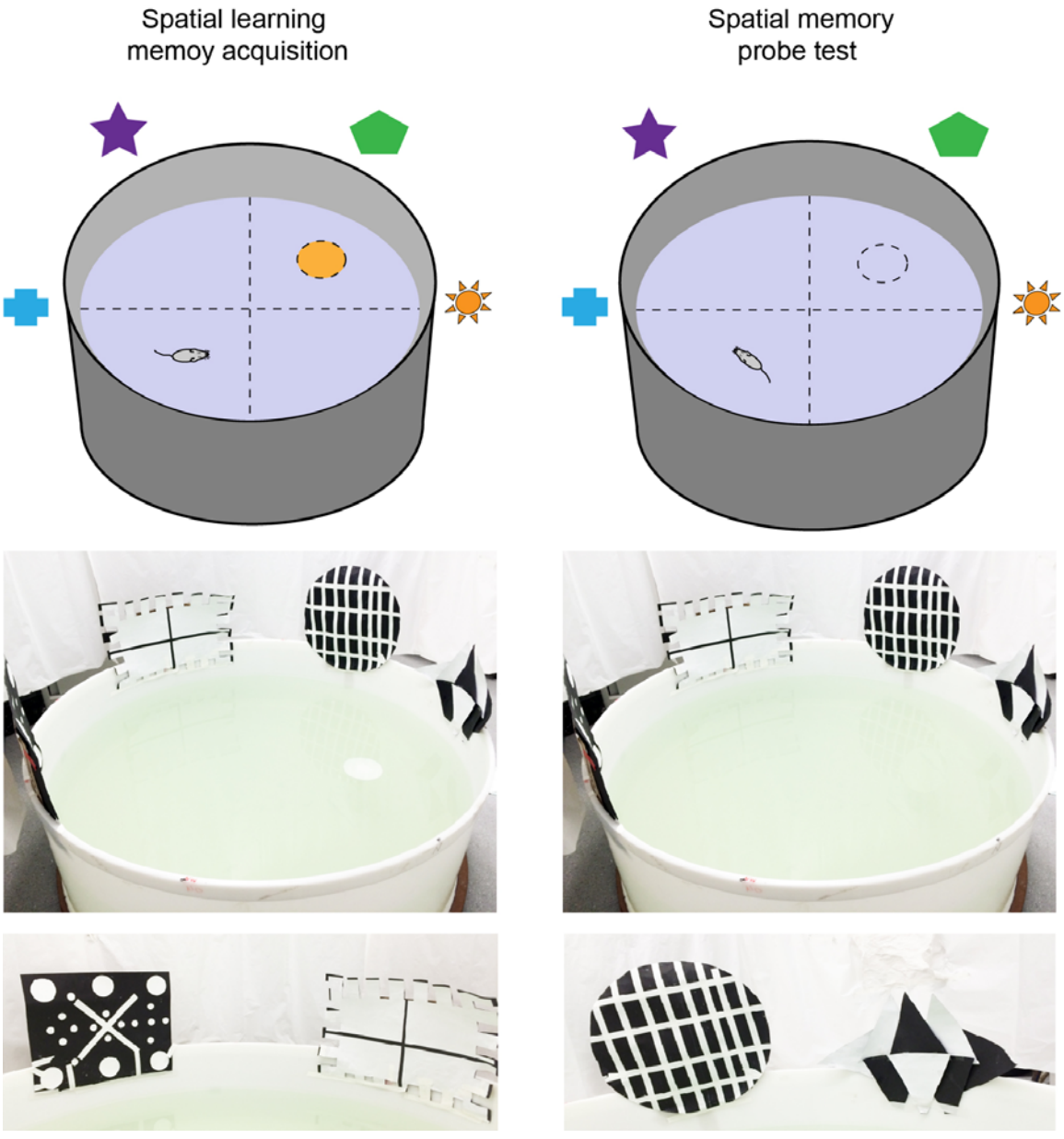

Fig. 4.10 Morris water maze apparatus and schematic diagram

Four starting positions were designated and mice were released from each starting position in a semi-random order every day. Mice were guided to the platform if they failed to find the hidden platform within 60 s and allowed to stay on it for another 60 s for the first trial of the first day, 30 s for the second trial of the first day, and 15 s for the rest of following trials. Four acquisition trials were performed daily for 6 to 10 consecutive days. Learning curve was generated from the time mice spent in finding the submerged platform (Escape latency to the platform) and from the total distance moved during exploring (Path length). To assess the long-term spatial memory, mice were subjected to a single probe trial (60 s) 1 day, 7 days or 21 days after termination of training. During the probe trial, the platform was removed from the maze and mice were released from a starting position in the opposite quadrant. Memory precision was evaluated from the probe trial by measuring: 1. the time spent in an annulus zone covering twice the platform area, virtually drawn over its previous location. For comparison, identical zones were virtually drawn in each maze quadrant. 2. The number of crossings of the annulus zone. Higher percentage of time and larger number of crossings of the annulus zone indicate better memory for the previously trained platform location. During the acquisition stage, learning of the platform location was judged as successful when WT mice reached escape latencies < 20 s and exhibited significantly more annulus crossings over the target zone, compared to the averaged crossings over three comparable zones drawn virtually over each of the non-target quadrants. If these criteria were not met in the first probe test, mice were subjected to additional training for 4 subsequent days. In these cases, the 1 day memory test was performed after completion of the entire training phase. After the last probe test, mice were tested in the visually-cued version of the water maze to test possible perceptual or motor deficits (abnormal eyesight or motor disability) of the mice. A three days visible platform test was performed in the end of the experiment to test the possible spatial deficits (abnormal eyesight or motoric disability) of the mice. During this test, the platform was kept submerged but a flag was mounted that extends approximately 12 cm above the water surface. To ensure that the animal was using this flag to locate the platform, the flag location and the mouse starting points were both moved to new positions in each trial (60 s). Experiments were video-recorded and tracked with Ethovision XT (Noldus Information Technology).

4.23 Multiple electrodes local field potential recordings *in vivo*

Adult male mice were injected with 0.8 mg/g b.w. urethane (10% w/v; Sigma in NaCl 0.9%) and 0.05 µg/g b.w. of buprenorphine (Temgesic). Initial anesthesia was induced with 4% isoflurane in 100% water-saturated oxygen, which was decreased to 1.0–1.5% isoflurane during surgery. Animals were placed in a stereotaxic apparatus (Stoelting). Body temperature was maintained at 36.5 °C using a homeothermic heating pad (WPI) throughout the experiment. A midline skin incision was made on the top of the skull. For a common

ground and reference electrode, a 0.8 mm wide craniotomy was drilled above the cerebellum (1.5 mm posterior to lambda, 1.0 mm lateral to the midline) and a stainless steel screw connected to the ground wire was inserted. After drilling 0.6 mm wide craniotomies, two linear 16-site silicon probes with a 100 µm inter-electrode distance and 177 μm^2 electrode surface (a1x16–5 mm-100-177; NeuroNexus Technologies) were vertically lowered into the right hemisphere: one into the dorsal hippocampus along the CA1-DG axis (2 mm posterior to bregma, 1.4 mm lateral to midline, depth 2.1 mm), the other into the PFC (1.54 mm anterior to bregma, 0.3 mm lateral to midline, depth 2.8 mm). Prior to insertion, probes were dipped in a DiI-solution, for post-experimental probe position verification. Both probes were connected to a 1x preamplifier (Neuralynx) mounted to the stereotaxic instrument. Animal breathing rate and movement was recorded with a piezoelectric sensor placed under the animal's thorax. When probes and sensor were in place, isoflurane anesthesia was discontinued. Recording was immediately started and lasted for at least 2 hours. Data from both probes and the sensor were digitally filtered (0.5–9000 Hz bandpass) and digitized as 16-bit integers with a sampling rate of 32 kHz using a Digital Lynx 4SX data acquisition system (Neuralynx). During the recording, anesthetic depth was observed from beathing rates, twitching and electrophysiological properties. If required, additional 0.2 mg/g b.w. urethane doses were given. After the experiment, mice were deeply anesthetized with 4% isoflurane for 5 mins, before quick decapitation and excision of the brain, which was put into 4% PFA. Probe positions were verified in NeuroTrace fluorescent Nissl-stained (Invitrogen) coronal slices, which were used in combination with the local field potential (LFP) depth profile for layer identification (Buzsaki et al., 2003).

All *in vivo* data were analyzed and visualized in MATLAB (MathWorks) or NeuroScope (Hazan et al., 2006). LFPs were downsampled to 1.28 kHz from raw traces. Multitaper time-frequency spectra were computed using Chronux (www.chronux.org). A CSD calculation for hippocampal signals was based on the inversion of the electrostatic forward solution, using the spline method, assuming a 0.5 mm source diameter and 0.3S tissue conductivity (Pettersen et al., 2006). Power between 0.2-1.2 Hz was used to mark SWS-like periods. For automatic ripple detection during these periods, recordings were band filtered (Butterworth; 14th order, 100-250 Hz). Ripples were defined as events during which the instantaneous amplitudes, calculated by the absolute of the Hilbert transform, exceeded four times the SD above the mean. The left and right borders of detected ripple events were defined as the time points where the instantaneous power dropped < 1.75 SDs above the mean. Events shorter than 25 ms were excluded.

For each individual ripple, we calculated its amplitude and estimated its frequency. Ripple amplitude was obtained by measuring the average peak-to-peak amplitude per ripple

on the band filtered signal. Ripple frequency was obtained by calculating the mean inverse distance between subsequent troughs. To obtain the ripple amplitude and frequency per animal, a mean was calculated for all detected ripples throughout a recording. Ripple occurrence was defined as the number of ripples per second of SWS-like brain states. The amplitudes of sharp waves co-occurring with ripples (SPW-Rs) were obtained by taking the mean of the most negative point of the CSD in str.Rad during pre-detected ripple events. We also detected SPWs independent from ripples by filtering the CSD from str. Rad (Butterworth, 12^{th} order, low-pass, 30 Hz cut-off) and detecting negative peaks larger than 2 SD below 0 during SWS. Sharp wave borders were defined where the negative peaks reached 1 SD below 0.

Paradoxical/REM-like epochs were manually selected and defined by the absence of slow wave power, the presence of continuous theta (4–6 Hz) oscillations and co-occurring gamma frequency (20-50 Hz) activity. Theta and gamma power was calculated for the selected REM-like epochs by integrating the area below the theta and gamma ranges (nFFT = 4096 points, sliding window 2048 points).

4.24 Long-term potentiation recordings *in vivo*

Mouse was anesthetized with urethane (1.5 g/kg b.w., i.p., Sigma) and maintained at a surgical level with supplemental injections if needed, and then was positioned in a stereotaxic apparatus (Fig. 4.11). Skull was exposed by making a midline skin incision on the top of the skull. Mouse body temperature was maintained at 37 °C through a CMA 450 temperature controller. Heart beating rate was monitored throughout the experiment. For the recordings in the hippocampus, a concentric bipolar stimulating electrode (SNE-100, David Kopf Instruments) was placed in the perforant path fibers in the angular bundle (coordinates with the skull surface flat: 2.7-2.8 mm lateral to the lambda, and 1.8-1.9 mm below the surface of the skull). A Epoxy-insulated stainless steel recording electrode (A-M Systems) was placed in the dentate gyrus (DG: 2.0-2.1 mm posterior to bregma, 1.5-1.6 mm lateral to the midline, and 1.6-1.8 mm below the surface of the skull). For the recordings in the prefrontal cortex, the stimulating electrode was placed in the ventral CA1 (coordinates: 3.3-3.4 mm posterior to bregma, 3.1-3.2 mm lateral to the midline, and 1.7-1.8 mm below the surface of the skull), and the recording electrode was placed in the medial prefrontal cortex (mPFC, coordinates: 1.7-1.8 mm anterior to bregma, 0.4-0.5 mm lateral to the midline, and 1.6-1.7 mm below the surface of the skull). Basic synaptic transmission was evaluated by input/output (I/O) curve which was generated by injecting systematic variation of the stimulus current from 0.1-1.0 mA with steps of 0.1 mA. Stimulus pulses were delivered at 0.05 Hz and three responses at each current level were averaged.

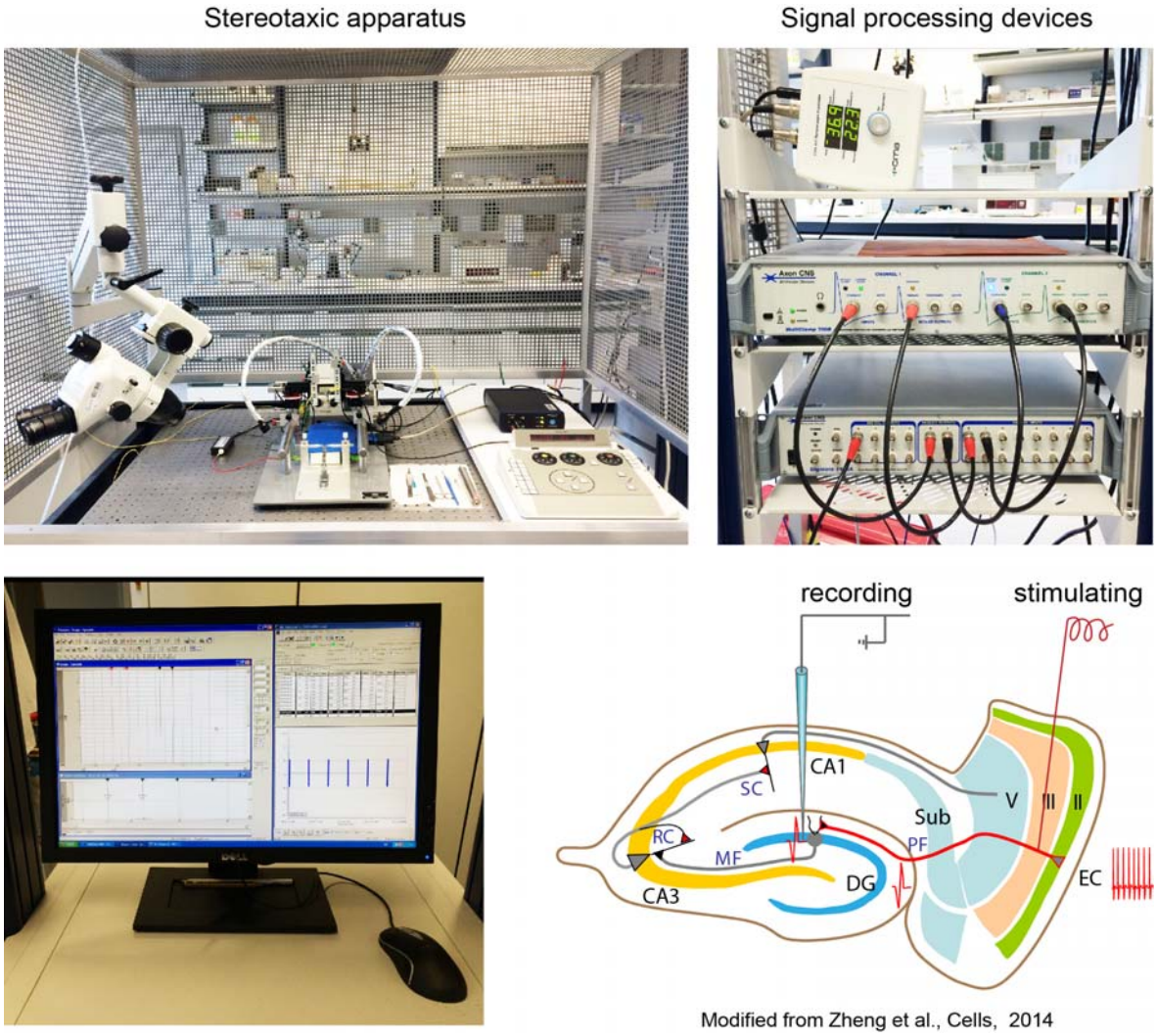

Fig. 4.11 *In vivo* extracellular field potential recordings system configuration

Stimulus intensity was adjusted to evoke a fEPSP slope approx. 50% of maximum and a superimposed population spike of approx. 1 mV in the DG for 20 min baseline recordings. LTP in the hippocampus (DG-LTP) was induced by theta-burst stimulation (TBS) which consists 6 series of 6 trains of 6 stimuli at 400 Hz, 200 ms between trains, 20 s between series (Jones et al., 2001; Cooke et al., 2006; Jedlicka et al., 2013). LTP in the medial prefrontal cortex (mPFC-LTP) was induced by applying high frequency stimulation (HFS) consisting 2 series of 10 trains of 50 stimuli at 250 Hz, 10 seconds between trains, and 10 min between series (Izaki et al., 2001; Kawashima et al., 2006). Post-titanic recordings were performed for 2.5-3 hours with single pulse applied at a frequency of 0.05 Hz. The wave width and current intensity was doubled during DG-LTP induction. Whereas during mPFC-LTP induction, the wave width and current intensity was kept the same as that used in the baseline recordings. In the end, the electrodes positions were verified by brain slice histology. Slopes of the fEPSP and/or amplitudes of the population spike were normalized to the mean value of 20 min baseline. Electrodes placement was controlled by a Display SM-5

manipulator (Luigs & Neumann). Stimulation was generated by STG 4002 stimulus generator (Multichannel Systems). Signals were captured by Digidata 1440A digitizer (Molecular Devices), amplified 1000x and filtered at 3K Hz by MultiClamp 700B amplifier (Molecular Devices). Data were acquired with Clampex software (Version 10.2) and analyzed with Clampfit 10.2.

4.25 Statistical analysis

Two-tailed Student's *t*-tests were applied when data were normally distributed. In the novel object recognition test, preference index was compared to the chance level performance (50%) with one sample *t*-test. In the experiments of western blot quantification, open field, elevated zero/plus maze, fear conditioning and conditioned taste aversion, two sample *t*-tests were used to make comparison between genotypes. For the flinch-jump and local field recording data, Mann-Whitney test was applied between genotypes. For the cell mapping data, Kruskal-Wallis with Dunn's multiple comparison *post hoc* tests was used among groups. For the acquisition phase of Morris water maze and fear conditioning and *in vivo* LTP recordings, two-way ANOVA with repeated measures was performed within subjects following time or trials and Fisher's LSD *post hoc* test was utilized between genotypes. For the probe tests of the water maze, paired *t*-test comparison was made between time percentage or crossings in target quadrant/annulus zone and average time percentage or crossings in other three quadrants/annulus zones within subjects. All statistics were done with IBM SPSS software (Version 19) and $p < 0.05$ was considered as significant. All graphs were generated with Origin 9.0, Adobe Illustrator CS5 (version 15.2) and Matlab (MathWorks). Values presented in figures are mean ± s.e.m or median ± s.d. or median with 25^{th} and 75^{th} percentile, as indicated.

5 Appendix

5.1 References

(1997) Mutant mice and neuroscience: recommendations concerning genetic background. Banbury Conference on genetic background in mice. Neuron 19:755-759.

Addis DR, Moscovitch M, Crawley AP, McAndrews MP (2004) Recollective qualities modulate hippocampal activation during autobiographical memory retrieval. Hippocampus 14:752-762.

Alberi L, Liu SX, Wang Y, Badie R, Smith-Hicks C, Wu J, Pierfelice TJ, Abazyan B, Mattson MP, Kuhl D, Pletnikov M, Worley PF, Gaiano N (2011) Activity-Induced Notch Signaling in Neurons Requires Arc/Arg3.1 and Is Essential for Synaptic Plasticity in Hippocampal Networks. Neuron 69:437-444.

Alberini CM (2009) Transcription factors in long-term memory and synaptic plasticity. Physiological reviews 89:121-145.

Alvarez P, Squire LR (1994) Memory consolidation and the medial temporal lobe: a simple network model. Proc Natl Acad Sci U S A 91:7041-7045.

Anagnostaras SG, Maren S, Fanselow MS (1999) Temporally graded retrograde amnesia of contextual fear after hippocampal damage in rats: within-subjects examination. J Neurosci 19:1106-1114.

Anagnostaras SG, Gale GD, Fanselow MS (2001) Hippocampus and contextual fear conditioning: recent controversies and advances. Hippocampus 11:8-17.

Axmacher N, Mormann F, Fernandez G, Elger CE, Fell J (2006) Memory formation by neuronal synchronization. Brain research reviews 52:170-182.

Bacon C, Schneider M, Le Magueresse C, Froehlich H, Sticht C, Gluch C, Monyer H, Rappold GA (2015) Brain-specific Foxp1 deletion impairs neuronal development and causes autistic-like behaviour. Molecular psychiatry 20:632-639.

Bannerman DM, Yee BK, Good MA, Heupel MJ, Iversen SD, Rawlins JN (1999) Double dissociation of function within the hippocampus: a comparison of dorsal, ventral, and complete hippocampal cytotoxic lesions. Behavioral neuroscience 113:1170-1188.

Beeman CL, Bauer PS, Pierson JL, Quinn JJ (2013) Hippocampus and medial prefrontal cortex contributions to trace and contextual fear memory expression over time. Learn Mem 20:336-343.

Beique JC, Na Y, Kuhl D, Worley PF, Huganir RL (2011) Arc-dependent synapse-specific homeostatic plasticity. Proc Natl Acad Sci U S A 108:816-821.

Bero AW, Meng J, Cho S, Shen AH, Canter RG, Ericsson M, Tsai LH (2014) Early remodeling of the neocortex upon episodic memory encoding. Proc Natl Acad Sci U S A 111:11852-11857.

Berry SD, Seager MA (2001) Hippocampal theta oscillations and classical conditioning. Neurobiol Learn Mem 76:298-313.

Bi GQ, Poo MM (1998) Synaptic modifications in cultured hippocampal neurons: dependence on spike timing, synaptic strength, and postsynaptic cell type. J Neurosci 18:10464-10472.

Bick-Sander A (2002) Modifikation des genomischen Arg3.1 Lokus in embryonalen Stammzellen. In: Fachbereich Medizin, p 117. Hamburg: Universität Hamburg.

Blaser R, Heyser C (2015) Spontaneous object recognition: a promising approach to the comparative study of memory. Front Behav Neurosci 9:183.

Bliss TV, Lomo T (1973) Long-lasting potentiation of synaptic transmission in the dentate area of the anaesthetized rabbit following stimulation of the perforant path. The Journal of physiology 232:331-356.

Boyce R, Glasgow SD, Williams S, Adamantidis A (2016) Causal evidence for the role of REM sleep theta rhythm in contextual memory consolidation. Science 352:812-816.

Buhl DL, Buzsaki G (2005) Developmental emergence of hippocampal fast-field "ripple" oscillations in the behaving rat pups. Neuroscience 134:1423-1430.

Buzsaki G (2002) Theta oscillations in the hippocampus. Neuron 33:325-340.

Buzsaki G (2005) Theta rhythm of navigation: link between path integration and landmark navigation, episodic and semantic memory. Hippocampus 15:827-840.

Buzsaki G (2015) Hippocampal sharp wave-ripple: A cognitive biomarker for episodic memory and planning. Hippocampus 25:1073-1188.

Buzsaki G, Draguhn A (2004) Neuronal oscillations in cortical networks. Science 304:1926-1929.

Buzsaki G, Moser EI (2013a) Memory, navigation and theta rhythm in the hippocampal-entorhinal system. Nat Neurosci 16:130-138.

Buzsaki G, Moser EI (2013b) Memory, navigation and theta rhythm in the hippocampal-entorhinal system. Nat Neurosci 16:130-138.

Buzsaki G, Horvath Z, Urioste R, Hetke J, Wise K (1992) High-frequency network oscillation in the hippocampus. Science 256:1025-1027.

Buzsaki G, Buhl DL, Harris KD, Csicsvari J, Czeh B, Morozov A (2003) Hippocampal network patterns of activity in the mouse. Neuroscience 116:201-211.

Byers CE, Barylko B, Ross JA, Southworth DR, James NG, Taylor CAt, Wang L, Collins KA, Estrada A, Waung M, Tassin TC, Huber KM, Jameson DM, Albanesi JP (2015) Enhancement of dynamin polymerization and GTPase activity by Arc/Arg3.1. Biochimica et biophysica acta.

Cao VY, Ye Y, Mastwal S, Ren M, Coon M, Liu Q, Costa RM, Wang KH (2015) Motor Learning Consolidates Arc-Expressing Neuronal Ensembles in Secondary Motor Cortex. Neuron 86:1385-1392.

Castellucci V, Pinsker H, Kupfermann I, Kandel ER (1970) Neuronal mechanisms of habituation and dishabituation of the gill-withdrawal reflex in Aplysia. Science 167:1745-1748.

Chao OY, Huston JP, Li JS, Wang AL, de Souza Silva MA (2016) The medial prefrontal cortex-lateral entorhinal cortex circuit is essential for episodic-like memory and associative object-recognition. Hippocampus 26:633-645.

Chau LS, Prakapenka A, Fleming SA, Davis AS, Galvez R (2013) Elevated Arc/Arg 3.1 protein expression in the basolateral amygdala following auditory trace-cued fear conditioning. Neurobiol Learn Mem 106:127-133.

Chee SS, Menard JL, Dringenberg HC (2015) The lateral septum as a regulator of hippocampal theta oscillations and defensive behavior in rats. J Neurophysiol 113:1831-1841.

Chen G, Zou X, Watanabe H, van Deursen JM, Shen J (2010) CREB binding protein is required for both short-term and long-term memory formation. J Neurosci 30:13066-13077.

Chia C, Otto T (2013) Hippocampal Arc (Arg3.1) expression is induced by memory recall and required for memory reconsolidation in trace fear conditioning. Neurobiol Learn Mem 106:48-55.

Chinnakkaruppan A, Wintzer ME, McHugh TJ, Rosenblum K (2014) Differential contribution of hippocampal subfields to components of associative taste learning. J Neurosci 34:11007-11015.

Chotiner JK, Nielson J, Farris S, Lewandowski G, Huang F, Banos K, de Leon R, Steward O (2010) Assessment of the role of MAP kinase in mediating activity-dependent transcriptional activation of the immediate early gene Arc/Arg3.1 in the dentate gyrus in vivo. Learn Memory 17:117-129.

Chowdhury S, Shepherd JD, Okuno H, Lyford G, Petralia RS, Plath N, Kuhl D, Huganir RL, Worley PF (2006) Arc/Arg3.1 interacts with the endocytic machinery to regulate AMPA receptor trafficking. Neuron 52:445-459.

Clark RE, Squire LR (1998) Classical conditioning and brain systems: the role of awareness. Science 280:77-81.

Clopath C (2012) Synaptic consolidation: an approach to long-term learning. Cognitive neurodynamics 6:251-257.

Colgin LL (2013) Mechanisms and functions of theta rhythms. Annual review of neuroscience 36:295-312.

Colgin LL (2016) Rhythms of the hippocampal network. Nature reviews Neuroscience 17:239-249.

Colgin LL, Denninger T, Fyhn M, Hafting T, Bonnevie T, Jensen O, Moser MB, Moser EI (2009) Frequency of gamma oscillations routes flow of information in the hippocampus. Nature 462:353-357.

Cooke SF, Wu J, Plattner F, Errington M, Rowan M, Peters M, Hirano A, Bradshaw KD, Anwyl R, Bliss TV, Giese KP (2006) Autophosphorylation of alphaCaMKII is not a general requirement for NMDA receptor-dependent LTP in the adult mouse. The Journal of physiology 574:805-818.

Corcoran KA, Donnan MD, Tronson NC, Guzman YF, Gao C, Jovasevic V, Guedea AL, Radulovic J (2011) NMDA receptors in retrosplenial cortex are necessary for retrieval of recent and remote context fear memory. J Neurosci 31:11655-11659.

Corkin S (2002) What's new with the amnesic patient H.M.? Nature reviews Neuroscience 3:153-160.

Craig TJ, Henley JM (2012) SUMOylation, Arc and the regulation homeostatic synaptic scaling: Implications in health and disease. Communicative & integrative biology 5:634-636.

Craig TJ, Jaafari N, Petrovic MM, Jacobs SC, Rubin PP, Mellor JR, Henley JM (2012) Homeostatic synaptic scaling is regulated by protein SUMOylation. J Biol Chem 287:22781-22788.

Csicsvari J, Jamieson B, Wise KD, Buzsaki G (2003) Mechanisms of gamma oscillations in the hippocampus of the behaving rat. Neuron 37:311-322.

Curzon P, Rustay NR, Browman KE (2009) Cued and Contextual Fear Conditioning for Rodents. In: Methods of Behavior Analysis in Neuroscience, 2nd Edition (Buccafusco JJ, ed). Boca Raton (FL).

Czajkowski R, Jayaprakash B, Wiltgen B, Rogerson T, Guzman-Karlsson MC, Barth AL, Trachtenberg JT, Silva AJ (2014) Encoding and storage of spatial information in the retrosplenial cortex. Proc Natl Acad Sci U S A 111:8661-8666.

Czerniawski J, Ree F, Chia C, Ramamoorthi K, Kumata Y, Otto TA (2011) The Importance of Having Arc: Expression of the Immediate-Early Gene Arc Is Required for Hippocampus-Dependent Fear Conditioning and Blocked by NMDA Receptor Antagonism. J Neurosci 31:11200-11207.

D'Hooge R, De Deyn PP (2001) Applications of the Morris water maze in the study of learning and memory. Brain research Brain research reviews 36:60-90.

da Silva BM, Bast T, Morris RG (2014) Spatial memory: behavioral determinants of persistence in the watermaze delayed matching-to-place task. Learn Mem 21:28-36.

Dammermann B (1999) Herstellung und Charakterisierung einer arg3.1-Knockout-Maus. In: Fachbereich Chemie, p 164. Berlin: Universität Hamburg.

Dayawansa S, Ruch S, Norgren R (2014) Parabrachial-hypothalamic interactions are required for normal conditioned taste aversions. American journal of physiology Regulatory, integrative and comparative physiology 306:R190-200.

Denny CA, Kheirbek MA, Alba EL, Tanaka KF, Brachman RA, Laughman KB, Tomm NK, Turi GF, Losonczy A, Hen R (2014) Hippocampal memory traces are differentially modulated by experience, time, and adult neurogenesis. Neuron 83:189-201.

Dew IT, Cabeza R (2011) The porous boundaries between explicit and implicit memory: behavioral and neural evidence. Annals of the New York Academy of Sciences 1224:174-190.

Dillon C, Goda Y (2005) The actin cytoskeleton: integrating form and function at the synapse. Annual review of neuroscience 28:25-55.

Dittgen T, Nimmerjahn A, Komai S, Licznerski P, Waters J, Margrie TW, Helmchen F, Denk W, Brecht M, Osten P (2004) Lentivirus-based genetic manipulations of cortical neurons and their optical and electrophysiological monitoring in vivo. Proc Natl Acad Sci U S A 101:18206-18211.

Dudai Y (2012) The restless engram: consolidations never end. Annual review of neuroscience 35:227-247.

Dudai Y, Karni A, Born J (2015) The Consolidation and Transformation of Memory. Neuron 88:20-32.

Duvarci S, Pare D (2014) Amygdala microcircuits controlling learned fear. Neuron 82:966-980.

Ego-Stengel V, Wilson MA (2010) Disruption of ripple-associated hippocampal activity during rest impairs spatial learning in the rat. Hippocampus 20:1-10.

Einarsson EO, Nader K (2012) Involvement of the anterior cingulate cortex in formation, consolidation, and reconsolidation of recent and remote contextual fear memory. Learn Mem 19:449-452.

Engert F, Bonhoeffer T (1999) Dendritic spine changes associated with hippocampal long-term synaptic plasticity. Nature 399:66-70.

Erdmann G, Schutz G, Berger S (2007) Inducible gene inactivation in neurons of the adult mouse forebrain. Bmc Neurosci 8:63.

Fanselow MS (2010) From contextual fear to a dynamic view of memory systems. Trends in cognitive sciences 14:7-15.

Floresco SB (2014) Spatial Learning in Animals. Encyclopedia of Psychopharmacology:1-5.

Forni PE, Scuoppo C, Imayoshi I, Taulli R, Dastru W, Sala V, Betz UA, Muzzi P, Martinuzzi D, Vercelli AE, Kageyama R, Ponzetto C (2006) High levels of Cre expression in neuronal progenitors cause defects in brain development leading to microencephaly and hydrocephaly. J Neurosci 26:9593-9602.

Frankland PW, Bontempi B (2005) The organization of recent and remote memories. Nature reviews Neuroscience 6:119-130.

Frankland PW, Cestari V, Filipkowski RK, McDonald RJ, Silva AJ (1998) The dorsal hippocampus is essential for context discrimination but not for contextual conditioning. Behavioral neuroscience 112:863-874.

Frankland PW, O'Brien C, Ohno M, Kirkwood A, Silva AJ (2001) Alpha-CaMKII-dependent plasticity in the cortex is required for permanent memory. Nature 411:309-313.

Gale GD, Anagnostaras SG, Godsil BP, Mitchell S, Nozawa T, Sage JR, Wiltgen B, Fanselow MS (2004) Role of the basolateral amygdala in the storage of fear memories across the adult lifetime of rats. J Neurosci 24:3810-3815.

Gao M, Sossa K, Song LH, Errington L, Cummings L, Hwang H, Kuhl D, Worley P, Lee HK (2010) A Specific Requirement of Arc/Arg3.1 for Visual Experience-Induced Homeostatic Synaptic Plasticity in Mouse Primary Visual Cortex. J Neurosci 30:7168-7178.

Giorgi C, Yeo GW, Stone ME, Katz DB, Burge C, Turrigiano G, Moore MJ (2007) The EJC factor eIF4AIII modulates synaptic strength and neuronal protein expression. Cell 130:179-191.

Girardeau G, Zugaro M (2011) Hippocampal ripples and memory consolidation. Curr Opin Neurobiol 21:452-459.

Girardeau G, Benchenane K, Wiener SI, Buzsaki G, Zugaro MB (2009) Selective suppression of hippocampal ripples impairs spatial memory. Nat Neurosci 12:1222-1223.

Goshen I, Brodsky M, Prakash R, Wallace J, Gradinaru V, Ramakrishnan C, Deisseroth K (2011) Dynamics of retrieval strategies for remote memories. Cell 147:678-689.

Gouty-Colomer LA, Hosseini B, Marcelo IM, Schreiber J, Slump DE, Yamaguchi S, Houweling AR, Jaarsma D, Elgersma Y, Kushner SA (2015) Arc expression identifies the lateral amygdala fear memory trace. Molecular psychiatry.

Greenstein YJ, Pavlides C, Winson J (1988) Long-term potentiation in the dentate gyrus is preferentially induced at theta rhythm periodicity. Brain Res 438:331-334.

Grigson PS, Reilly S, Shimura T, Norgren R (1998) Ibotenic acid lesions of the parabrachial nucleus and conditioned taste aversion: further evidence for an associative deficit in rats. Behavioral neuroscience 112:160-171.

Gusev PA, Gubin AN (2010a) Arc/Arg3.1 mRNA global expression patterns elicited by memory recall in cerebral cortex differ for remote versus recent spatial memories. Frontiers in integrative neuroscience 4:15.

Gusev PA, Gubin AN (2010b) Recent and remote memory recalls modulate different sets of stereotypical interlaminar correlations in Arc/Arg3.1 mRNA expression in cortical areas. Brain Res 1352:118-139.

Gusev PA, Cui C, Alkon DL, Gubin AN (2005) Topography of Arc/Arg3.1 mRNA expression in the dorsal and ventral hippocampus induced by recent and remote spatial memory recall: Dissociation of CA3 and CA1 activation. J Neurosci 25:9384-9397.

Guzowski JF, Lyford GL, Stevenson GD, Houston FP, McGaugh JL, Worley PF, Barnes CA (2000) Inhibition of activity-dependent arc protein expression in the rat hippocampus impairs the maintenance of long-term potentiation and the consolidation of long-term memory. J Neurosci 20:3993-4001.

Hafting T, Fyhn M, Molden S, Moser MB, Moser EI (2005) Microstructure of a spatial map in the entorhinal cortex. Nature 436:801-806.

Hameyer D, Loonstra A, Eshkind L, Schmitt S, Antunes C, Groen A, Bindels E, Jonkers J, Krimpenfort P, Meuwissen R, Rijswijk L, Bex A, Berns A, Bockamp E (2007) Toxicity of ligand-dependent Cre recombinases and generation of a conditional Cre deleter mouse allowing mosaic recombination in peripheral tissues. Physiol Genomics 31:32-41.

Han JH, Kushner SA, Yiu AP, Hsiang HL, Buch T, Waisman A, Bontempi B, Neve RL, Frankland PW, Josselyn SA (2009) Selective erasure of a fear memory. Science 323:1492-1496.

Hardman R, Evans DJ, Fellows L, Hayes B, Rupniak HT, Barnes JC, Higgins GA (1997) Evidence for recovery of spatial learning following entorhinal cortex lesions in mice. Brain Res 758:187-200.

Hazan L, Zugaro M, Buzsaki G (2006) Klusters, NeuroScope, NDManager: a free software suite for neurophysiological data processing and visualization. J Neurosci Methods 155:207-216.

Hebb D (1949) The organization of behavior; a neuropsychological theory. New York: Wiley.

Hermey G, Mahlke C, Gutzmann JJ, Schreiber J, Bluthgen N, Kuhl D (2013) Genome-wide profiling of the activity-dependent hippocampal transcriptome. Plos One 8:e76903.

Herry C, Johansen JP (2014) Encoding of fear learning and memory in distributed neuronal circuits. Nat Neurosci 17:1644-1654.

Ho JW, Poeta DL, Jacobson TK, Zolnik TA, Neske GT, Connors BW, Burwell RD (2015) Bidirectional Modulation of Recognition Memory. J Neurosci 35:13323-13335.

Holloway CM, McIntyre CK (2011) Post-training disruption of Arc protein expression in the anterior cingulate cortex impairs long-term memory for inhibitory avoidance training. Neurobiol Learn Mem 95:425-432.

Hollup SA, Molden S, Donnett JG, Moser MB, Moser EI (2001) Accumulation of hippocampal place fields at the goal location in an annular watermaze task. J Neurosci 21:1635-1644.

Huerta PT, Lisman JE (1995) Bidirectional synaptic plasticity induced by a single burst during cholinergic theta oscillation in CA1 in vitro. Neuron 15:1053-1063.

Hughes JR (1958) Post-tetanic potentiation. Physiological reviews 38:91-113.

Inostroza M, Born J (2013) Sleep for preserving and transforming episodic memory. Annual review of neuroscience 36:79-102.

Ito-Ishida A, Ure K, Chen H, Swann John W, Zoghbi Huda Y (2015) Loss of MeCP2 in Parvalbumin-and Somatostatin-Expressing Neurons in Mice Leads to Distinct Rett Syndrome-like Phenotypes. Neuron 88:651-658.

Izaki Y, Takita M, Nomura M (2001) Mouse hippocampo-prefrontal paired-pulse facilitation and long-term potentiation in vivo. Neuroreport 12:1191-1193.

Izquierdo I, Furini CR, Myskiw JC (2016) Fear Memory. Physiological reviews 96:695-750.

Jadhav SP, Kemere C, German PW, Frank LM (2012) Awake hippocampal sharp-wave ripples support spatial memory. Science 336:1454-1458.

Jakkamsetti V, Tsai NP, Gross C, Molinaro G, Collins KA, Nicoletti F, Wang KH, Osten P, Bassell GJ, Gibson JR, Huber KM (2013) Experience-Induced Arc/Arg3.1 Primes CA1 Pyramidal Neurons for Metabotropic Glutamate Receptor-Dependent Long-Term Synaptic Depression. Neuron 80:72-79.

Jedlicka P, Vnencak M, Krueger DD, Jungenitz T, Brose N, Schwarzacher SW (2013) Neuroligin-1 regulates excitatory synaptic transmission, LTP and EPSP-spike coupling in the dentate gyrus in vivo. Brain Struct Funct.

Jin J, Maren S (2015) Prefrontal-Hippocampal Interactions in Memory and Emotion. Frontiers in systems neuroscience 9:170.

Johansen JP, Cain CK, Ostroff LE, LeDoux JE (2011) Molecular mechanisms of fear learning and memory. Cell 147:509-524.

Jones MW, Errington ML, French PJ, Fine A, Bliss TV, Garel S, Charnay P, Bozon B, Laroche S, Davis S (2001) A requirement for the immediate early gene Zif268 in the expression of late LTP and long-term memories. Nat Neurosci 4:289-296.

Joseph R (1996) Neuropsychiatry, neuropsychology and clinical neuroscience: Emotion,

evolution, cognition, language, memory, brain damage, and abnormal behavior, 2nd edition. Edition. Baltimore, MD: Lippincott Williams & Wilkins.

Josselyn SA, Köhler S, Frankland PW (2015) Finding the engram. Nature Reviews Neuroscience 16:521-534.

Jouvet M (1969) Biogenic amines and the states of sleep. Science 163:32-41.

Kandel ER (2001) The molecular biology of memory storage: a dialogue between genes and synapses. Science 294:1030-1038.

Kandel ER, Dudai Y, Mayford MR (2014) The molecular and systems biology of memory. Cell 157:163-186.

Kaplan R, Adhikari MH, Hindriks R, Mantini D, Murayama Y, Logothetis NK, Deco G (2016) Hippocampal Sharp-Wave Ripples Influence Selective Activation of the Default Mode Network. Current biology : CB 26:686-691.

Karlsson MP, Frank LM (2009) Awake replay of remote experiences in the hippocampus. Nat Neurosci 12:913-918.

Katche C, Cammarota M, Medina JH (2013a) Molecular signatures and mechanisms of long-lasting memory consolidation and storage. Neurobiol Learn Mem 106:40-47.

Katche C, Dorman G, Slipczuk L, Cammarota M, Medina JH (2013b) Functional integrity of the retrosplenial cortex is essential for rapid consolidation and recall of fear memory. Learn Mem 20:170-173.

Kawashima H, Izaki Y, Grace AA, Takita M (2006) Cooperativity between hippocampal-prefrontal short-term plasticity through associative long-term potentiation. Brain Res 1109:37-44.

Kawashima T, Okuno H, Nonaka M, Adachi-Morishima A, Kyo N, Okamura M, Takemoto-Kimura S, Worley PF, Bito H (2009) Synaptic activity-responsive element in the Arc/Arg3.1 promoter essential for synapse-to-nucleus signaling in activated neurons. P Natl Acad Sci USA 106:316-321.

Kay LM (2003) Two species of gamma oscillations in the olfactory bulb: dependence on behavioral state and synaptic interactions. Journal of integrative neuroscience 2:31-44.

Keene CS, Bucci DJ (2008) Neurotoxic lesions of retrosplenial cortex disrupt signaled and unsignaled contextual fear conditioning. Behavioral neuroscience 122:1070-1077.

Kim IH, Wang H, Soderling SH, Yasuda R (2014) Loss of Cdc42 leads to defects in synaptic plasticity and remote memory recall. eLife 3.

Kim JJ, Fanselow MS (1992) Modality-specific retrograde amnesia of fear. Science 256:675-677.

Kim S, Martin KC (2015) Neuron-wide RNA transport combines with netrin-mediated local translation to spatially regulate the synaptic proteome. eLife 4.

Kobayashi H, Yamamoto S, Maruo T, Murakami F (2005) Identification of a cis-acting element required for dendritic targeting of activity-regulated cytoskeleton-associated protein mRNA. Eur J Neurosci 22:2977-2984.

Korb E, Finkbeiner S (2011) Arc in synaptic plasticity: from gene to behavior. Trends in neurosciences 34:591-598.

Korb E, Wilkinson CL, Delgado RN, Lovero KL, Finkbeiner S (2013) Arc in the nucleus regulates PML-dependent GluA1 transcription and homeostatic plasticity. Nat Neurosci 16:874-U266.

Kubik S, Miyashita T, Kubik-Zahorodna A, Guzowski JF (2012) Loss of activity-dependent Arc gene expression in the retrosplenial cortex after hippocampal inactivation: interaction in a higher-order memory circuit. Neurobiol Learn Mem 97:124-131.

Kuipers SD, Trentani A, Tiron A, Mao X, Kuhl D, Bramham CR (2016) BDNF-induced LTP is associated with rapid Arc/Arg3.1-dependent enhancement in adult hippocampal neurogenesis. Scientific reports 6:21222.

Lahtinen H, Palva JM, Sumanen S, Voipio J, Kaila K, Taira T (2002) Postnatal development of rat hippocampal gamma rhythm in vivo. J Neurophysiol 88:1469-1474.

Larson J, Lynch G (1986) Induction of synaptic potentiation in hippocampus by patterned stimulation involves two events. Science 232:985-988.

Le Be JV, Markram H (2006) Spontaneous and evoked synaptic rewiring in the neonatal neocortex. Proc Natl Acad Sci U S A 103:13214-13219.

Leblanc MO, Bland BH (1979) Developmental aspects of hippocampal electrical activity and motor behavior in the rat. Experimental neurology 66:220-237.

LeDoux J (2003) The emotional brain, fear, and the amygdala. Cellular and molecular neurobiology 23:727-738.

LeDoux JE (1995) Emotion: clues from the brain. Annual review of psychology 46:209-235.

LeDoux JE (2000) Emotion circuits in the brain. Annual review of neuroscience 23:155-184.

Lee AK, Wilson MA (2002) Memory of sequential experience in the hippocampus during slow wave sleep. Neuron 36:1183-1194.

Lehmann H, Lacanilao S, Sutherland RJ (2007) Complete or partial hippocampal damage produces equivalent retrograde amnesia for remote contextual fear memories. Eur J Neurosci 25:1278-1286.

Leinekugel X, Khazipov R, Cannon R, Hirase H, Ben-Ari Y, Buzsaki G (2002) Correlated bursts of activity in the neonatal hippocampus in vivo. Science 296:2049-2052.

Liao D, Hessler NA, Malinow R (1995) Activation of postsynaptically silent synapses during pairing-induced LTP in CA1 region of hippocampal slice. Nature 375:400-404.

Link W, Konietzko U, Kauselmann G, Krug M, Schwanke B, Frey U, Kuhl D (1995) Somatodendritic expression of an immediate early gene is regulated by synaptic activity. Proc Natl Acad Sci U S A 92:5734-5738.

Lonergan ME, Gafford GM, Jarome TJ, Helmstetter FJ (2010) Time-dependent expression of Arc and zif268 after acquisition of fear conditioning. Neural plasticity 2010:139891.

Lv XF, Xu Y, Han JS, Cui CL (2011) Expression of activity-regulated cytoskeleton-associated protein (Arc/Arg3.1) in the nucleus accumbens is critical for the acquisition, expression and reinstatement of morphine-induced conditioned place preference. Behav Brain Res 223:182-191.

Lyford GL, Yamagata K, Kaufmann WE, Barnes CA, Sanders LK, Copeland NG, Gilbert DJ, Jenkins NA, Lanahan AA, Worley PF (1995) Arc, a growth factor and activity-regulated gene, encodes a novel cytoskeleton-associated protein that is enriched in neuronal dendrites. Neuron 14:433-445.

Lynch GS, Dunwiddie T, Gribkoff V (1977) Heterosynaptic depression: a postsynaptic correlate of long-term potentiation. Nature 266:737-739.

Lynch MA (2004) Long-term potentiation and memory. Physiological reviews 84:87-136.

Mabb AM, Je HS, Wall MJ, Robinson CG, Larsen RS, Qiang Y, Correa SA, Ehlers MD (2014) Triad3A Regulates Synaptic Strength by Ubiquitination of Arc. Neuron 82:1299-1316.

Maddox SA, Schafe GE (2011) The Activity-Regulated Cytoskeletal-Associated Protein (Arc/Arg3.1) Is Required for Reconsolidation of a Pavlovian Fear Memory. J Neurosci 31:7073-7082.

Malkki HA, Mertens PE, Lankelma JV, Vinck M, van Schalkwijk FJ, van Mourik-Donga LB, Battaglia FP, Mahlke C, Kuhl D, Pennartz CM (2016) Effects of Arc/Arg3.1 gene deletion on rhythmic synchronization of hippocampal CA1 neurons during locomotor activity and sleep. Neurobiol Learn Mem 131:155-165.

Maren S (1999) Neurotoxic basolateral amygdala lesions impair learning and memory but not the performance of conditional fear in rats. J Neurosci 19:8696-8703.

Maren S, Phan KL, Liberzon I (2013) The contextual brain: implications for fear conditioning, extinction and psychopathology. Nature reviews Neuroscience 14:417-428.

Markram H, Lubke J, Frotscher M, Sakmann B (1997) Regulation of synaptic efficacy by coincidence of postsynaptic APs and EPSPs. Science 275:213-215.

Marshall L, Helgadottir H, Molle M, Born J (2006) Boosting slow oscillations during sleep potentiates memory. Nature 444:610-613.

Matsuda T, Cepko CL (2007) Controlled expression of transgenes introduced by in vivo electroporation. Proc Natl Acad Sci U S A 104:1027-1032.

McClelland JL, McNaughton BL, O'Reilly RC (1995) Why there are complementary learning systems in the hippocampus and neocortex: insights from the successes and failures of connectionist models of learning and memory. Psychological review 102:419-457.

McCurry CL, Shepherd JD, Tropea D, Wang KH, Bear MF, Sur M (2010) Loss of Arc renders the visual cortex impervious to the effects of sensory experience or deprivation. Nat Neurosci 13:450-457.

McHugh TJ, Blum KI, Tsien JZ, Tonegawa S, Wilson MA (1996) Impaired hippocampal representation of space in CA1-specific NMDAR1 knockout mice. Cell 87:1339-1349.

Messaoudi E, Kanhema T, Soule J, Tiron A, Dagyte G, da Silva B, Bramham CR (2007a) Sustained Arc/Arg3.1 synthesis controls long-term potentiation consolidation through regulation of local actin polymerization in the dentate gyrus In vivo. J Neurosci 27:10445-10455.

Messaoudi E, Kanhema T, Soule J, Tiron A, Dagyte G, da Silva B, Bramham CR (2007b) Sustained Arc/Arg3.1 synthesis controls long-term potentiation consolidation through regulation of local actin polymerization in the dentate gyrus in vivo. J Neurosci 27:10445-10455.

Mishiba T, Tanaka M, Mita N, He X, Sasamoto K, Itohara S, Ohshima T (2014) Cdk5/p35 functions as a crucial regulator of spatial learning and memory. Molecular brain 7:82.

Miyashiro K, Dichter M, Eberwine J (1994) On the nature and differential distribution of mRNAs in hippocampal neurites: implications for neuronal functioning. Proc Natl Acad Sci U S A 91:10800-10804.

Mizunuma M, Norimoto H, Tao K, Egawa T, Hanaoka K, Sakaguchi T, Hioki H, Kaneko T, Yamaguchi S, Nagano T, Matsuki N, Ikegaya Y (2014) Unbalanced excitability underlies offline reactivation of behaviorally activated neurons. Nat Neurosci 17:503-505.

Moga DE, Calhoun ME, Chowdhury A, Worley P, Morrison JH, Shapiro ML (2004) Activity-regulated cytoskeletal-associated protein is localized to recently activated excitatory synapses. Neuroscience 125:7-11.

Monteggia LM, Barrot M, Powell CM, Berton O, Galanis V, Gemelli T, Meuth S, Nagy A, Greene RW, Nestler EJ (2004) Essential role of brain-derived neurotrophic factor in adult hippocampal function. Proc Natl Acad Sci U S A 101:10827-10832.

Montgomery SM, Buzsaki G (2007) Gamma oscillations dynamically couple hippocampal CA3 and CA1 regions during memory task performance. Proc Natl Acad Sci U S A 104:14495-14500.

Morris R (1984) Developments of a water-maze procedure for studying spatial learning in the rat. J Neurosci Methods 11:47-60.

Morris RG, Garrud P, Rawlins JN, O'Keefe J (1982) Place navigation impaired in rats with hippocampal lesions. Nature 297:681-683.

Moser EI, Roudi Y, Witter MP, Kentros C, Bonhoeffer T, Moser MB (2014) Grid cells and cortical representation. Nature reviews Neuroscience 15:466-481.

Nabavi S, Fox R, Proulx CD, Lin JY, Tsien RY, Malinow R (2014) Engineering a memory with LTD and LTP. Nature.

Nadasdy Z, Hirase H, Czurko A, Csicsvari J, Buzsaki G (1999) Replay and time compression of recurring spike sequences in the hippocampus. J Neurosci 19:9497-9507.

Nadel L, Moscovitch M (1997) Memory consolidation, retrograde amnesia and the hippocampal complex. Curr Opin Neurobiol 7:217-227.

Nadel L, Hupbach A, Gomez R, Newman-Smith K (2012) Memory formation, consolidation and transformation. Neuroscience and biobehavioral reviews 36:1640-1645.

Nakayama D, Hashikawa-Yamasaki Y, Ikegaya Y, Matsuki N, Nomura H (2016) Late Arc/Arg3.1 expression in the basolateral amygdala is essential for persistence of newly-acquired and reactivated contextual fear memories. Scientific reports 6:21007.

Nakayama D, Iwata H, Teshirogi C, Ikegaya Y, Matsuki N, Nomura H (2015) Long-delayed expression of the immediate early gene Arc/Arg3.1 refines neuronal circuits to perpetuate fear memory. J Neurosci 35:819-830.

Nakazawa K, Sun LD, Quirk MC, Rondi-Reig L, Wilson MA, Tonegawa S (2003) Hippocampal CA3 NMDA receptors are crucial for memory acquisition of one-time experience. Neuron 38:305-315.

Nakazawa K, Quirk MC, Chitwood RA, Watanabe M, Yeckel MF, Sun LD, Kato A, Carr CA, Johnston D, Wilson MA, Tonegawa S (2002) Requirement for hippocampal CA3 NMDA receptors in associative memory recall. Science 297:211-218.

Nonaka A, Toyoda T, Miura Y, Hitora-Imamura N, Naka M, Eguchi M, Yamaguchi S, Ikegaya Y, Matsuki N, Nomura H (2014) Synaptic plasticity associated with a memory engram in the basolateral amygdala. J Neurosci 34:9305-9309.

Nyhus E, Curran T (2010) Functional role of gamma and theta oscillations in episodic memory. Neuroscience and biobehavioral reviews 34:1023-1035.

O'Keefe J (1976) Place units in the hippocampus of the freely moving rat. Experimental neurology 51:78-109.

Okuno H, Akashi K, Ishii Y, Yagishita-Kyo N, Suzuki K, Nonaka M, Kawashima T, Fujii H, Takemoto-Kimura S, Abe M, Natsume R, Chowdhury S, Sakimura K, Worley PF, Bito H (2012) Inverse Synaptic Tagging of Inactive Synapses via Dynamic Interaction of Arc/Arg3.1 with CaMKII beta. Cell 149:886-898.

Olarte-Sanchez CM, Amin E, Warburton EC, Aggleton JP (2015) Perirhinal cortex lesions impair tests of object recognition memory but spare novelty detection. Eur J Neurosci 42:3117-3127.

Olvera-Cortes E, Cervantes M, Gonzalez-Burgos I (2002) Place-learning, but not cue-learning training, modifies the hippocampal theta rhythm in rats. Brain research bulletin 58:261-270.

Onoue K, Nakayama D, Ikegaya Y, Matsuki N, Nomura H (2014) Fear extinction requires Arc/Arg3.1 expression in the basolateral amygdala. Molecular brain 7:30.

Park S, Park JM, Kim S, Kim JA, Shepherd JD, Smith-Hicks CL, Chowdhury S, Kaufmann W, Kuhl D, Ryazanov AG, Huganir RL, Linden DJ, Worley PF (2008) Elongation factor 2 and fragile X mental retardation protein control the dynamic translation of Arc/Arg3.1 essential for mGluR-LTD. Neuron 59:70-83.

Pastalkova E, Serrano P, Pinkhasova D, Wallace E, Fenton AA, Sacktor TC (2006) Storage of spatial information by the maintenance mechanism of LTP. Science 313:1141-1144.

Pedemonte M, Barrenechea C, Nunez A, Gambini JP, Garcia-Austt E (1998) Membrane and circuit properties of lateral septum neurons: relationships with hippocampal rhythms. Brain Res 800:145-153.

Peebles CL, Yoo J, Thwin MT, Palop JJ, Noebels JL, Finkbeiner S (2010) Arc regulates spine morphology and maintains network stability in vivo. P Natl Acad Sci USA 107:18173-18178.

Penfield W, Milner B (1958) Memory deficit produced by bilateral lesions in the hippocampal zone. AMA archives of neurology and psychiatry 79:475-497.

Pettersen KH, Devor A, Ulbert I, Dale AM, Einevoll GT (2006) Current-source density estimation based on inversion of electrostatic forward solution: effects of finite extent of neuronal activity and conductivity discontinuities. J Neurosci Methods 154:116-133.

Phillips RG, LeDoux JE (1992) Differential contribution of amygdala and hippocampus to cued and contextual fear conditioning. Behavioral neuroscience 106:274-285.

Pinsker H, Kandel ER, Castellucci V, Kupfermann I (1970) An analysis of habituation and dishabituation in Aplysia. Advances in biochemical psychopharmacology 2:351-373.

Pintchovski SA, Peebles CL, Kim HJ, Verdin E, Finkbeiner S (2009) The serum response factor and a putative novel transcription factor regulate expression of the immediate-early gene Arc/Arg3.1 in neurons. J Neurosci 29:1525-1537.

Plath N et al. (2006) Arc/Arg3.1 is essential for the consolidation of synaptic plasticity and memories. Neuron 52:437-444.

Ploski JE, Pierre VJ, Smucny J, Park K, Monsey MS, Overeem KA, Schafe GE (2008) The Activity-Regulated Cytoskeletal-Associated Protein (Arc/Arg3.1) Is Required for Memory Consolidation of Pavlovian Fear Conditioning in the Lateral Amygdala. J Neurosci 28:12383-12395.

Ponnusamy R, Poulos AM, Fanselow MS (2007) Amygdala-dependent and amygdala-independent pathways for contextual fear conditioning. Neuroscience 147:919-927.

Popov VI, Davies HA, Rogachevsky VV, Patrushev IV, Errington ML, Gabbott PL, Bliss TV, Stewart MG (2004) Remodelling of synaptic morphology but unchanged synaptic density during late phase long-term potentiation (LTP): a serial section electron micrograph study in the dentate gyrus in the anaesthetised rat. Neuroscience 128:251-262.

Poulos AM, Ponnusamy R, Dong HW, Fanselow MS (2010) Compensation in the neural circuitry of fear conditioning awakens learning circuits in the bed nuclei of the stria terminalis. Proc Natl Acad Sci U S A 107:14881-14886.

Poulos AM, Li V, Sterlace SS, Tokushige F, Ponnusamy R, Fanselow MS (2009) Persistence of fear memory across time requires the basolateral amygdala complex. Proc Natl Acad Sci U S A 106:11737-11741.

Rajasethupathy P, Sankaran S, Marshel JH, Kim CK, Ferenczi E, Lee SY, Berndt A, Ramakrishnan C, Jaffe A, Lo M, Liston C, Deisseroth K (2015) Projections from neocortex mediate top-down control of memory retrieval. Nature 526:653-659.

Ramirez-Lugo L, Nunez-Jaramillo L, Bermudez-Rattoni F (2007) Taste memory formation: role of nucleus accumbens. Chemical senses 32:93-97.

Redondo RL, Morris RG (2011) Making memories last: the synaptic tagging and capture hypothesis. Nature reviews Neuroscience 12:17-30.

Reilly S (1999) The parabrachial nucleus and conditioned taste aversion. Brain research bulletin 48:239-254.

Reilly S, Bornovalova MA (2005) Conditioned taste aversion and amygdala lesions in the rat: a critical review. Neuroscience and biobehavioral reviews 29:1067-1088.

Ren M, Cao V, Ye Y, Manji HK, Wang KH (2014) Arc Regulates Experience-Dependent Persistent Firing Patterns in Frontal Cortex. J Neurosci 34:6583-6595.

Rial Verde EM, Lee-Osbourne J, Worley PF, Malinow R, Cline HT (2006) Increased expression of the immediate-early gene arc/arg3.1 reduces AMPA receptor-mediated synaptic transmission. Neuron 52:461-474.

Rios M, Fan G, Fekete C, Kelly J, Bates B, Kuehn R, Lechan RM, Jaenisch R (2001) Conditional deletion of brain-derived neurotrophic factor in the postnatal brain leads to obesity and hyperactivity. Molecular endocrinology 15:1748-1757.

Robinson J, Manseau F, Ducharme G, Amilhon B, Vigneault E, El Mestikawy S, Williams S (2016) Optogenetic Activation of Septal Glutamatergic Neurons Drive Hippocampal Theta Rhythms. J Neurosci 36:3016-3023.

Robinson S, Poorman CE, Marder TJ, Bucci DJ (2012) Identification of functional circuitry between retrosplenial and postrhinal cortices during fear conditioning. J Neurosci 32:12076-12086.

Rodriguez JJ, Davies HA, Silva AT, De Souza IE, Peddie CJ, Colyer FM, Lancashire CL, Fine A, Errington ML, Bliss TV, Stewart MG (2005) Long-term potentiation in the rat dentate gyrus is associated with enhanced Arc/Arg3.1 protein expression in spines, dendrites and glia. Eur J Neurosci 21:2384-2396.

Roediger HL, 3rd (1990) Implicit memory. Retention without remembering. The American psychologist 45:1043-1056.

Romanski LM, LeDoux JE (1992) Equipotentiality of thalamo-amygdala and thalamo-cortico-amygdala circuits in auditory fear conditioning. J Neurosci 12:4501-4509.

Rondi-Reig L, Libbey M, Eichenbaum H, Tonegawa S (2001) CA1-specific N-methyl-D-aspartate receptor knockout mice are deficient in solving a nonspatial transverse patterning task. Proc Natl Acad Sci U S A 98:3543-3548.

Rosenblum K, Meiri N, Dudai Y (1993) Taste memory: the role of protein synthesis in gustatory cortex. Behavioral and neural biology 59:49-56.

Rudenko A, Seo J, Hu J, Su SC, de Anda FC, Durak O, Ericsson M, Carlen M, Tsai LH (2015) Loss of cyclin-dependent kinase 5 from parvalbumin interneurons leads to hyperinhibition, decreased anxiety, and memory impairment. J Neurosci 35:2372-2383.

Ryan L, Nadel L, Keil K, Putnam K, Schnyer D, Trouard T, Moscovitch M (2001) Hippocampal complex and retrieval of recent and very remote autobiographical memories: evidence from functional magnetic resonance imaging in neurologically intact people. Hippocampus 11:707-714.

Sakai N, Yamamoto T (1998) Role of the medial and lateral parabrachial nucleus in acquisition and retention of conditioned taste aversion in rats. Behav Brain Res 93:63-70.

Sano Y, Shobe JL, Zhou M, Huang S, Shuman T, Cai DJ, Golshani P, Kamata M, Silva AJ (2014) CREB Regulates Memory Allocation in the Insular Cortex. Current biology : CB 24:2833-2837.

Santini MA, Klein AB, El-Sayed M, Ratner C, Knudsen GM, Mikkelsen JD, Aznar S (2011) Novelty-Induced Activity-Regulated Cytoskeletal-Associated Protein (Arc) Expression in Frontal Cortex Requires Serotonin 2a Receptor Activation. Neuroscience 190:251-257.

Sauer B (1987) Functional expression of the cre-lox site-specific recombination system in the yeast Saccharomyces cerevisiae. Molecular and cellular biology 7:2087-2096.

Sauer B, Henderson N (1988) Site-specific DNA recombination in mammalian cells by the Cre recombinase of bacteriophage P1. Proc Natl Acad Sci U S A 85:5166-5170.

Schomburg EW, Fernandez-Ruiz A, Mizuseki K, Berenyi A, Anastassiou CA, Koch C, Buzsaki G (2014) Theta phase segregation of input-specific gamma patterns in entorhinal-hippocampal networks. Neuron 84:470-485.

Schwenk F, Baron U, Rajewsky K (1995) A cre-transgenic mouse strain for the ubiquitous deletion of loxP-flanked gene segments including deletion in germ cells. Nucleic acids research 23:5080-5081.

Scoville WB, Milner B (1957) Loss of recent memory after bilateral hippocampal lesions. Journal of neurology, neurosurgery, and psychiatry 20:11-21.

Shepherd JD, Bear MF (2011) New views of Arc, a master regulator of synaptic plasticity. Nat Neurosci 14:279-284.

Shepherd JD, Rumbaugh G, Wu J, Chowdhury S, Plath N, Kuhl D, Huganir RL, Worley PF (2006) Arc/Arg3.1 mediates homeostatic synaptic scaling of AMPA receptors. Neuron 52:475-484.

Shi SH, Hayashi Y, Petralia RS, Zaman SH, Wenthold RJ, Svoboda K, Malinow R (1999) Rapid spine delivery and redistribution of AMPA receptors after synaptic NMDA receptor activation. Science 284:1811-1816.

Shimamura AP JJ, Squire LR. (1991) What is the role of frontal lobe damage in memory disorders? In Frontal lobe functioning and dysfunction. New York: Oxford University Press.

Siapas AG, Wilson MA (1998) Coordinated interactions between hippocampal ripples and cortical spindles during slow-wave sleep. Neuron 21:1123-1128.

Siegel D (1999) The developing mind: Toward a neurobiology of interpersonal experience. New York, NY: Guilford.

Sirota A, Csicsvari J, Buhl D, Buzsaki G (2003) Communication between neocortex and hippocampus during sleep in rodents. Proc Natl Acad Sci U S A 100:2065-2069.

Skaggs WE, McNaughton BL (1996) Replay of neuronal firing sequences in rat hippocampus during sleep following spatial experience. Science 271:1870-1873.

Smith-Hicks C, Xiao B, Deng RK, Ji YF, Zhao X, Shepherd JD, Posern G, Kuhl D, Huganir RL, Ginty DD, Worley PF, Linden DJ (2010) SRF binding to SRE 6.9 in the Arc promoter is essential for LTD in cultured Purkinje cells. Nat Neurosci 13:1082-U1073.

Solstad T, Boccara CN, Kropff E, Moser MB, Moser EI (2008) Representation of geometric borders in the entorhinal cortex. Science 322:1865-1868.

Soriano P (1999) Generalized lacZ expression with the ROSA26 Cre reporter strain. Nature genetics 21:70-71.

Squire LR (1992) Declarative and nondeclarative memory: multiple brain systems supporting learning and memory. Journal of cognitive neuroscience 4:232-243.

Squire LR (2004) Memory systems of the brain: a brief history and current perspective. Neurobiol Learn Mem 82:171-177.

Squire LR, Zola-Morgan S (1991) The medial temporal lobe memory system. Science 253:1380-1386.

Squire LR, Bayley PJ (2007) The neuroscience of remote memory. Curr Opin Neurobiol 17:185-196.

Squire LR, Wixted JT (2011) The cognitive neuroscience of human memory since H.M. Annual review of neuroscience 34:259-288.

Squire LR, Dede AJ (2015) Conscious and unconscious memory systems. Cold Spring Harbor perspectives in biology 7:a021667.

Squire LR, Stark CE, Clark RE (2004) The medial temporal lobe. Annual review of neuroscience 27:279-306.

Staresina BP, Duncan KD, Davachi L (2011) Perirhinal and parahippocampal cortices differentially contribute to later recollection of object- and scene-related event details. J Neurosci 31:8739-8747.

Steward O, Wallace CS, Lyford GL, Worley PF (1998) Synaptic activation causes the mRNA for the IEG Arc to localize selectively near activated postsynaptic sites on dendrites. Neuron 21:741-751.

Stewart M, Fox SE (1990) Do septal neurons pace the hippocampal theta rhythm? Trends in neurosciences 13:163-168.

Stumpf C, Petsche H, Gogolak G (1962) The significance of the rabbit's septum as a relay station between the midbrain and the hippocampus. II. The differential influence of drugs upon both the septal cell firing pattern and the hippocampus theta activity. Electroencephalography and clinical neurophysiology 14:212-219.

Tanaka KZ, Pevzner A, Hamidi AB, Nakazawa Y, Graham J, Wiltgen BJ (2014) Cortical representations are reinstated by the hippocampus during memory retrieval. Neuron 84:347-354.

Tang JC, Rudolph S, Dhande OS, Abraira VE, Choi S, Lapan SW, Drew IR, Drokhlyansky E, Huberman AD, Regehr WG, Cepko CL (2015) Cell type-specific manipulation with GFP-dependent Cre recombinase. Nat Neurosci 18:1334-1341.

Tang W, Ehrlich I, Wolff SB, Michalski AM, Wolfl S, Hasan MT, Luthi A, Sprengel R (2009) Faithful expression of multiple proteins via 2A-peptide self-processing: a versatile and reliable method for manipulating brain circuits. J Neurosci 29:8621-8629.

Tayler KK, Tanaka KZ, Reijmers LG, Wiltgen BJ (2013) Reactivation of neural ensembles during the retrieval of recent and remote memory. Current biology : CB 23:99-106.

Teixeira CM, Pomedli SR, Maei HR, Kee N, Frankland PW (2006) Involvement of the anterior cingulate cortex in the expression of remote spatial memory. J Neurosci 26:7555-7564.

Tse D, Langston RF, Kakeyama M, Bethus I, Spooner PA, Wood ER, Witter MP, Morris RG (2007) Schemas and memory consolidation. Science 316:76-82.

Tse D, Takeuchi T, Kakeyama M, Kajii Y, Okuno H, Tohyama C, Bito H, Morris RG (2011) Schema-dependent gene activation and memory encoding in neocortex. Science 333:891-895.

Tsien JZ, Chen DF, Gerber D, Tom C, Mercer EH, Anderson DJ, Mayford M, Kandel ER, Tonegawa S (1996) Subregion- and cell type-restricted gene knockout in mouse brain. Cell 87:1317-1326.

Tulving E (1972) Episodic and Semantic Memory: Organization of Memory (E. Tulving & W. Donaldson ed.). New York, NY: Academic Press.

Turrigiano G (2012) Homeostatic synaptic plasticity: local and global mechanisms for stabilizing neuronal function. Cold Spring Harbor perspectives in biology 4:a005736.

van der Meer MA, Redish AD (2009) Low and High Gamma Oscillations in Rat Ventral Striatum have Distinct Relationships to Behavior, Reward, and Spiking Activity on a Learned Spatial Decision Task. Frontiers in integrative neuroscience 3:9.

van Eden CG, Kros JM, Uylings HB (1990) The development of the rat prefrontal cortex. Its size and development of connections with thalamus, spinal cord and other cortical areas. Progress in brain research 85:169-183.

Vandecasteele M, Varga V, Berenyi A, Papp E, Bartho P, Venance L, Freund TF, Buzsaki G (2014) Optogenetic activation of septal cholinergic neurons suppresses sharp wave ripples and enhances theta oscillations in the hippocampus. Proc Natl Acad Sci U S A 111:13535-13540.

Vanderwolf CH (1969) Hippocampal electrical activity and voluntary movement in the rat. Electroencephalography and clinical neurophysiology 26:407-418.

Verde EMR, Lee-Osbourne J, Worley PF, Malinow R, Cline HT (2006) Increased expression of the immediate-early gene Arc/Arg3.1 reduces AMPA receptor-mediated synaptic transmission. Neuron 52:461-474.

Vinogradova OS (1995) Expression, control, and probable functional significance of the neuronal theta-rhythm. Prog Neurobiol 45:523-583.

Viskontas IV, McAndrews MP, Moscovitch M (2000) Remote episodic memory deficits in patients with unilateral temporal lobe epilepsy and excisions. J Neurosci 20:5853-5857.

Voglis G, Tavernarakis N (2006) The role of synaptic ion channels in synaptic plasticity. EMBO reports 7:1104-1110.

Vogt MA, Inta D, Luoni A, Elkin H, Pfeiffer N, Riva MA, Gass P (2014) Inducible forebrain-specific ablation of the transcription factor Creb during adulthood induces anxiety but no spatial/contextual learning deficits. Front Behav Neurosci 8:407.

Vorhees CV, Williams MT (2006) Morris water maze: procedures for assessing spatial and related forms of learning and memory. Nat Protoc 1:848-858.

Vorhees CV, Williams MT (2014) Assessing spatial learning and memory in rodents. ILAR journal / National Research Council, Institute of Laboratory Animal Resources 55:310-332.

Vousden DA, Epp J, Okuno H, Nieman BJ, van Eede M, Dazai J, Ragan T, Bito H, Frankland PW, Lerch JP, Henkelman RM (2015) Whole-brain mapping of behaviourally induced neural activation in mice. Brain Struct Funct 220:2043-2057.

Walker MP, Robertson EM (2016) Memory Processing: Ripples in the Resting Brain. Current biology : CB 26:R239-241.

Waltereit R, Dammermann B, Wulff P, Scafidi J, Staubli U, Kauselmann G, Bundman M, Kuhl D (2001) Arg3.1/Arc mRNA induction by Ca2+ and cAMP requires protein kinase A and mitogen-activated protein kinase/extracellular regulated kinase activation. J Neurosci 21:5484-5493.

Wang DO, Kim SM, Zhao Y, Hwang H, Miura SK, Sossin WS, Martin KC (2009) Synapse- and stimulus-specific local translation during long-term neuronal plasticity. Science 324:1536-1540.

Warburton EC, Brown MW (2010) Findings from animals concerning when interactions between perirhinal cortex, hippocampus and medial prefrontal cortex are necessary for recognition memory. Neuropsychologia 48:2262-2272.

Waung MW, Pfeiffer BE, Nosyreva ED, Ronesi JA, Huber KM (2008) Rapid translation of Arc/Arg3.1 selectively mediates mGluR-dependent LTD through persistent increases in AMPAR endocytosis rate. Neuron 59:84-97.

Welzl H, D'Adamo P, Lipp HP (2001a) Conditioned taste aversion as a learning and memory paradigm. Behav Brain Res 125:205-213.

Welzl H, D'Adamo P, Lipp HP (2001b) Conditioned taste aversion as a learning and memory paradigm. Behav Brain Res 125:205-213.

Whitlock JR, Heynen AJ, Shuler MG, Bear MF (2006) Learning induces long-term potentiation in the hippocampus. Science 313:1093-1097.

Wilkenfield J, Nickel M, Blakely E, Poling A (1992) Acquisition of lever-press responding in rats with delayed reinforcement: A comparison of three procedures. Journal of the experimental analysis of behavior 58:431-443.

Wiltgen BJ, Tanaka KZ (2013) Systems consolidation and the content of memory. Neurobiol Learn Mem 106:365-371.

Wiltgen BJ, Sanders MJ, Anagnostaras SG, Sage JR, Fanselow MS (2006) Context fear learning in the absence of the hippocampus. J Neurosci 26:5484-5491.

Wiltgen BJ, Zhou M, Cai Y, Balaji J, Karlsson MG, Parivash SN, Li W, Silva AJ (2010) The hippocampus plays a selective role in the retrieval of detailed contextual memories. Current biology : CB 20:1336-1344.

Winocur G, Moscovitch M (2011) Memory transformation and systems consolidation. Journal of the International Neuropsychological Society : JINS 17:766-780.

Winocur G, Moscovitch M, Bontempi B (2010) Memory formation and long-term retention in humans and animals: convergence towards a transformation account of hippocampal-neocortical interactions. Neuropsychologia 48:2339-2356.

Winocur G, Sekeres MJ, Binns MA, Moscovitch M (2013) Hippocampal lesions produce both nongraded and temporally graded retrograde amnesia in the same rat. Hippocampus 23:330-341.

Winocur G, Frankland PW, Sekeres M, Fogel S, Moscovitch M (2009) Changes in context-specificity during memory reconsolidation: selective effects of hippocampal lesions. Learn Mem 16:722-729.

Winson J (1978) Loss of hippocampal theta rhythm results in spatial memory deficit in the rat. Science 201:160-163.

Yamada K (2011) Analyses of fear memory in Arc/Arg3.1-deficient mice: intact short-term memory and impaired long-term and remote memory. World Journal of Neuroscience 01:1-8.

Yamamoto T (2007) Brain regions responsible for the expression of conditioned taste aversion in rats. Chemical senses 32:105-109.

Yin Y, Edelman GM, Vanderklish PW (2002) The brain-derived neurotrophic factor enhances synthesis of Arc in synaptoneurosomes. Proc Natl Acad Sci U S A 99:2368-2373.

Ying SW, Futter M, Rosenblum K, Webber MJ, Hunt SP, Bliss TV, Bramham CR (2002) Brain-derived neurotrophic factor induces long-term potentiation in intact adult hippocampus: requirement for ERK activation coupled to CREB and upregulation of Arc synthesis. J Neurosci 22:1532-1540.

Yiu AP, Mercaldo V, Yan C, Richards B, Rashid AJ, Hsiang HL, Pressey J, Mahadevan V, Tran MM, Kushner SA, Woodin MA, Frankland PW, Josselyn SA (2014) Neurons are recruited to a memory trace based on relative neuronal excitability immediately before training. Neuron 83:722-735.

Yuste R, Bonhoeffer T (2001) Morphological changes in dendritic spines associated with long-term synaptic plasticity. Annual review of neuroscience 24:1071-1089.

Zelikowsky M, Bissiere S, Fanselow MS (2012) Contextual fear memories formed in the absence of the dorsal hippocampus decay across time. J Neurosci 32:3393-3397.

Zelikowsky M, Bissiere S, Hast TA, Bennett RZ, Abdipranoto A, Vissel B, Fanselow MS (2013) Prefrontal microcircuit underlies contextual learning after hippocampal loss. Proc Natl Acad Sci U S A 110:9938-9943.

Zhao MG, Toyoda H, Lee YS, Wu LJ, Ko SW, Zhang XH, Jia Y, Shum F, Xu H, Li BM, Kaang BK, Zhuo M (2005) Roles of NMDA NR2B subtype receptor in prefrontal long-term potentiation and contextual fear memory. Neuron 47:859-872.

Zheng B, Sage M, Sheppeard EA, Jurecic V, Bradley A (2000) Engineering mouse chromosomes with Cre-loxP: range, efficiency, and somatic applications. Molecular and cellular biology 20:648-655

5.2 Statement of contribution

Arc/Arg3.1 floxed mouse line was generated by Prof. Dietmar Kuhl and former colleagues, Dr. Björn Dammermann, Dr. Anika Bick-Sander and Eric Therstappen. All behavioral, biochemical and histology experiments were designed and performed by Xiaoyan Gao and Mario Sergio Castro Gómez. *In vivo* LTP recordings were performed by Xiaoyan Gao. rISH was performed by Sabine Graf. Jasper Grendel performed and analyzed LFP recordings. Cell counting was performed with the help of Helia Saber and Jing Sun. Dr. Lars Binkle helped design rISH primers. Dr. Daniel Mensching cloned rAAV-CaMKIIα-CreER^{T2}-2AP-venus plasmid. Mario Sergio Castro Gómez did the quantification of Arc/Arg3.1 mRNA from mouse brain with different age based on the rISH images. Prof. Dirk Isbrandt (Group for Experimental Neurophysiology, Universitätsklinikum Köln) participated in design and supervision of LFP experiments. Prof. Dietmar Kuhl and Dr. Ora Ohana generated the concept of the project and provided funding. Dr. Ora Ohana performed initial experiments, oversaw and directed all experiments. The study was supported by a grant from DFG (SFB 936-project B4 from 2011 to 2014) and by the grant “Molekulare Mechanismen der NetzIrkmodifizierung” from the Federal State of Hamburg. Xiaoyan Gao was also supported with a stipend from China Scholarship Council (CSC).

Currently, some parts of the data presented in this thesis are used in a manuscript under revision.

Title: Arc/Arg3.1 Regulates a Critical Period for Learning and Memory Networks

Authors: Xiaoyan Gao[1#], Sergio Castro-Gomez[1#], Jasper Grendel[1#], Sabine Graf[1], Lars Binkle[1], Daniel Mensching[1], Dirk Isbrandt[2, †], Dietmar Kuhl[1*], Ora Ohana[1*]

Affiliations:

[1]Institute for Molecular and Cellular Cognition (IMCC), Center for Molecular Neurobiology (ZMNH), University Medical Center Hamburg-Eppendorf (UKE) Hamburg, Germany

[2] Research group Experimental Neuropediatrics, Center for Molecular Neurobiology (ZMNH), University Medical Center Hamburg-Eppendorf (UKE) Hamburg, Germany

[†]Current address: Institute for Molecular and Behavioral Neuroscience, DZNE and UzK Research Team Experimental Neurophysiology, University of Cologne, Cologne, Germany.

contributed to an equal extent

* Correspondence to: ora.ohana@zmnh.uni-hamburg.de

dietmar.kuhl@zmnh.uni-hamburg.de

Abstract

During early postnatal development primary sensory regions of the brain undergo periods of heightened plasticity which sculpt neural networks and lay the foundation for adult sensory perception. Such critical periods were also postulated for learning and memory, but remain elusive and poorly understood. Here we present evidence that expression of Arc/Arg3.1 is up-regulated during the first four weeks of postnatal development, drives the maturation of network activity in mnemonic regions and determines the capacity for learning and memory in adulthood. Conditional removal of Arc/Arg3.1 during the first three postnatal weeks causes a profound reduction of memory-linked theta and gamma oscillations, an alteration of hippocampal ripples, and deficits in spatial learning and memory consolidation. In contrast, a later removal of Arc/Arg3.1 only impairs long-term memory consolidation leaving learning and network activity patterns largely intact. These results demonstrate that Arc/Arg3.1 delineates a critical period in the development of learning and memory, during which it is required for proper wiring of hippocampal-cortical networks for future learning and memory storage.

5.3 Curriculum vitae

Personal information

Given name: Xiaoyan

Family name: Gao

Date of birth: 21.11.1982

Gender: Male

Nationality: P.R.China

Education

11.2011-Present Doctoral study in Neurobiology

Institute for Molecular and Cellular Cognition (IMCC)

Center for Molecular Neurobiology Hamburg (ZMNH)

University Medical Center (UKE)

University of Hamburg (UHH), Hamburg, Germany

Supervisors: Prof. Dietmar Kuhl and Dr. Ora Ohana

Co-supervisor in Department of Biology: Prof. Christian Lohr

09.2008-09.2011 Master study in Neurobiology

Department of Neurobiology and Biophysics, School of Life Sciences

University of Science and Technology of China (USTC), Hefei, China

Supervisors: Prof. Ming Wang and Prof. Di-yun Ruan

09.2004-07.2008 Bachelor study in Bioengineering

Department of Bioengineering, School of Life Sciences

Shandong University of Technology (SDUT), Zibo, China

Universitätsklinikum Hamburg-Eppendorf

Center for Molecular Neurobiology Hamburg

Research Group:
Neuronal Translational Control

Martinistraße 52
20246 Hamburg

Kent Duncan, PhD

Phone: +49(0)40 7410-56274
Fax: +49(0)40 7410-53436
Kent.Duncan@zmnh.uni-hamburg.de
www.zmnh.uni-hamburg.de

Delivery address:
Falkenried 94
20251 Hamburg

Universitätsklinikum Hamburg-Eppendorf Martinistraße 52 20246 Hamburg
Zentrum für Molekulare Neurobiologie - Forschergruppen

July 22, 2016

English language Thesis Certification: Xiaoyan Gao

To whom it may concern:

Xiaoyan Gao, who was born on 21.11.1982 in Shandong, China, is submitting his doctoral dissertation in English. The title of his thesis is: 'Dependence of learning and memory consolidation on spatiotemporal expression of Arc/Arg3.1 in hippocampal-cortical networks'.

I hereby certify as a native speaker and molecular biologist that the English language used in this thesis is sufficiently correct for submission.

Yours truly,

Universität Hamburg
Universitätsklinikum Hamburg-Eppendorf
Zentrum für Molekulare Neurobiologie
AG Duncan
Falkenried 94 · D-20251 Hamburg

Kent Duncan, Ph.D. **Hamburg, July 22, 2016**